NASA-CR-165419

MITRE Technical Report

MTR-8311

Final Technical Report On-Board Processing for Future Satellite Communications Systems: SATELLITE-ROUTED FDMA

George Berk, Paul F. Christopher, Murray Hoffman,
Paul N. Jean, Ersch Rotholz, Brian E. White

May 1981

CONTRACT SPONSOR	NASA/LeRC
CONTRACT NO.	F19628-81-C-0001
PROJECT NO.	8680
DEPT.	D-97

THE MITRE CORPORATION
BEDFORD, MASSACHUSETTS

Department Approval: W. T. Brandon

MITRE Project Approval: W. T. Brandon

To: Recipients of MTR-8311 Date: 4 November 1981

From: P. N. Jean Memo No.: D97-M-462

Subject: Missing NASA Report Number

Copies to: Technical Report Center, File

In the upper right-hand corner of the front cover, please correct the document to read as follows:

NASA/LeRC

CONTRACT No.: C-49029D
REPORT No.: CR-165419

Also, on page iii - update block 1 to read as follows:

1. Report No.

NASA/LeRC CR-165419

This report number should be written on each copy we receive so that future references to the report can be made through via their documentation control system. During publication, the report control number was inadvertently omitted.

P. N. Jean

PNJ:kc

NASA-CR-165419

1. Report No.	2. Government Accession No.	3. Recipient's Catalog No.
NASA/LeRC C-49029-D		

4. Title and Subtitle	5. Report Date
Final Technical Report On-Board Processing for Future Satellite Communications Systems SATELLITE-ROUTED FDMA	May 1981 6. Performing Organization Code
7. Author(s) George Berk, Paul F. Christopher, Murray Hoffman, Paul N. Jean Ersch Rotholz, Brian E. White	8. Performing Organization Report No. MTR-8311
9. Performing Organization Name and Address The Mitre Corporation P.O. Box 208 Bedford, MA 01730	10. Work Unit No. 11. Contract or Grant No. F19628-81-C-0001
12. Sponsoring Agency Name and Address National Aeronautics and Space Administration Lewis Research Center Cleveland, Ohio 44135	13. Type of Report and Period Covered Contractor Report 14. Sponsoring Agency Code

15. Supplementary Notes

Project Manager, James O. Rotnem, NASA Lewis Research Center, Cleveland, Ohio

16. Abstract

A frequency division multiple access (FDMA) 30/20 GHz satellite communications architecture without on-board baseband processing is investigated. Conceptual system designs are suggested for domestic traffic models totaling 4 Gb/s of customer premises service (CPS) traffic and 6 Gb/s of trunking traffic. Emphasis is given to the CPS portion of the system which includes thousands of earth terminals with digital traffic ranging from a single 64 kb/s voice channel to hundreds of channels of voice, data, and video with an aggregate data rate of 33 Mb/s. A unique regional design concept that effectively smooths the non-uniform traffic distribution and greatly simplifies the satellite design is employed. The satellite antenna system forms thirty-two 0.33° beams on ooth the uplinks and the downlinks in one design. In another design matched to a traffic model with more dispersed users, there are twenty-four 0.33°! beams and twenty-one 0.7° beams Detailed system design techniques show that a single satellite producing approximately 5 kW of DC power is capable of handling at least 75% of the postulated traffic. A detailed cost model of the ground segment and estimated system costs based on current information from manufacturers are presented.

17. Key Words (Suggested by Author(s))	18. Distribution Statement
• on-board processing • satellite communications • 30/20 GHz, EHF, K_a - Band • multibeam antenna • FDMA	Unclassified - Unlimited

19. Security Classif. (of this report)	20. Security Classif. (of this page)	21. No. of Pages	22. Price*
Unclassified	Unclassified	299	

* For sale by the National Technical Information Service, Springfield, Virginia 22161

ACKNOWLEDGMENTS

John M. Ruddy is the author of appendix B, and William R. Neal wrote appendixes C and D. Thomas J. Ferguson wrote the subsection on coding techniques in section 5. Norman A. Spier provided computer programming support in generating the crosstalk results. F. J. Zucker and A. P. Doohovskoy contributed to spacecraft antenna implementation and beam pattern considerations. Douglas O. Alwine and Warren K. Green served as consultants on technology issues. Helen E. King prepared most of the material of the text and supervised the organization of the final document with the assistance of Judith A. Laskey. Ruth W. Wales provided editing support. The principal authors thank these colleagues for their valuable help.

Special thanks is also extended to John D. Kiesling and his colleagues at General Electric/Space Division for helpful technological discussions during the early stages of this study.

ERRATA

NASA Contractor Report 165419

ON-BOARD PROCESSING FOR FUTURE SATELLITE COMMUNICATIONS SYSTEMS: SATELLITE-ROUTED FDMA

George Berk, Paul F. Christopher, Murray Hoffman, Paul N. Jean, Ersch Rotholz, and Brian E. White

May 1981

Cover and title page: The NASA Contractor Report number (CR-165419) should be added.

Report documentation page: The report number (block 1) should be changed to NASA CR-165419.

TABLE OF CONTENTS

TABLE OF CONTENTS (Continued)

TABLE OF CONTENTS (Continued)

TABLE OF CONTENTS (Concluded)

TABLE OF CONTENTS (Concluded)

LIST OF ILLUSTRATIONS

LIST OF ILLUSTRATIONS (Continued)

LIST OF ILLUSTRATIONS (Continued)

LIST OF ILLUSTRATIONS (Continued)

LIST OF ILLUSTRATIONS (Concluded)

LIST OF TABLES

LIST OF TABLES (Continued)

LIST OF TABLES (Continued)

LIST OF TABLES (Concluded)

SECTION 1

EXECUTIVE SUMMARY

This report describes a feasibility study for a frequency division multiple access (FDMA), multiple beam, satellite communications system, without on-board baseband processing, operating in the 30/20 GHz frequency bands.

This study of a satellite system operating in the 30/20 GHz bands has two major objectives:

1. A new satellite system must aim at conserving the orbital arc, thereby allowing a larger number of satellites in the geosynchronous arc. Orbital arc conservation can be obtained by:

    a. Using high-gain (narrow-beam) terminal antennas which have little gain in any but the desired direction. This approach is particularly suitable for domestic satellite systems where several satellites illuminate the same area.

    b. Using coding to combat rain attenuation and reducing the power margins proportionally. This is particularly suitable for downlink rain accomodation since adaptive equalization is not feasible.

    c. Using high capacity satellites to reduce the number of satellites required to provide service.

2. A new satellite system must also make efficient use of available bandwidth in order to handle the ever increasing communications capacity. Efficient bandwidth utilization can be achieved by:

    a. Conserving bandwidth by employing frequency reuse. High-gain (narrow-beam) satellite antennas allow beams that are sufficiently (spatially) separated to use the same frequency band with acceptably low interference.

This study indicates that satellite routed (SR)-FDMA systems may compare favorably in performance, flexibility, and cost with satellite switched (SS)-time division multiple access (TDMA) systems. The FDMA system concept developed by the MITRE Corporation

is unique in suggesting a regional approach to satisfying high density, non-uniform traffic models supplied by the National Aeronautics and Space Administration (NASA). This regional concept greatly simplifies the satellite design by reducing the number of filters, amplifiers, intermediate frequency (IF) frequency converters and down-converters.

The satellite services thousands of small, medium, and large earth stations located around the major cities of the continental United States (CONUS). Two categories of earth terminal are considered: Customer Premises Service (CPS) terminals which provide direct satellite access to local users, and trunking terminals which support high volume multiplexed traffic of area users organized by terrestrial networks. The CPS traffic comprises digital voice, data, and video channels at data rates ranging from 56 kb/s to 6.3 Mb/s. The total peak hour CPS traffic for CONUS is 4 Gb/s, while the trunking traffic totals 6 Gb/s. The amount of traffic associated with a given area is roughly proportional to its population.

A system of such high capacity is both power and bandwidth limited. The attainable satellite DC power is limited by weight and size restrictions on the solar cell array. The available 2.5 GHz bandwidth at Ka-band is insufficient for handling the specified traffic without frequency reuse. A high-gain multibeam satellite antenna system alleviates both problems. The high antenna gain reduces both spacecraft and earth terminal power requirements. In addition, the multiple beams allow frequency reuse of the available bandwidth. Frequency reuse requires careful consideration of the co-channel interference among the beams, and much attention has been given to this issue in the study.

Connectivity among frequency division multiplexed (FDM) users is achieved by frequency slot assignments and filtering in the satellite, whereas it is achieved in a time division multiplexed (TDM) system by time slot assignment and switching in the satellite. A network control center assigns specific transmit and receive frequencies for every link on a dynamic basis. The routing of traffic is performed in two steps: first, band allocation and filtering in the satellite provide the connectivity between uplink and downlink beams; second, conventional FDM connects the individual users within a beam.

Traffic is organized on a regional basis. The recommended beam and frequency design for one traffic model is shown in figure 1-1. This view of CONUS shows the locations of the 0.33° beams as seen from a satellite in a geostationary orbit at 90° west longitude. Each beam cell contains a code which identifies which sub-bands are

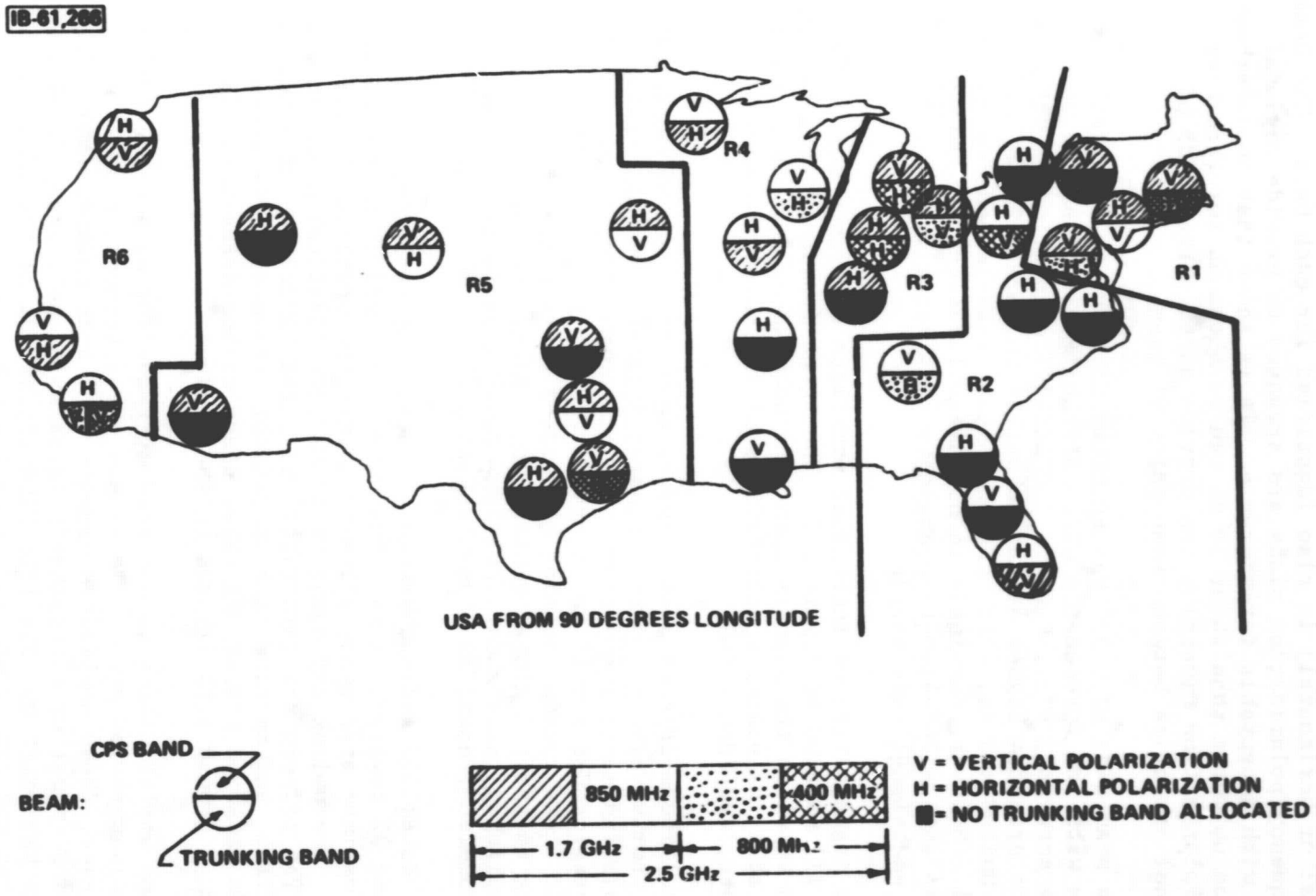

Figure 1-1. Beam and Frequency Plans for a Six Region CPS and Trunking FDMA Satellite System

allocated for CPS and trunking traffic. The assigned polarization (vertical or horizontal) is also identified for each beam. The beam and frequency/polarization plans are arranged to provide regional routing with acceptable interference. It is shown that an interbeam isolation no worse than about 30 dB can be obtained for this beam plan. Polarization diversity can provide up to about 20 dB of additional isolation between some pairs of beams.

The beam size of 0.33° was selected as about the smallest possible with the foreseeable state-of-the-art in satellite beam pointing accuracy, e.g., 0.04°. The satellite location of 90° west longitude provides higher elevation angles to terminals in the eastern United States, which has the higher traffic density and more rainfall. However, terminals in northwest locations of CONUS will have less than a 30° elevation angle to this satellite, which could require additional rain margin.

The organization of individual satellite downlinks for region 1 (R1) is illustrated in figure 1-2. The three frequency translations required to align the signals into continuous downlink bands, which is desirable for easing specifications of the satellite power amplifiers, are identified.

A multibeam antenna system and bandpass filters with bandwidths ranging from several to about a hundred megahertz are the essence of the simplified satellite design. The conceptual block diagram of the six-region CPS satellite is presented in figure 1-3. The satellite first routes incoming bandwidths containing many channels according to their regional destination. After the regional routing is accomplished, sub-bands containing fewer signals are routed to their individual downlink beam destinations.

The satellite antenna system includes four reflectors, and 32 uplink and 32 downlink horns. The beams are fixed (non-steerable) and for maximum efficiency illuminate only the specified traffic centers. The uplink and downlink beams have identical beamwidths of 0.33°. The filters are hard-wired, of fixed bandwidth (tailored to the traffic), and operate in a convenient intermediate frequency band. No baseband processing takes place on-board the satellite. (This was a ground rule imposed on the study.)

Power amplification is provided by traveling wave tubes (TWTs) with 75 W saturation power. To reduce the intermodulation interference, these amplifiers operate at a 5-dB backoff (BO). The projected DC power of a reasonably large solar cell array is 5000 W. This sets the limit on satellite capacity at 75% of the specified CPS traffic and 70% of the specified trunking traffic. If more satellite power is available, satellite capacity is still limited by

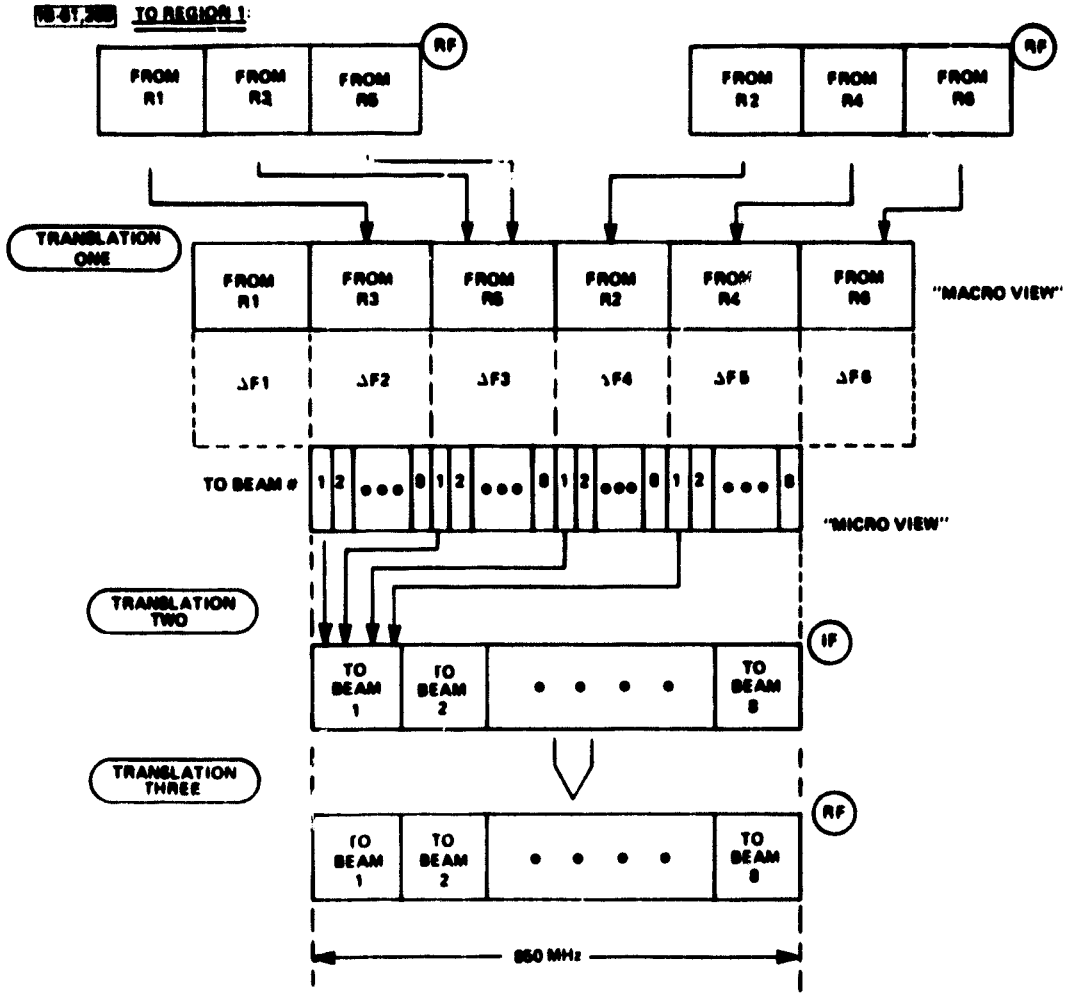

Figure 1-2. Satellite Downlink Organization for Region 1

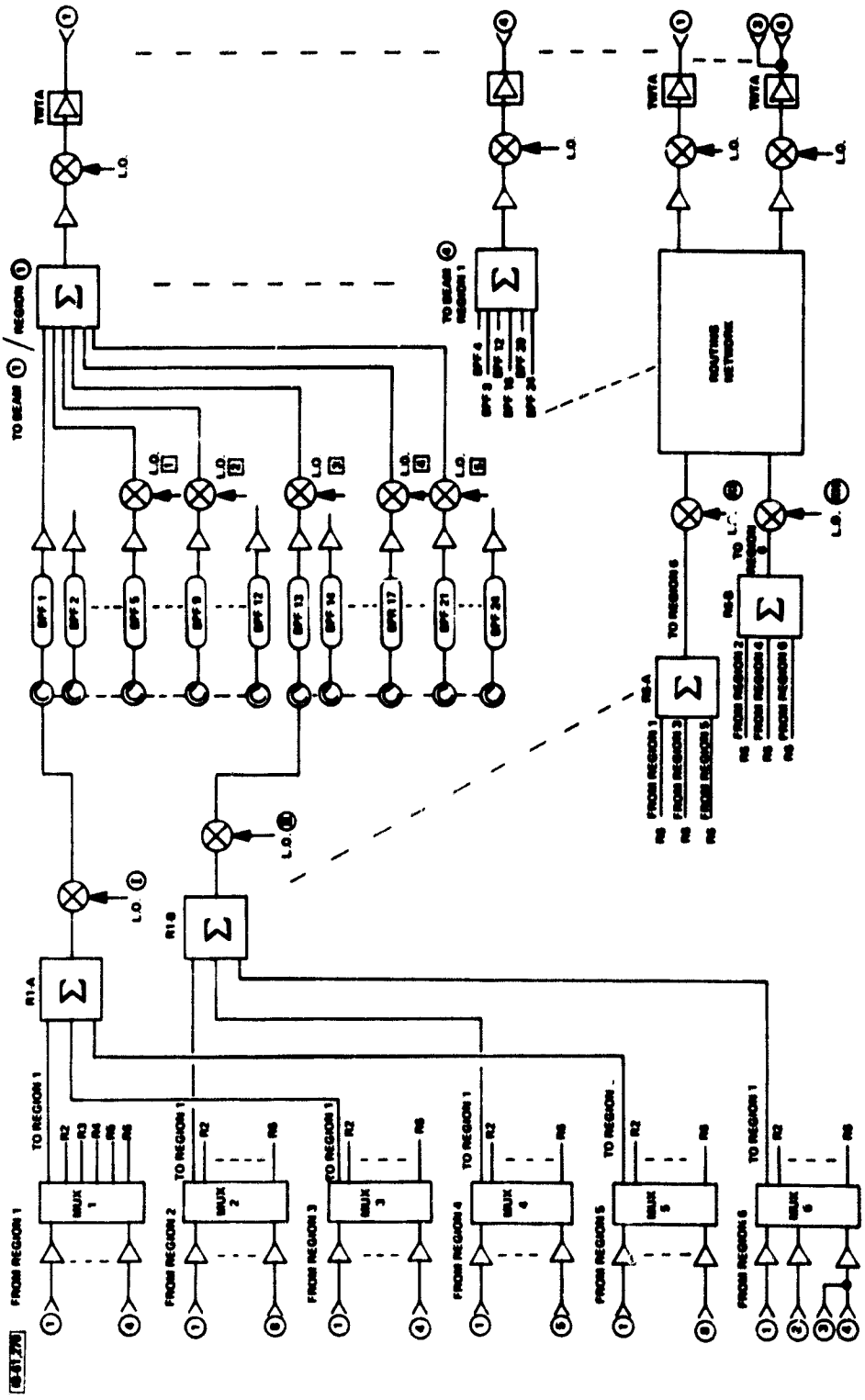

Figure 1-3. Satellite Configuration for a 6 Region CPS FDMA Satellite Concept

available bandwidth. Approximately 90% of the traffic can be handled if guard bands between satellite filters and excess bandwidth to reduce blocked calls are minimized, and if satellite DC power is not limited to 5000 W.

These limitations of traffic handling capability are governed by the beams with the highest traffic density. The non-uniformity of the traffic model has been preserved. (This was another ground rule of the study.) The greatest single factor which would ease the satellite design, other than a more uniform traffic model, is to place the trunking users on their own satellite. This would permit the satisfaction of all the CPS user traffic with a 5000 W satellite. Future work should also depart from the assumption of a single satellite and consider several satellites, perhaps one for each region of CONUS. Interconnectivity among regions can be accomplished either through crosslinks or ground networks.

The SR-FDMA satellite is conceptually different from an SS-FDMA satellite. The receive spectrum of a switching satellite would be divided into many more and much smaller sub-bands containing fewer signals. All the sub-bands would be downconverted to a common intermediate frequency band and sent to a large switching matrix. The switch settings would be determined by the destinations of the signals in the various input sub-bands and would be changed relatively frequently according to the real-time ebb and flow of the traffic demands. The sub-bands at the switch outputs would then each be upconverted to the appropriate bandwidth slot in the transmit band.

An SS-FDMA satellite would be much more complex than the SR-FDMA satellite discussed in this report. Some switching capability is provided in the SR-FDMA system designs for long-term changes in the distribution of traffic. This limited switching capability allows beams in the same region to compensate for traffic distribution changes by swapping bandwidths with one another. However, this is a second-order consideration philosophically since there is no need for satellite switching with SR-FDMA. Short-term switching is accomplished by frequency assignments on the ground.

In the 30/20 GHz bands, rain attenuation is another serious problem which requires careful consideration. In order to combat uplink fades during heavy rain storms, the earth stations must be able to boost their output power by at least 10 dB and/or use coding. Rain margins of 10 dB for the uplink and 4 dB for the downlink result in link availabilities of 99.5% which is a reasonable requirement for CPS. (There is less attenuation at the lower downlink frequencies.) More margin is necessary for a link availability goal of 99.9%. The link budgets adopted ensure total

uplink and downlink margins of at least 15 dB and 6 dB, respectively, in the absence of rain. (This was a study requirement.) An analysis suggesting how to select uplink margin according to the rain region location of a terminal is included in section 5.

Four sources of interference are considered in the system design: co-channel interference, interchannel interference (crosstalk), intermodulation interference, and additive white Gaussian noise (AWGN). Co-channel interference results from the finite isolation among beams that use the same frequency band. It can be reduced by carefully shaped antenna beam patterns, frequency planning, and cross-polarization. Crosstalk is caused by the spectral spreading of the modulation waveform of each channel into adjacent frequency channels. It can be reduced by a bandwidth-efficient modulation scheme like minimum shift keying (MSK) and by sufficient intercarrier frequency spacing. Extensive analysis is performed to show how to specify interchannel frequency spacings and interbeam isolation from a signal-to-noise ratio (SNR) point of view. Intermodulation interference is treated differently but also in considerable detail.

Table 1-1 contains details of the various trunking and CPS terminals. The link budgets of the CPS terminals are found in table 1-2. The weight and power budgets for a four-region and six-region CPS satellite are given in table 1-3. Table 1-4 lists the estimated costs of the CPS terminals and a four-region CPS satellite. There is no significant change for a six-region satellite

As is apparent, present Ka-band terminal costs are far too high to encourage a practical market for CPS. This is due to the large size (4.5 m for Traffic Model A) antenna system with step tracking and the full redundancy required to achieve high reliability within the limits of today's technology. In addition, the terminal incorporates several expensive up-and-down converters for multicarrier multidestination operation with several modems for the various information processing modes. Traffic Model B allows the use of simpler, non-redundant terminals with 2 m to 3 m antenna diameters, solid state high power amplifiers (HPAs) and a 4 to 6 voice channel capacity. These terminals can be made more cost effective. However, these terminals may never be as inexpensive as the C band satellite terminals being sold presently.

The need to develop system techniques and technologies for much lower cost terminals is perhaps the greatest single issue identified in this report.

Table 1-1

Definitions of Trunking and CPS Terminals

	TRUNKING				CPS		
TERMINAL TYPE	A	B	C	D	E	F	G
ANTENNA SIZE (m)	10	10	10	4.5	8.0	4.5	4.5
G/T (dB/^{o}K)	41	41	41	32.3	36.0	27.7	27.7
EIRP (dBW)	88.4	85.4	80.4	72.0	76.2	68.4	60.4
TRAFFIC (Mb/s)	548	274	87.5	12.6	33.0	5.5	0.88
VOICE (NO. 64 kb/s CHANNELS)					240	60	12
DATA (NO. CHANNELS)							
56 kb/s					20	5	1
1.5 Mb/s					2	0	0
VIDEO (NO. CHANNELS)							
56 kb/s					10	2	1
1.5 Mb/s					5	1	0
6.3 Mb/s					1	0	0
NO. TERMINALS	4	11	18	6	80	300	1824

Table 1-2

Link Budgets for CPS Terminals

Parameter	Terminal Type and Data Rate E 33.Mb/s	F 5.5Mb/s	G 0.88Mb/s
Uplink @ 30 GHz			
Ant. Size (m)	8.0	4.5	4.5
Gain (dB)	65.5	60.5	60.5
Terminal $EIRP_{eff}$ (dBW)	76.2	68.5	60.5
Path Loss (dB)	-213.0	-213.0	-213.0
Rain Loss (dB)	- 10.0	- 10.0	- 10.0
Misc. RF Losses (dB)	- 5.0	- 5.0	- 5.0
S/C Ant. $Gain_{eff}$ (dB)	48.0	48.0	48.0
S/C Noise $T_{S/C}$ (^{o}K)	1150.0	1150.0	1150.0
S/C $(G/T)_{eff}$ (dB/^{o}K)	17.4	17.4	17.4
$(C/kT)_{U.L.}$ (dB-Hz)	94.2	86.5	78.5
Margin (dB)	16.0	16.0	16.0
Downlink @ 20 GHz			
S/C $Gain_{eff}$(dB)	48.0	48.0	48.0
S/C $EIRP_{eff}$(dBW)	49.0	49.6	41.6
Rain Loss (dB)	- 4.0	- 4.0	- 4.0
Misc. RF Losses (dB)	- 5.5	- 5.5	- 5.5
Path Loss (dB)	-210.0	-210.0	-210.0
Term. Noise T_{ET}(^{o}K)	400.0	850.0	850.0
$(G/T_{ET})_{eff}$ (dB/^{o}K)	36.0	27.7	27.7
$(C/kT)_{D.L.}$ (dB-Hz)	94.1	86.4	78.4
Margin (dB)	10.0	10.0	10.0
Overall C/kT (dB-Hz)	91.1	83.1	75.1
$(E_b/N_o)_{eff}$ (dB)	16.0	16.0	16.0
Net Link Margin (dB)	3.0	3.0	3.0

Table 1-3

CPS Satellite Weight & Power Budget for Two Regional Concepts

Components or Subsystem	4 Region Satellite System			6 Region Satellite System		
	Weight/UNIT lb	Weight/TOTAL lb	Power TOTAL W	Weight/UNIT lb	Weight TOTAL lb	Power TOTAL W
Ant. System	55	220	-	55	220	-
RF Mux	2.5	10	36	2.5	15	36
IF Mux	10 ea	92	144	10 ea	138	173
Transponder	41.5	1660	3000	41.5	1660	3000
Other El. & Battery		240 -	300 250		300 -	375 250
T.T. & Contr.		40	300		40	300
Structure Mech. Therm.		200	-		200	-
Solar Array		312	196		312	196
Allowance EOL			800			800
Comm Payload		2774	5026		2885	5130
Liquid Fuel		300			300	
ap. - Per Eng.		2000			2000	
	TOTALS:	5074 lb	5026 W		5185 lb	5130 W

Table 1-4

Estimated 30/20 GHz System Costs

CPS TERMINAL COST SUMMARY

Terminal Type	E	F	G
Cost/Unit (Q=100)	$1,535K	$ $735K	$ $576.8K
(Q=1000)	--	$ $622K	$ $475.0K
Number of Sat. Term :	80	300	1824
Total Terminal Cost :	$122.80 M	$186.81 M	$866.40M
Total Ground Segment :	$ 1,176M		

CPS SATELLITE COST ESTIMATE (4 Regions)

Total Sat. Weight :	5074 lb	2283.3 kg
Transponder Weight :	44.5 lb	20.0 kg
Power DC Total :	5026 W	
Comm. Payload Weight :	2800 lb	1260.0 kg
Sat. Cost		
NRE:	$146M	
RE:	$ 49M	
Total Sat. System Cost:	Sat. Cost + Launching (two only)	
No. of Satellites (4)*:	(3 x $45) + $49M + $30M =	$214M
NRE:		$146M
Terminal Gr. Segment :		$1176M
TOTAL SYSTEM COST :		$1536M

* This quantity of satellites is based on the assumption of one separate CPS satellite and one trunking satellite (with one spare unit for each class of satellite).

In the SS-TDMA system which is a counterpart to the SR-FDMA system, only one channel per beam is active at a time and routing is achieved by steerable beams or switches in the satellite. However, this TDMA architecture is not economical for a system with many (moderate size) users. Such a system requires a high terminal effective isotropic radiated power (EIRP), a very high burst rate, and stringent waveform synchronization. These factors may increase terminal cost prohibitively.

SS-TDMA is clearly the favorite architecture for the relatively small number (less than 100) of large trunking terminals. TDMA with on-board baseband processing for CPS has also received considerable favor in the 30/20 GHz community. NASA is planning a demonstration satellite for testing the feasibility of these TDMA schemes. Based on the results of the present as well as previous MITRE studies, it is recommended that the capability to experiment with FDMA concepts also be included on the demonstration satellite. This should be possible with a moderate increase in satellite weight and power.

The conceptual design of the SR-FDMA system involves careful beam positioning, interference-free frequency planning, a regional routing technique, efficient satellite and terminal designs, realistic link margins, and detailed weight and cost analyses. Further detail on all these topics may be found in the body of this report.

Future work should emphasize FDMA techniques for lower cost terminals. On-board baseband processing would permit FDMA/TDM architectures which may be optimum for CPS applications.

SECTION 2

INTRODUCTION

This brief introduction to the FDMA study provides some background for the work, a review of the traffic models employed, a summary of the MITRE contributions, and an overview of the report.

STUDY BACKGROUND

Previous MITRE studies for NASA/Lewis Research Center (LeRC) have emphasized FDMA/TDM with on-board baseband processing for improved system flexibility and performance. At the request of NASA/LeRC, the present study examines the feasibility of FDMA/FDM with no on-board baseband processing. This decision was motivated in part by the preponderance of contractor studies and proposals and common-carrier sentiment for TDMA/TDM with on-board baseband processing or satellite switching. Only the General Electric/Space Systems Division has advocated an all FDM concept (Kiesling, 1980). Therefore, NASA/LeRC asked for another independent opinion on the feasibility of FDMA.

The GE approach was aimed at a system permitting very low cost terminals with price tags in the $20-$50K range. They felt such terminal costs were necessary to generate a sufficiently large market for Customer Premises Service (CPS). Most of the terminals considered by GE were single channel voice or data terminals with bit rates ranging from 32 kb/s to about 1 Mb/s. FDMA appears to have a better chance of achieving lower system cost for such data rates when the significantly higher burst rates and output powers required by single channel TDMA terminals in the CPS system context are considered. In addition, since burst rates are typically two or three orders of magnitude greater, TDMA generates the need for sophisticated synchronization techniques.

Present day satellite communications technology in the 30/20 GHz frequency bands is relatively underdeveloped. The foreseeable military and commercial markets for this band are somewhat limited and tend to involve trunking rather than CPS users. GE based their estimated low terminal cost on a projected mass market, presuming the heavy involvement and investment of consumer manufacturers. It is conceivable that if a potential market for CPS can be demonstrated, these manufacturers will be attracted by the prospect of meeting the demand for thousands of small earth stations.

The main hope for CPS is to reduce the cost of the terrestrial tails in present common-carrier satellite communications by providing satellite service directly to user premises. For the initial phases, at least, the customer may not own his on-site earth terminal but would lease it or pay a monthly service charge which would be included in his CPS "telephone bill." Market studies have suggested that CPS will only become viable compared to terrestrial services if the break-even distance can be reduced to no more than a few hundred miles. This means that satellite service has to become competitive with terrestrial service at shorter and shorter distances for CPS to become an attractive alternative.

Another important factor for selling telecommunication service from a common-carrier point of view is extremely high end-to-end availability. Some estimates claim that CPS could not be sold unless this availability is 0.9999. Others suggest that 0.999 is sufficient. The availability for CPS suggested by NASA/LeRC for CPS is 0.995, with 0.999 as a goal. These availabilities may be difficult to achieve at low terminal cost. Users of existing service which already provides a high availability may not be willing to sacrifice this availability at comparable cost. On the other hand, new services may well be economically attractive at considerably less availability when compared to the prospect of no service at all.

Rain attenuation is the principal factor determining link availability in the 30/20 GHz band. Dual diversity terminals for heavy trunking users, and flexible dynamic power diversity and coding schemes for smaller users under a centralized or subcentralized network control scheme are keys to successful performance in this frequency regime. Additional power and bandwidth margins must be provided in regions of CONUS experiencing more rainfall.

Comparing alternative system approaches is difficult if each approach is based on a different set of requirements. One of the major contributions of NASA/LeRC is the development of a standardized set of traffic models on which system designs can be based and fairly compared. Although these models may not be totally realistic or accurate, they represent a useful starting point for conceptual system designs and cost estimates.

The NASA traffic models were not available to GE at the time of their FDMA study. They chose to focus on relatively low data rate, single-channel terminals where FDMA has an excellent chance of success. In the present study MITRE adhered closely to the NASA-supplied traffic models throughout the course of the work. During this effort, it became clear that, because the traffic models are so

ambitious, FDMA is not necessarily superior to TDMA, if reasonable projections for satellite technology in the 30/20 GHz bands are assumed. On the other hand, it appears that FDMA is a competitor to TDMA, even with the postulated heavy mixtures of high data rate multichannel terminals.

NASA plans to launch a 30/20 GHz CPS/trunking demonstration satellite in 1987. The architecture currently favored by the community involved appears to be TDMA with on-board baseband processing and radio frequency/intermediate frequency (RF/IF) switching. If FDMA is indeed a viable alternative, NASA does not wish to preclude the feasibility of demonstrating FDMA concepts. However, budget constraints impose a limitation of one demonstration satellite. Thus, in any experimental joint flight of TDMA and FDMA 30/20 GHz technology, satellite hardware should be shared as much as possible between the TDMA and FDMA portions. An economical way of including the MITRE FDMA concept in a satellite primarily intended to demonstrate TDMA is suggested in section 9.

TRAFFIC MODELS

Two traffic models were supplied by NASA: Traffic Model A and Traffic Model B. The original Traffic Model A was based on three types of trunking terminal and three types of CPS terminal. A fourth type of trunking terminal was added to traffic Model A after the MITRE work was underway. Both versions of Model A were used, so not all the examples are self-consistent. However, there are no major differences and the final system designs are based on the more recent model.

Traffic Model B is similar to Traffic Model A. The total capacity for Traffic Model B is the same as that for Traffic Model A. The principal differences are in the larger number of terminals, their smaller sizes, and their distribution at greater distances from the major cities. In Traffic Model B there are six types of CPS terminal with lower data rates and fewer channels per terminal. The smallest terminal has a single 64 kb/s voice channel. There are approximately 45 major cities listed in the CPS traffic models. In Traffic Model A, the terminals are essentially confined to these cities. In Traffic Model B, they are distributed roughly in proportion to population based on the 277 Standard Metropolitan Statistical Areas (SMSAs) in CONUS (Census, 1979).

The MITRE study was mainly concerned with CPS to CPS traffic but some attention was paid to intercommunication between CPS and trunking users. There was no requirement to consider trunking to trunking users except to assume that the trunking to trunking

service would be handled by the same satellite. In order to deal adequately with the interface between CPS and trunking, the trunking to trunking traffic model was also provided. Only 18 metropolitan centers require trunking in the NASA-supplied traffic model. The trunking traffic and CPS Traffic Models A and B are summarized in tables 2-1 through 2-3. Under NASA/LeRC guidance, a 50% duty factor was assumed for CPS traffic only. This is interpreted to mean that half the CPS terminals are operating at full capacity during the peak busy hour.

Table 2-1

Trunking Terminal to Trunking Terminal Traffic Generated by Major Metropolitan Centers

Population Center	Total Peak Hour Traffic (Mb/s)
New York	968
Washington, DC	639
Los Angeles	560
Chicago	560
Detroit/Cleveland	484
San Francisco/Sacramento	484
Boston/Hartford	484
Cincinnati/Columbus	320
Houston	242
Dallas	242
Minneapolis/St. Paul	154
Miami	154
St. Louis	154
Pittsburgh	154
Atlanta	154
Denver	100
Kansas City	100
Seattle	100
Total:	6053

MITRE CONTRIBUTIONS

The principal MITRE contribution in this study has been to show that 75% of the NASA traffic models can be satisfied with an FDMA satellite that consumes approximately 6 kW of DC power and weighs approximately 6200 lb. The satellite would consume about 5 kW of

Table 2-2

Definition of Terminals

A. Trunking Terminals for CPS Traffic Models A and B

Type	Number	Total Data Rate (Mb/s)
A	4	548
B	11	274
C	18	87.5
D	6	12.6

B. CPS Terminals for CPS Traffic Model A

			Number of Channels					
			Video			Data		Voice
Type	Number	Total Data Rate (Mb/s)	6.3 Mb/s	1.5 Mb/s	56 kb/s	1.5 Mb/s	56 kb/s	64 kb/s
E	80	33.84	1	5	10	2	20	240
F	300	5.564	0	1	2	0	5	60
G	1824	0.88	0	0	1	0	1	12

C. CPS Terminals for CPS Traffic Model B

			Number of Channels					
			Video			Data		Voice
Type	Number	Total Data Rate (Mb/s)	6.3 Mb/s	1.5 Mb/s	56 kb/s	1.5 Mb/s	56 kb/s	64 kb/s
E	200	9.944	1	1*	2	1*	2	30
F	600	1.988	0	1*	1	1*	2	5
G	1600	0.696	0	0	0	0	1	10
H	1600	0.432	0	0	1	0	1	5
I	2400	0.320	0	0	0	0	0	5
J	3600	0.064	0	0	0	0	0	1

* One 1.5 Mb/s Video or Data Channel but not both.

Table 2-3

Distribution of Terminal Types for Traffic Model A

	Terminal Types						
	Trunking				CPR		
	A	B	C	D	E	F	G
New York	1	2	-	-	3	12	140
Detroit	-	1	-	-	2	8	60
Cleveland	-	1	-	-	-	2	22
San Francisco	1	-	-	-	1	7	50
Boston	-	1	-	-	1	5	35
Buffalo	-	-	-	-	3	6	30
Milwaukee	-	-	-	-	6	11	44
Indianapolis	-	-	-	-	6	11	44
Greensboro	-	-	-	-	5	8	44
San Diego	-	-	-	-	5	7	40
Phoenix	-	-	-	-	5	7	40
Tampa	-	-	-	-	5	7	40
Portland	-	-	-	-	5	6	34
Salt Lake City	-	-	-	-	5	6	34
Lansing	-	-	-	-	2	6	40
Harrisburg	-	-	-	-	2	6	40
New Orleans	-	-	-	-	2	6	40
Norfolk	-	-	-	-	-	9	20
Syracuse	-	-	-	-	-	9	20
Oklahoma City	-	-	-	-	-	9	20
Nashville	-	-	-	-	-	9	20
Fresno	-	-	-	-	-	4	32
San Antonio	-	-	-	-	-	4	32
Louisville	-	-	-	-	-	4	32
Memphis	-	-	-	-	-	4	32
Omaha	-	-	-	-	-	4	32
Jacksonville	-	-	-	-	-	4	32
[illegible]ington, DC	-	1	1	-	2	6	75
Los Angeles	1	-	1	-	4	7	80
Chicago	1	-	1	-	4	7	80
Cincinnati	-	1	-	-	0	2	30
Houston	-	1	-	-	2	9	60
Dallas	-	1	-	-	2	6	40
Minneapolis/St Paul	-	-	2	-	1	6	40
Miami	-	-	2	-	1	6	40
St. Louis	-	-	2	-	0	10	30
Pittsburgh	-	-	2	-	0	10	30
Atlanta	-	-	2	-	0	9	30
Denver	-	-	1	2	0	9	30
Kansas City	-	-	1	2	0	6	30
Seattle	-	-	1	2	0	6	30
Hartford	-	1	-	-	-	2	15
Rochester	-	-	-	-	3	5	30
Columbus	-	-	1	-	2	7	30
Philadelphia	-	1	1	-	1	6	75
Totals:	4	11	18	6	80	300	1824

power and would weigh approximately 5200 lb without the trunking to trunking portion.

The MITRE system concept is unique in suggesting a regional approach to the organization of multiple beams. This greatly simplified the satellite design by saving filters, mixers, and switches.

This work on FDMA has generated some insight into the proper system approach. The fundamental FDMA concept of greatest potential is the interbeam satellite routing of distinct bandwidths, with each bandwidth containing many individual channels. Each channel reaches its destination independently of other channels by means of proper frequency assignment on the ground, based on network control instructions. This is in sharp contrast to the TDMA approach, which requires satellite switching. Although some switching is useful on an FDMA satellite, primarily to implement daily or longer-term changes in traffic demand, the FDMA approach essentially requires no switching at all. Therefore, satellite routed FDMA (SR-FDMA) is a more accurate description than satellite switched FDMA (SS-FDMA). Again, it is not the individual channels which are routed by the satellite but relatively large chunks of bandwidth each containing many channels. It will be useful to keep this vision in mind throughout this report for a better understanding of SR-FDMA. These notions are defined further in the next section.

During this work, MITRE has developed a useful methodology for deriving an efficient frequency plan from a non-uniform traffic model and a postulated beam plan. This methodology is sufficiently well-defined to be programmed on a computer.

Another significant aspect of the MITRE effort is in the area of terminal cost. Realistic cost models have been applied to present 30/20 GHz technological efforts of commercial and military manufacturers. These cost models are in close agreement with industry-quoted figures for terminal costs. The models cost each major cost-driving subsystem in proportion to the total hardware cost, and the total hardware cost is calculated to be in proportion to the overhead cost. About 50% of the total hardware cost of most current satellite terminals is due to the antenna and transmitter (if a tracking antenna is required). The up-down converters constitute around 15% to 20% of the total hardware cost and the modems constitute about 5% to 20%. All cost figures in this report are in 1980 dollars and the cost model was revised in 1979. All cost model inputs for the data base are derived from manufacturers' cost data gathered by MITRE between 1976 and 1980, and are applicable only to specific technologies. If an alternate lower cost technology can be applied to a specified task or subsystem, the

overall terminal cost is reduced in proportion to that subsystems contribution to the total terminal cost (including overhead). In order to achieve a substantial overall cost reduction, all hardware costs (including assembly costs) must be reduced simultaneously.

The costing methods used by MITRE are described in detail in section 10. However, in a brief summary, the cost analysis procedure works as follows: first, the subassembly unit costs are either computed from a model (based on manufacturer supplied data) or based directly on quotes if the model is not available or not applicable to a specific unit or task. The total hardware cost includes: the antenna, transmitter, low noise amplifier (LNA), up-down converters, frequency synthesizers, and modems. This total hardware cost is then used in several K-factor multiplication calculations to derive the cost of assembly, integration, test engineering, quality control, management, administration, and profit. The total sum of all the above contributions is the cost of the first production terminal. When this cost is applied to a learning curve (both industry and MITRE use a 95% learning curve), it becomes reduced during production. Therefore, an N quantity of terminals yields an Nth unit cost. The equation for the average cost computation in section 10 is a mathematical model used to approximate the summation of N quantity costs and supports a cost calculation in a simple algebraic form for any N quantity and X learning curve. The accuracy of this approximation is well within 0.1%.

This conservative view of system cost is offered to temper overly optimistic expections for low cost terminals capable of generating a large CPS market. It seems clear from the following estimates that the cost of 30/20 GHz terminal technology must be reduced dramatically.

The estimated total CPS system cost is approximately $1.5B for Traffic Model A. Satellite cost is in the neighborhood of $400M, including launch and non-recurring engineering costs. Thus, too much of the cost is in the terminals which range in price from $300K to $700K each. Present technology does not permit 30/20 GHz terminal costs below $100K (based on manufacturer quoted costs in 1980 dollars) for the types of high data rate, multichannel terminals postulated in Traffic Model A. Even the 64 kb/s single channel terminal of Traffic Model B is too expensive.

Satellite weight, power, and cost are only slightly larger for Traffic Model B. Individual terminal costs are reduced to about $250K for the smallest single channel terminals. However, since there are 10,000 terminals in this model, the total system cost exceeds $5B with near-term 30/20 GHz technology projections. Since

TDMA terminals are generally more expensive than FDMA terminals, and because of the large number of terminals, the cost of a TDMA system for Traffic Model B would be even higher.

OVERVIEW OF REPORT

Section 3 presents the basic ideas of SR-FDMA system operation with respect to user connectivity by means of simplified terminal and satellite functional block diagrams. Multiple beam patterns, interbeam isolation, and frequency reuse are explored in section 4. The advantages of a larger number of smaller beams for reducing spacecraft power and serving more users are pointed out. A sandwich construction for implementing a more compact spacecraft antenna system is suggested.

Section 5 covers modulation and coding. A carrier-to-interference analysis is performed for constant-envelope, offset-quadrature modulations such as MSK and co-channel, cross-channel, and receiver interference. An optimization of residual rain margins is performed. Rate 1/2 codes are suggested. Intermodulation interference is analyzed in section 6. The effect of strong and weak centrally located carriers within a satellite RF/IF frequency band is examined. Carrier-to-intermodulation (C/IM) interference behavior as a function of output power backoff in a non-linear high power amplifier is reviewed. The relationship between satellite and terminal C/IM ratios is explained.

Section 7 outlines a general methodology for determining frequency allocation by beams for SR-FDMA, after showing the infeasibility of full switching for the specified traffic model. A discussion of channel blocking within a satellite (RF/IF bandwidth is provided. The network control and technical aspects of power diversity schemes to mitigate rain are discussed in section 8.

Critical spacecraft technologies for SR-FDMA are discussed in section 9. The main issue is spacecraft antenna implementation for realizing sufficient interbeam isolation. Because of the regional system concept, filtering and switching technologies are relatively unstressed. A concept for including SR-FDMA on a demonstration satellite is also presented in this section.

Preliminary system design efforts for handling the traffic models are documented in section 10. The numbers of transponders required for specific candidate beam plans are computed. The state-of-the-art of solar cell array power generation and power conversion efficiencies are discussed. An estimate of satellite power required to support the trunking to trunking users is provided. The terminal

and satellite cost models used in deriving estimated system costs are defined.

Section 11 contains two recommended baseline system designs, one for each of the traffic models provided by NASA. This section is the culmination of the study and reflects all the work discussed in other sections of the report. The major conclusions of the study are accumulated in section 12.

There are five appendixes. Appendix A compares FDMA and TDMA with respect to burst rate and transmitter power requirements. Appendix B discusses the issues of where CPS-trunking traffic interconnection should be accomplished, in the satellite or on the ground. Appendix C contains an alternative SR-FDMA system that does not use the regional approach. Appendixes D and E discuss surface acoustic wave (SAW) filter technology and solid state switch technology, respectively.

References are listed at the end of the section in which they are cited. A glossary is provided at the end of the report.

REFERENCES

(Census, 1979) Statistical Abstract of the United States: 1979, 100th edition, U. S. Bureau of the Census, Washington, DC, 1979, pp. 2, 17-26.

(Kiesling, 1980) J. D. Kiesling, "Study of Advanced Communications Satellite Systems Based on SS-FDMA," Document No. 80SDS4217, Contract No. NAS-3-21745, Philadelphia, PA: General Electric/Space Division, Valley Forge Space Center, May 1980.

SECTION 3

GENERIC SR-FDMA SYSTEM DESCRIPTION

The fundamental ideas for understanding satellite routed (SR)-FDMA communication system concepts are presented. A simple example is used for clarity.

SYSTEM ELEMENTS AND DEFINITIONS

A user consists of one active data source which employs one data channel. An earth station or terminal serves several users and accesses the satellite for each user individually. The terminal consists of an antenna, a transmitter, and several modems, one for each user class. The frequencies of transmission and reception for each modem are determined by a control center. Since there are many terminals, the earth station must be as inexpensive as possible.

The satellite consists of multi-beam antenna arrays, multiplexers (signal splitters which use filters passing different frequency bands), and high power transmitters. The multiplexers channel the signals received by a receive antenna to a transmit antenna for transmission. Although there are no switches on the satellite (no switching matrices) in the most fundamental concept, the satellite is large and relatively expensive.

Either the satellite or one large earth station could serve as a control center which assigns the transmit and receive frequencies to each user. A narrow frequency band called an orderwire channel is used for special communications between the earth stations and the control center through the satellite. An earth station requests and receives frequency assignments for its users over the orderwire channel. A users' matrix represents statistical data specifying the long term connectivity of users among beams. The users' matrix determines the bandwidth of each filter comprising the satellite multiplexer. This information is also stored in the control center computer.

The frequency plan consists of the frequency bands assigned to all users and must satisfy the compatibility requirement that only users which are sufficiently isolated in space or time may use the same frequency. The frequency plan can be obtained from the users' matrix in a procedure described below.

Antenna beam isolation permits frequency reuse and therefore increases the system capacity. Beams which are sufficiently far apart may use the same frequency with tolerable co-channel interference. This is explained in more detail in section 4.

COMMUNICATIONS NETWORK CONNECTIVITY EXAMPLE

This example shows how to design the satellite multiplexer and how the system works. Suppose an uplink beam and a downlink beam service the same area on the earth. The uplink beam is designated with an upper case letter, and the downlink beam is designated with the same letter in lower case form. Either the upper or lower case form of the letter identifies the area.

Figure 3-1 shows part of a users' matrix; the element in row one, column three (A,c) = 2 means that, on the average, two users from area A transmit to two users of area c. However, for duplex traffic the same number of users in C transmit to a, so (C,a) = (A,c), i.e., the users' matrix is symmetrical.

In the simplest example, the antenna beam footprints areas form a row of circles, as shown in figure 3-2. The purpose of frequency reuse (by means of multi-beams) is to employ the same frequency band by as many users as possible with acceptably low interference (co-channel interference) between users. In this example there are four coverage areas, and acceptable isolation between beams two or more beamwidths apart is assumed; such beams can therefore use the same frequency. All beams which can use the same frequency have the same shading, as illustrated in figure 3-2.

The eight-frequency plan for the connections shown in figure 3-2 is plotted in figure 3-3A. All the elements of the first row and column of figure 3-1 are satisfied except (B,a) = 1. There is double frequency reuse because two users employ the same frequency. Note that both the uplink and the downlink beams are sufficiently isolated for each frequency assignment. Without loss of generality, the above frequency plan can be rearranged as shown in figure 3-3B. Multiplexers for these two frequency plans are now compared.

Multiplexer Design

Consider the frequency plan shown in figure 3-3A. The entry in the first row and column defines the need for a filter passing frequency f_1, whose input is connected to uplink (receive antenna) A and whose output is connected to downlink (transmit antenna) a. Another filter passing f_1 connects antennas D and d, etc. The resulting transponder is drawn in figure 3-4A. Since the frequency

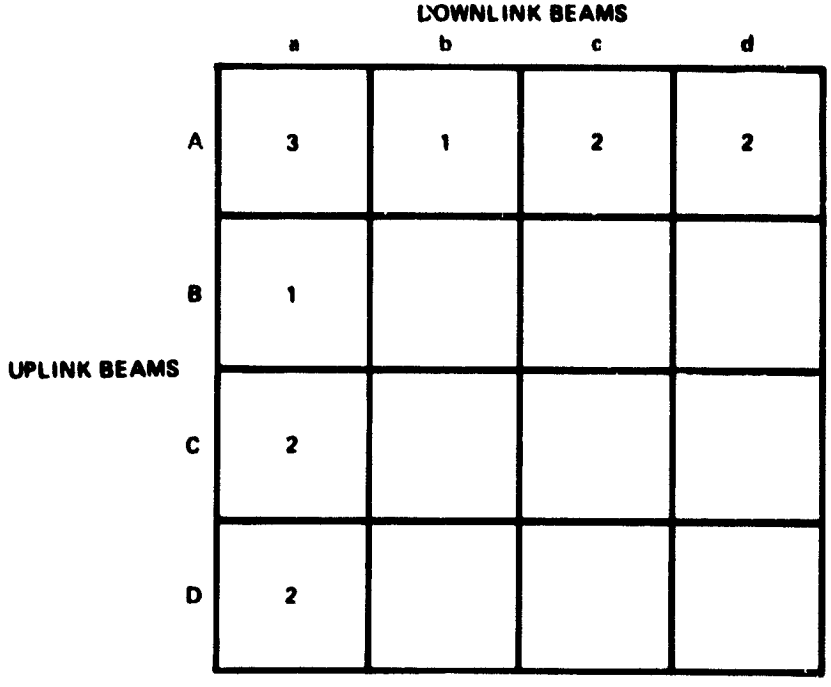

IA-88,428

Figure 3-1. Users Matrix

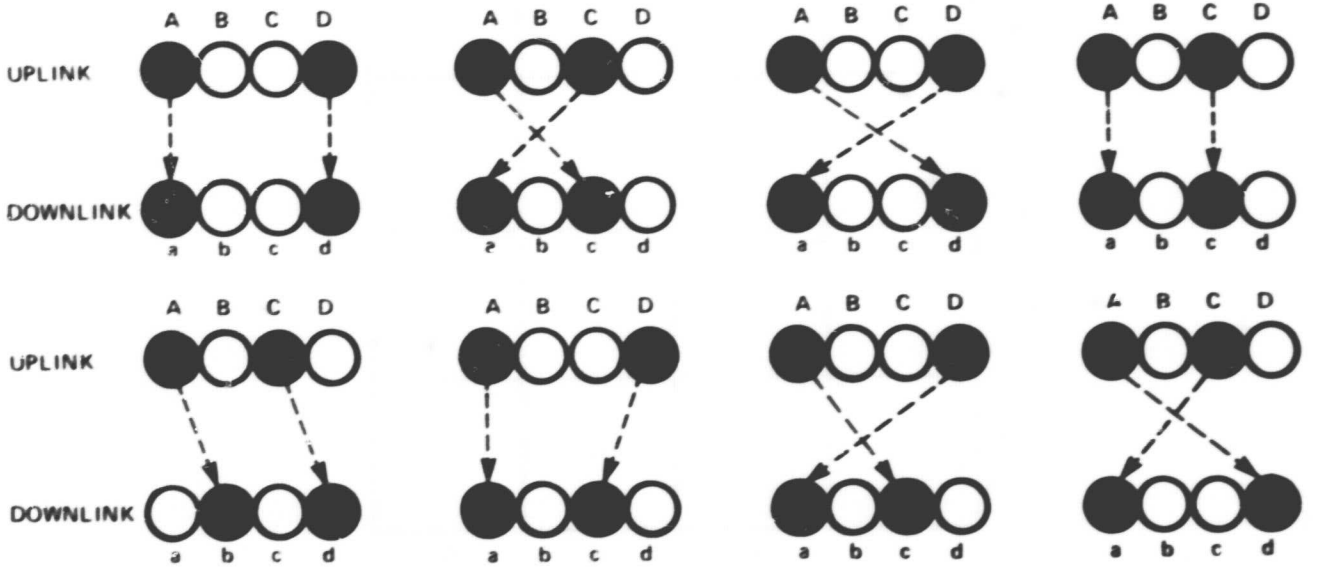

Figure 3-2. Some Permissible Beam Connections on the Same Frequency

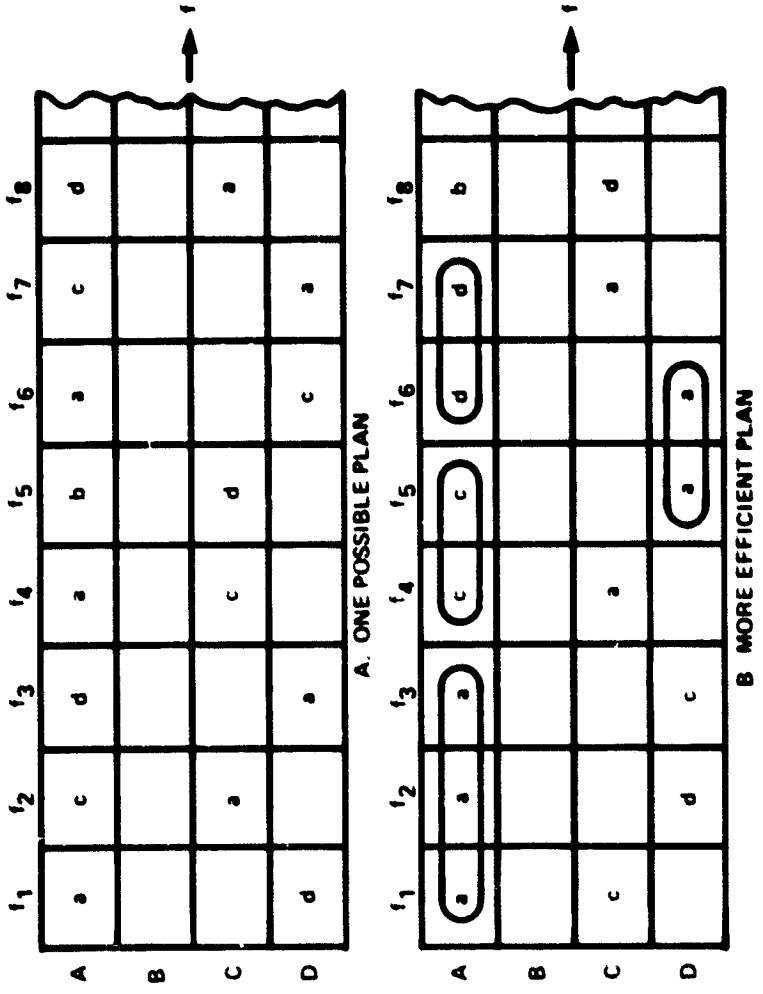

Figure 3-3. Equivalent Frequency Plans

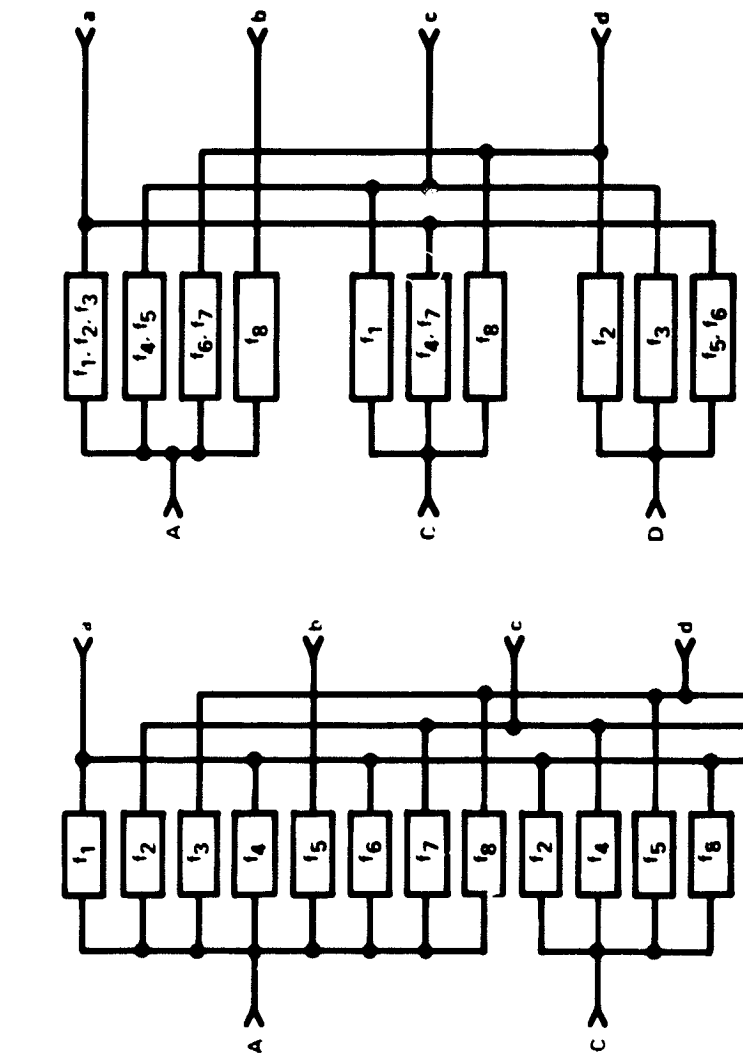

B TRANSPONDER FOR FIGURE 3-3B.

A TRANSPONDER FOR FIGURE 3 3A

Figure 3-4. Corresponding Multiplexer Realizations

IA-60,413

plan of figure 3-3B allows grouping of adjacent frequencies in the same downlink beam, the corresponding transponder of figure 3-4B has fewer filters.

Row A gives the filters in the multiplexer connected to receive antenna A, etc. The appropriate outputs are summed by means of combiners into the corresponding transmit antennas. Multiplexers are much more difficult to design than combiners.

System Operation

System operation is explained with reference to the frequency plan shown in figure 3-3A and its multiplexer shown in figure 3-4A. A user of an earth station located in beam A that wants to transmit to area d is assigned frequency f_3. (A subsequent reply from D to a is assigned f_7. While (A,d) uses f_3, the same frequency can be used between other users from D to a.) If another user in beam A wants to transmit to b, he is assigned a transmit frequency f_5, etc., as depicted in figure 3-5.

The satellite multiplexer of figure 3-4A does the routing between uplink and downlink antennas. No satellite switching is required. An appropriate transmit frequency on earth ensures that the transmission arrives at the right destination.

Multiplexer Implementation

The multiplexers in the satellite are difficult to implement directly at 20 or 30 GHz on a beam basis because the small percentage bandwidths of the filters require very high quality factors. Therefore, filters will be implemented at conveniently chosen intermediate frequencies (IFs) by using up and down convertors as sketched in figure 3-6A.

Another possibility is to implement the multiplexers with mixers and IF bandpass filters (BPFs) as shown in figure 3-6B. All BPFs are centered at the same IF and may even have the same bandwidth if the traffic is uniformly distributed. The IF frequency may be chosen in the region where surface acoustic wave (SAW) filters are feasible.

The local oscillator (LO) frequencies f_{LO1} and $f_{LO1'}$ are offset by the same amount in all filter channels. The LO frequencies are chosen so that only the appropriate input signals are routed to the desired destination via the bandpass filters. The LO frequencies are essentially fixed, making the satellite synthesizer design quite

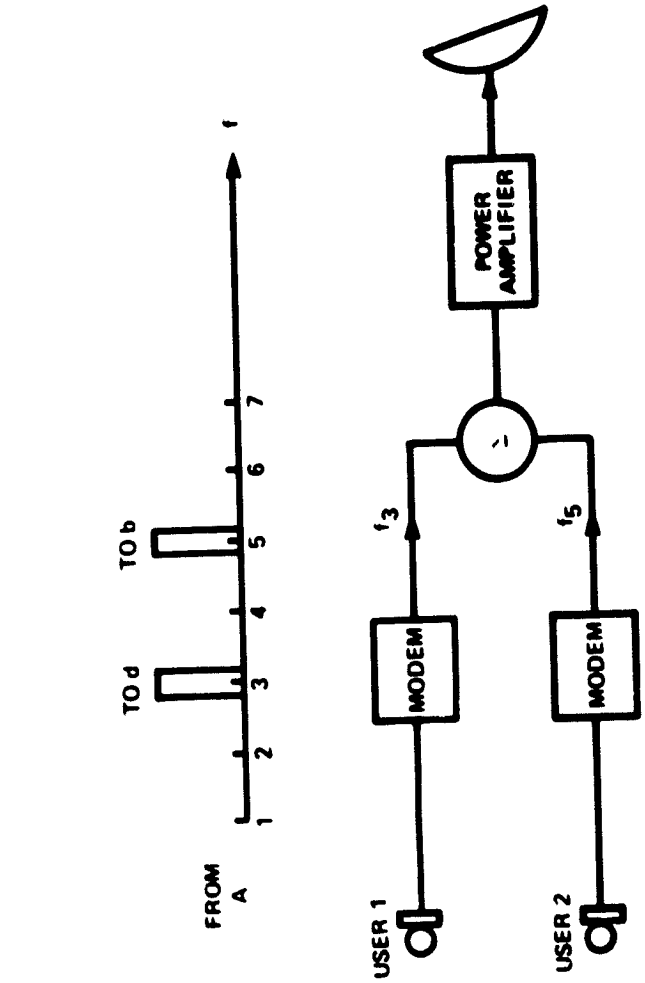

Figure 3-5. Earth Station in Beam A

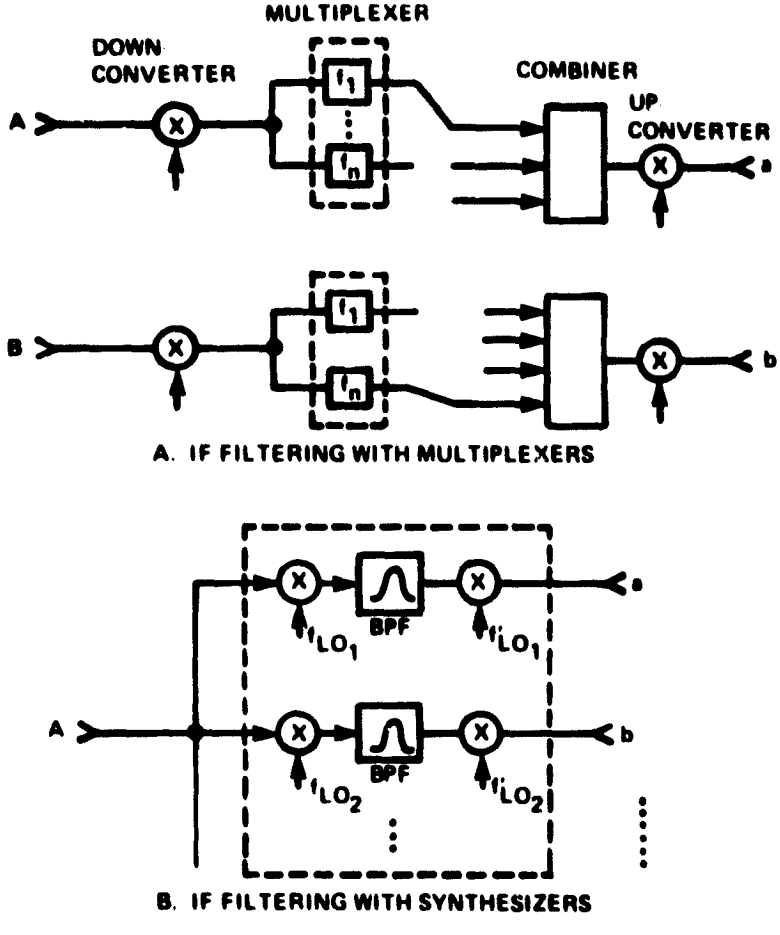

Figure 3-6. Multiplexer Implementations

reasonable. However, if they can vary, system flexibility in reconfiguring the satellite to handle long-term variations in traffic is achievable. Synthesizer switching speed is not an issue in this context.

SECTION 4

MULTIPLE BEAMS

The theory of multiple beam patterns, interbeam isolation, and frequency reuse is discussed. Implications for the spacecraft realization of on-board power and multiple beam antennas are developed.

BEAM PATTERNS

Assume that the coverage of a single beam cell is defined by the area where the received signal does not vary by more than X(dB) of the peak gain, where X is a constant in the 3 to 6 dB range. The coverage area of the cell is enclosed by the X(dB)-down contour; see figure 4-1. The -X(dB) contours touch each other and form a multiple beam pattern of cells.

If adjacent cells use the same frequency, significant signal interference will generally result. However, cells which are farther away may use the same frequency with some tolerable level of mutual interference. The situation can be visualized by coloring (selecting designs for) the cells; all cells using the same frequency will be of the same color. Figure 4-2 shows example rectangular arrays of cell patterns for several values of the number of colors (designs), N. If the angular separation between the centers of adjacent cells is θ_o, then, from figure 4-2, it would appear that the shortest distance between cell centers of the same color is

$$d_1 = \sqrt{N}\,\theta_o \tag{4.1}$$

and the next shortest distance is

$$d_2 = \sqrt{2N}\,\theta_o \tag{4.2}$$

The separation θ_o corresponds to the X(dB) beamwidth contour.

Beam Isolation

If d is the angular distance between the centers of two beams, and if $G(\theta)$ denotes the gain of each singlet beam as a function of beamwidth θ_o, then the isolation between the beam patterns of figure 4-3 is defined as

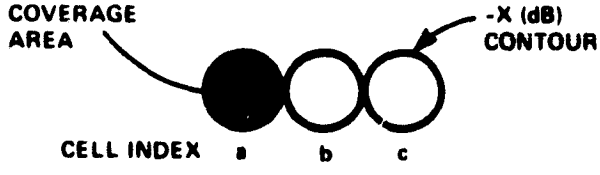

A. COVERAGE PATTERN

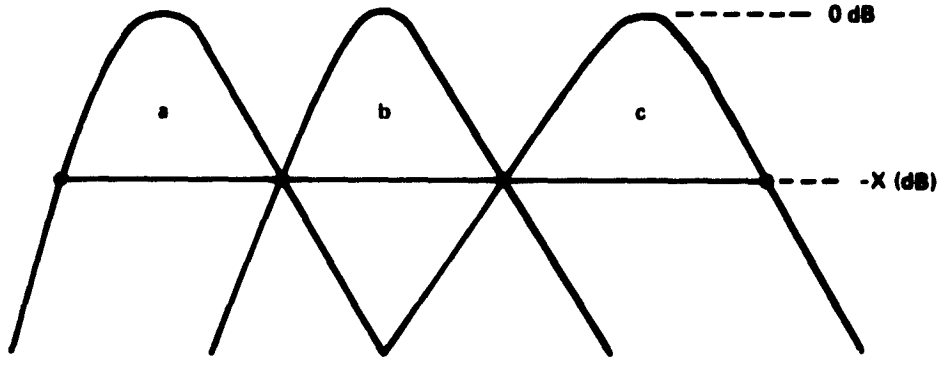

B. GAIN VERSUS FREQUENCY

IA 60,427

Figure 4-1. Definition of Multiple Beam Cells

A. DEFINITIONS

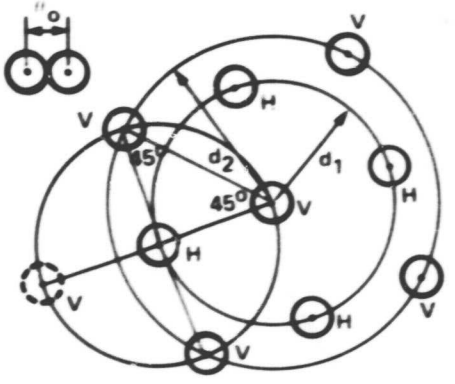

θ_o: ANGULAR SEPARATION BETWEEN CENTERS OF ADJACENT CELLS

V: VERTICAL POLARIZATION

H: HORIZONTAL POLARIZATION

d_1: MINIMUM DISTANCE BETWEEN CELL CENTERS OF THE SAME COLOR (DESIGN)

d_2: NEXT TO MINIMUM DISTANCE BETWEEN CELL CENTERS OF THE SAME COLOR (DESIGN)

B. N = 4

$d_1 = 2\theta_o = \sqrt{4}\,\theta_o$

$d_2 = \sqrt{8}\,\theta_o$

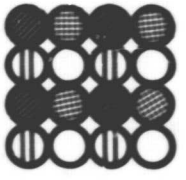

C. N = 5

$d_1 = \sqrt{5}\,\theta_o$

$d_2 = \sqrt{10}\,\theta_o$

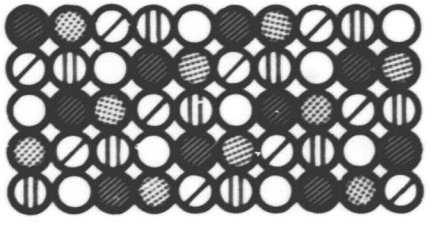

D. N = 10

$d_1 = \sqrt{10}\,\theta_o$

$d_2 = \sqrt{20}\,\theta_o$

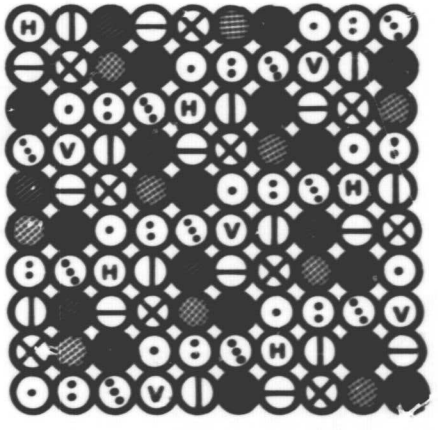

Figure 4-2. Rectangular Arrays of Circular Cell Patterns

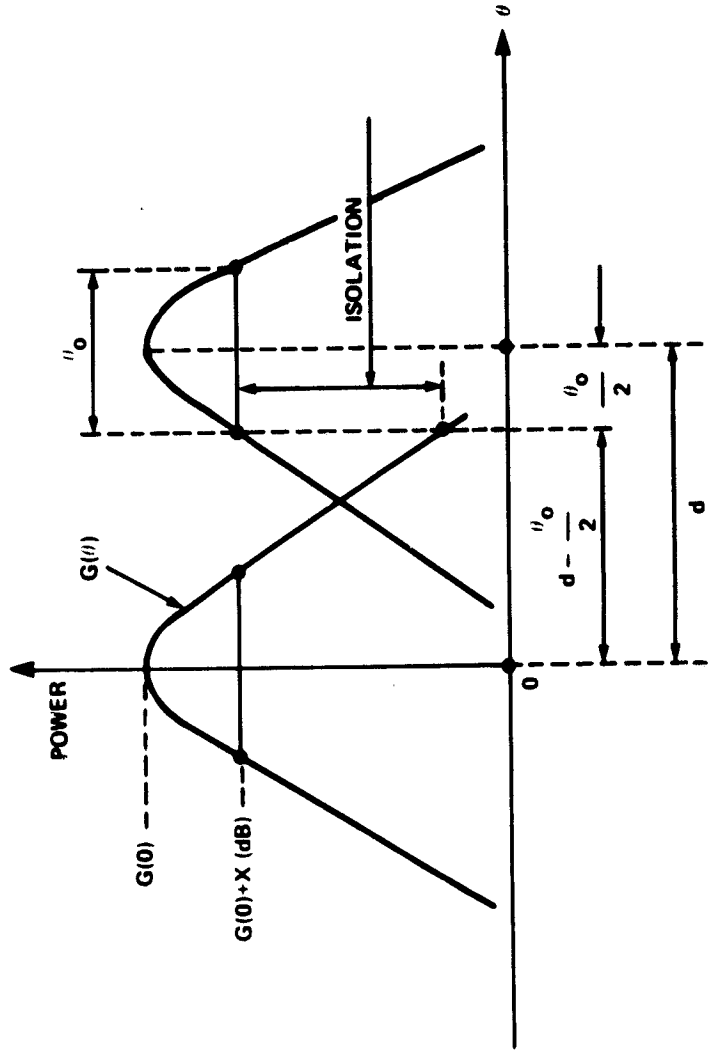

Figure 4-3. Inter-Beam Pattern Isolation

IA-60.423

$$I(d) = \frac{G(\theta_o/2)}{G(d-\theta_o/2)} \quad \text{or} \quad I(d) = G(o) + X - G(d-\theta_o/2) \text{ in dB} \tag{4.3}$$

For example, if X = -3 dB, and if the singlet beam pattern is described by

$$G(\theta) = \frac{1}{1 + (2\theta/\theta_o)^{2.5}} \tag{4.4}$$

then,

$$I(d_1) = 10 \log \left[1 + (2\sqrt{N}-1)^{2.5}\right] - 3 \text{ (dB)} \tag{4.5a}$$

and

$$I(d_2) = 10 \log \left[1 + (2\sqrt{2N}-1)^{2.5}\right] - 3 \text{ (dB)}. \tag{4.5b}$$

Table 4-1 gives $I(d_1)$ and $I(d_2)$ as a function of the number of colors, N.

Table 4-1

Isolations for Rectangular Cell Arrays

N	4	5	6	7	8	9	10
$I(d_1)$ (dB)	9.2	10.7	11.9	12.9	13.8	14.6	15.2
$I(d_2)$ (dB)	13.8	15.2	16.4	17.3	18.2	18.9	19.5

Cross-Polarization

Cross-polarization may increase the isolation. However, according to figure 4-2A and figure 4-2D, cross-polarization increases only $I(d_1)$ and does not affect $I(d_2)$. Therefore, $I(d_2)$, given in the bottom row of table 4-1, is the highest isolation attainable with rectangular arrays of cells for a given number of colors, N and 3-dB down cell contours. $I(d_2)$ can be increased by two means:

1. increasing N; however, this reduces the frequency reuse, as shown below;

2. shaping the singlet beam to obtain a faster roll-off than the radiation pattern given by equation (4.4).

Frequency Reuse

Multiple beam satellite antennas allow:

1. earth terminals to have lower values of effective isotropic radiated power (EIRP) and gain to noise temperature ratio (G/T), which is very desirable for small earth stations;

2. frequency reuse.

Two links will operate with acceptably low mutual interference on the same frequency if the isolation between them is sufficiently large. If the allocated bandwidth for a particular satellite system is B, frequency reuse increases the effective bandwidth to FB; F is the frequency reuse factor defined as

$$F = M/N \tag{4.6}$$

where M is the number of beams, and N is the number of colors or disjoint frequency bands.

F should be as large as possible, i.e., for fixed M, N should be as small as possible. However, as has been shown, a small N means less isolation between the beams.

The number of frequency bands, N, imposed by the beam isolation, will also depend on the system requirements. These, in turn, will be determined by the desired link quality and the type of modulation, since some modulations are less susceptible to co-channel interference.

Example

Suppose that the number of beams is chosen as M = 50, and that a beam isolation of at least 15 dB is required. From table 4-1, $I(d_1)$ = 15.2 dB for N = 10 and $I(d_2)$ = 15.2 dB for N = 5. This means that without additional cross-polarization isolation, N = 10 frequency bands are needed. The frequency reuse factor then will be F = 50/10 = 5. Such a system will have five times the effective bandwidth of a system without multiple beams. If cross-polarization is used, F = 50/5 = 10.

Table 4-1 illustrates that the capacity of the system (effective bandwidth, or number of users) can at most double when cross-polarization is employed for rectangular cell arrays, regardless of the level of isolation due solely to polarization diversity. This can also be seen directly from equation (4.5).

CLOSE-PACKED CIRCULAR CELL ARRAYS

Consider the four-color example of figure 4-4 where the cells are packed close together to reduce gaps in coverage above the X(dB)-down gain level. As shown in figure 4-4A, the smallest distances between cells of the same color are now only

$$d_1 = \sqrt{3}\ \theta_o \qquad (4.7a)$$

$$d_2 = 2\ \theta_o \qquad \text{(close packed; N = 4)} \qquad (4.7b)$$

$$d_3 = \sqrt{7}\ \theta_o \qquad (4.7c)$$

where θ_o is the single cell beamwidth. This means that the isolation between beams will be slightly less than in the rectangular array. If cross-polarization is used as in figure 4-4B, then typically d_3, the shortest distance between cells of the same frequency band and polarization, will determine the minimum interbeam isolation.

A non-symmetrical array like that of figure 4-5 may be needed to achieve a specified isolation. However, this cell pattern would require two more colors.

Both of the preceding beam/frequency plans are superior to beam plan 5 of the GE report (Kiesling, 1980). The figure 4-4 configuration provides twice the bandwidth with the same minimum co-polarized interbeam isolation, while figure 4-5 achieves a better minimum isolation with one-third more bandwidth.

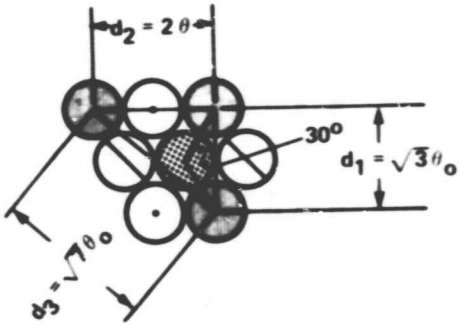

A. BASIC CLUSTER

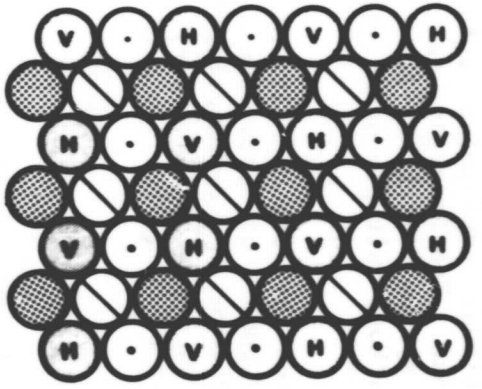

B. LARGER ARRAY

Figure 4-4. Close-Packed Circular Cell Four-Color Configurations

GE Beam Plan Number 5

GE has proposed a composite beam method of uniformly covering the continental United States (CONUS) with sixty eight 0.5° degree cells and eight disjoint frequency bands. A western section of the GE plan is sketched in figure 4-6. Uncircled integers represent frequency band assignments with one polarization and circled integers represent bands with the other polarization. A composite beam area, indicated by a heavy outline in the figure, consists of a close-packed cluster of four cells containing a given frequency band, number 8 in this case, of the same polarization. These composite beams are overlapped so that four frequency bands are assigned to each cell. For uniformly distributed users each cell must share every band with three other cells of the corresponding cluster. This means that each cell has access only to one-eighth the total bandwidth.

The minimum distances corresponding to equation (4.7) are indicated in figure 4-6. The smallest distance d_1 is only $1/\sqrt{3} = 0.577$ that of figure 4-4. This means that greater reliance must be placed on cross-polarization isolation because adjacent cells use the same frequency band in this GE plan. Isolation due to polarization alone is limited to roughly 20 dB at 30/20 GHz; signals at these frequencies will tend to depolarize in heavy rain (Arnold, et al., 1980). The next smallest distance d_2 is $\sqrt{3}/2 = 0.867$ that of figure 4-4 but cross-polarization is again involved. The smallest distance with co-polarization is the same in both plans. This is the critical isolation distance since additional cross-polarization isolation is not available in this case. The beam plan in figure 4-4 achieves twice the frequency reuse of figure 4-6 because only four frequency bands are used. Inspection of figure 4-5 reveals a plan which improves the interbeam isolation with one-third more bandwidth than the GE plan.

If adjacent frequency bands are numbered sequentially, the GE plan of figure 4-6 also has the apparent drawback of adjacent co-polarization bands in adjacent cells. Although not shown here, it is possible to number the bands of figures 4-4 and 4-5 in such a way that adjacent bands in adjacent cells are cross-polarized for greater isolation against crosstalk interference. This idea is applied to the extent possible in the sample beam/frequency plan for the eastern United States shown in figure 4-7.

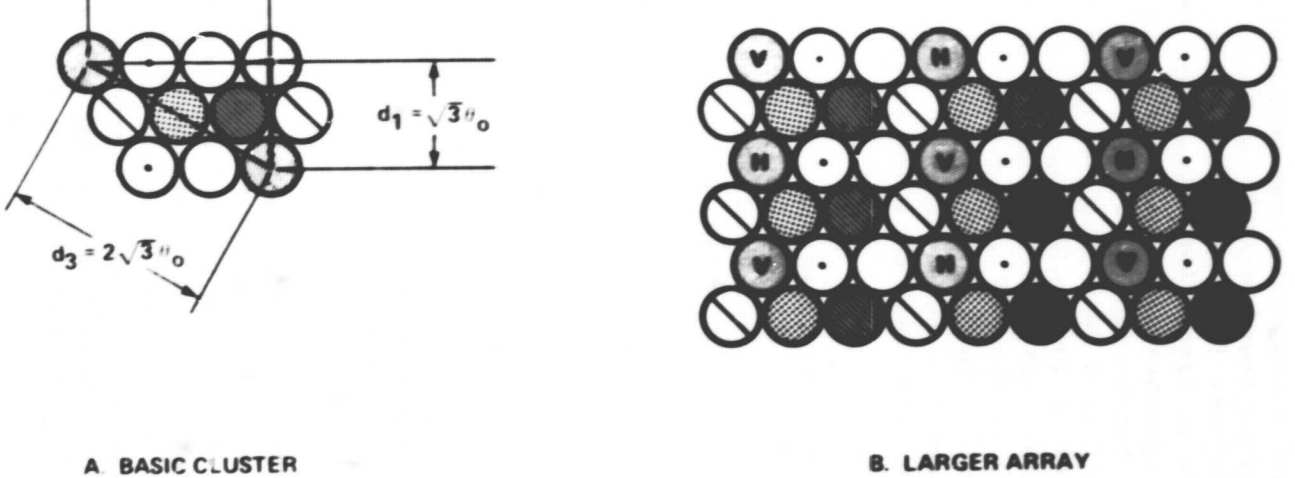

A. BASIC CLUSTER

B. LARGER ARRAY

Figure 4-5. Close-Packed Circular Cell Six-Color Configurations

IA-60,907

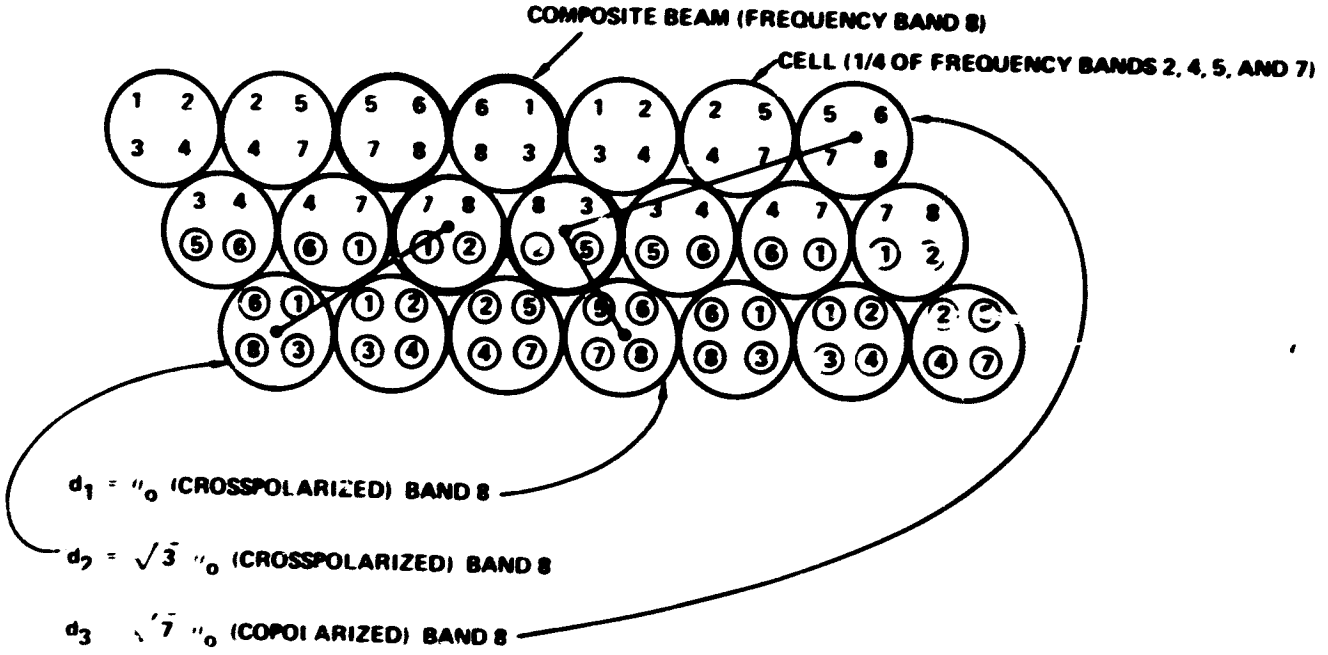

Figure 4-6. Portion of GE Beam Plan 5

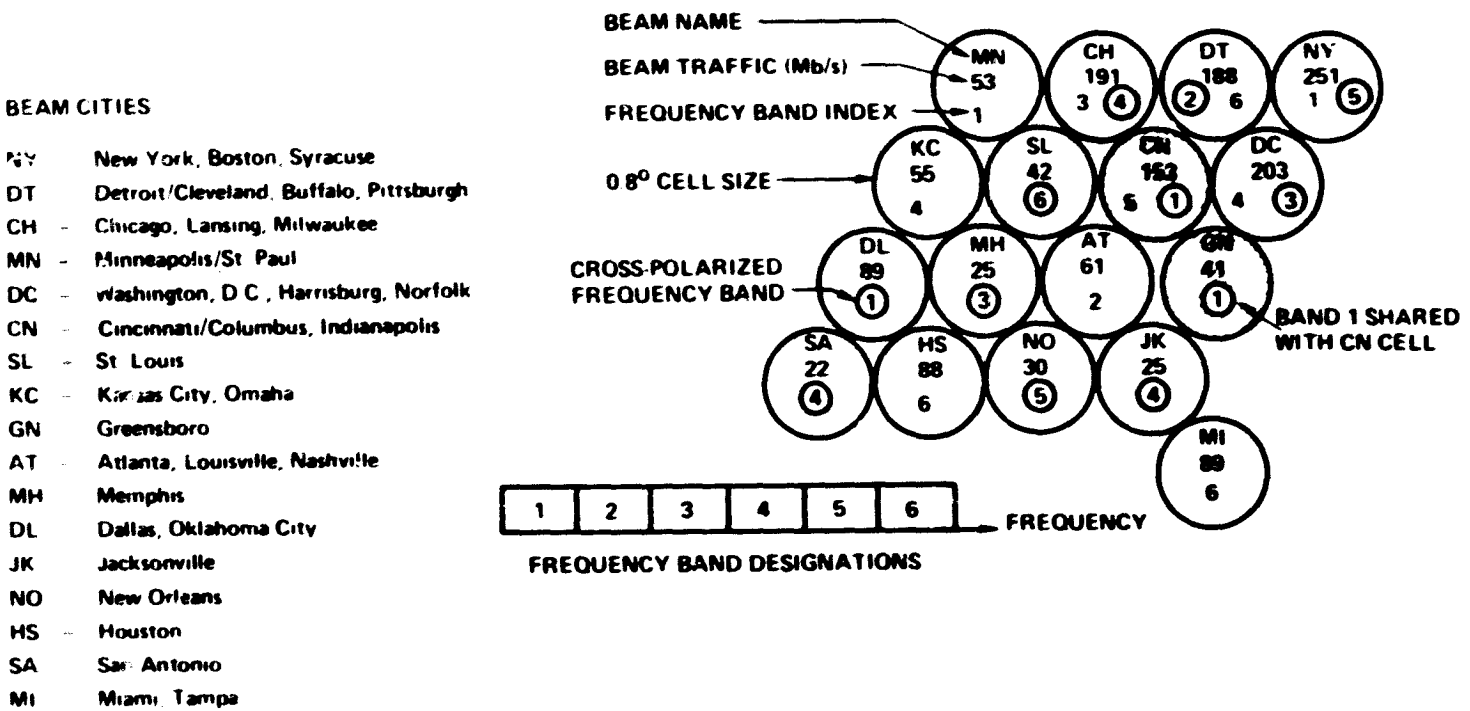

NOTES
- BANDS (5) 6 (4) (3) AND (1) ADDED TO NY, DT, CH, DC, AND CN BEAMS TO BETTER ACCOMMODATE NON UNIFORM TRAFFIC DISTRIBUTION
- BANDWIDTH POTENTIALLY WASTED IN LOWER TRAFFIC BEAMS
- GOOD INTERBEAM AND INTERBAND ISOLATION

Figure 4-7. Example Beam/Frequency Plan for Eastern U.S. (CPS to CPS Traffic Only)

SATELLITE DC POWER IMPLICATIONS

The relationship between antenna beam cell size and the DC power required on the satellite is investigated in this subsection. It is assumed that user terminals are distributed uniformly throughout the coverage area and that each beam is driven by a dedicated traveling wave tube (TWT). Two cell sizes of 1.2° and 0.6° beamwidth are considered in the following examples. It is shown that the 0.6° cells lead to better frequency reuse, i.e., more users can be served, and that less DC power is required on the satellite. Smaller beams provide greater antenna gain but imply a larger number of beams for CONUS and a more complex spacecraft antenna implementation. The exchange of a larger antenna for lower power is considered a favorable trade-off in spacecraft weight (Katz, et al., 1979).

Let N be the number of colors, i.e., disjoint frequency sub-bands, used in a multiple beam plan of M individual beam cells. As before, $F = M/N$ is defined as the frequency reuse factor. Let U be the total number of users, and let B be the bandwidth available to a single user. A nominal total CPS bandwidth of $W = 1$ GHz is taken as fixed. It is apparent that bandwidth is conserved, i.e., $BU = WF$, or

$$U = \left(\frac{W}{B}\right)F = \left(\frac{W}{B}\right)\left(\frac{M}{N}\right) \tag{4.8a}$$

The number of users per beam is

$$u = \frac{U}{M} = \left(\frac{W}{B}\right)\left(\frac{1}{N}\right) \tag{4.8b}$$

The two beam/frequency plan examples considered are shown in figure 4-8A and B. The following assumptions are common to these 10 and 40 beam CONUS coverage plans: Each user is characterized by an $R = 1$ Mb/s signal occupying $B = 1.25$ MHz and a single-channel earth station with a 2 m diameter antenna and a $T = 1000^\circ K$ system noise temperature. The satellite DC to RF power conversion efficiency is taken as $\eta = 10\%$, and a power amplifier back-off $BO = 3$-dB is assumed.

Suppose the desired signal-to-noise ratio (SNR) is $E_b/N_o = 8.5$ dB and there is an implementation loss of $L = 3.5$ dB. Then the required overall carrier-to-noise ratio (CNR) is approximately $C/N_o = (E_b/N_o)\ L\ R = 72$ dB-Hz. For the 1.2° cell of figure 4-8A, the CNRs for the uplink and downlink are equal, i.e., the system is balanced, and

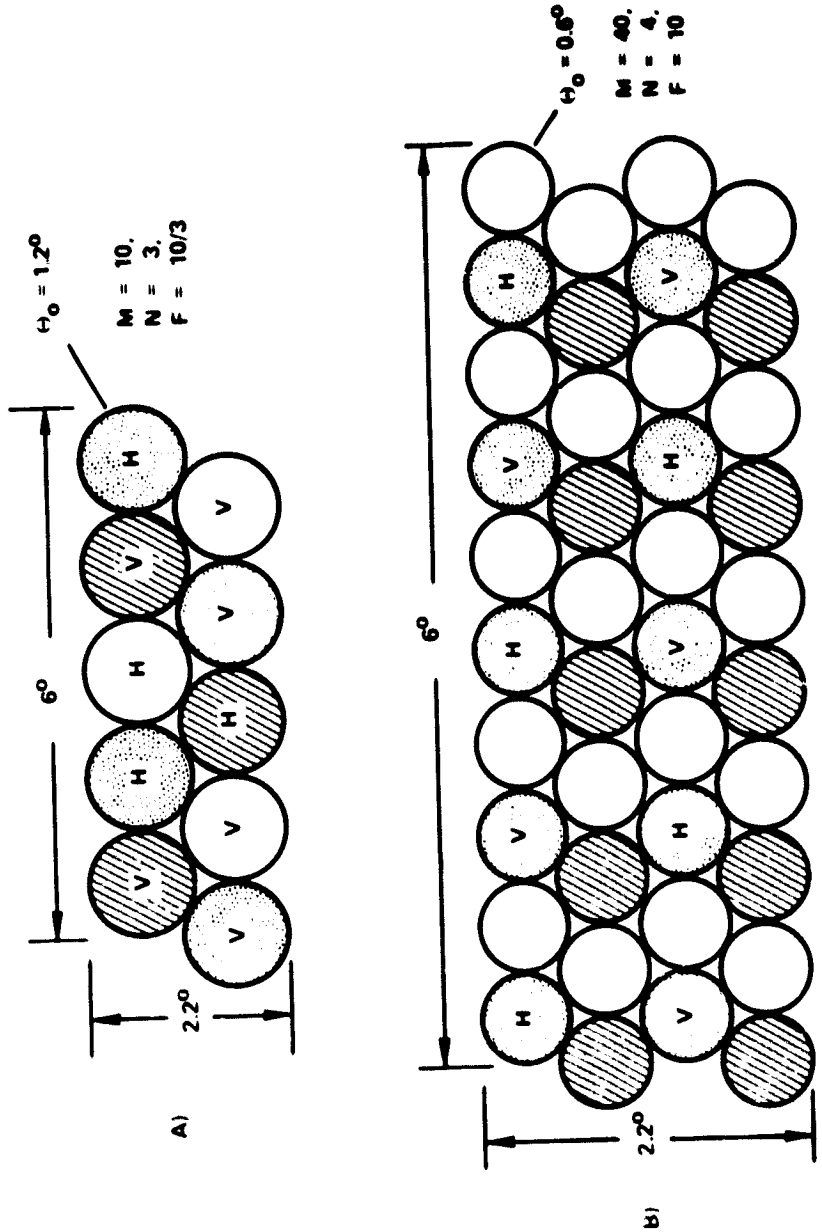

Figure 4-8. Two Possible Beam/Frequency Plans for CONUS Coverage

IA-60,996

$$\left(\frac{C}{N_o}\right)_u = \left(\frac{C}{N_o}\right)_d \cong 2\left(\frac{C}{N_o}\right) = 75 \text{ dB-Hz} \tag{4.9}$$

since

$$\frac{1}{\frac{C}{N_o}} \cong \frac{1}{\left(\frac{C}{N_o}\right)_u} + \frac{1}{\left(\frac{C}{N_o}\right)_d} . \tag{4.10}$$

A simple downlink budget calculation shows for a 1 Mb/s user that the RF power at the satellite TWT output is

$$P = \frac{(EIRP)_d}{G_{sd}} = \frac{(C/N_o)_d \; k \; L_d T}{G_{sd} \; G_{ed}}$$

$$= 75 \text{ dB-Hz} - 228.6 \text{ dB-j/°K} + 210 \text{ dB} + 30 \text{ dB-°K}$$

$$-42.7 \text{ dB} - 49.8 \text{ dB}$$

$$= -6.1 \text{ dBW} = 0.245 \text{ W.} \tag{4.11}$$

Here $k = 1.38 \times 10^{-23}$ j/°K (Boltzmann's constant), L_d is the downlink path loss at 20 GHz, and G_{sd} and G_{ed} are the spacecraft and earth station antenna gains, respectively. Therefore, the total satellite DC power in this case is

$$P_{T\,DC} = M \, P_{DC} = M \frac{(BO) \; P_{RF}}{\eta} = \frac{(BO)(uP)}{\eta}$$

$$= \frac{(BO)}{\eta} \left(\frac{W}{B}\right)\left(\frac{M}{N}\right) P = 13.1 \text{ kW} \tag{4.12}$$

where P_{DC} and P_{RF} are the satellite DC and RF power per beam. The number of users served is $U = Mu = 2667$, from equations (4.8a) and (4.8b).

With the 0.6° cells of figure 4-8B, the uplink satellite antenna gain is 6-dB larger. Since nothing else has changed to affect the uplink power budget, $(C/N_O)_u = 81$ dB-Hz, cf. equation (4.9). Now only about $(C/N_O)_d = 73$ dB-Hz is required to maintain

the desired C/N_o of 72 dB-Hz, according to equation (4.10). Such an unbalanced system is really preferred to accommodate larger uplink fades due to rain. Since G_{sd} has also increased by 6-dB in this case, P = -6.1 - 2.0 - 6 dBW = -14.1 dBW = 0.039 W. The total satellite DC power drops to P_{TDC} = 6.24 kW, using equation (4.12), since M = 40 and N = 4. In this case U = 8000 users are served.

Since P_{TDC} is proportional to UR, the total data rate, the satellite DC power consumption is constant for a fixed total data rate. The principal conclusion is that the 40-beam system can serve three times the users with less than half the spacecraft power compared with the 10-beam system. Two-meter earth terminals spread uniformly over CONUS can just about be supported by a single 1985 satellite using 1982 technology which promises 5 kW of DC power. A slightly larger antenna for the earth terminals would make up the necessary difference.

COMPACT MULTIPLE-BEAM SPACECRAFT ANTENNA

Since SS-FDMA beam plans may involve more than one cell size, it is appropriate to consider designs of spacecraft antennas that promise more compact realizations than a collection of separate designs for each cell size. The generation of up to five cell sizes at 30/20 GHz with a single sandwich-type reflector and two sets of feed horns is suggested in this section.

The half-power beamwidth θ_o in degrees of a parabolic reflector is given by

$$\theta_o \approx \frac{70\lambda}{D} = \frac{21}{fD} \qquad (4.13)$$

where λ is the wavelength in meters, D is the reflector diameter in meters, and f is the frequency in GHz. Consider four different sized reflectors constructed from either vertical (V) or horizontal (H) wires and the beamwidths listed in table 4-2. A sandwich reflector consisting of the two larger diameters can be utilized as follows. A small set of feed horns completely illuminates both reflectors and produces 0.5 and 0.75 degree cells on the downlink with vertical and horizontal polarizations, respectively. A larger set of feed horns illuminates smaller portions of these reflectors, corresponding to D = 0.93 and 0.62 m, and produces 1.1 and 1.7 degree cells on the downlink with vertical and horizontal polarizations, respectively. On the uplink the small feed horns collect vertically and horizontally polarized energy from 0.33 and 0.5 degree cells, while the larger feed horns see smaller portions of the reflectors and collect vertically and horizontally polarized energy from 0.75 and 1.1 degree cells.

Thus, up to five cell sizes are possible with two reflectors and two sets of feed horns at 30/20 GHz. By eliminating the 30 GHz, small feed horn illumination of the larger reflector, and the 20 GHz, large feed horn illumination of the smaller reflector, three cell sizes common to both the uplink and downlink are produced. These sizes are 0.5, 0.75, and 1.1 degrees in this example; the polarity alternates with increasing cell size. The smaller cells would be used in heavier traffic areas. Some polarization isolation has been lost, however.

Table 4-2

Elements for Synthesizing a Multi-Cell-Size Sandwich Reflector

D (m)	Polarization	Frequency (GHz)	Half-Power Beamwidth (degrees)
2.1	V	30	0.33
		20	0.5
1.4	H	30	0.5
		20	0.75
0.93	V	30	0.75
		20	1.1
0.62	H	30	1.1
		20	1.7

A more serious problem is the physical colocation of the two sets of feed horns. For example, if the 0.75 degree cells were pointed identically on the uplink and downlink, the larger and smaller feed horns for these beams would clash. This implies that cell overlaps with either the 0.5 degree size or 1.1 degree size may be permissible only with a common-size set of feed horns using filtering of the distinct uplink and downlink frequency bands. Further analytical work to quantify this horn clash issue is required before such a sandwich reflector configuration for the spacecraft antenna can be recommended.

REFERENCES

(Arnold, et al., 1980) H. W. Arnold, et al., "Measurements and Prediction of the Polarization - Dependent Properties of Rain and Ice Depolarization," IEEE Nat. Telecomm. Conference (NTC '80), Houston, TX, 30 November - 4 December 1980, pp. 43.3.1 - 43.3.6.

(Katz, et al., 1979) J. L. Katz, et al., "Final Report - Application of Advanced On-Board Processing Concepts for Future Satellite Communications Systems," MTR-3787, Vol. I, F19628-79-C-0001, Bedford, MA 01730: The MITRE Corporation, June 1979.

(Kiesling, 1980) J. D. Kiesling, "Study of Advanced Communications Satellite System Based on SS-FDMA," Document No. 80SDS4217, General Electric/Space Division, Valley Force Space Center, P. O. Box 8555, Philadelphia, PA 19101, May 1980, Contract No. NAS-3-21745 for NASA/Lewis Research Center.

SECTION 5

MODULATION AND CODING

A signal-to-noise ratio (SNR) model for handling crosstalk and interbeam interference is developed. The relative amplitude of interfering carriers in adjacent channels due to differences in rain attenuation is treated. An optimum way of specifying uplink margins as a function of typical rain region fades is derived. A discussion of block versus convolutional coding is presented.

EFFECTIVE SIGNAL-TO-NOISE RATIO

An effective SNR including the effects of interchannel interference (crosstalk), co-channel interference and channel (receiver) noise is derived in this section. This will be useful for estimating the interchannel spacings and interbeam isolations required for FDMA waveforms with the data rates and traffic types specified in the traffic model. The results to be obtained hold for any modulation in a large class of constant-envelope, offset-quadrature, minimum shift keying (MSK)-type modulations having the same bit error rate (BER) performance as binary or quadrature phase shift keying (BPSK or QPSK) in additive white Gaussian noise (AWGN). Complex variable notation will be employed for ease in derivation.

Consider a desired signal at carrier frequency ω(rad/s) of the form $s(t)\exp(j\omega t)$ where the baseband signal

$$s(t) = \sum_{\substack{n \\ \text{even}}} b_n\, v(t-nT) + j \sum_{\substack{n \\ \text{odd}}} b_n\, v(t-nT) \qquad (5.1)$$

is composed of data symbols $b_n = \pm\sqrt{E_b}$ (E_b is the energy per data bit and the elementary signals are called antipodal) and a baseband window defined as

$$v(t) \equiv 0, \quad t > |T| \qquad \text{(finite support)} \qquad (5.2a)$$

$$\int_{-T}^{T} v^2(t)\, dt = 1 \qquad \text{(unit energy)} \qquad (5.2b)$$

$$v^2(t) + v^2(t-T) = \frac{1}{T}, \quad t \in (0,T) \qquad \text{(constant envelope)} \qquad (5.2c)$$

($R = 1/T$ (b/s) is the data rate). The window $v(t)$ is rectangular for offset or staggered QPSK (SQPSK) and a half sinusoid for MSK.

The shape and degree of continuity of the baseband window affects the extent to which multiple FDMA carriers can be packed into a given bandwidth, i.e., v(t) determines bandwidth efficiency or crosstalk performance (Kalet, White, 1977).

Interchannel and co-channel interference can be expressed as summations of signals of the same format as the desired signal. They have arbitrary relative amplitudes, symbol timing, frequency and phase offsets, except for the co-channel interfering frequency which is the same as that for the desired signal carrier, by definition. The data rates of all the interfering signals are the same as the desired signal data rate R in this model. The usual channel noise is taken as zero-mean AWGN with a single-sided power spectral density of N_0. The coherent correlation receiver statistic is the real (imaginary) part of $r_n/2$ for determining the b_n's for n even (odd), where

$$r_n = \int_{(n-1)T}^{(n+1)T} (s(t)\exp(j\omega t) + (\text{interchannel interference}) + (\text{co-channel interference}) + \text{AWGN})\, v(t)\exp(-j\omega t)\, dt \qquad (5.3)$$

and the decision rule is

$$b_n = \begin{cases} +\sqrt{E_b}, & \text{Re}\{r_n\} > 0 \\ -\sqrt{E_b}, & \text{Re}\{r_n\} < 0 \end{cases}, \quad n \text{ even} \qquad (5.4a)$$

$$b_n = \begin{cases} +\sqrt{E_b}, & \text{Im}\{r_n\} > 0 \\ -\sqrt{E_b}, & \text{Im}\{r_n\} < 0 \end{cases}, \quad n \text{ odd} \; . \qquad (5.4b)$$

Statistical independence among user signals, types of interference, and random variables representing data symbols is assumed. Relative signal amplitudes, symbol timing, frequencies and phases, neglecting sum frequency terms, are also assumed. Sin $\Delta_i\tau$ is an odd function of τ and cos $\Delta_i\tau$ and $\rho(\tau)$ are even functions of τ. It can be shown that ensemble averaging yields a mean and variance of

$$\bar{r}_n = \begin{cases} b_n, & n \text{ even} \\ jb_n, & n \text{ odd} \end{cases} \qquad (5.5a)$$

$$\left.\begin{array}{l}\overline{(R_e\ (r_n) - b_n)^2},\ n \text{ even} \\ \overline{(I_m\ (r_n) - b_n)^2},\ n \text{ odd}\end{array}\right\} = \frac{E_b}{T}\left(\sum_i \overline{A_i^2} \int_0^{2T} \rho^2(\tau)\ \cos\Delta_i\tau d\tau + \sum_k \overline{B_k^2} \int_0^{2T} \rho^2(\tau) d\tau\right) + \frac{N_o}{2} \qquad (5.5b)$$

where the autocorrelation function of the baseband window is

$$\rho(\tau) = \begin{cases} \int_{-T}^{T} v\ (t + \tau)\ v\ (t)\ dt, & -2T \leq \tau \leq 2T \\ 0, & \tau > |2T| \end{cases} \qquad (5.6)$$

where the frequency offset of the ith crosstalk term is

$$\Delta_i = \omega_i - \omega \qquad (5.7)$$

and where $\overline{A_i^2}$ and $\overline{B_k^2}$ are the second-order moments of the ith interchannel and kth co-channel interfering signal amplitude random variables, respectively. The effective SNR is defined as the magnitude squared (E_b) of the mean of equation (5.5a) divided by the variance of equation (5.5b). In the absence of crosstalk and co-channel interference, this would be $2E_b/N_o$ which is the correct SNR at the output of a coherent correlation receiver for antipodal elementary signals in AWGN (Wozencraft, Jacobs, 1965).

For simplicity of calculation it is assumed that there are I (even) interchannel interferers all of second moment $A_i^2 = A^2$ and carrier offsets

$$\Delta_i = \pm\Delta,\ \pm 2\Delta,\ \pm\ldots\pm\frac{I}{2}\Delta \qquad (5.8)$$

around the desired signal carrier, and K co-channel interferers with the same second moment $B_k^2 = B^2 = A^2X^2$ where X^2 is determined by interbeam isolation.

For

$$C(\Delta_i) = \frac{1}{T}\int_0^{2T} \rho^2(\tau)\ \cos\Delta_i\tau\ d\tau \qquad (5.9a)$$

the effective SNR becomes

$$SNR_{eff} = \frac{1}{2A^2\sum_{m=1}^{I/2} C(m\Delta) + KA^2X^2C(0) + \frac{N_o}{2E_b}}. \qquad (5.9b)$$

Typical Crosstalk Results

Let r be the code rate (so far, r = 1), i.e., the ratio of the number of bits into the coder to the number of bits out of the coder. Define the normalized carrier frequency spacing as

$$\beta = \frac{\Delta r}{2\pi R} . \tag{5.10}$$

Then typical crosstalk levels for SQPSK, MSK and sinusoidal frequency shift keying (SFSK) (Kalet, Weiner, 1979) are as listed in table 5-1 along with the optimum window (Eaves, Wheatley, 1979). Note that $C(2\pi R\beta/r)$ can be below -20 dB for $\beta \gtrsim 1$, i.e., bandwidth efficiencies $(1/\beta)$ approaching 1 b/s per Hz are feasible for equal strength signals ($A^2 = 1$) and an E_b/N_o in the order of 10, cf. equation (5.9b).

Table 5-1

Crosstalk Level $C(2\pi R\beta/r)$ (dB) From Equiamplitude Interfering Carrier $\beta R/r$ Hz Away in Frequency

	β		
Modulation	1	2	3
SQPSK	-16	-21.5	-25
MSK	-21.5	-36.2	-43.7
SFSK	-16.5	-33.9	-56.1
Optimum	-22.1	-46.0	-63.5

For purposes of comparison, the variances of quantization noise for a real signal of unit amplitude are listed in table 5-2 for one to eight bits of quantization. Note that with an assumed 6-bit quantization, for example, carrier separations in hertz which exceed three times the channel burst rate R/r are unnecessary, at least for $A^2 = 1$.

Table 5-2

Quantization Noise for Real Signal of Unit Amplitude

Number of Bits (b) in Quantization	Quantization Noise Variance $2^{-2b}/12$ (dB)
1	-16.8
2	-22.8
3	-28.9
4	-34.9
5	-40.9
6	-46.9
7	-52.9
8	-59.0

Methodology for Determining Channel Spacings

An example is used to illustrate the procedure for determining the necessary carrier frequency spacing between unsynchronized signals of the same type traffic, modulation, and data rate. Suppose an R = 1.5 Mb/s video channel is to be communicated with a BER of $P_b \leq 10^{-3}$. This requires an E_b/N_o of 6.7 dB in AWGN as determined from the standard BER curve for antipodal signals of

$$P_b = \frac{1}{\sqrt{2\pi}} \int_{\sqrt{2E_b/N_o}}^{\infty} \exp\,(-x^2/2)\,dx \qquad (5.11)$$

as a function of E_b/N_o. Allowing an equipment implementation loss factor L = 1 dB, and designing a balanced system where the three interference terms of equation (5.9b) must each be no larger than $(1/3)/2L\,(E_b/N_o)$, guarantees the desired

$$SNR_{eff} \geq \frac{1}{3(1/3)/2L(E_b/N_o)} = \frac{2L\,E_b}{N_o}$$
$$= 2(E_b/N_o)_{eff} = 10.7 \text{ dB}. \qquad (5.12)$$

The margin inherent in the balanced design is 10 log 3 = 4.8 dB in the sense that SNR_{eff} would be approximately three times as large if the crosstalk and co-channel interference terms were negligible. Finally, the single link residual fade margin of the desired signal after adaptation is defined as $A^2 \geq 1$, since $A^2 = 10$, for instance, represents a fade in the desired signal of 10 dB compared to all the surrounding signals.

Next, suppose that there are K = 4 adjacent antenna beam cells operating at the same frequency which introduce significant co-channel interference. Computing C(0) ≈ -3 dB for the selected modulation, say, SFSK, the required interbeam isolation can be determined from

$$X^2 \leq \frac{1}{KA^2 C(0) 6L(E_b/N_o)} = -28.5 \text{ dB}.$$

This must be accomplished by a combination of beam shaping and cross-polarization.

A carrier frequency separation must now be selected so that the crosstalk interference satisfies

$$\sum_{m=1}^{I/2} C(m\Delta) \leq \frac{1}{2A^2 6\, L(E_b/N_o)} = -28.5 \text{ dB}.$$

From crosstalk curves for SFSK, it is seen that only the first (m = 1) term is significant and that $\beta \approx 1.75$ is sufficient. This means that without additional channel filtering, the 1.5 Mb/s video channels must be spaced no more than 1.5β MHz ≈ 2.6 MHz apart. From previous results it is noted that MSK has a smaller crosstalk than SFSK for $\beta \lesssim 2.3$. A β of only about 1.33 is required for the above crosstalk level with MSK signals; this implies a corresponding channel spacing of only 1.5 x 1.33 MHz = 2 MHz with MSK. If MSK is used, of course, the value of C(0) for MSK should be used to determine the interbeam isolation X^2.

Design Example for Channel Spacings

Sets of design curves for MSK are provided in figures 5-1 and 5-2. The crosstalk performance curves used to demonstrate the application of the foregoing modulation theory and methodology in a system design.

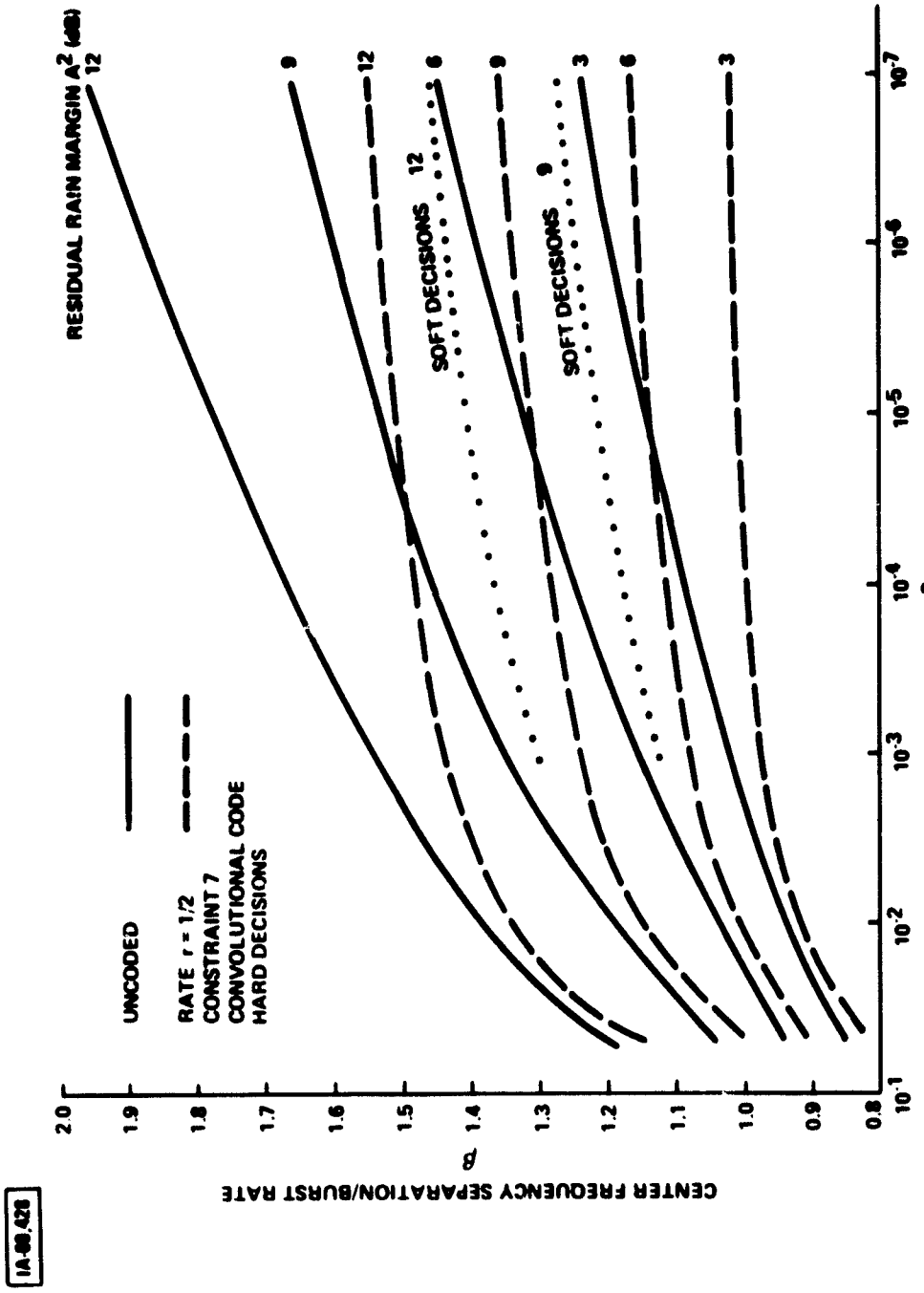

Figure 5-1. Crosstalk Performance for MSK (Equipment Margin L = 1.5 dB; I = 2 Interchannel Interferers; Balanced System Margin 10 $Log_{10}3$ = 4.8 dB)

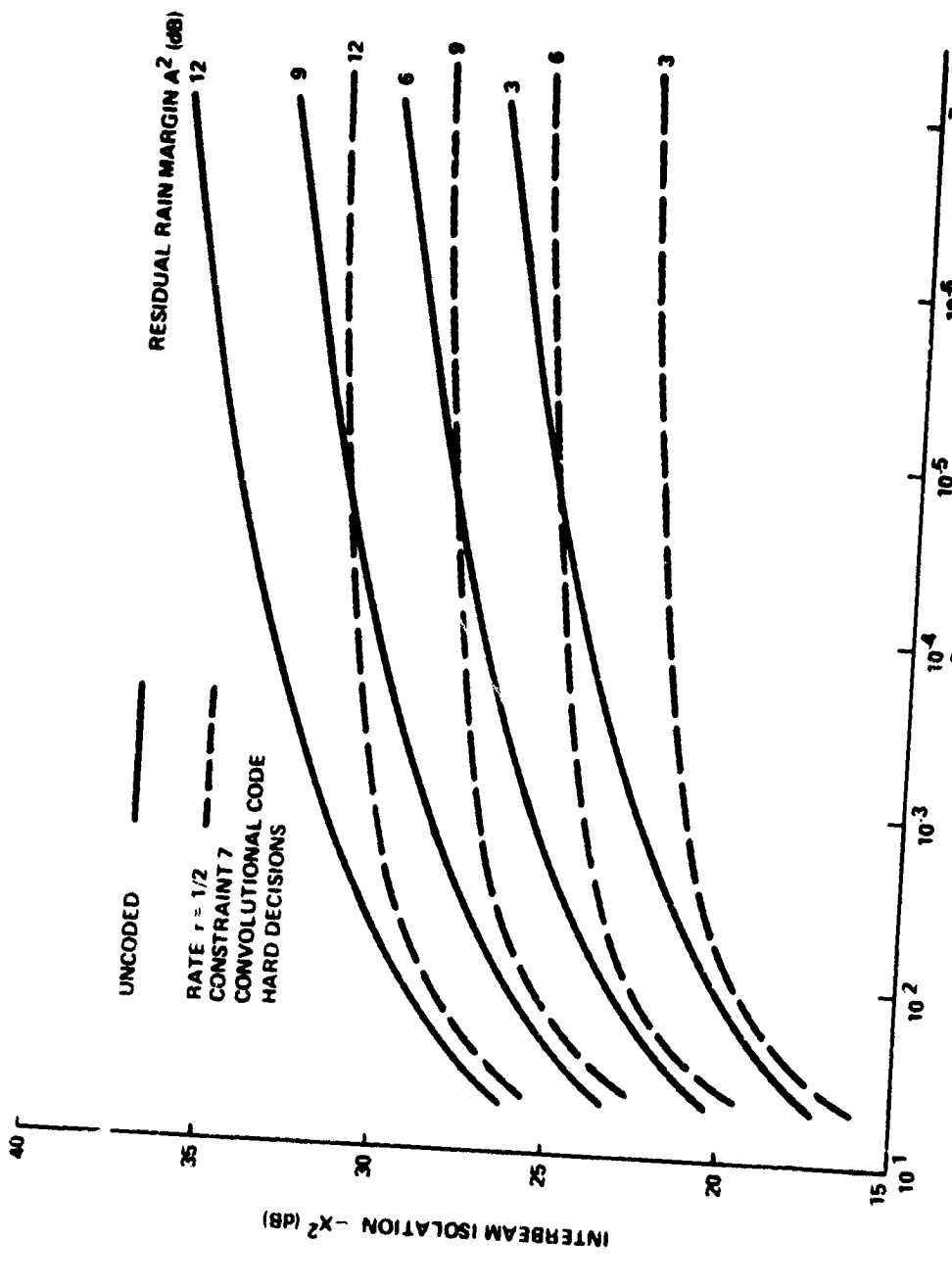

IA-88,987

Figure 5-2. Co-Channel Interference for MSK (Equipment Margin L = 1.5 dB: K = 4 Co-Channel Interferers; Balanced System Margin 10 $\log_{10}3$ = 4.8 dB)

The six types of digital channels included in the CPS traffic model are listed in table 5-3. A broad range of BERs adequate for these channels is selected in the Bit Error Probability column for illustration. For the most part, the indicated error probabilities may be less stringent than a uniform requirement of $P_b \leq 10^{-6}$, for example, which would not distinguish among different types of traffic. The Residual Fade Margin column contains example values of A^2 chosen with the rationale that certain channels may enjoy a higher degree of signal strength fading control and, therefore, a lower residual fade margin. It will probably be more effective in practice to select the A^2 according to the terminal size (total data rate based on the composite of channels) and/or terminal location (the rain region which will impact the residual margin statistics). This criterion is adopted in a subsequent example. As indicated in the next column, the data channels and lowest rate video channel are coded with a rate 1/2, constraint length 7, convolutional code in this example. The implied normalized carrier frequency spacings resulting from the application of figure 5-1 are listed in the Normalized Channel Spacing column. The corresponding channel spacings in hertz are shown in the last column, taking into account a doubling in burst rate for the coded channels.

By using these channel spacings and the traffic model, version A (see section 2), specifying the distribution of channels within CPS terminals and distribution of active CPS terminals by metropolitan area, the bandwidth required per beam is computed for the candidate eastern United States beam plan discussed in section 4. The results for CPS to CPS traffic only are shown in table 5-4. The average bandwidth efficiency for MSK on a beam basis is 1.3 MHz/Mb/s in this case. The approximate number of standard 36 MHz transponders required for each beam is also indicated.

A possible frequency/polarization plan for this 0.8 degree beam pattern is suggested in figure 5-3. This figure shows that no more than 23 disjoint 36 MHz bandwidth segments, or a total of 828 MHz of bandwidth, are required. This implies a frequency reuse factor of only about 59 transponders/23 bandwidths = 2.6. This rather small factor is a consequence of the highly non-uniform traffic distribution and the finite extent of the beam pattern.

This example suggests several issues for further investigation: clustered beams, non-uniform cell sizes, additional coding, and inclusion of CPS/trunking cross traffic. These topics are addressed in sections 4, 7, 10 and 11 of this report.

Table 5-3

Channel Spacings for MSK Design Example

Channel Type	Bit Error Probability P_b	Residual Fade Margin A^2(dB)	Coded	Normalized Channel Spacing β	Channel Spacing (MHz)
(1) 6.3 Mb/s Video	10^{-3}	3	no	1.02	6.43
(2) 1.5 Mb/s Data	10^{-6}	3	yes	1.02	3.06
(3) 1.5 Mb/s Video	10^{-4}	6	no	1.25	1.88
(4) 56 kb/s Data	10^{-7}	6	yes	1.17	0.131
(5) 56 kb/s Video	10^{-5}	6	yes	1.13	0.127
(6) 64 kb/s Voice	10^{-2}	9	no	1.18	0.076

Table 5-4

Bandwidth/Beam Required for Traffic Model (Version A: 50% CPS Terminals Active; CPS to CPS Traffic Only) Using MSK

BEAM	TOTAL BANDWIDTH (MHz)	TOTAL DATA RATE (Mb/s)	AVERAGE MHz/Mb/s	NUMBER OF 36 MHz TRANSPONDERS
NY	327	251	1.30	9
DT	244	188	1.30	7
CH	244	191	1.28	7
MN	69	53	1.30	2
DC	265	203	1.31	7
CN	199	153	1.30	6
SL	54	42	1.29	2
KC	72	55	1.31	2
GN	53	41	1.29	2
AT	79	61	1.30	2
MH	32	25	1.28	1
DL	116	89	1.30	3
JK	32	25	1.28	1
NO	39	30	1.30	1
HS	114	88	1.30	3
SA	32	22	1.45	1
MI	115	89	1.29	3
17 Beams (Eastern U.S.)	2086	1606	1.30 (Average)	59

IA-60,908

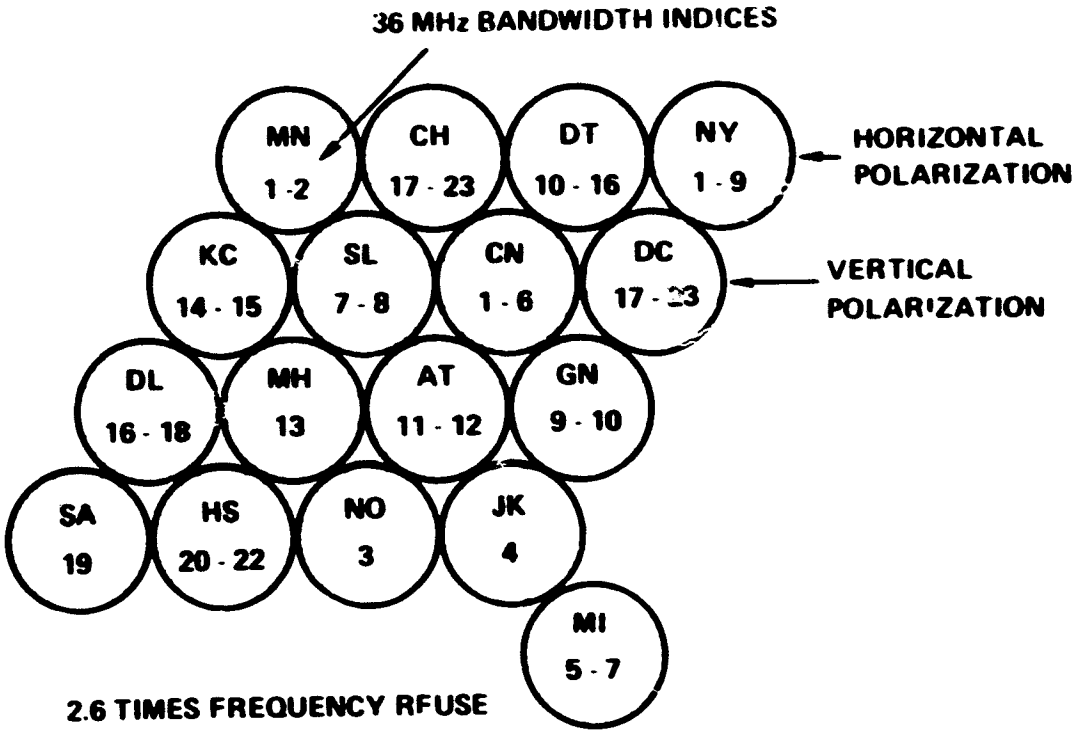

Figure 5-3. Frequency/Polarization Plan for 0.8° Beam Pattern Covering the Eastern U.S.

RESIDUAL RAIN MARGIN ESTIMATES

Recall that $A^2 = \overline{A_1^2}$ represents the average power of an interfering signal at an earth station receiver relative to the desired signal. This quantity is called the residual fade margin because it is assumed that some form of compensation for rain attenuation has already been made. Compensation would be necessary if the required center frequency spacing or interbeam isolation implied by a large A^2 cannot be achieved within the allocated bandwidth or spacecraft antenna implementation, respectively. On the other hand, exact compensation may be infeasible because of imperfections in measuring rain attenuation and the sheer complexity of perfect network control.

The smaller A^2 is, the smaller the crosstalk, co-channel interference, and IM interference will be. Strategies for minimizing and estimating A^2 are discussed in the following paragraphs.

The centralized assignment of the carrier frequency of each channel transmitted by an earth station according to the destination of that transmission is a basic notion of SR-FDMA. The key idea for minimizing A^2 with respect to the vast majority of signals is to further constrain carrier frequency assignments so that signals of roughly the same strength occupy any portion of the frequency band of every earth station receiver. If this condition is met, then each group of uplink signals destined for a given terminal will possess the same property at the satellite since these signals will all be attenuated by the same amount on the downlink. This assumes that the satellite is nearly linear so that the relative power levels within each group of signals are maintained from input to output. Thus, the frequency assignment problem for minimizing A^2 may be reduced to that of compensating for differences in uplink fades from different terminal locations. Proper frequency assignment could therefore permit the maintenance of an A^2 within the uplink rain fade compensation error, at least locally in any sub-band containing the center frequencies of a few adjacent signals. This may be adequate since it is only necessary to maintain a reasonably small A^2 within one or two adjacent signals with the low crosstalk modulations being contemplated.

All 16 possible combinations of uplink and downlink rain fades for two transmitting and two receiving earth stations are considered in figure 5-4. Full generality is assured by connecting the two channels of each transmitting terminal to different receiving terminals. Channels 1 and 2 (C1 and C2) of uplink terminal 1 (T1) are connected to channel 5 (C5) of downlink terminal 3 (R3) and channel 7 (C7) of downlink terminal 4 (R4), respectively; similarly,

DOWNLINK FADE COMPENSATION (dB)

UPLINK FADE COMPENSATION ERROR (dB)			0		0		0		d		c		d		c		0	
			R3		R4		R3		R4		R3		R4		R3		R4	
			C5	C6	C7	C8	C5	C6	C7	C8	C5	C6	C7	C8	C5	C6	C7	C8
0	T1	C1	0				0				c				c			
		C2			0				d				d				0	
0	T2	C3				0				d				d				0
		C4		0				0				c				c		
0	T1	C1	0				0				c				c			
		C2			0				d				d				0	
b	T2	C3				b				b+d				b+d				b
		C4		b				b				b+c				b+c		
a	T1	C1	a				a				a+c				a+c			
		C2			a				a+d				a+d				a	
b	T2	C3				b				b+d				b+d				b
		C4		b				b				b+c				b+c		
a	T1	C1	a				a				a+c				a+c			
		C2			a				a+d				a+d				a	
0	T2	C3				0				d				d				0
		C4		0				0				c				c		

T - TRANSMITTING TERMINAL
R - RECEIVING TERMINAL
C - CHANNEL

IA-60,909

Figure 5-4. Relative Signal Strength Possibilities at the Satellite

channels 3 and 4 (C3 and C4) of uplink terminal 2 (T2) are connected to channel 8 (C8) of R4 and channel 6 (C6) of R3, respectively. This connection pattern is repeated in each of 16 major squares.

The four entries in each square represent the power level of each channel at the satellite relative to the no fading case of the upper-leftmost square. These entries are expressed in terms of downlink fade compensation for R3 and R4 and uplink fade compensation error from T1 and T2. For example, if there is rain on the uplink from T2 and on the downlink to R4 but no rain on the T1 uplink or R3 downlink, then the four signals have the relative power levels, 0, b, d, and b + d (dB) at the satellite. Note that C2 of T1 and C3 of T2 were boosted in power by d to compensate for the downlink rain and both T2 channels were boosted by some amount at T2 to compensate for the uplink rain; b represents the difference between this amount and the actual uplink fade. Although c and d are positive, a and b could be negative as well.

As can be seen by taking differences between entries in figure 5-4, in every case, the relative signal strengths of the two channels received by R3 or R4 will be independent of any downlink fade compensation. In the preceding example, for C5 and C6 and for C7 and C8, this difference is b, the value of the uplink fade compensation error for T2. If the uplink fades are measured accurately, and if full uplink power diversity control can be employed, then the power differences among channels destined for the same earth station will be small. Otherwise, in order to minimize crosstalk, the center frequencies of such signals with disparate powers should not be in the same segment of the receiver frequency band. In other words, there is a possible trade-off between power and frequency control to compensate for rain fades.

From the viewpoint of satellite intermodulation (IM) interference signals being boosted in power to compensate for downlink fades should use a different portion of satellite bandwidth than other uplink signals use. In the preceding example, this suggests that the C2 and C3 signals from T1 and T2, which are d (dB) higher in power than the C1 and C4 signals, should be assigned center frequencies sufficiently separate from those of the C1 and C4 signals.

Co-channel interference will be affected mainly by differences in uplink fade compensation errors among different beam locations. It remains to estimate rain fade compensation errors based on rain statistics for the various beam areas and representative power control strategies. Before doing this, a few practical issues are considered.

Downlink fading can be compensated for by using power diversity in several ways. The most specific method is to further amplify only the affected signals either at the satellite or at the transmitting earth stations. The former might be accomplished by assigning frequencies so that the uplink signals pass through a satellite amplifier with a higher gain characteristic. In this instance, the signals have the same relative power at the satellite input as the signals passing through an amplifier with lower gain. This should be favorable for minimizing IM interference problems in the satellite. If power boosting occurs at the terminals, the satellite input will have different power levels but the center frequencies of the amplified signals should still be assigned to the same segment of the receiving band of the destination terminal. In this case, satellite IM interference will increase to the extent that downlink power amplifiers pass earth station receiver sub-bands containing signals of disparate powers.

Practical difficulties of hardware proliferation and protocol complexity can arise if there is an attempt to compensate downlink rain fades exactly. For example, the number of downlink power (pre?) amplifiers in a beam must be finite, which implies an equal number of possible instantaneous gains. It would be desirable to be able to adjust the gain of each amplifier so that no amplifier is idle for want of signals needing the proper gain factor. Of greater concern, perhaps, is the possibility that a given earth station may have difficulty in boosting different channels by different amounts according to various downlink rain conditions. If the earth station simply boosts a single power amplifier output power by an amount governed by one downlink fade, say the maximum fade for any channel of that terminal, then other channels would be boosted unnecessarily high. This may cause massive reassignments of center frequencies of the latter signals in order to maintain a relatively uniform power level across each earth station receiver band. Therefore, if it is infeasible to individually boost uplink channels over the downlink fading range, it appears to be more attractive to effect downlink power control by adjusting uplink frequencies at the terminals and amplifier gains at the satellite. Frequency assignments should be made with the center frequency roughly proportional to amplifier gain.

Another issue concerns the fact that the crosstalk and co-channel interference model presented earlier applies only for signals of the same data rate. In practice, it may be convenient to determine center frequency assignments in such a way that signals adjacent in frequency are not necessarily at the same data rate. In this case, it is not clear what the center frequency spacing should be between a given signal already assigned and a newly assigned signal at a different data rate. Since the higher rate signal would

tend to produce more crosstalk in the band of the lower rate signal than the reverse, the center frequer spacing should probably be governed by the higher rate using the crosstalk model. This will not be as bandwidth efficient as the procedure of assigning signals of approximately the same data rate, as well as power level, to the same part of the frequency band. On the other hand, the interstitial type spacing arising from groups of signals at mixed rates might reduce IM interference. Both approaches should be tried through simulation and experiment, not only to test the validity of the crosstalk model but to also establish the more attractive operational procedure.

Optimization of Relative Uplink Margins

Attention now returns to the task of minimizing and estimating A^2. Rather than computing a true mean of the relative power level of interfering signals nearby in center frequency, a more pessimistic viewpoint is adopted. Let only the desired signal be attenuated by uplink rain at the 0.995 level of link availability, a value considered acceptable for CPS traffic. Nominal uplink attenuations for the seven regions of CONUS according to a Crane model (Crane, 1980) are shown in figure 5-5; 30 degree elevation angles are assumed. The total CPS to CPS and CPS to trunking traffic out of each region based on the traffic model of section 2 is also shown. A conservative estimate of A^2 for each region is computed as follows.

Let P_r be the ratio of the traffic from region r to the total traffic from all regions. These ratios will serve as probabilities that determine the likelihood of an adjacent signal from each of the seven regions. Let F_r denote the loss factor due to uplink rain fading of a desired signal in region r, e.g., the rain attenuation is expressed as $10 \log_{10} F_r$ (dB) in figure 5-5. Let M_r be the relative margin or factor by which power is boosted by each terminal in region r relative to a nominal uplink reference power. Therefore, if a desired signal from region s starts with margin M_s but experiences an uplink fade F_s, and if an interfering signal from region r has a margin M_r but is unfaded, then the relative power of the interfering to desired signal at the satellite is $M_r F_s / M_s$; the average relative power for that desired signal is

$$A_s^2 = \sum_r P_r M_r F_s / M_s = \frac{F_s}{M_s} \sum_r P_r M_r. \qquad (5.13)$$

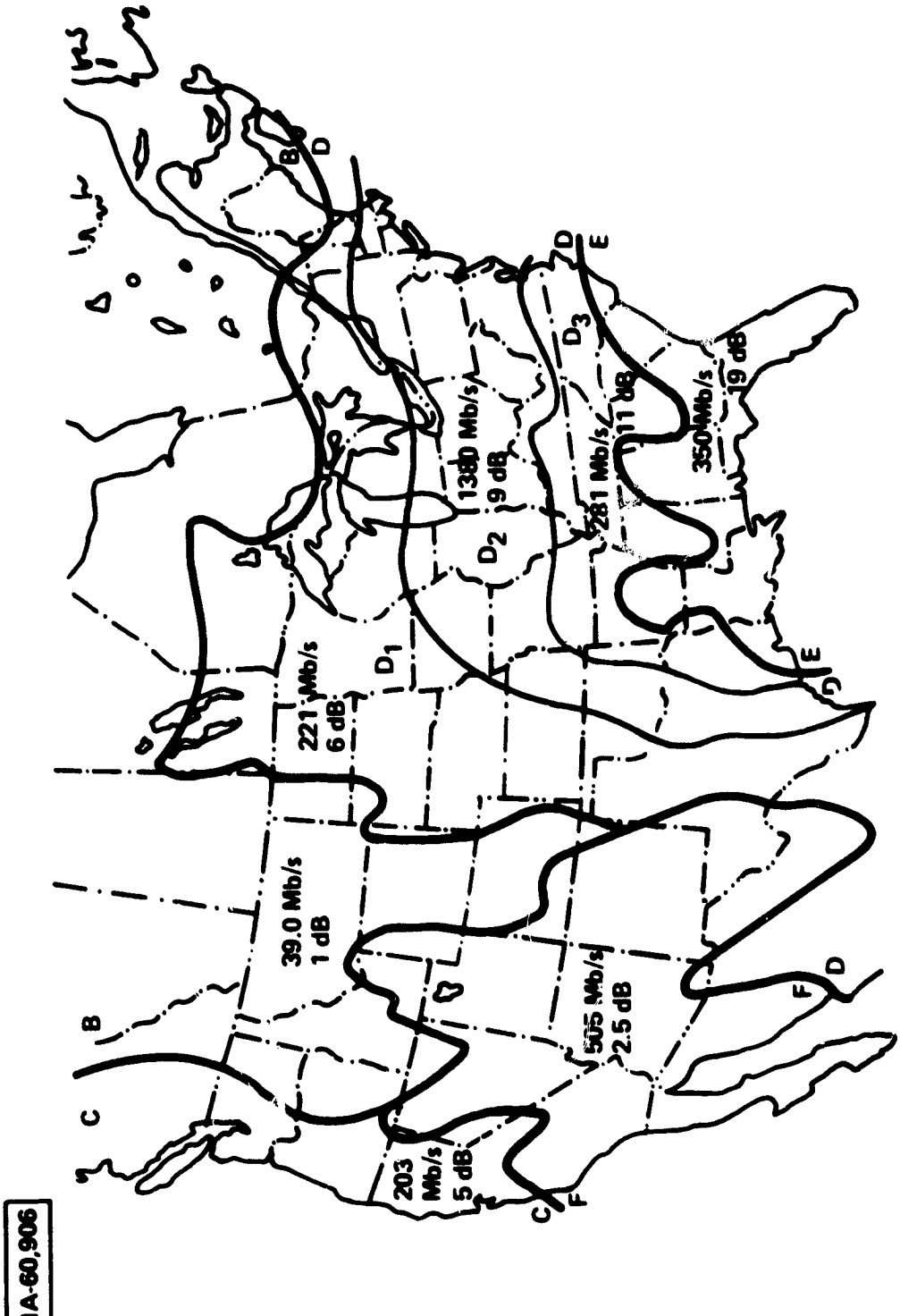

Figure 5-5. Rain Regions of the United States with Total CPS to CPS and CPS to Trunking Traffic and Nominal Uplink Attenuation (30 GHz, 0.995 Availability, 30° Elevation) by Region

The objective here is to select the unknown margins M_r to minimize the average of A_s^2 over the seven regions, again weighted according to the probabilities P_s. Thus, the margins M_r will be optimized to minimize

$$A^2 = \sum_r P_s A_s^2 = \sum_s P_s \frac{F_s}{M_s} \sum_r P_r M_r \tag{5.14}$$

by using equation (5.13). Zeroing the derivatives of equation (5.14) with respect to M_k, one obtains

$$\begin{aligned} 0 = \frac{dA^2}{dM_k} &= -\frac{P_k F_k}{M_k^2} \sum_{r \neq k} P_r M_r + \sum_{s \neq k} P_s \frac{F_s}{M_s} P_k \\ &= P_k \left[\sum_r P_r \left(\frac{F_r}{M_r} - \frac{F_k}{M_k^2} M_r \right) \right], \text{ for all k.} \end{aligned} \tag{5.15}$$

One solution of equation (5.15) arises from setting each term to zero, i.e.,

$$M_k = \sqrt{F_k/F_r}\, M_r, \text{ for all k.} \tag{5.16}$$

By substituting equation (5.16) into equation (5.14), A^2 becomes

$$\begin{aligned} A_{min}^2 &= \sum_s \sum_r P_s P_r F_s \frac{M_r}{M_s} = \sum_s \sum_r P_s P_r F_s \sqrt{\frac{F_r}{F_s}} \\ &= \sum_s P_s \sqrt{F_s} \sum_r P_r \sqrt{F_r} = \left(\sum_s P_s \sqrt{F_s} \right)^2 . \end{aligned} \tag{5.17}$$

This corresponds to a minimum because the second derivatives of the objective function are positive, i.e.,

$$\frac{d^2A^2}{dM_k^2} = P_k \left[-P_k \frac{F_k}{M_k^2} + \sum_{r \neq k} P_r \frac{2F_k}{M_k^3} M_r + P_k \frac{F_k}{M_k^2} \right]$$

$$= \frac{2P_k F_k}{M_k^3} \sum_{r \neq k} P_r M_r > 0, \text{ for all } k. \qquad (5.18)$$

Equation (5.15) is used and P_r, F_r, and M_r are all positive quantities.

The optimum (relative) margins are determined by selecting an arbitrary reference value of unity for region B (r = 1), for example, and using equation (5.16):

$$M_1 = 1 \text{ and } M_2 = \sqrt{F_2/F_1} = \sqrt{3.16/1.26} = 1.58 = 2 \text{ dB}.$$

The other margins determined by using equation (5.13) are shown in table 5-5 along with P_r, F_r and A_r^2.

The main conclusion of this analysis is that A^2 = 10 dB is an excellent value to employ in the modulation and coding model of crosstalk and co-channel interference. (See equation (5.9b) and figures 5-1 and 5-2.) This value is conservative since it was computed by assuming that only the desired signal experiences uplink rain fading and that center frequencies are not influenced by uplink margins.

Given a beam plan, the A_r^2 column of table 5-5 may be used to determine the appropriate A^2 value to employ in any uplink beam according to its region. Again, it is emphasized that the effective A^2 values will be smaller to the extent that center frequencies are assigned according to expected signal strengths at the satellite. The uplink margins M_r of table 5-5 and relative boosts in signal power to compensate for downlink fades are good average indicators of relative signal strengths expected.

SUITABLE CODING TECHNIQUES

At this point various options for error control coding are discussed. The two usual types of linear codes -- block or convolutional -- as well as the choice between a hard decision or soft decision demodulator are available. Throughout the discussion it is assumed that the channel is memoryless. If necessary, this assumption can be made valid by employing an interleaving device which has memory longer than that of the channel noise source. Common interleaving techniques include the block or matrix type interleavers, the convolutional interleavers (Ramsey, 1970) or

Table 5-5

Optimization of Relative Uplink Margins M_r to Minimize Relative Power Level A^2 of Interfering Signal

Region Index r	Region Name	Probability P_r^*	Uplink Fade F_r^{**}	Uplink Margin M_r	Net Fade $F_r M_r$	Relative Power A_r^2
1	B	0.013	1.26 = 1 dB	1 = 0 dB	1.26 = 1 dB	3.59 = 5.55 dB
2	C	0.068	3.16 = 5 dB	1.58 = 2 dB	2 = 3 dB	5.7 = 7.56 dB
3	D_1	0.074	3.98 = 6 dB	1.78 = 2.5 dB	2.24 = 3.5 dB	6.38 = 8.05 dB
4	D_2	0.463	7.94 = 9 dB	2.51 = 4 dB	3.16 = 5 dB	9.01 = 9.55 dB
5	D_3	0.094	12.6 = 11 dB	3.16 = 5 dB	3.99 = 6 dB	11.4 = 10.6 dB
6	E	0.118	79.4 = 19 dB	7.94 = 9 dB	10 = 10 dB	28.5 = 14.5 dB
7	F	0.170	1.78 = 2.5 dB	1.19 = 0.75 dB	1.50 = 1.75 dB	4.28 = 6.31 dB

NOTES: $\sum_r P_r M_r = 2.85$

$A^2_{min} = 10.2 = 10.1$ dB

*Fraction of CPS to CPS and CPS to Trunking Traffic

**0.995 Availability, 30° Elevation Angle, 30 GHz

random interleaving via a random access memory (RAM). An interleaving memory of several constraint lengths for convolutional codes or several block lengths for blocks codes is usually sufficient. The first topic discussed is quantization of the received signal.

In a binary system like MSK, the demodulator is said to have made a hard decision if it decides that a 0 or 1 was sent by the modulator. An unquantized decision is made when the demodulator determines the probability of a 0 or 1 being sent, given the received version of the elementary signal. Between these two extremes lie the soft decisons wherein the demodulator estimate of the signal must assume one of N discrete values. Typically, N is a power of two. It can easily be shown that receiver quantization destroys some of the information which was presented to the receiver about the data. The coarser the quantization, the more information is lost. As has been shown (Viterbi, Omura 1979), less that 0.25 dB is lost with 3-bit (N = 8) quantization compared to unquantized decisions, while hard decisions imply a loss of between 2 and 3 dB. Note that finite quantization is required by any digital implementation of a decoder. Quantization is usually done uniformly although this is not necessary.

When the interference is AWGN, a quantized receiver constitutes a discrete memoryless channel which can be characterized by its transition probabilities; that is, the receiver must be able to determine the probability of obtaining each quantization level for either 0 or 1 being sent. These probabilities depend on noise background and signal level. Thus, in order to make use of soft decisions, the receiver must employ automatic gain control (AGC). Not needing AGC for hard decisions is one positive aspect of a hard decision receiver for antipodal signals like MSK.

Two advantages of block codes are that they can operate at very high speeds and can be chosen so as to make error rates quite low. A 100 Mb/s Reed-Solomon decoder can be fairly inexpensive to build (Berlekamp, 1980). However, the well known algebraic decoding techniques for block codes force the demodulator to make hard decisions, since the decoder requires 0s and 1s in order to operate in a finite field. Although there is still a coding gain, at least for reasonable SNRs, there is a 2-dB loss when the Reed-Solomon decoder is compared to an unquantized decoder.

Block codes or convolutional codes, either linear or nonlinear, can be decoded with soft decisions via correlation decoding, which compares the quantized version of the received signal with each possible codeword and chooses the codeword which is closest in some predetermined metric. This method is impractical for any but the

smallest codes since the work factor is proportional to 2^K, where K is the number of information bits per codeword. Many ideas have appeared in the literature on methods of approximating correlation decoding with soft decisions via algorithms which are claimed to be faster and easier to implement. The greatest drawback of such algorithms is that they are still fairly slow and expensive and require significant processing. For this reason, it is assumed that a block code would make hard decisions using an algebraic decoding algorithm.

For comparison purposes, the 10 error correcting BCH (127,64) code and the (24,12) Golay code have been selected. The latter is capable of correcting all codeword error patterns of less than four bits and 8855 of the 10,626 possible error patterns of weight four, i.e., a complete decoder instead of the more usual bounded distance decoder is used. As is shown in figure 5-6, the BCH code is superior for the range of BERs from 10^{-7} to 10^{-2}. The decoding of the BCH code is easily accomplished via the Berlekamp-Massey algorithm (Massey, 1969).

A convolutional code (CC) of constraint length K, memory M = K-1, and rate r = 1/2 consists of a K-stage shift register which has two sets of taps, each with a different output, which are interleaved to produce a codeword. The results presented for a certain constraint length do not hold for all CCs of that length, but only for the non-catastrophic codes with maximal free distance. The maximal free distance can be shown to be a nondecreasing function of the constraint length that determines performance. As a result, an increase in constraint length can lead to a better code. However, the traditional maximum likelihood decoder -- the Viterbi algorithm -- has a work factor which is proportional to 2^K. Thus, increasing the constraint length, while increasing the maximal free distance, makes the decoder more complex as well as slower. The constraint length K = 7 is generally accepted as a good compromise between free distance and decoder speed and complexity.

One of the great advantages of CCs is that the Viterbi algorithm can be applied not only to the hard decision channel, but also to the quantized output of a soft decision demodulator. As shown in figure 5-6, BCH (127,64) code requires slightly less E_b/N_o than the K = 7 CC on a channel with hard decisions. However, on the 8-level quantized channel, the CC achieves more than a 1.5-dB advantage over the BCH code.

The error curves for the CCs are obtained via the union bound on an unquantized channel and the Viterbi algorithm. However, the original algorithm requires large memory since a decision is made on the entire message. Traditionally, the path memory (the length of

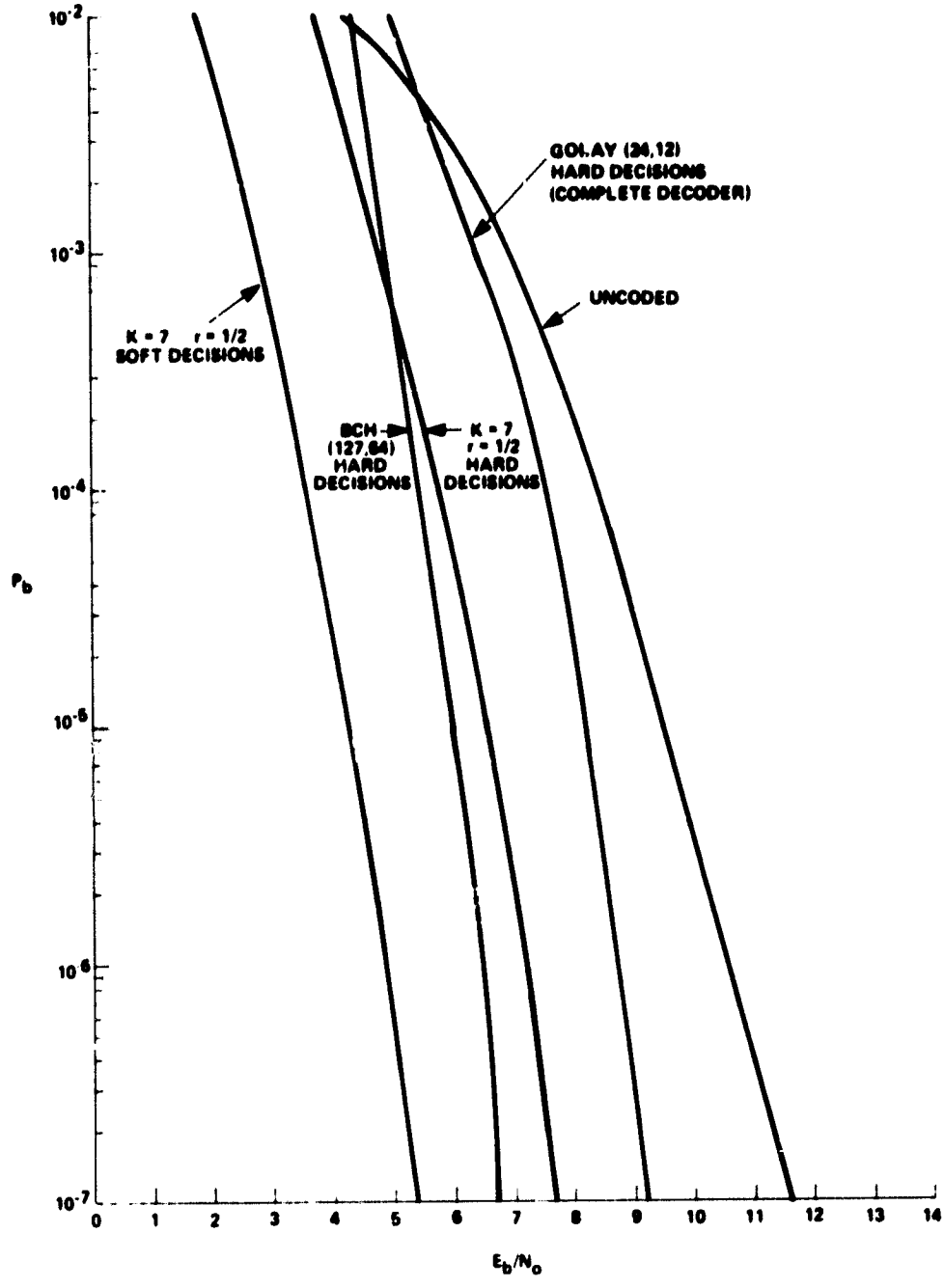

Figure 5-6. Performance of Several Rate 1/2 Binary Codes

the path through the code's trellis) is truncated at roughly four times the constraint length, or about 32 bits for K = 7. That is, a decision is made, at a certain time, on the bit which was sent 32 bit-times earlier based on all bits received in between.

Heller and Jacobs did extensive simulations of CC performance with 8-level quantization and 32-bit path memory (Heller, Jacobs, 1971). The results show a loss of only 0.25 dB compared to the theoretical performance without quantization and with no path memory truncation. This suggests that the K = 7 convolutional code would provide very good performance.

One objection might come from SR-FDMA users who require a very high data rate and a very low bit error rate. In this situation, the above CC may not meet the requirements. If this were the case, then one might use a higher rate but long and powerful block code, such as a Reed-Solomon code, with an erasure correcting algorithm. It is felt though, that error rates from 10^{-6} to 10^{-2} and reasonable data rates can be handled quite well with the convolutional code.

REFERENCES

(Berlekamp, 1980) E. R. Berlekamp, "The Technology of Error Correcting Codes," Proc. IEEE, Vol. 68, No. 5, May 1980, 564-593.

(Crane, 1980) R. K. Crane, "Prediction of Attenuation by Rain," IEEE Trans. Commun. Vol. COM-28, No. 9, September 1980, 1717-1733.

(Eaves, Wheatley, 1979), R. E. Eaves and S. M. Wheatley, "Optimization of Quadrature-Carrier Modulation for Low Crosstalk and Close Packing of Users," IEEE Trans. Commun. Vol. COM-27, No. 1, January 1979, 176-185.

(Heller, Jacobs, 1971) J. A. Heller and I. M. Jacobs, "Viterbi Decoding for Satellite and Space Communications," IEEE Trans. Commun. Tech., Vol. COM-19, 1971, 835-848.

(Kalet, Weiner, 1979) J. Kalet and L. N. Weiner, "Close Packing of PCSFSK Signals - Model and Simulation Results," IEEE Trans. Commun. Vol. COM-27, No. 8, 1234-1239.

(Kalet, White, 1977) J. Kalet and B. E. White, "Suboptimal Continuous Shift Keyed (CSK) Demodulation for Efficient Implementation of Low Crosstalk Data Communication," IEEE Trans. Commun. Vol. COM-25, No. 9, September 1977, 1037-1041.

(Massey, 1969) J. L. Massey, "Shift Register Synthesis and BCH Decoding," IEEE Trans. Inf. Th., Vol. IT-15, No. 1, January, 1969, 122-127.

(Ramsey, 1970) J. L. Ramsey, "Realization of Optimum Interleavers," IEEE Trans. Inf. Th., Vol. IT-16, No. 3, May 1970, 338-345.

(Viterbi, Omura, 1979) A. J. Viterbi and J. K. Omura, Principles of Digital Communication and Coding, New York: McGraw-Hill, 1979.

(Wozencraft, Jacobs, 1965) J. M. Wozencraft and I. M. Jacobs, Principles of Communication Engineering, New York: Wiley, 1965.

SECTION 6

INTERMODULATION

Intermodulation (IM) interference at the satellite and the relation between satellite and earth terminal IM interference-to-carrier-power ratios are examined in this section.

SATELLITE INTERFERENCE MODELS

Let there be I (even) interfering equally-spaced carriers all of amplitude A surrounding another carrier of amplitude B as depicted in figure 6-1. These situations model signals at the input to the satellite where one center carrier of index i = 1/2 corresponds to a user signal whose uplink power has been increased to overcome a downlink fade to the destination user (Case 1), or who is experiencing an uplink fade (Case 2). IM products will be generated when these signals pass through satellite nonlinearities. Case 1 is more serious than Case 2 in that the larger carrier can induce significant IM interference in other channels (Case 1B) as well as the same channel (Case 1A): the weaker carrier alone (Case 2) may not survive satellite downlink power robbing and/or suppression due to IM interference. On the other hand, Case 2 may represent a serious limitation if the satellite power amplifier must operate with a sufficiently high back-off to permit a weak center carrier signal to survive.

The purpose of this section is to consider degradations in SNR caused by third-order IM products. It is assumed that higher-order IM products can be neglected. Similarly, of the third-order products, only those of the frequency form $f_i + f_j - f_k$ (i,j,k distinct) are considered; products of the form $2f_i - f_j$ have 6-dB smaller amplitude and are fewer in number for large I.

A single such IM product in a given channel is assumed to be proportional to the product of the amplitudes of the generating carriers. The total IM power in that channel from all these IM products is assumed to be the sum of the squares of the individual IM product amplitudes. This results from assuming that the IM products have statistically independent and zero mean phases so that the ensemble average of the cross terms arising from squaring a sum of IM products is zero. Hence, the average IM power includes only the square of each IM product.

C-2

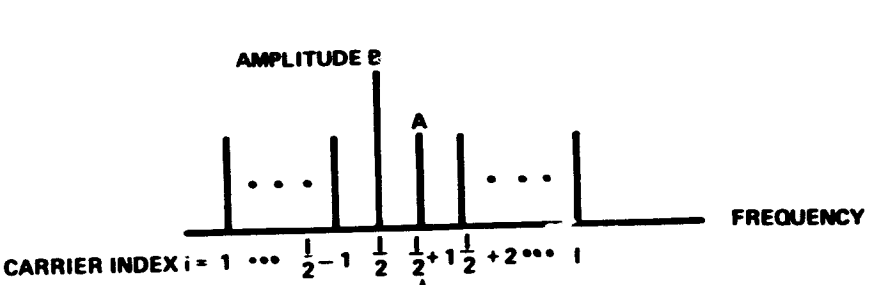

A. STRONG CENTRAL CARRIER AT i = I/2

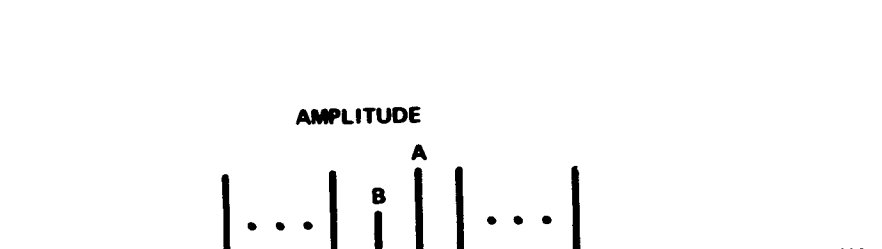

B. WEAK CENTRAL CARRIER AT i = I/2

Figure 6-1. Intermodulation Channels of Interest for I(Even) Carriers

The number of IM products being considered that fall in channel i is (Westcott, 1967)

$$n_i(I) = \frac{i}{2}(I-i-1) + \frac{1}{4}((I-3)^2 - 5). \tag{6.1}$$

Note that $n_{I+i+1}(I) = n_i(I)$, by symmetry. The number of IM products falling in the central channels $i = I/2$ and $i = I/2 + 1$ is therefore

$$n_{I/2}(I) = n_{I/2+1}(I) = \frac{1}{8}(3I-4)(I-2). \tag{6.2}$$

When all carriers have the same amplitude A, the net IM amplitude in a central channel is

$$a_{I/2}(A,I) = a_{I/2+1}(A,I) = C\, n_{I/2}^{1/2}(I)\, A^3 \tag{6.3}$$

where C is a proportionality constant that is hardware dependent. The next step is the calculation of the net IM amplitudes in the central channels when the carrier index $i = I/2$ has a larger amplitude $B > A$.

Strong Central Carrier

It can be shown that the number $m_{I/2}(I)$ of IM products in channel I/2 generated by carrier I/2 is

$$m_{I/2}(I) = \frac{I}{2} - 1 \tag{6.4a}$$

and the number $m_{I/2+1}(I)$ of IM products in channel I/2 + 1 generated by carrier I/2 is

$$m_{I/2+1}(I) = 3(\frac{I}{2} - 1) = 3m_{I/2}(I). \tag{6.4b}$$

Thus, the net IM amplitude at $i = I/2$ is

$$\begin{aligned} a_{I/2}(B,I) &= C\,(m_{I/2}(I)\, A^4 B^2 + (n_{I/2}(I) - m_{I/2}(I))A^6)^{1/2} \\ &= CA^2\,((\frac{I}{2} - 1)B^2 + \frac{1}{4}(3I - 8)A^2))^{1/2} \end{aligned} \tag{6.5}$$

with equations (6.3) and (6.4a). Similarly, at $i = I/2 + 1$

$$\begin{aligned} a_{I/2+1}(B,I) &= C\, A^2\,(m_{I/2+1}(I)\, B^2 + (n_{I/2+1}(I) - m_{I/2+1}(I))A^2)^{1/2} \\ &= CA^2((\frac{I}{2} - 1)(3B^2 + \frac{1}{4}(3I - 16)A^2))^{1/2}. \end{aligned} \tag{6.6}$$

The relative IM power ratio in channel I/2 is

$$\frac{a^2_{I/2}(B,I)}{a^2_{I/2}(A,I)} = 1 + \frac{4\left(\left(\frac{B}{A}\right)^2 - 1\right)}{3I - 4} \tag{6.7a}$$

from equations (6.2), (6.3), and (6.5). At I/2 + 1

$$\frac{a^2_{I/2+1}(B,I)}{a^2_{I/2+1}(A,I)} = 1 + \frac{12\left(\left(\frac{B}{A}\right)^2 - 1\right)}{3I - 4} \tag{6.7b}$$

The IM power increases in the central channels for a 10 dB increase in the relative power of the carrier in channel I/2 are listed in table 6-1. Note that this power increase is significantly greater in the adjacent central channel I/2 + 1.

Table 6-1

Relative IM Power Increase for Carrier Power Increase of (B/A) = 10 at Channel I/2 (dB)

	I		
Channel	10	50	100
I/2	3.77	0.96	0.50
I/2+1	7.12	1.40	1.35

The IM power in other channels will be less than channel I/2 + 1 by symmetrical and physical arguments. As a check, the adjacent channel I/2 - 1 is examined. From equation (6.1)

$$n_{I/2-1}(I) = \frac{I}{4}\left(\frac{3I}{2} - 5\right) = n_{I/2+1}(I) - 1. \tag{6.8}$$

It can be shown that the number of IM products at I/2-1 affected by the strong carrier is

$$m_{I/2-1}(I) = \frac{3I}{2} - 4 = m_{I/2+1}(I) - 1. \tag{6.9}$$

Taken together, equations (6.6), (6.8), and (6.9) imply that the power increase in channel I/2 - 1 relative to the quiescent IM power in a central channel is strictly less than that in channel I/2 + 1, i.e.,

$$a^2_{I/2+1}(B,I) - a^2_{I/2-1}(B,I) = C^2A^4B^2. \qquad (6.10)$$

Therefore, the worst-case IM situation (Case 1B) is represented by equation (6.7b), which is shown graphically in figure 6-2.

Weak Central Carrier

In Case 2, the central carrier in channel I/2 is assumed to be weaker than the other carriers by $Y = (A/B)^2$ (dB), where $B \leq A$. Suppose the minimum acceptable carrier to IM interference ratio (C/I) is Z (dB). Then if the weaker carrier is to satisfy this requirement, each of the other carriers will have a C/I of at least Y + Z (dB). This ratio may be difficult to achieve in a nonlinear power amplifier unless the output power backoff is so great that the device efficiency is unacceptable. On the other hand, if the backoff is limited to provide some minimally acceptable efficiency, the weak carrier will not be detectable with the desired reliability because IM interference in that channel will be too large.

This is illustrated with the typical C/I vs. backoff characteristic of figure 6-3. Suppose there are I = 10 carriers and that the saturated output power of the amplifier is 20 W, for example. Then each of the stronger carriers would be allocated $20/(9+10^{-Y/10})$ W and the weaker carrier would receive only $20/(1+9\times10^{+Y/10})$ W. If all the carriers were of equal power, then B = A and Y = 0 dB. This implies that each carrier would receive 2 W of saturated output power and that C/I = 14 dB, according to figure 6-3. However, suppose that the minimum acceptable C/I is Z = 16 dB. This would imply a 3-dB backoff for equal carriers and 1 W per carrier.

Alternatively, a 6-dB backoff implies that the weaker carrier can be no more than Y = 19.5 - 16 = 3.5 dB down for an acceptable C/I in that channel. This corresponds to 0.24 W in the weak channel and 0.53 W in the strong channels. If Y = 10 dB, then a 10-dB backoff is necessary to maintain the weak channel quality. This would mean a C/I = Y + Z = 26 dB in the strong channels, cf. figure 6-3. This corresponds to 0.022 W in the weak channel and 0.22 W in the strong channels. Unfortunately, a 10-dB backoff usually implies an intolerably low power amplifier efficiency. Thus, the depth of

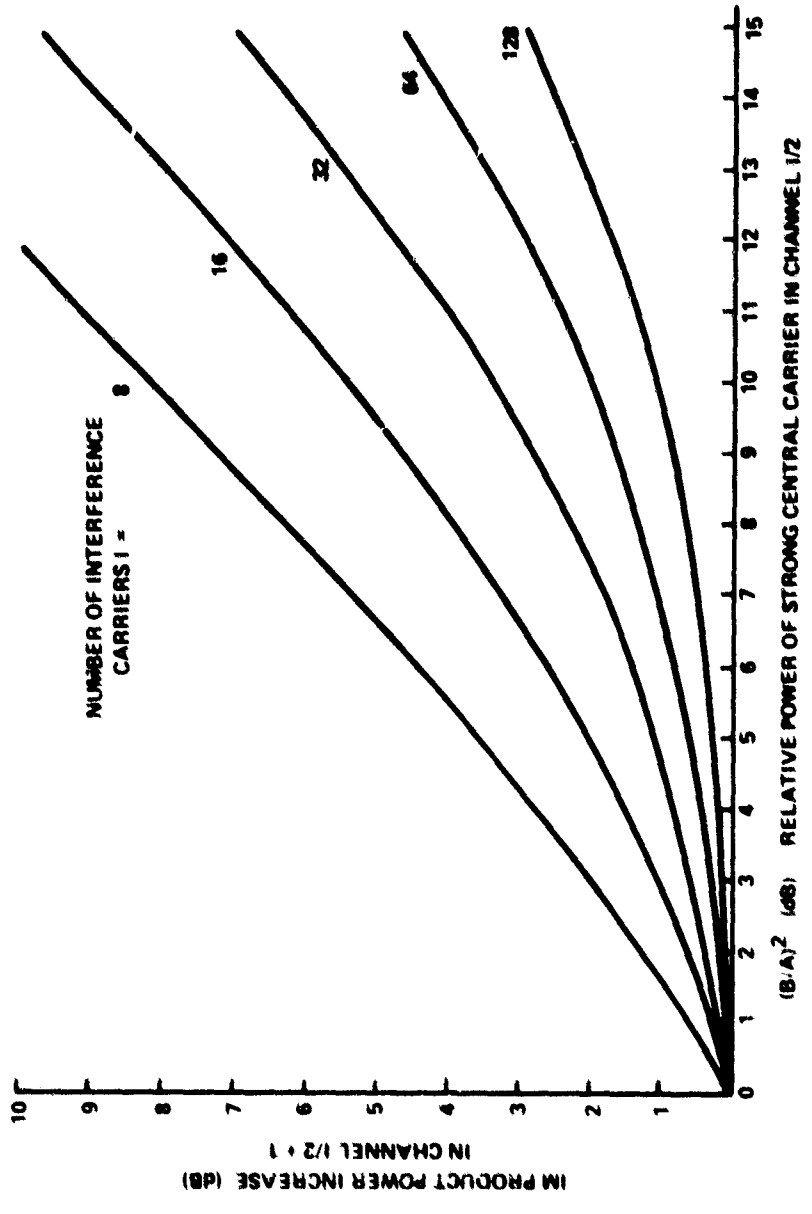

Figure 6-2. Worst-Case Degradation From 3rd Order IM Products

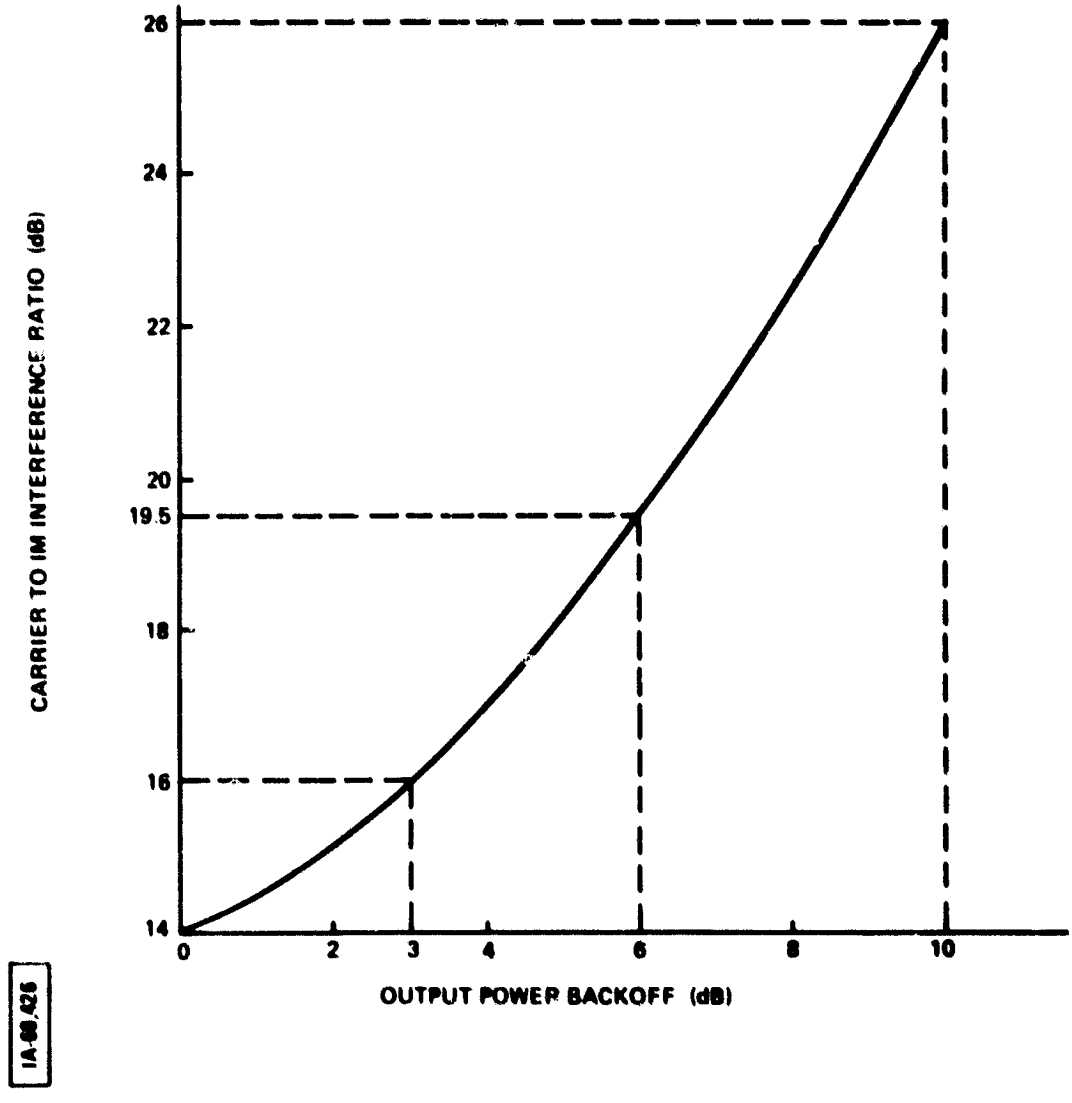

Figure 6-3. Typical Behavior of Nonlinear Power Amplifier

the weak signal may be limited to just a few dB by the particular power amplifier characteristics.

EARTH STATION REQUIREMENT

Four factors contribute to communication interference: Gaussian noise, co-channel noise (interbeam interference due to a finite beam isolation), cross-channel noise (crosstalk due to modulation spreading), and intermodulation. Let an equal contribution be assigned to each of these factors; in particular, suppose the noise power of each factor is at least 20 dB below the signal power. The total interference will therefore be at least 14 dB below the carrier power (C), which is sufficient for digital transmission.

Intermodulation interference power originates in earth station power amplifiers and in satellite TWTs. The overall C/IM power ratio must be no less than 20 dB. There are two options: 1) to place the burden on the earth station (i.e., to have a high C/IM at the terminal) and 2) to require equal contributions from the satellite (S) and earth station (E).

Option 1:

$(C/IM) = 27$ dB $\quad (C/IM) = 21$ dB $\quad C/IM = 20$ dB

(The relationship $(IM/S) = (IM/C)_E + (IM/C)_S$ has been used.)

Experimentally, a multicarrier signal produces about C/IM = 19 dB for an output backoff of 5 dB, as suggested from figure 6-3. Also, if it is assumed that C/IM increases 2 dB for each additional dB of output backoff, $(C/IM)_E = 27$ dB for an output backoff of 9 dB and $(C/IM)_E = 21$ dB for an output backoff of 6 dB. This is somewhat more optimistic than suggested by figure 6-3. In this case, the 20 dB C/IM could be achieved if the satellite TWT operates with a 6 dB backoff and the earth station TWT operates with a 9 dB backoff.

In this option, it is not worthwhile to reduce the satellite's C/IM much below 21 dB because it would require a very high C/IM from the earth station. For example,

$(C/IM)_S = 20.5$ dB $\quad (C/IM)_E = 30$ dB $\quad (C/IM) = 20$ dB

implies that a reduction of the satellite (C/IM) by only 0.5 dB requires a 3 dB higher C/IM from the earth station, which is probably undesirable.

Option 2:

$(C/IM)_E$ = 23 dB $(C/IM)_S$ = 23 dB C/IM = 20 dB

The same experimental data as above yields $(C/IM)_E = (C/IM)_S$ = 23 dB for an output backoff of 7 dB. In this case the desired C/IM = 20 dB is achieved if both the satellite and the earth station operate at 1/5 the saturation level.

There are problems with options 1 and 2 in that link budget calculations show that it is undesirable to operate satellite TWTs at a backoff higher than 5 dB, i.e., with a C/IM exceeding 19 dB. Hence, it might be more acceptable to have C/IM = 18 dB, with $(C/IM)_S$ = 19 dB and $(C/IM)_E$ = 25 dB.

Therefore, instead of having the four interference factors equal to 20 dB with an overall C/I of 14 dB, a mix such as this may be preferred:

Option 3:

(C/IM) = 18 dB $(C/I)_{Gaussian}$ = 21 dB

$(C/I)_{co\text{-}channel}$ = 20 dB $(C/I)_{crosstalk}$ = 22 dB

which still yields a net C/I of 14 dB.

The beam isolation of 20 dB must be maintained because of the possibility of nearby beams using the same frequency band and the same polarization. The spacing between carriers needs to be increased slightly to obtain $(C/I)_{crosstalk}$ = 22 dB instead of 20 dB.

The principal conclusion follows. Since the satellite cannot operate at a backoff higher than 5 dB (due to power supply limitations), $(C/IM)_S$ = 19 dB, and therefore, the required C/IM from an earth station is at least 25 dB.

REFERENCE

(Westcott, 1967) R. J. Westcott, "Investigation of Multiple F.M./F.D.M. Carriers Through a Satellite T.W.T. Operating Near to Saturation," Proc. IEE Vol. 114, No. 6, June, 1967, 726-740.

SECTION 7

SATELLITE ROUTING

This section shows that it is not feasible to provide full interchannel switching capability in the satellite for the assumed traffic models. A limited switching capability for long-term changes in traffic distribution is recommended. The main subject of this section is satellite routing, and, in particular, a method by which frequencies and bandwidth can be efficiently allocated to beams. Channel blocking is also discussed.

MATRIX SIZES FOR FULL SWITCHING

For the three CPS terminals types D, E, and F in the earlier traffic model (old version A), there are six types of channel. The number of terminals of each type and the number of channels of each type in a given terminal are listed in table 7-1. In order to greatly simplify the problem of full satellite switching, each switch is restricted to handling traffic of one channel type only. As will be seen, even this implies too much complexity for fully switching lower data rate channels.

Let m_i be the total number of terminals of type i and let n_{ij} be the number of channels of type j in a terminal of type i. Then the number of input or output ports on a switch handling just channels of type j is given by

$$L_j = \sum_i m_i n_{ij} \tag{7.1}$$

The number of crosspoints in the switch for channels of type j is L_j^2. These parameters are listed in table 7-1. Note that these numbers of ports and crosspoints depend only on the number of terminals and channel distribution within these terminals and are independent of the number of beams.

From another point of view, suppose there are N channels of one type per beam and M beams. In this case, complexity is proportional to the square of the number of channels per beam times the square of the number of beams. For example, if 100 56 kb/s data channels per beam were to be fully switched among M = 40 uplink and 40 downlink beams, a microwave switch with

$$(MN)^2 = (4000)^2 = 16 \times 10^6$$

crosspoints is implied.

IA-88,411

Table 7-1

Switch Sizes Required for Full Switching of Identical Channels of CPS Terminal and Channel Types in Version A of Traffic Model

CHANNEL TYPE i	TERMINAL POPULATION AND NUMBER OF CHANNELS PER TERMINAL BY TYPE			NUMBER OF INPUT OR OUTPUT PORTS	NUMBER OF CROSSPOINTS
	m_i = 26 D	276 E	1800 F	N_j	N^2_j
56 kb/s VIDEO	n_{ij} = 10	2	1	2612	6.8 M
1.5 Mb/s VIDEO	5	1	0	406	165 k
6.3 Mb/s VIDEO	1	0	0	26	676
56 kb/s DATA	20	5	1	3700	13.7 M
1.5 Mb/s DATA	2	0	0	52	2704
64 kb/s VOICE	240	60	12	44,400	2 G

Clearly, full switching capabilities for all types of channel in the traffic model postulated are formidable if not impossible.

FREQUENCY ALLOCATION PRINCIPLES

For Traffic Model A, the uplink and downlink beam sizes are assumed to be identical with a 4-dB contour of 0.33°. Since the available DC satellite power is limited, a small beam size is desirable to achieve a high antenna gain. Two factors restrict the beam size: 1) satellite antenna pointing accuracy, probably on the order of 0.05°, and 2) several pairs of cities are about 0.3° apart (Buffalo-Pittsburgh, Indianapolis-Cincinnati, Louisville-Nashville, Omaha-Kansas City, and Seattle-Portland); if the beam site is reduced below 0.3°, many more beams would be required.

The 45 major cities specified by NASA are grouped into 31 beams as shown in figure 7-1. The map represents CONUS as it appears from a geostationary satellite located at 90° W longitude. In this map the antenna beam contours appear as circles, which is very convenient.

Table 7-2 lists the cities and the total channel data rate in each beam based on Traffic model A. It is conservatively assumed that 20% of the users in each beam experience rain attenuation. When a user experiences rain attenuation, he switches to coding in order to restore link margin. The assumed coding rate is r = 1/2, so the transmission rate in each beam is 1.2R, where R is the total uncoded data rate computed from the NASA Traffic Model A for CPS to CPS and CPS to trunking traffic. Five cities lie in the heaviest rain region of the country (Miami, Tampa, Jacksonville, Atlanta, and New Orleans). An additional 50% bandwidth is given to these five beams to allow increased carrier spacing and to reduce crosstalk. Therefore, the transmission rate in each such beam is 1.5 x (1.2R).

The traffic matrix of table 7-3 shows the approximate distribution of traffic among the 31 beams. The traffic T_{ij} in Mb/s from beam i to beam j is

$$T_{ij} = \frac{R_i R_j}{\sum_{i=1}^{31} R_i} = \frac{R_i R_j}{3755} \qquad (7.2)$$

where R_j and R_j is the total traffic in beam i and beam j, respectively. For example, the traffic from beam 2 to beam 12 (from New York/Philadelphia to Atlanta) is

$$T_{2,12} = \frac{254 \times 70}{3755} = 4.7 \simeq 5.$$

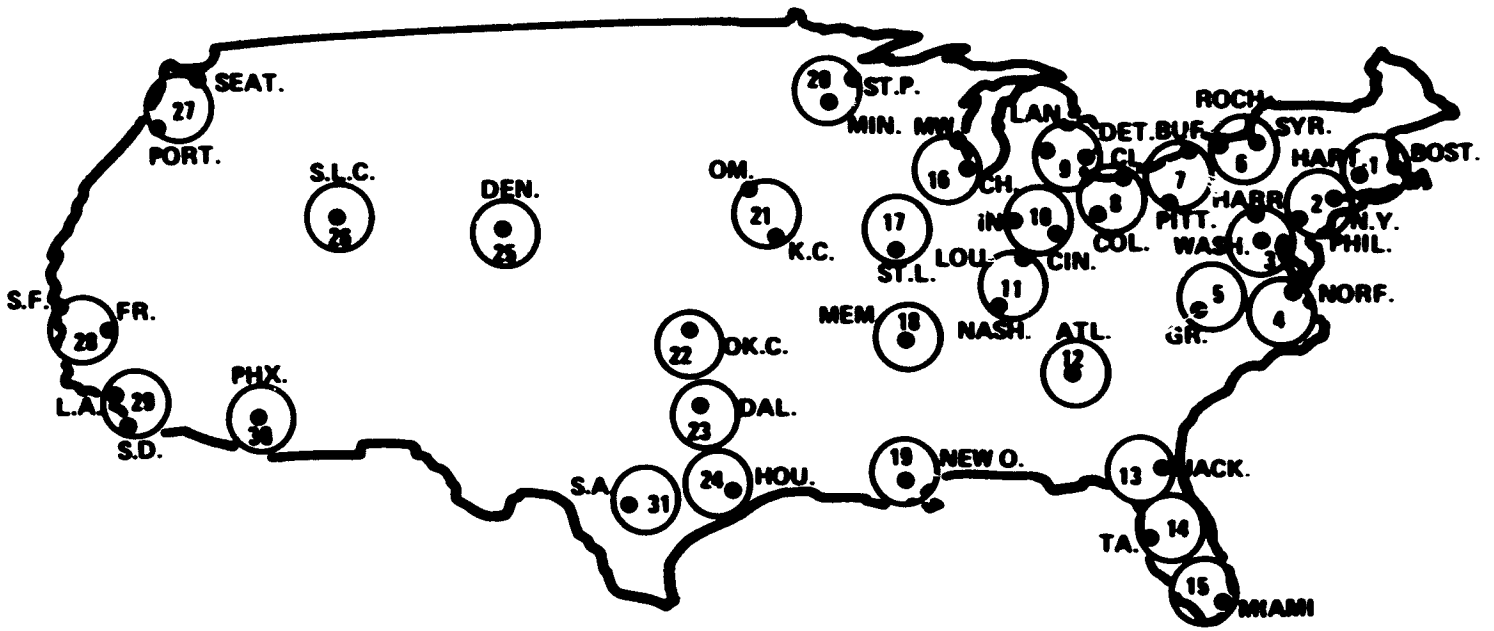

Figure 7-1. CONUS from 90° Longitude Showing 31 Beam Plan for Traffic Model A

Table 7-2

Channel Data Rate Distribution for Beam Plan A

BEAM NUMBER (J)	CITIES IN BEAM	DATA RATE/BEAM (R_j) (Mb/s) WITH CODING FACTOR OF 20%	
		1.2 R	(1.2 R 1.5)*
1	Boston/Hartford	70	
2	New York/Philadelphia	254	
3	Washington/Harrisburg	181	
4	Norfolk	40	
5	Greensboro	151	
6	Syracuse/Rochester	133	
7	Buffalo/Pittsburgh	145	
8	Cleveland/Columbus	99	
9	Detroit/Lansing	181	
10	Indianapolis/Cincinnati	203	
11	Nashville/Louisville	70	
12	Atlanta	47	(70)
13	Jacksonville	30	(45)
14	Tampa	145	(218)
15	Miami	61	(92)
16	Chicago/Milwaukee	328	
17	St. Louis	48	
18	Memphis	30	
19	New Orleans	82	(122)
20	Minneapolis/ St Paul[+]	61	
21	Omaha/Kansas City	65	
22	Oklahoma City	40	
23	Dallas	80	
24	Houston	102	
25	Denver	47	
26	Salt Lake City	139	
27	Seattle/Portland	174	
28	San Francisco/Fresno	100	
29	Los Angeles/San Diego	292	
30	Phoenix	145	
31	San Antonio	30	
	Total:		3755 Mb/s

*With expansion factor of 50% for beams in rain region E.
[+]Counted as one city

Table 7-3

Traffic Matrix for CPS to CPS and CPS to Trunking Traffic in Traffic Model A Assuming a Distribution in Proportion to Total Traffic in an Uplink Beam (Entry i, j - $R_i R_j / \sum_i R_i$ to Nearest Mb/s Constrained to ≥ 1 Mb/s)

Uplink Beam \ Downlink Beam	1	2	3	4	5	6	7	8	9	10	11	12	13	14	15	16	17	18	19	20	21	22	23	24	25	26	27	28	29	30	31
1	1	5	3	1	3	2	3	2	3	4	1	1	1	4	2	6	1	1	2	1	1	1	1	2	1	3	3	2	5	3	
2	17	12	3	10	9	10	7	12	14	5	5	3	15	6	22	3	2	8	4	4	3	5	7	3	9	12	7	20	10		
3		9	2	7	6	7	5	9	10	3	3	2	11	4	16	2	1	6	3	3	2	4	5	2	7	8	5	14	7	1	
4			1	2	1	2	1	2	2	1	1	1	2	1	3	1	1	1	1	1	1	1	1	1	1	2	1	3	2	1	
5				6	5	6	4	7	8	3	3	2	9	4	13	2	1	5	2	3	2	3	4	2	6	7	4	12	6	1	
6					5	5	4	6	7	2	2	2	8	3	12	2	1	4	2	2	1	3	4	2	5	6	4	10	5	1	
7						6	4	7	8	3	3	2	8	4	13	2	1	5	2	3	2	3	4	2	5	7	4	11	6	1	
8							3	5	5	2	2	1	6	2	9	1	1	3	2	2	1	2	3	1	4	5	3	8	4	1	
9								9	10	3	3	2	11	4	16	2	1	6	3	3	2	4	5	2	7	8	5	14	7	1	
10									11	4	4	2	12	5	18	3	2	7	3	4	2	4	6	3	8	9	5	16	8	2	
11										1	1	1	4	2	6	1	1	2	1	1	1	1	2	1	3	3	2	5	3	1	
12											1	1	4	2	6	1	1	2	1	1	1	1	2	1	3	3	2	5	3	1	
13												1	3	1	4	1	1	1	1	1	1	1	1	1	2	2	1	3	2	1	
14													13	5	19	3	2	7	4	4	2	5	6	3	8	10	6	17	8	2	
15														2	8	1	1	3	1	2	1	2	2	1	3	4	2	7	4	1	
16															29	4	3	11	5	6	3	7	9	4	12	15	9	26	13	3	
17																1	1	2	1	1	1	1	1	1	2	2	1	4	2	1	
18																	1	1	1	1	1	1	1	1	1	1	1	2	1	1	
19																		4	2	2	1	3	3	2	5	6	3	9	5	1	
20																			1	1	1	1	2	1	2	3	2	5	2	1	
21																				1	1	1	2	1	2	3	2	5	3	1	
22																					1	1	1	1	1	2	1	3	2	1	
23																						2	2	1	3	4	2	6	3	1	
24																							3	1	4	5	3	8	4	1	
25																								1	2	2	1	4	2	1	
26																									5	6	4	11	5	1	
27																										8	5	14	7	1	
28																											3	8	4	1	
29																												23	11	2	
30																													6	1	
31																														1	

Here it is assumed that $T_{ij} = T_{ji}$, which is an approximation because the cross-traffic between CPS and trunking users is not symmetrical. Traffic matrix entries have been rounded in the usual manner except that numbers smaller than 0.5 are replaced by 1 and not rounded to 0 in order to provide at least some connectivity.

The following beam isolation rules are applied. Beams which lie less than $2\theta_0$ apart cannot operate on the same frequency band under any circumstances. Beams which lie between $2\theta_0$ to $3\theta_0$ apart can use the same frequency band only if cross-polarization is used. The extra 20 dB cross-polarization isolation will help achieve a total 40-dB isolation in this case. Beams which lie more than $3\theta_0$ apart can use the same frequency band even with the same polarization. Unfortunately, the resulting beam isolation in this case is not much more than 20 dB according to the CCIR curve shown in figure 7-2 (CCIR, 1978).

In the beam plan of figure 7-1, many beams lie less than $2\theta_0$ apart. This can be indicated in graphical form with a solid line (branch) connecting the two beams (nodes). When two beams lie from $2\theta_0$ to $3\theta_0$ apart their nodes are connected with a dashed line. The resulting graph is shown in figure 7-3. This graph can be used for establishing a possible set of polarizations for the beams.

Starting at an arbitrary node, say, node 5 (representing beam 5, Greensboro), arbitrarily assign a horizontal polarization to it (H for horizontal, V for vertical): follow a dashed line to another node, say node 2, which must be assigned a vertical polarization. Continue this procedure along dashed lines until all nodes are assigned a polarization.

Conflicts can arise. For example, in going from node 5 to node 6 to node 8 to node 5 (a closed loop formed from an odd number of nodes), the same polarization must be assigned to two adjacent nodes, e.g., H to both nodes 5 and 8. Therefore, the adjacent nodes in question must be connected with a solid line, signifying that the corresponding beams cannot use the same frequency band.

The next task is to partition the 31 beams into several groups determined by constraints in sharing frequency bands. The three major traffic centers are beam 16 (Chicago/Milwaukee) with 328 Mb/s, beam 29 (Los Angeles/San Diego) with 292 Mb/s, and beam 2 (New York/Philadelphia) with 254 Mb/s. These three beams are a natural choice for the nuclei of three groups.

Since beam 16 is the busiest, it and its immediate neighbors, beam 10 (Cincinnati/Indianapolis), beam 9 (Detroit/Lansing), and beam 17 (St. Louis) are examined first. Since beams 10, 9 and 17

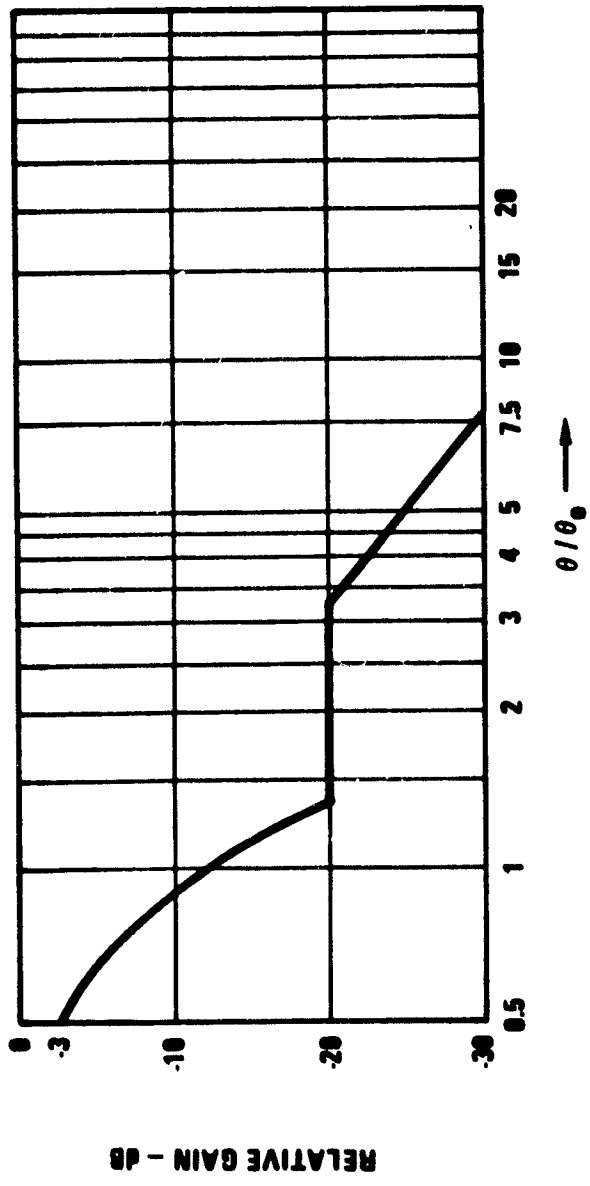

Figure 7-2. Typical Worst-Case Antenna Gain Relative to Peak Gain as a Function of Angle θ from Beam Center Normalized by 3-dB Beamwidth θ_0

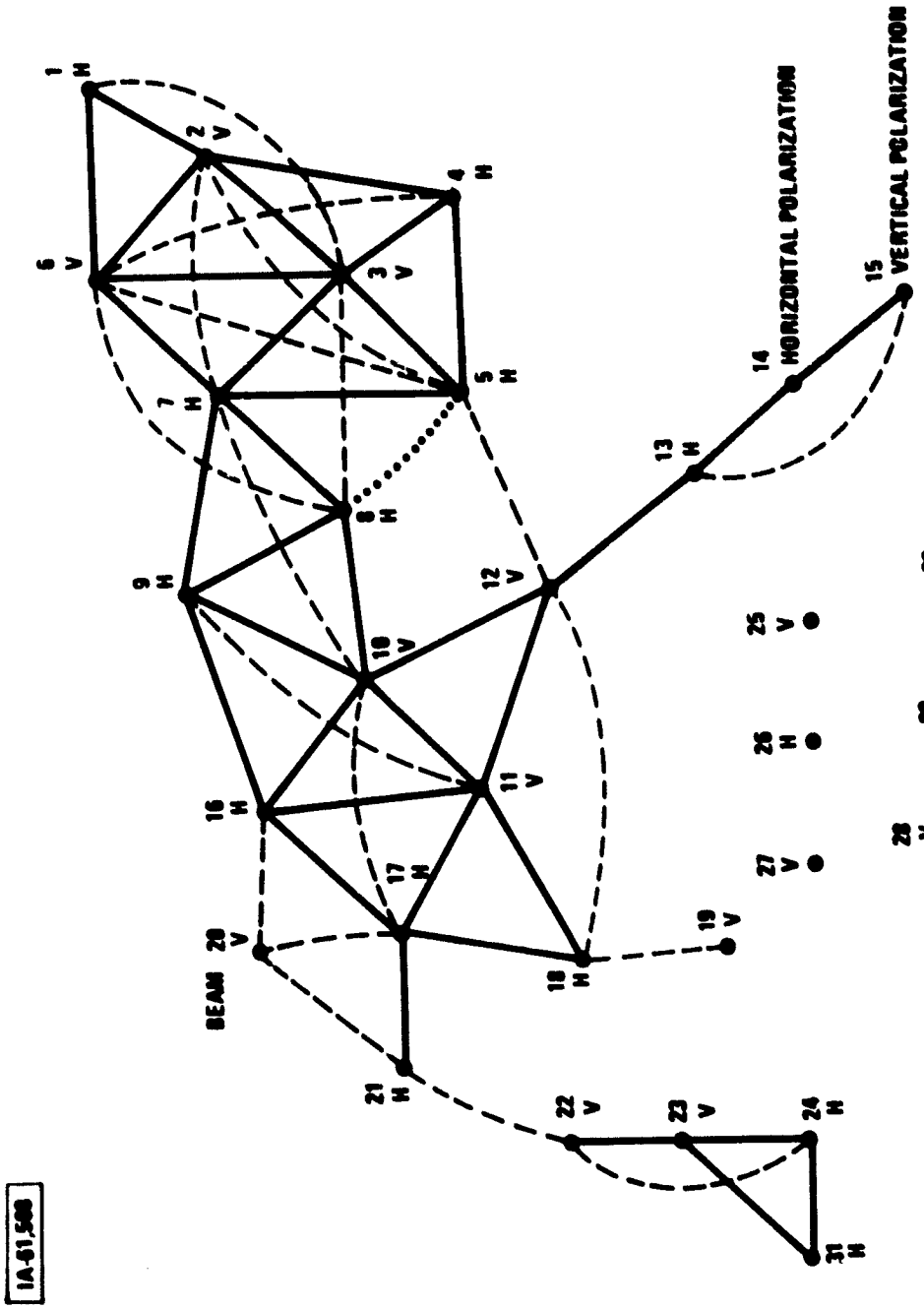

Figure 7-3. Graph Corresponding to the Interbeam Separation for The Beam Plan of Figure 7-1.

are less than $2\theta_o$ away from beam 16, all four beams must use a different frequency band from beam 16. The total traffic of this group is 760 Mb/s. With a nominal Hz/(b/s) factor of 1.25, this group will occupy nearly all the 1 GHz bandwidth planned to be allocated to CPS traffic. If more beams were included, the available CPS bandwidth would be exceeded. Therefore, these four beams will form the Chicago group named after its largest city.

Now, because the total CPS traffic is 3755 Mb/s, it is logical to search for five disjoint non-interfering groups with about 760 Mb/s of traffic per group.

Another natural group is formed by beams 2, 3, 4, 1, and 6. The total traffic for these five beams is 678 Mb/s, short of the 760 Mb/s goal. Beam 5 (Greensboro) with 151 Mb/s, etc., cannot be included because it will increase the total traffic too much. After some cut and try attempts, it turns out that beam 20 can be added to yield a total of 739 Mb/s. The Chicago group is isolated from the New York group, and they can therefore use the same frequency band without interference.

Beams 7, 8, and 5 are between these two groups. If the Florida beams 13, 14, and 15 are included in a kind of a vertical slice through the country, a 750 Mb/s Tampa group is obtained.

Similarly, the Los Angeles group includes beams 29, 30, and 28. The question is which other beams should be part of this group? Beams 23, 24, 31, and 22 have too much traffic. If beams 25 and 27 are included, there would be five beams in the Los Angeles group, but this would leave ten beams for the last group. This is not desirable because the insertion loss penalty in attempting to combine ten beams would be too great. Therefore, beams 12, 11, 18, and 21 are added to the Los Angeles group for a total traffic of 772 Mb/s.

The last group includes all remaining beams with a total of 734 Mb/s. This Seattle group is completely isolated from the other four groups in the sense that it cannot cause interference to the other groups, as shown in figure 7-3. The resulting graph of the five groups, showing the solid line constraints, is given in figure 7-4.

The next step is to establish a frequency plan for each group of beams. For example, the traffic matrix of figure 7-3 shows that 5 Mb/s are sent from beam 2 to beam 12. This implies that five 1 Mb/s bandwidth units or slots must be assigned for this traffic. Since beams 1, 3, 4, and 6 are too close to beam 2, they cannot use the same frequency allocations assigned to beam 2. However, beam 5 is $2\theta_o$ away from beam 2 and (with cross-polarization) can use the

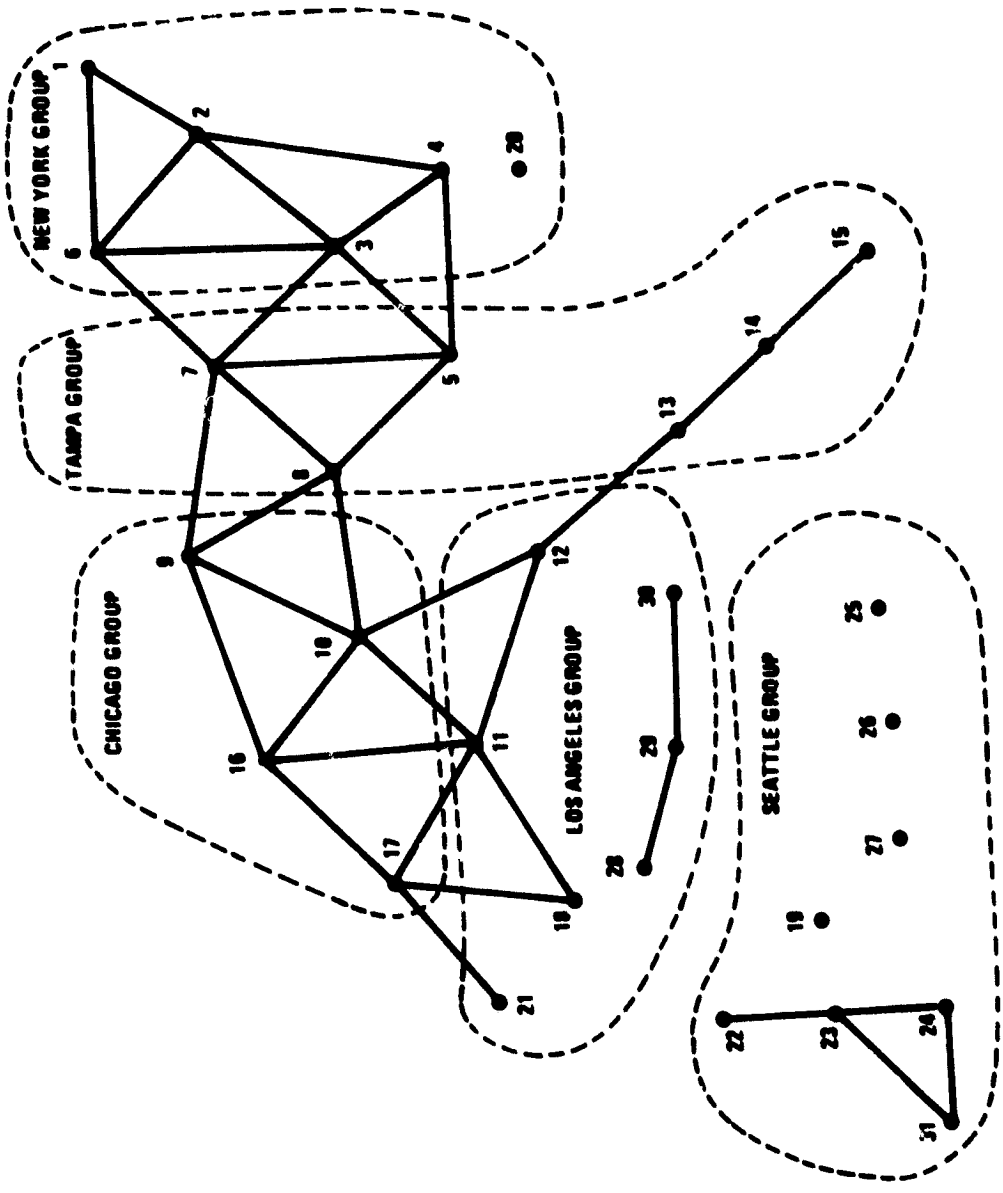

Figure 7-4. Resulting Graph of the Five Beam Groups

same band as beam 2. Therefore, beam 5 can use the frequency band prescribed by the traffic matrix to send four traffic units to beam 8. Note from figure 7-4 that the uplink beams 2 and 5 are isolated and the downlink beams 12 and 8 are isolated.

There are two general principles for establishing the frequency plan:

1. All beams in a group use distinct frequency bands; there is no frequency reuse among the beams of a group.

2. Bandwidths in a downlink beam should be contiguous. One way to accomplish this is shown in figure 7-5.

In more detail, the frequency plan proceeds as follows:

a) The traffic matrix entries for the traffic units from the Chicago group to the Chicago beam, (column 16, from rows 9, 10, 16, and 17) are examined. The largest number of units, 29, determines the assignment of the first 29 frequency units for the transmission from beam 16 to itself.

b) Next, the connected graph is examined to see which beams outside the Chicago group, if any, are connected to beam 16. Since node 11 is connected to node 16 in the 29-unit band for beam 16 to beam 16, transmission from or to beam 11 is forbidden.

c) When cut and try methods have completed the frequency assignments for the 29-unit band, a page of the overall frequency plan has been formed. When the entire section of bandwidth determined by traffic destined for beam 16 has been assigned, a book in the overall frequency plan has been completed.

The pages forming the first beam book are shown in figure 7-6. The transponder block diagram associated with this frequency plan is sketched in figure 7-7.

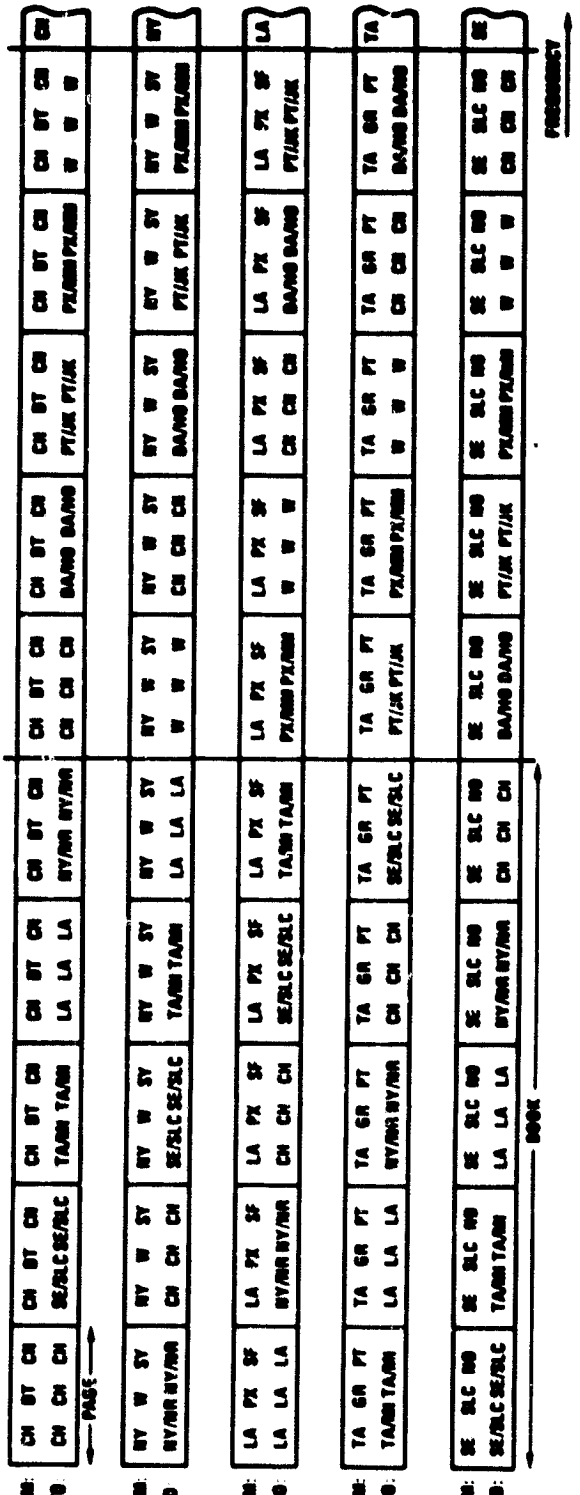

Figure 7-5. Sample Macroscopic Frequency Plan

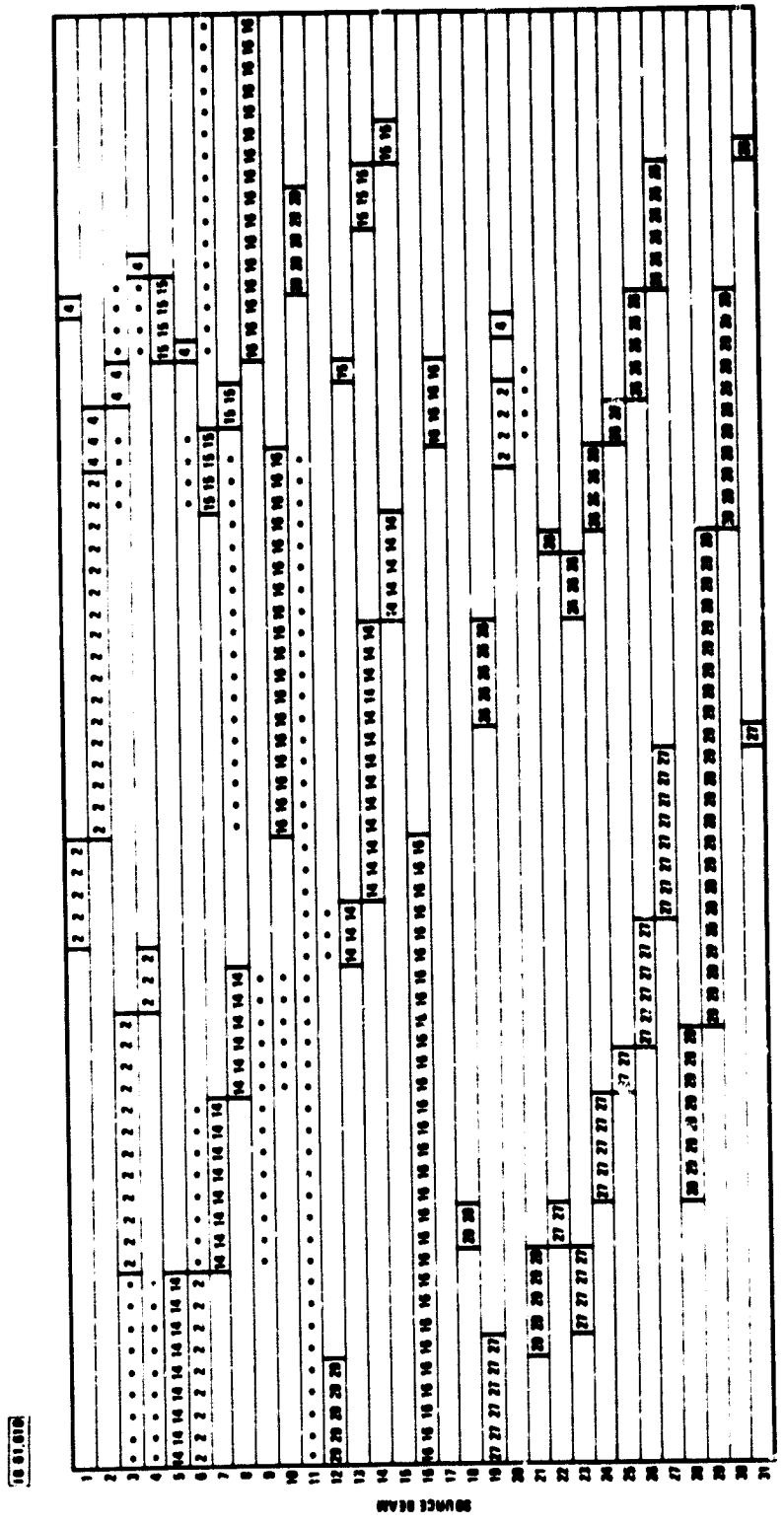

Figure 7-6. Sample Microscopic Frequency Plan Showing Destination Beams

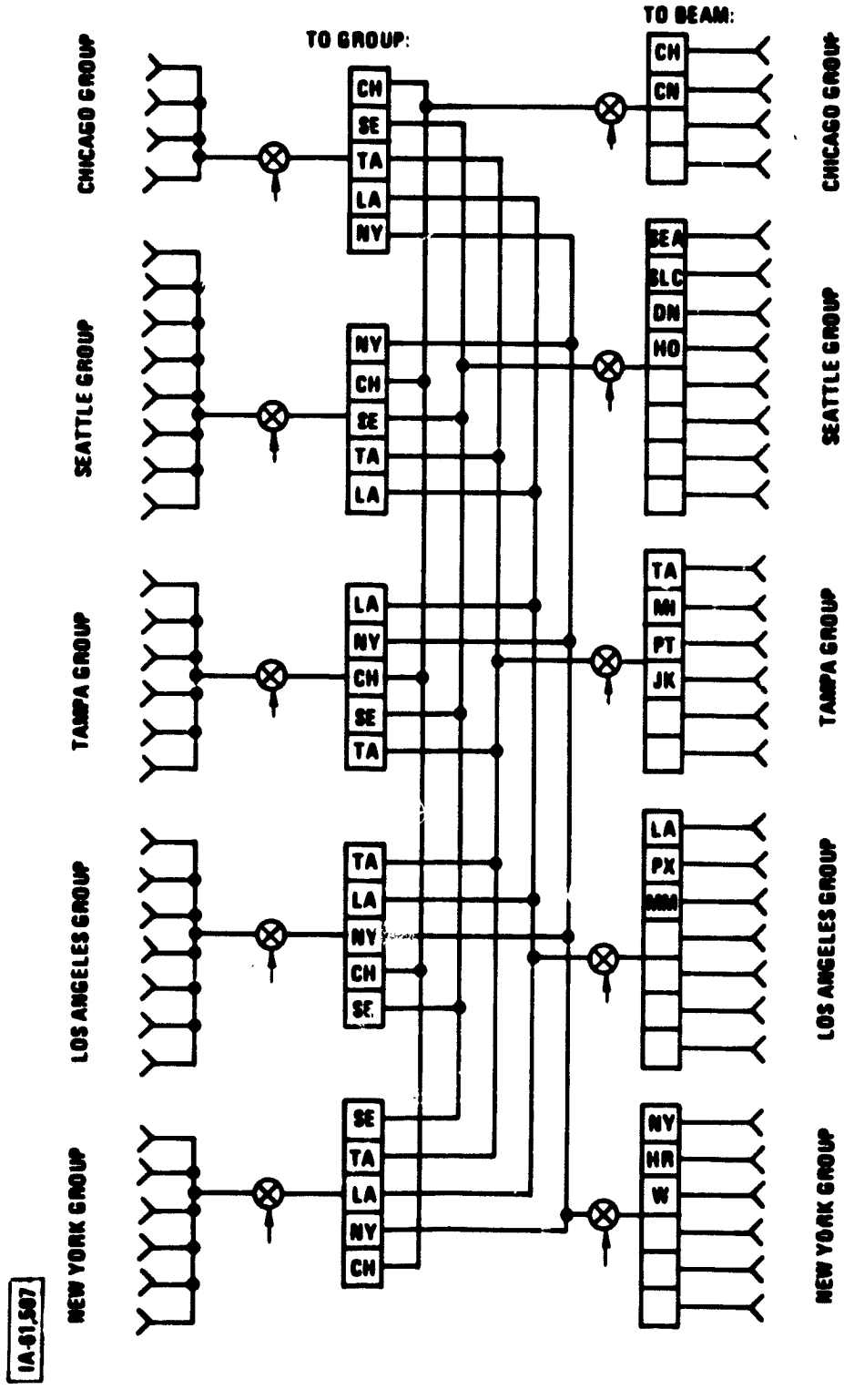

Figure 7-7. Transponder Block Diagram for Five Group Frequency Plan

CHANNELIZATION OF SATELLITE BANDWIDTHS

Some extra bandwidth should be included in each IF/RF path routed by the satellite to permit an acceptable blocking probability when users request channel connections on a first-come, first-served basis. For simplicity of illustration, suppose that each channel consumes the same bandwidth. Then, the greater the number of channels available, s, in a given satellite bandwidth, the lower the blocking probability B(s,a); for a fixed offered traffic load a, in Erlangs, and a fixed bandwidth utilization efficiency, ρ, or carried traffic load per channel the following relationship holds:

$$\rho = a(1-B(s,a))/s \qquad (7.3)$$

The parameter a represents the number of channels required and a(1-B(s,a)), the number of channels served. Any pair of the four variables s, a, B, and ρ may be specified independently, but then the other two variables are completely determined.

For example, suppose that a 20% bandwidth expansion is acceptable. This implies that $\rho = 0.8$. A $B(s,a) = 0.005$ is desirable for a 99.5% CPS availability. This results in $s \approx 90$ from the standard blocked-calls-cleared Poisson queueing model (Katz, et al., 1979), and $a \approx 72$ from equation (7.3). Thus, a 90-channel bandwidth is required to service 72 channels with an availability of 99.5% and an 80% bandwidth utilization.

If there is a total of about 140 56 kb/s data channels to be serviced, for instance, then two separate satellite bandwidths of $1.44 \times 90 \times 56$ kb/s $\approx$ 7.3 MHz each are required. Here the modulation and coding bandwidth expansion factor of $1.2 \times 1.2 = 1.44$ is employed. Other examples can be constructed using blocking formulas and queueing theory curves available in the literature.

SWITCHING CONCEPT

One of the advantages of FDMA is that satellite switching is not a fundamental requirement. However, some switching may be necessary to accommodate periodic or long term changes in traffic flows. For example, it may be necessary to increase the bandwidth assigned to certain beams at the expense of other beams. This might be done on a daily basis to handle the redistribution of busy-hour vs. non-busy-hour traffic. In addition, unforeseen changes in the traffic matrix may develop in the course of several years of satellite operation. It is desirable to be able to handle such changes in beam capacities without a large impact on spacecraft design. A satellite switch may be required for the necessary

bandwidth expansion flexibility in beams which are bandwidth limited in the basic hard-wired design.

NASA/LeRC has suggested the following criterion for redistributing beam capacities. If a given beam has a traffic demand that is less than 1.5 times the average beam capacity, then the spacecraft must be able to adapt to a 50% change in traffic in that beam; otherwise, a 30% change in traffic in that beam must be accommodated.

For instance, with a total CPS traffic of 3.8 Gb/s and 32 beams, 1.5 times the average beam capacity is approximately 178 Mb/s. The Boston/Hartford beam has a CPS to CPS traffic demand of 58 Mb/s according to the Traffic Model A. Since this is less than 180 Mb/s, a 50% or 29 Mb/s increase in CPS to CPS beam traffic must be accommodated. For a 1.44 bandwidth to data rate expansion factor, this implies that 1.44 x 29 Mb/s ≈ 42 MHz of additional bandwidth must be made available to the Boston/Hartford beam. Similarly, the Chicago/Milwaukee beam has 273 Mb/s of CPS to CPS traffic, which means a potential beam bandwidth expansion capability of 1.44 x 273 Mb/s x 0.3 ≈ 118 MHz. The smallest bandwidth expansion of 18 MHz occurs in the Jacksonville beam. Even though the Chicago/Milwaukee beam has the heaviest traffic, the Indianapolis/Cincinnati beam requires the greatest bandwidth expansion of 1.44 x 169 Mb/s x 0.5 ≈ 122 MHz, since the latter beam traffic falls just below the 180 Mb/s threshold.

Therefore, the bandwidth expansion range for the 32-beam plan is roughly 18 to 122 MHz. One way to implement beam bandwidth changes is to employ satellite switches which rearrange the input/output connections of a collection of IF bandwidth filters. For maximum flexibility, the bandwidths of these filters should probably be distributed roughly according to powers of two with the largest and smallest bandwidths corresponding to the upper and lower end of the bandwidth expansion range, respectively. Specifically, there might be one 128 MHz bandwidth filter, two 64 MHz filters, four 32 MHz filters, and eight 16 MHz filters available for switching. The optimum mix requires further analysis and would depend on the actual beam plan and traffic model employed. Several switches could be employed, one for each group of beams. The number of inputs to each switch would equal the number of bandpass filters in the collection mentioned above, in this case 15. The number of switch outputs could equal the number of beams, e.g., 32. Although the total number of crosspoints of each switch might be 15 x 32 = 480, considerably fewer crosspoints could be activated simultaneously to realize significant beam bandwidth expansions.

REFERENCES

(CCIR, 1978) CCIR Report 558-1, figure 11, in Recommendations and Reports of the CCIR, 1978, Vol. IV, XIV Plenary Assembly, Kyoto, Japan, 1978.

(Katz, et al., 1979) J. L. Katz, et al. "Final Report - Application of Advanced On-Board Processing Concepts to Future Satellite Communications Systems," MTR-3787, Vol. I, F19628-79-C-0001, Bedford, MA 01730: The MITRE Corporation, June 1979.

SECTION 8

POWER DIVERSITY FOR ADAPTIVE RAIN COMPENSATION

Network control issues for earth station transmitter power diversity are discussed. The feasibility of satellite downlink power diversity is examined quantitatively. Possible means of sensing propagation attenuation and controlling power diversity from the satellite are explored.

NETWORK CONTROL ISSUES

Some rain attenuation compensation techniques require the use of centralized network control mechanisms. Along with providing power diversity control, these control systems can offer the users automatic demand assignment multiple access (DAMA) operation, automatic fault diagnostics, and status monitoring with record keeping. In addition, billing, satellite control, operator-assisted calls and switch reconfigurations can also be handled by the control system.

Implementation of central control systems may involve the use of one or more common signaling channels (CSCs) and a network control center (NCC). GE suggested the use of one CSC per beam and dedicated frequency bands for network control using a TDM signaling format. Before investigating these systems, the concepts of ground-controlled rain attenuation compensation techniques for SR-FDMA systems are examined to provide a background to the design of the network control.

Power Adaptation to Compensate for Link Fading

One possible solution to the problem of uplink rain attenuation is to require all users affected by rain to boost their uplink power to overcome the uplink fade. Users transmitting to a user in the rain also boost their uplink power in order to overcome the downlink fade suffered by the user in the rain. An alternative for downlink fade compensation is to require the satellite to boost its downlink power to the user in the rain.

In order to understand the implications of power adaptation, two examples are studied. The network has 12 users (U_1 through U_{12}), a linear satellite, and four uplink and four downlink beams. Each uplink (downlink) beam supports three users. Beams 1, 2, 3,

and 4 contain users U_1 - U_3, U_4 - U_6, U_7 - U_8, and U_9 - U_{12}, respectively. Also, in both examples, user U_2 is suffering from rain attenuation. User U_2 is currently communicating with user U_{11}. In the first example, both U_2 and U_{11} boost their uplink power to overcome the fade on the uplink from or downlink to U_2. As shown in figure 8-1, as long as U_2 does not overcompensate, there will be no increases in satellite intermodulation interference on the U_2-to-U_{11} link. However, when U_{11} boosts his uplink power, the satellite intermodulation interference increases in the satellite RF path containing the U_{11} to U_2 signal. In addition, if U_{11} is also transmitting to users U_7 and U_9, user U_8 will also suffer from increased intermodulation interference due to power-robbing.

The second example, shown in figure 8-2, avoids the intermodulation problems found in the first example because the satellite boosts its downlink power. This is useful in overcoming the downlink fade on the U_{11}-to-U_2 link. However, satellite power is wasted on the downlink beams to users U_1 and U_3. As in the first example, user U_2 boosts his uplink power to maintain the U_2-to-U_{11} link.

Selecting one scheme rather than the other requires knowing more about the available satellite power, the link budgets, the network parameters (number of users, number of beams and the data rates, etc.), rain margins, and the associated control problems. The problem of network control is investigated next.

Central Control of Power Diversity Schemes

In order to implement a power diversity scheme, control commands must be issued to the users and/or the satellite to increase or decrease the power output on the link(s) being affected by rain. If a form of centralized network control is implemented, those commands are issued from an NCC and are transmitted over CSCs. In addition, status reports from the users arrive at the NCC via the CSCs. (DAMA, billing, and diagnostics operations are also carried out between the NCC and the users via the CSCs.)

A distributed closed loop control scheme could also be considered. Here each earth station would monitor its own uplink/downlink via the CSC beacon. Reductions in signal strengths are interpreted as fades. The uplink power is boosted by increments under microprocessor control until the signal level is deemed adequate. Status reports are sent to the NCC so that a possible override capability can be exercised.

IA-62,062

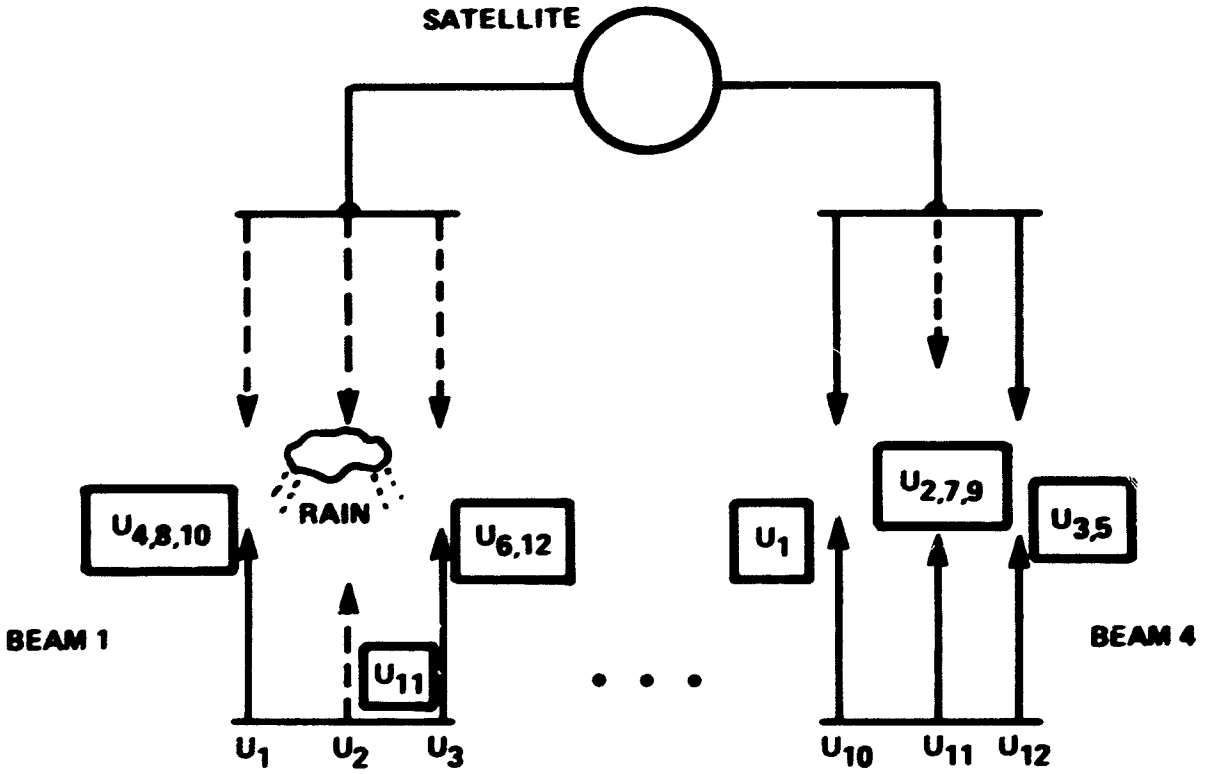

① SATELLITE BOOSTS DOWNLINK BEAM POWER TO AVOID INTERMODULATION PROBLEMS ON THE U_{11} - U_2 LINK

② USER U_2's BOOSTS UPLINK POWER

Figure 8-1. The Concept of Power Adaptation to Compensate for Fade (System 1)

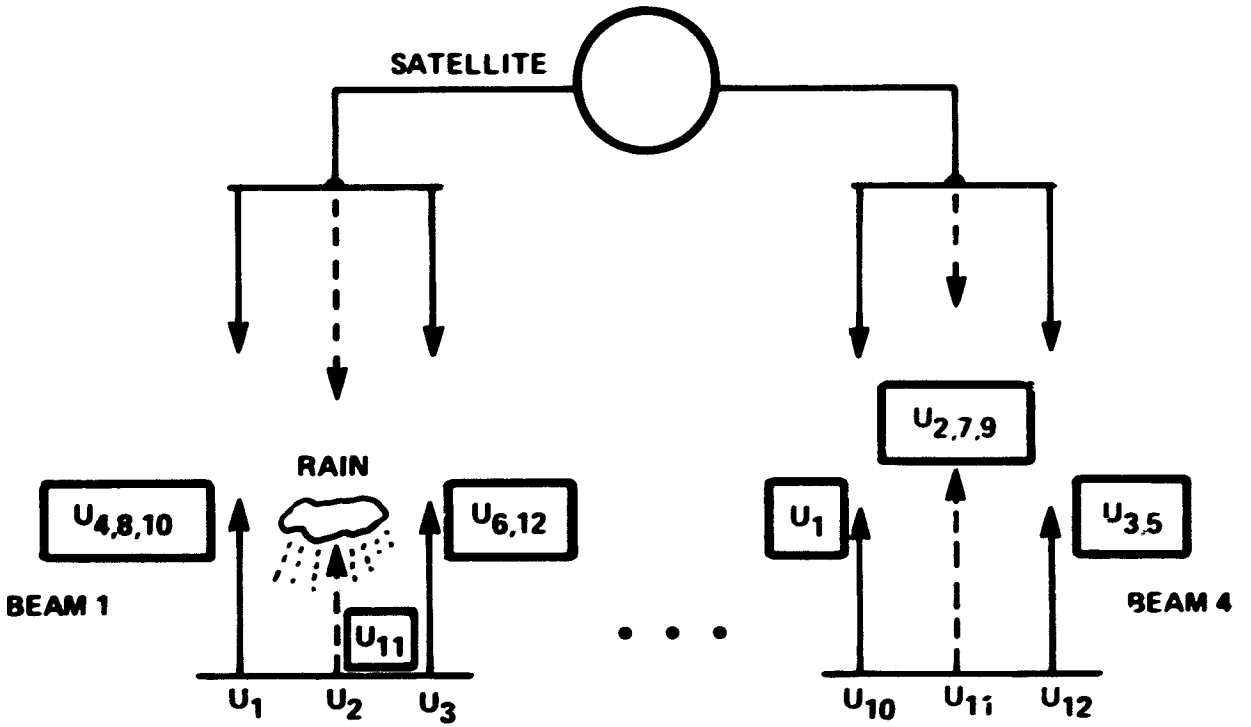

① LINK U_2 - U_{11} SUFFERS FROM UPLINK RAIN ATTENUATION

② LINK U_{11} - U_2 SUFFERS FROM DOWNLINK ATTENUATION

③ SATELLITE INTERMODULATION INTERFERENCE INCREASES WITH INCREASES IN U_{11}'s UPLINK POWER

Figure 8-2. The Concept of Power Adaptation to Compensate for Fade (System 2)

In a 1980 report to NASA (Kiesling, 1980), General Electric presented their approach for a network control system that handles power diversity operations and other communications-related functions. Their control scheme is reviewed here briefly.

GE Approach to Central Control

In the GE concept, each earth station measures the level of the received power in the CSC. Reductions in this power level are interpreted as fades and a quantized description of level changes are transmitted to the NCC. The NCC processes such data from all earth terminals and provides instructions to individual earth stations which control their transmitter power adaptation. The satellite transponders operate at constant gain throughout this procedure.

For ease of analysis, they assumed that power would be boosted at an earth terminal by a fixed amount, say 20 or 30 dB. Ideally, step-wise changes in transmitter power would be more effective. Over compensation can cause intermodulation interference, as mentioned previously. Since rain induced attenuations last in the order of minutes and because high speed computer processing can be accomplished quite rapidly, the control system response time is dominated by propagation and queueing delays which should not exceed several seconds. Since the connectivity between any pair of users typically lasts for at least tens of seconds, a response time of several seconds is quite adequate for power adaptation control.

GE performed an extensive statistical analysis involving desired availability, carrier-to-noise ratio, number of excited carriers, and the total margin defined as the sum of an interference margin and a fade margin. Their study showed that there exists a broad minimum for the total fixed margin in a proper FDMA system design. Results were presented for the overall signal-to-noise ratio (SNR) versus the number of excited carriers as a function of the signal-to-thermal noise ratio, and for the required signal-to-thermal noise ratio versus the fade margin as a function of intermodulation interference, polarization isolation, and co-channel interference. Analyses such as these should be quite useful in future system designs of the FDMA alternative.

MITRE verified certain portions of the GE analysis with regard to the preference for more rather than fewer carriers in a given satellite bandwidth. To verify GE's results, MITRE assumed that the terminals are uniformly distributed and the probability of a fade at one terminal is independent of the probability of a fade at another terminal. This suggests that terminals are spaced at least 15 km

apart. If the diameter of a coverage area is approximately 500 km, up to about 1,000 terminals can be accommodated under these conditions. It is further assumed that the satellite downlink power is fixed at a level which is sufficiently large to accommodate up to M_0 excited uplink carriers while still maintaining adequate SNRs for all the channels in the downlink beam. The satellite is assumed to be linear to a first approximation, i.e., there is no suppression in weak uplink signals, only power robbing. If the satellite power in the downlink beam is fixed at P_0, and if there are a total of N terminals in the beam, and M excited uplink terminals transmitting to that beam, then N - M terminals have a downlink power X, and M terminals have a downlink power $Y = D_0X$, where D_0 is the fixed level for a dynamic margin of, say, 20 dB.

If the values assumed by GE for a 99.99% availability level are used (too stringent for CPS), with 1,000 carriers per beam there can be up to 12 excited carriers and a dynamic margin of 20 dB, while still closing all the downlinks. If X = 1 W and Y = 100 W, with 12 excited carriers, P_0 = 2188 W. Therefore, with no excited carriers X would be approximately 2.19 W for every downlink carrier in the beam. On the other hand, with only 100 carriers in a beam, the equivalent performance is achieved with no more than four excited carriers. The total power in a beam in this case is P_0 = 496 W, or approximately 5 W per downlink carrier with no excited carriers. Thus, the downlink power per carrier is only 40% in the 1,000 carrier per beam case compared to the 100 carrier per beam case. This is consistent with the GE conclusion that wider bandwidth transponders handling more carriers per beam should be employed.

Single Modem Considerations for Small Earth Terminals

GE dedicated a modem to the common signaling channel (CSC). This has several advantages: the CSC is always available, there are fewer synchronization problems, and the modem is less complex than if the modem were shared with communications functions. However, there is a possible disadvantage for a small single-channel earth terminal which might be able to utilize a single modem for both signaling and communications. This is feasible because the common signaling functions tend to be low duty cycle compared to the communications function.

MITRE examined several alternatives for incorporating signaling functions into a single communication modem. In the first approach, a dedicated frequency band was allocated to the signaling function for a small fraction of the time. Since the terminal already has ample frequency agility for assigning a comunications carrier frequency according to the message destination, an additional

frequency slot for signaling is a minimal extension of capability. Periodically the terminal would dwell in the signaling frequency band to accomplish network control functions. Since the satellite signaling channels must be shared, the same signaling frequency band could be assigned to each user in a beam but to be used at a distinct time interval. This way there would be no interference among users in a beam during their signaling functions. However, this architecture has the disadvantage of lost traffic when one user is trying to communicate with another that is performing its signaling functions.

In a preferred architecture, each user in a beam can signal at the same time, but at fixed, disjoint frequency bands. The signaling times among beams can be staggered for non-overlaps so that the satellite signaling hardware is dedicated to one beam at a time, using the same signaling bandwidth for every beam. In this way, less communications time is lost due to signaling compared to the first architecture.

FEASIBILITY OF DOWNLINK POWER DIVERSITY

General Electric has restated an attractive power diversity concept for earth station transmitter power control which can reduce primary power requirements on-board a satellite (Kiesling, 1980). If the satellite must service a large number of coverage areas in CONUS, a large fixed distribution of satellite power to downlink beams might be avoided by adaptively sharing a smaller total power among the downlink beams according to the varying attenuations experienced within the beam areas. Extra power would be allocated to the relatively few beams encountering rain, and the margins of the remaining beams would be reduced accordingly. A few heavy or many lighter rain occurrences, if fully compensated, may require inordinate amounts of satellite power and lead to system instabilities. The feasibility of providing limited power compensation with stability is examined quantitatively in this section.

A comprehensive rain model by R. K. Crane (Frediani, 1979) has been modified to yield a lower attenuation with frequency dependence at EHF. In addition, the rain loss statistics have been represented as an exponential probability density in the higher attenuation regions of interest (Kamal, Christopher, 1981). (See figure 8-3.) This model permits extensive high link availability rain attenuation calculations on a small computer while still agreeing reasonably well with existing rain attenuation measurements, which generally show an f^2 dependence of attenuation with frequency.

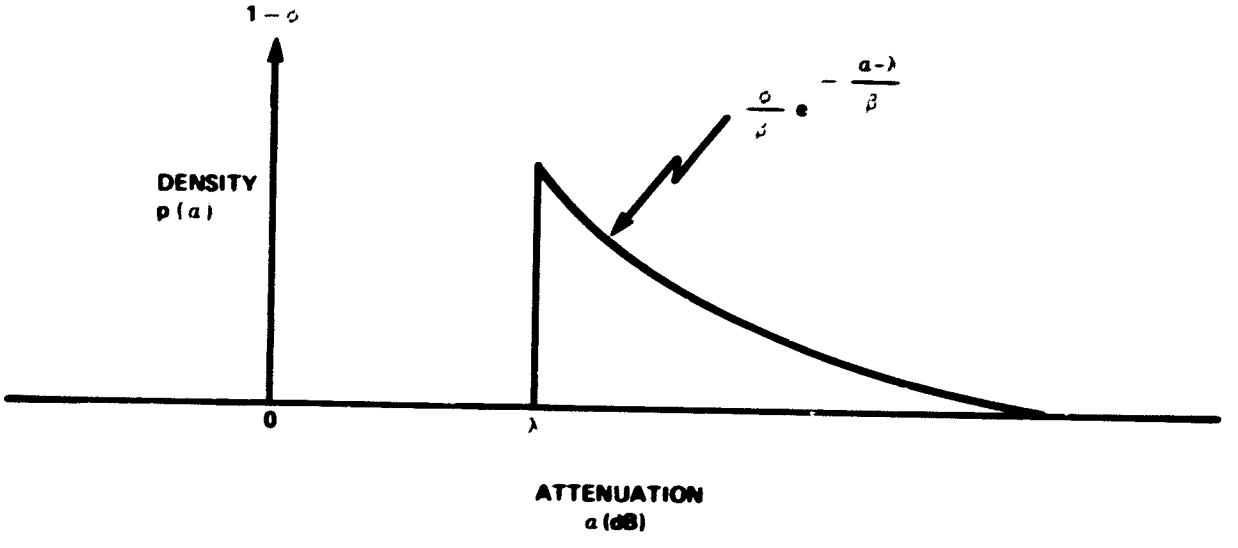

Figure 8-3. Assumed Rain Loss Probability Density Function

By converting the probability density function of downlink attenuation from decibels to the corresponding loss factor A by

$$A = 10^{\alpha/10} \tag{8.1}$$

$$p(A) = p(\alpha)\Big/\frac{dA}{d\alpha} \tag{8.2}$$

it can be shown that the mean and variance of the attenuation on a given downlink is

$$\mu_A = \bar{A} = \frac{(10 \log e)\,\phi}{\beta - 10 \log e} \exp\left(\frac{\lambda}{10 \log e}\right) + (1 - \phi) \tag{8.3a}$$

$$\sigma_A^2 = \overline{(A-\bar{A})^2} = \frac{(10 \log e)\,\phi}{2\beta - 10 \log e} \exp\left(\frac{2\lambda}{10 \log e}\right) + (1 - \phi) - \bar{A}^2. \tag{8.3b}$$

Note that the mean or variance of the power required to compensate a link modeled by the density of figure 8-3 can be infinite if the parameter β equals one or one-half times $10 \log_{10} e \approx 4.34$, respectively. In other words, rain losses on the downlink cannot be compensated, with many downlinks even in the statistical sense, for some combinations of rain, frequency, and elevation angle, at least for this rain model.

For M statistically independent downlinks, the distribution of downlink power required on the satellite will tend to a Gaussian distribution with a mean and standard deviation of $M\mu_A$ and $\sqrt{M}\sigma_A$, respectively, for large M. The ability of a satellite to satisfy downlink power demands can be found by subtracting the marginal satellite power required when the downlinks are shared, from the power necessary to support M separate downlinks with no power sharing. Suppose the desired single downlink availability is

$$P = 1 - \int_{A(P)}^{\infty} p(A)\,dA \tag{8.4a}$$

i.e., the link fade exceeds A(P) with probability 1-P. With M such downlinks and no power sharing, the marginal satellite power required is 10 log MA(P) (dB). With power sharing and large M, the marginal power required is approximately 10 log B(P) (dB) for the same overall availability

$$P = 1 - \frac{1}{\sqrt{2\pi M}\ \sigma_A} \int_{B(P)}^{\infty} \exp((B-M\mu_A)^2/2M\sigma_A^2)\ \text{dB}. \qquad (8.4b)$$

The satellite power margin advantage with power sharing is therefore given by 10 log MA(P)/B(P) (dB).

This advantage was computed as a function of frequency, with and without site diversity, for rain regions D (East Coast) and E (Florida), for M = 20, 50 and 100 downlink beams, for availabilities of P = 0.99, 0.999, and 0.9999, and for elevation angles of 10°, 20°, 30°, 40°, and 50°. For M = 100, angles less than 30° and frequencies above 17.5 GHz, essentially no power sharing advantage was observed. This is because complete power sharing implies allocation of whatever power is required for an arbitrarily deep rain fade. Therefore, the advantage of complete downlink power diversity is very doubtful.

However, if the satellite limits the power allocation in each downlink to that required for a link availability P_o, then power sharing can have a significant advantage. This requires a revised computation of the mean standard deviation of the downlink power distribution. The advantage of limited downlink power diversity is illustrated in figures 8-4 through 8-6 for P_o = 0.999. For example, limited power diversity has approximately a 5.5 dB advantage in region D for P = 0.999 with M = 100 downlink beams, an elevation angle of 30°, and no site diversity at 20 GHz (see figure 8-5A). The corresponding advantage for region E is about 10.5 dB.

Compensation for uplink rain has been discussed in section 5 and previously in this section. Since uplink fades will not be compensated exactly, the weaker signals entering the satellite will experience crosstalk interference. It is possible to calculate the crosstalk by estimating errors in compensating for uplink rain. Toward this end, the mean and variance of the conditional uplink attenuation factor A (given that it is raining) would be of interest. The conditional probability density function of the attenuation α_2 in dB is that of figure 8-1 with ϕ set to unity. The mean and variance of x are $\lambda + \beta$ and β^2, respectively. The parameters were computed for 30 GHz, single site diversity, a 30

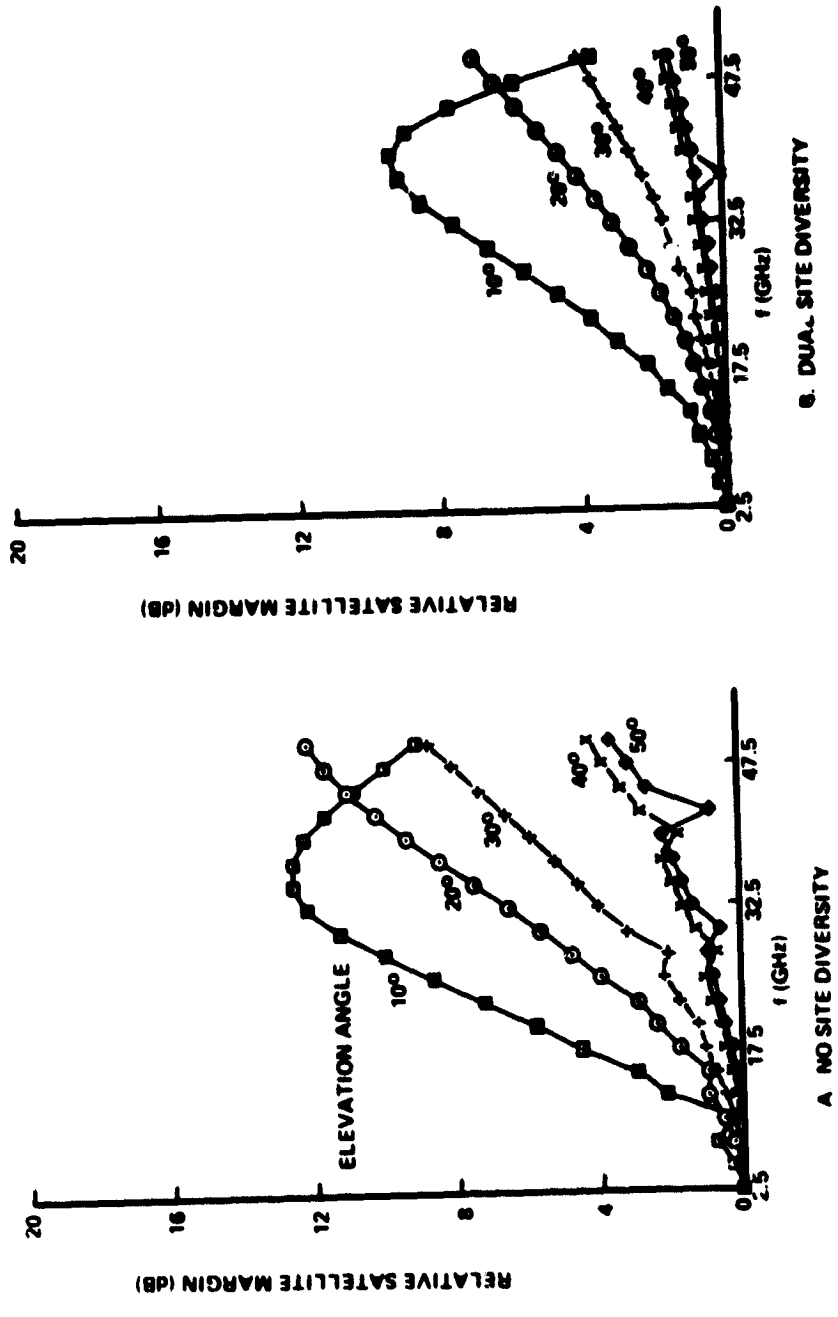

Figure 8-4. Satellite Margin Advantage Using Downlink Power Diversity Limited to P_0 = 0.999 Availability; P = 0.99, East Coast (Region D), M = 100 Beams

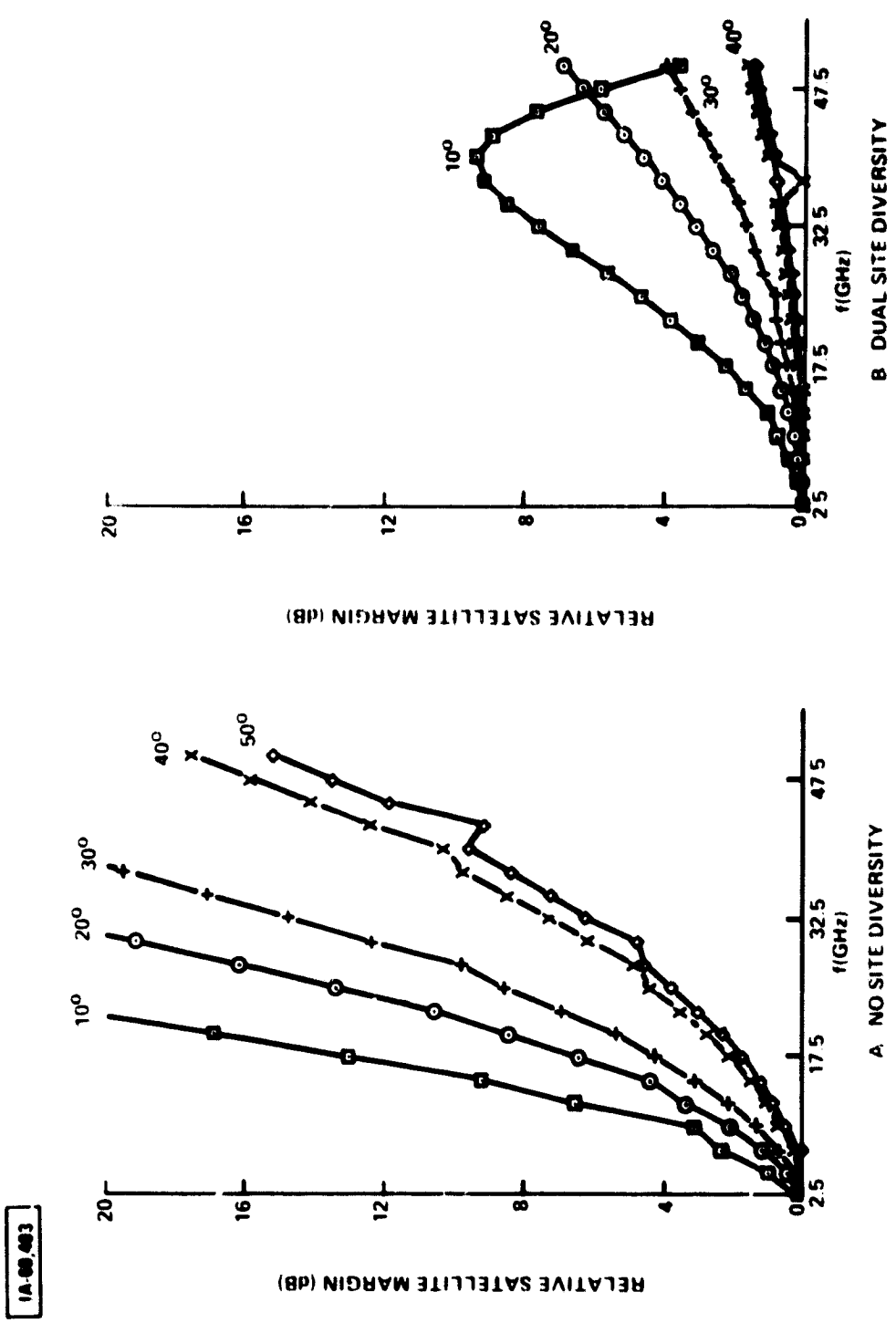

Figure 8-5. Satellite Margin Advantage Using Downlink Power Diversity Limited to P_o = 0.999 Availability; P = 0.999, East Coast (Region D), M = 100 Beams

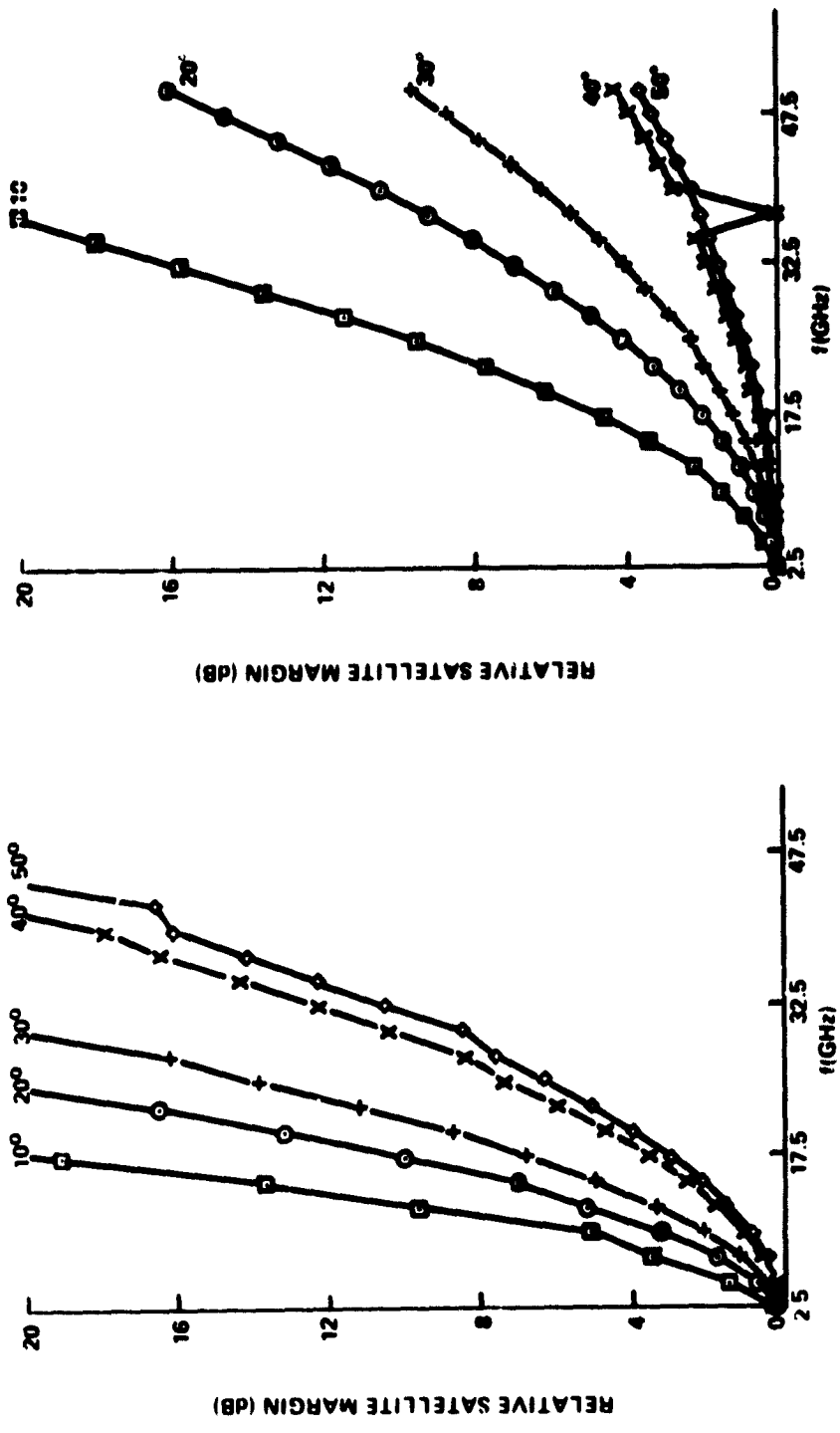

Figure 8-6. Satellite Margin Advantage Using Downlink Power Diversity Limited to P_o = 0.999 Availability; P = 0.9999, East Coast (Region D), M=100 Beams

IA-88,484

degree elevation angle, and each of the rain regions of CONUS. The results are compared in table 8-1.

Table 8-1

Attenuation Statistics for Conditional Rain Fade Probability Density

Region	Mean $\bar{A}_c$ (dB)	Standard Deviation (dB)	λ (dB)	β (dB)	$\lambda+\beta$ (dB)
B	4.22	1.66	2.34	2.71	5.05
C	4.44	2.05	2.44	2.84	5.28
D	8.48	8.72	3.51	5.46	8.97
E	18.86	22.66	4.42	11.63	16.05
F	3.60	0.43	2.23	2.18	4.41

POSSIBILITY OF POWER SENSING AND CONTROL AT THE SATELLITE

Sensing rain attenuation in each of the beams at the satellite itself may be useful. Satellite sensing and control may offer system economic advantages by avoiding multiple sensing sites on the ground, and by using only one atmospheric path for sensing or control, as opposed to multiple paths for the GE power control scheme.

During the past decade, Professor D. Staelin of M.I.T. has shown extensively (Staelin, 1969) that many atmospheric conditions can be sensed readily and accurately from satellites at geosynchronous altitude. One condition which can be sensed accurately is liquid water in the atmosphere (Staelin, et al., 1977). Passive microwave sensing at satellite altitude offers many possibilities; three are mentioned:

1. Each uplink 30 GHz beam can be radiometrically sensed at the satellite. The satellite could insist that each beam contribute constant power. If the power detected in beam (i) drops, the satellite commands all transmitters in beam (i) to raise their power. The disadvantages of this

sensing scheme are that all transmitters within more than 100 miles are raised together, whether they need it or not. Also, variations in number of ground sites might be interpreted as weather changes.

The advantages are that no sensing equipment is required at the ground stations, and a minimal number of intermodulation product surprises are introduced at the satellite because of constant power inputs.

2. Staelin (Staelin, et al., 1977) has shown that two separate radiometers, operating at 22 and 31 GHz, can yield very accurate measurements of liquid water content in the atmosphere. The 22 GHz radiometer reacts strongly with the water vapor content of the lower atmosphere and the 31 GHz radiometer reacts mostly with liquid water. By processing the two results, the ambiguity between the two sensors can be removed and liquid water content calculated.

The disadvantages of this two frequency passive microwave sensing include extra satellite weight and difficult measurements over land. This latter disadvantage may be too serious for use over CONUS. However, this method is not influenced by variations in the number of ground transmitters.

3. An infrared spectrometer can give estimates of liquid water content in the atmosphere. Over ocean areas, it would give less accurate rainfall rate estimates than 22/31 GHz radiometers, but it may be smaller and less costly.

An infrared spectrometer may be the most attractive passive sensing device for the satellite. Modest estimates of liquid water content of the atmosphere, combined with low weight and high resolution, may allow good system control at low system cost.

REFERENCES

(Frediani, 1979) D. J. Frediani, "Technology Assessment for Future MILSATCOM Systems: The EHF Bands," Project Report DCA-5, Lincoln Laboratory, M.I.T., P. O. Box 273, Lexington, MA 02173, 12 April 1979, Contract No. F19628-78-C-0002.

(Kamal, Christopher, 1981) A. K. Kamal and P. F. Christopher, "Communicationat Millimeter Waves," Intern. Conf. Commun. ICC'81, Denver, CO, 14-18 June 1981.

(Kiesling, 1980) J. D. Kiesling, "Study of Advanced Communications Satellite Systems Based on SS-FDMA," Document No. 80SDS4217, General Electric/Valley Force Space Division, P. O. Box 8555, Philadelphia, PA 19101, May 1980, Contract No. NAS 3-21745.

(Staelin, 1969) D. H. Staelin, "Passive Remote Sensing at Microwave Wavelengths," Proc. IEEE, Vol. 37, No. 4, April 1969, pp. 427 - 439.

(Staelin, et al., 1977) D. H. Staelin, et al., "Microwave Spectroscopic Imagery of the Earth," Science, Vol. 197, 2 September 1977, pp. 991-993.

SECTION 9

CRITICAL TECHNOLOGY AND SYSTEM ISSUES

This section discusses technology issues which are important for a satellite in which message traffic is routed by frequency assignment, i.e, an SR-FDMA satellite. The special needs of such a satellite with regard to antenna beams are covered in the first subsection. The following subsections provide a technology assessment of satellite and terminal equipment operating in the 30/20 GHz band.

The final subsection discusses the important topic of how an experimental satellite design, whose purpose is to demonstrate the TDMA system, can be modified to demonstrate both TDMA and SR-FDMA at some additional cost in weight and power.

BEAM SYSTEMS

The FDMA system proposed requires 31 spot beams having 0.3° half-power beamwidths. The placement of the beam footprints on a map of the United States is shown in figure 9-1. The 0.3° value was chosen to provide the gain necessary to support the traffic volume and to minimize interbeam interferences. Even at this beamwidth, the beam edges cluster and touch in several areas such as the eastern seaboard, the Midwest, etc. Signals originating in or intended for one area in a given frequency band must not be intercepted at too high a level in another beam using the same band. Unacceptable co-channel interference will result. Thus, the sum of the in-band sidelobe powers from all other beams falling in any of the footprints of figure 9-1 should not exceed -30 dB relative to the peak gain of the beam. (See section 5.)

This requirement will be a driving consideration in the antenna design. Other considerations include beam distortion and minimizing the number of antenna reflectors that the spacecraft must carry. Figure 9-1 presents not only the beam locations but their angular distribution. The United States is shown to subtend an azimuthal angle of 6.81° and an elevation angle of 2.99° at a synchronous equatorial satellite located at 90° W. Thus, if the axis of a satellite-borne reflector were aimed at the center of the country, (slightly below beam 21 for Omaha/Kansas City) the extreme beams would have to point 3.4° east and west of the axis if all beams were to come from one reflector.

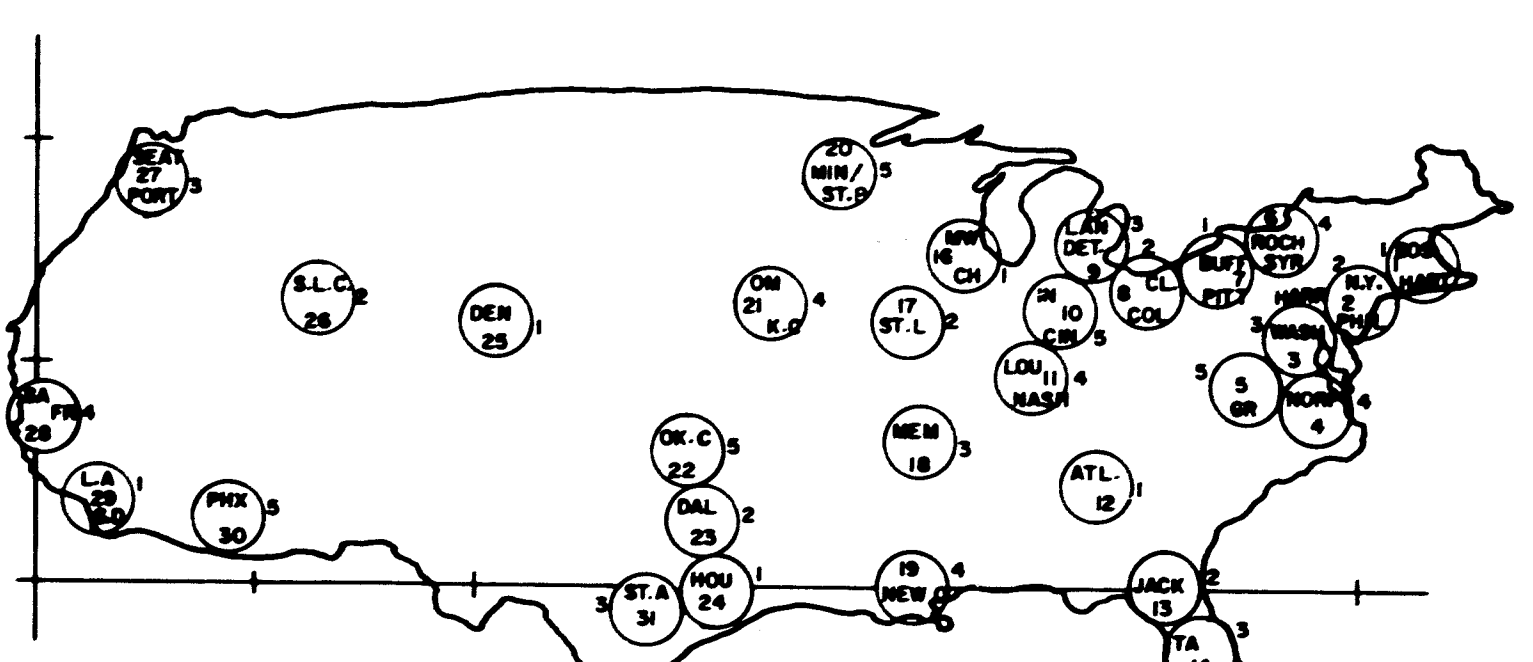

MIN PHI	-4.14	MIN THETA	4.26
MAX PHI	2.67	MAX THETA	7.25
RANGE PHI	6.81	RANGE THETA	2.99
PHI INTERCEPT	-4.00	THETA INTERCEPT	5.00

Figure 9-1. Beam Plan for Traffic Model A

When a beam is pointed (scanned) off axis in a reflector, coma distortion results. The first and other sidelobes become wider and higher. The first lobe joins the main beam on one side of the antenna pattern, thus reducing gain and increasing the potential for beam interferences. A well-known rule (Silver, 1948) states that the limit for scanning a beam off the axis of a reflector is five beamwidths before coma becomes too severe. This would be 1.5° for 0.3° beams, casting doubt on the azimuthal coverage of the country by one antenna. Using two reflectors, one for the eastern half and the other for the western half of the United States, could help. However, different size reflectors are needed for the uplink and downlink satellite beams. Using two reflectors for the downlink beams and two for the uplink beams will give the satellite a complement of four reflectors.

Recent work employing geometrical optics has shown that locating feed-horns radially out of the focal plane reduces coma. Therefore, a design study for the beam system of figure 9-1 should be carried out to determine whether only a single reflector could be used for all downlink beams and another single reflector used for all uplink beams. This is an effort of some magnitude and beyond the scope of the current program.

Matters could be helped if the same feed-horn could be used for both the uplink and downlink beams. There is no barrier to diplexing the uplink and downlink frequency bands onto the same horn. However, the fixed horn aperture will give a different beamwidth from the horn for each band, and one of these will very inefficiently illuminate a reflector of the size needed to give a 0.3° beam. In order to design an effective antenna, the designer must be able to control both the reflector and the horn aperture. This means that he must be free to design uplink and downlink antennas independently. Thus, the hope of having only two reflectors depends on the success of a program to reduce coma by refocusing. Beam interferences are not affected whether or not refocusing is successful. The requirement of two reflectors each for both uplink and downlink will not change the principles discussed below.

The reduction of beam interferences requires low sidelobes in the 0.3° beams. This is accomplished by illuminating the reflector most intensely at the center and tapering off the intensity toward the reflector edges. Illumination taper is controlled by the beam from the illuminating horn (called the primary beam). If a narrow beam is achieved by using a larger opening on the horn, then the intensity, high at the center of the reflector, will drop off enough at the edges to give low secondary sidelobes. Thus, large horn

apertures are required and it is necessary to determine what horn aperture sizes the beam system of figure 9-1 permits.

Each beam of figure 9-1 requires a separate horn. The horns are positioned relative to the axis of the reflector in the same way as the beams, but in mirror image locations because of the laws of reflection. Thus, we may speak of relative horn positions just as if the beams were the horns. The figure shows that a large number of the beams are touching. Horns located at those angular positions can be enlarged until the two horns just touch. That is the largest the horn can be. The size of the horn in this touching condition is calculated at the lowest downlink frequency, 17.5 GHz. It is known that a reflector diameter of 4 m is needed to produce a 0.3° beam at this frequency.

A common value of focal length, f, to diameter ratio for reflectors is 0.5. Thus, the focus of the reflector is expected to be 2 m from the vertex. Horns will be positioned on a surface at approximately this distance and the angular separation of the horn centers of two touching beams will be 0.3° subtended at the vertex of the parabola, as shown in figure 9-2. The arc length corresponding to this angle will also be the aperture opening of the horn. This is found from the relationship among radius, arc, and angle to be 1.047 cm. The question next arises as to how much amplitude taper a horn aperture of such a size produces. This requires a formula for the pattern of a horn.

A simple closed form for the pattern of an electromagnetic horn does not exist; the phase front curvature emanating from the horn does not lead to mathematical functions integrable in closed form and expressed as simple functions. However, if the horn sides are not flared at too wide an angle, a condition easy to satisfy with the small horns used in the 20-30 GHz band, it is possible to derive an approximate formula.

The formula is accurate enough for finding amplitude taper on reflectors when the curvature of the phase front in the horn aperture is less than a quarter wavelength, $\lambda/4$. Then, the phase front may be taken to be plane which leads to integrable functions. The Schelkunoff equivalence theorem and the vector potential are used to derive the approximate horn pattern, which is given in spherical polar coordinates with the plane of polarization in the Φ direction as:

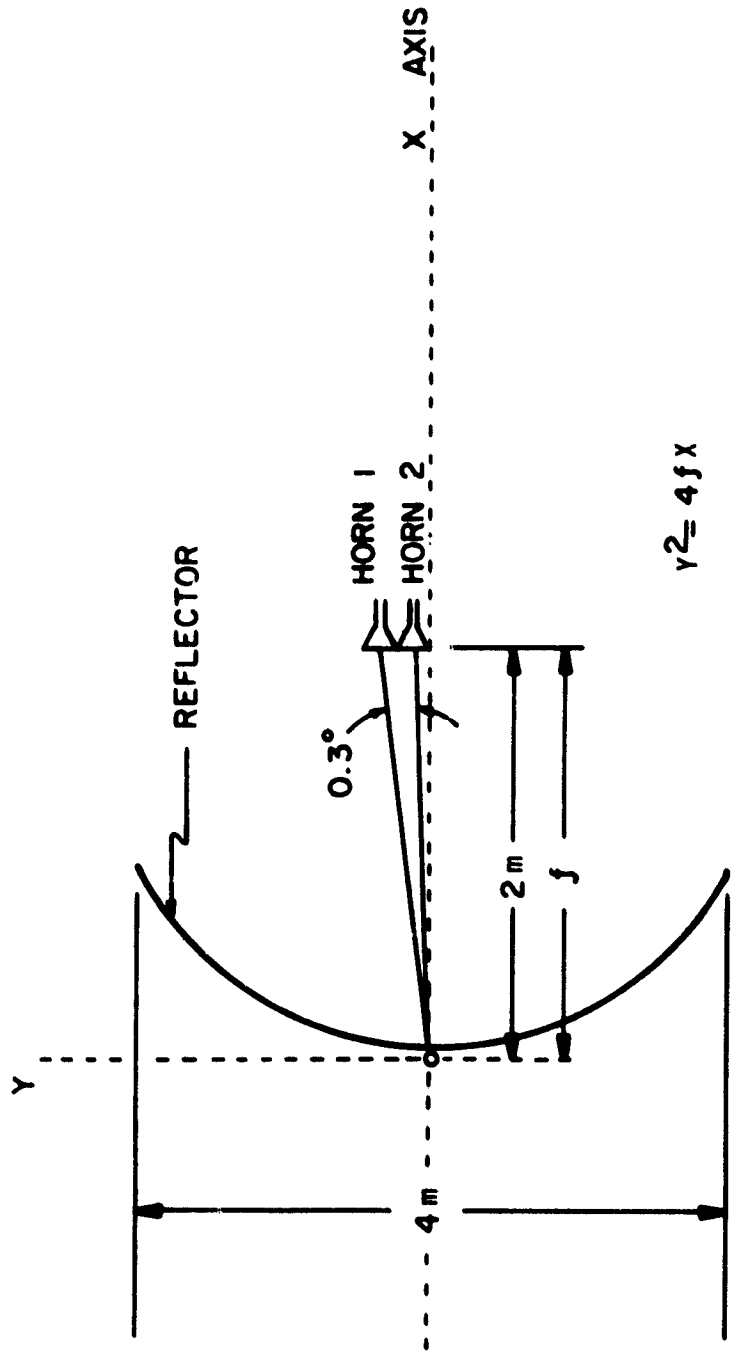

Figure 9-2. Determination of Horn Aperture

$$E_\phi = \frac{abE_{max}\exp(-jkr)(\sin\theta + \cos\phi)}{8\lambda r} \times \frac{\sin\left(\frac{kb}{2}\sin\theta\sin\phi\right)}{\left(\frac{kb}{2}\sin\theta\sin\phi\right)}$$

$$\times \left[\frac{\sin\left(\frac{ka}{2}\cos\theta + \frac{\pi}{2}\right)}{\left(\frac{ka}{2}\cos\theta + \frac{\pi}{2}\right)} - \frac{\sin\left(\frac{ka}{2}\cos\theta - \frac{\pi}{2}\right)}{\left(\frac{ka}{2}\cos\theta - \frac{\pi}{2}\right)}\right] \qquad (9.1)$$

where

Emax is the peak field intensity in the horn aperture

$k = 2\pi/\lambda$

a = H plane horn dimension

b = E plane horn dimension

r = radius in spherical polar coordinates

Equation (9.1) for E_Φ is next applied to the 4 m reflector using the size derived for the horn dimensions, namely: a = b = 1.047 cm. The reflector illumination found is given in table 9-1 as a function of Y, the radial distance from the axis X.

Table 9-1

Aperture Distribution for 4 m Reflector and 1.047 cm Horn
(f = 17.5 GHz)

Y (cm)	Distance Horn-Reflector (cm)	Relative Intensity (V/m)	dB Down From Peak
0	200	0.012732	0
50	203.125	0.012095	-0.44
100	212.500	0.010466	-1.70
150	228.125	0.008445	-3.56
200	250.000	0.006536	-5.79

Table 9-1 shows that the illumination taper produces a level only -5.79 dB down relative to the center (Y = 0). The secondary pattern of a 4 m antenna illuminated by this distribution may be

deduced using the well-known family of patterns for a round aperture derived from an in-phase illumination with amplitude distributed according to the parametric formula

$$A + B\left(1 - \frac{\rho^2}{a^2}\right)^P \tag{9.2}$$

where

A is the uniform component of aperture illumination, which is also the relative intensity at the edge.

B is the difference between the peak value of unity and A. $B = 1 - A$

ρ is the radial variable for the distance from the vertex axis to a point on the aperture inside the outer circumference.

a is the radius to the aperture circumference (or edge).

P is the algebraic power which determines how fast the intensity falls off from the peak value.

The pattern resulting from the aperture illumination of table 9-1 is given in figure 9-3. The resulting first sidelobes are only 21.5 dB down, and subsequent sidelobes are at too high a level for the addition of sidelobes of several antennas to produce an acceptably low carrier-to-interference ratio. It will be necessary to use a larger horn to reduce the first and all subsequent sidelobes. However, the horns would clash if their apertures were made larger; there is not enough area on the focal surface since the beam edges touch in figure 9-1.

A second focal surface will be provided by using a polarization sensitive reflecting screen. The screen reflects say, vertical polarization, and transmits horizontal polarization. The screen, reflector, and horns are shown in figure 9-4. An offset reflector is used so that, although it has a 4 m aperture, the horns are below the reflector and do not block the energy. Half the horns are behind the screen but are horizontally polarized, and so their radiation passes right through to the reflector. The other horns are in front of the screen and their patterns reflect off the screen to illuminate the reflector properly. These front horns are the same optical distance from the reflector as the rear horns on the original focal surface. In effect, the screen provides two focal surfaces so that the horns can be larger. Since half the horns will be located on the front and half on the back focal surfaces, the horns can be twice as large or 2.094 cm in both a and b horn

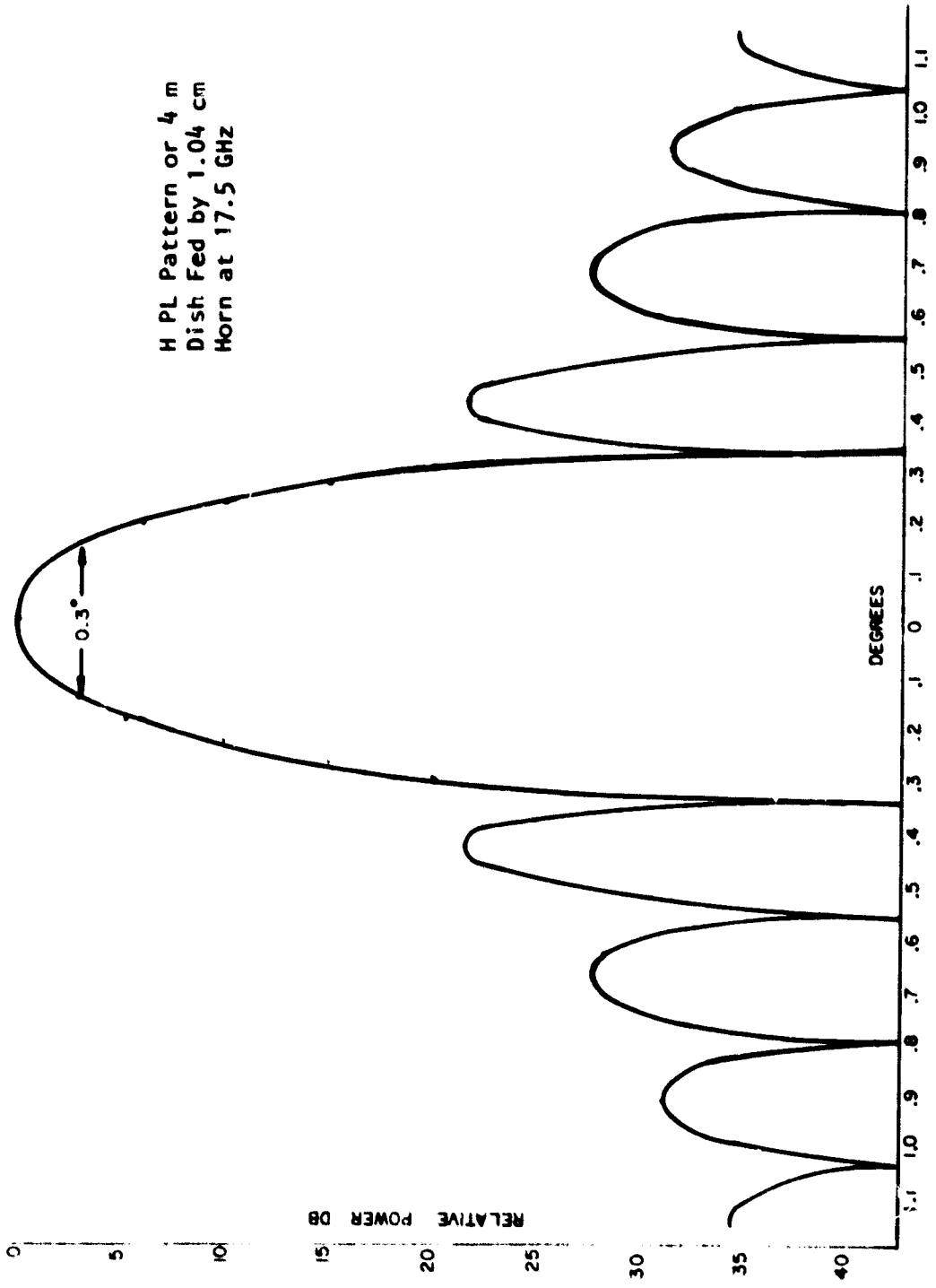

Figure 9-3. H Plane Pattern for Aperture Illumination of Table 9-1

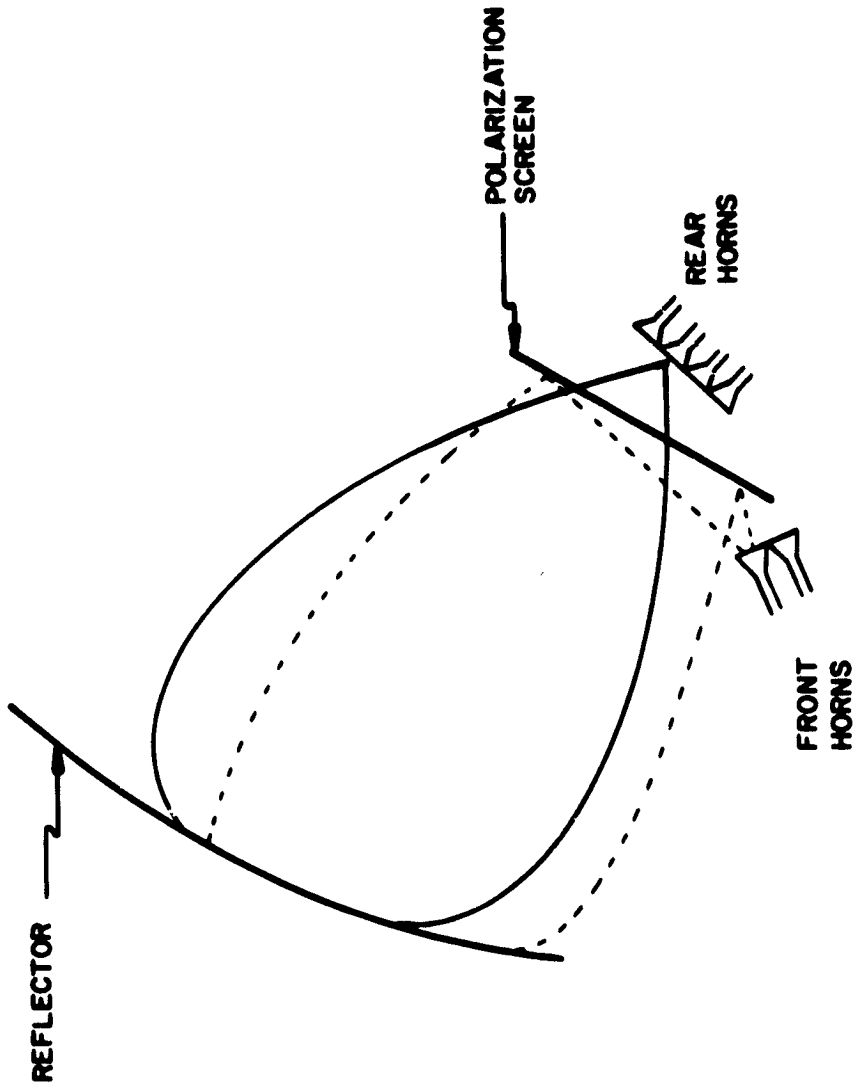

Figure 9-4. Dual Focusing Surface

dimensions. The amplitude taper on the reflector for this case is given in table 9-2.

Table 9-2

Aperture Distribution for a 4 m Reflector and 2.094 cm Horn, (f = 17.5 GHz)

Y (cm)	Distance Horn-Reflector (cm)	Relative Intensity (V/m)	dB Down From Peak
0	200	0.012732	0.0
50	203.125	0.011331	- 1.0
100	212.500	0.008162	- 3.9
150	228.125	0.005041	- 8.0
200	250.00	0.002878	-12 9

The 2.094 cm horn provides an edge illumination 7 dB lower than the 1.047 cm horn. The secondary pattern shape can be estimated as before from the class of canonical antenna patterns.

In this case:

A = 0.05

B = 0.95

By curve fitting tc table 9-2, P is found to be:

P = 1.5

The canonical form for this case was used in the anticipated antenna pattern shown in figure 9-5. Its first sidelobes are -26 dB down, the other sidelobes taper off in an acceptable manner, and the half-power beamwidth is indeed 0.3°. This pattern is used in conjunction with figure 9-1 and another graphical chart to estimate beam interferences for a specific system in Appendix C.

CURRENT SR-FDMA TECHNOLOGY ASSESSMENT

This subsection summarizes technology advances, status, and system impacts of satellite and terminal equipment operating in the 30/20 GHz band.

Space and Ground Subassemblies and Subsystems

Technology advancements, which will make significant impact on system performance and/or cost effectiveness, are needed for the following subassemblies and subsystems of both the space segment and the ground segment:

a. Solid state power amplifiers as transmitters

The following technologies are identified for further development;

1. GASFET transistor amplifiers (1-2 W power level at 20 GHz);

2. Impatt and Gunn device amplifiers (1-5 W power level at 30 GHz);

3. Techniques for power combining several medium power amplifiers (1-2 W).

b. Low power TWT amplifier development for small terminals

The low power (5-10 W) 30/20 GHz helix TWT technology for both the space and the ground segment in the United States is lagging far behind other nations. In Japan and Germany, helix TWTs for space applications at 20 GHz are already under development. Ground terminal TWTs in production today deliver only 1 W of RF power at 30 GHz. Higher power tubes are only laboratory samples.

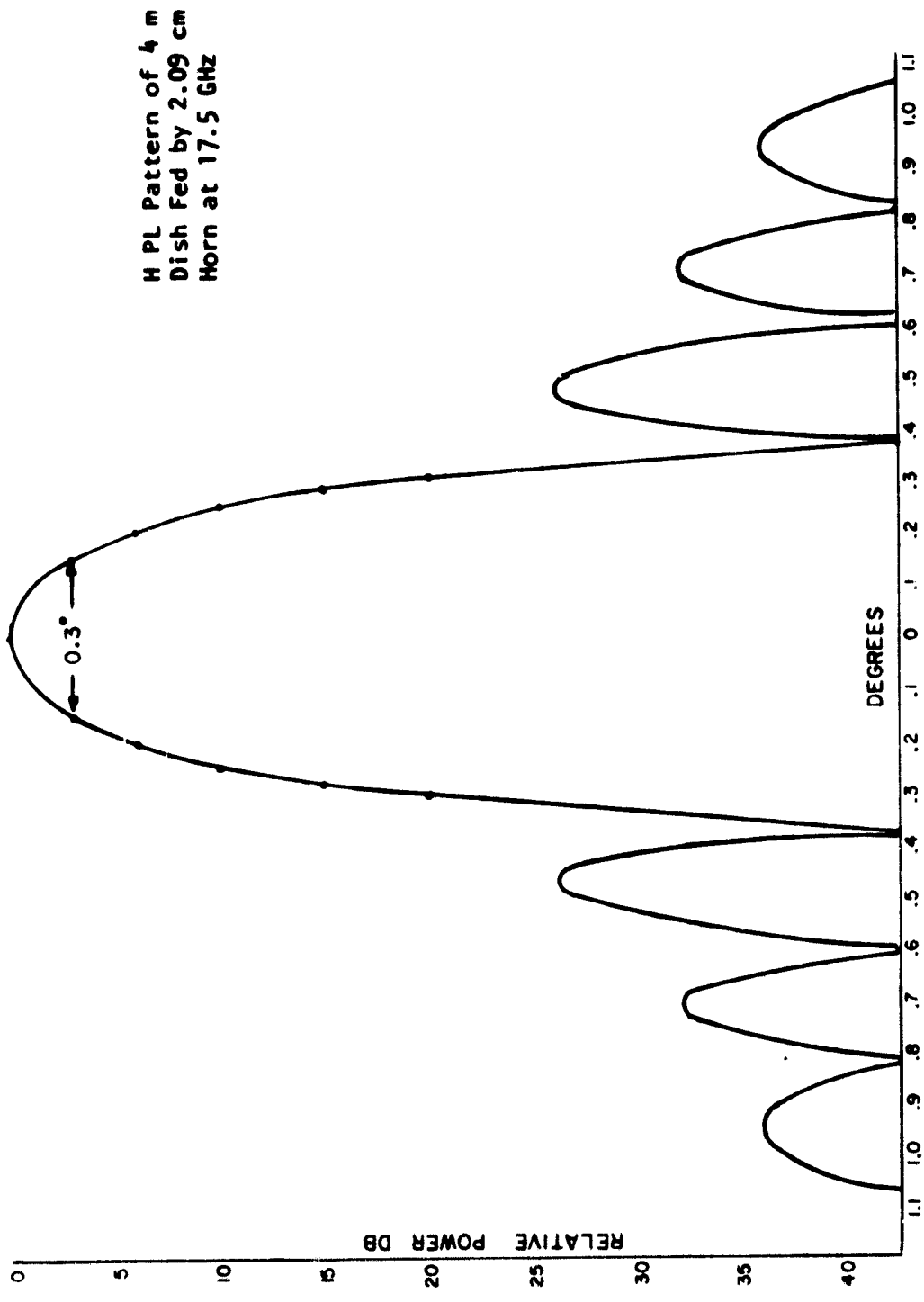

Figure 9-5. H Plane Pattern for Aperture Illumination of Table 9-2

c. Integrated front end receiver with dual frequency conversion

Development of this technology would result in reduced labor for the wiring of each assembly and the testing of each functional subassembly, improved performance, and a more compact receiver.

d. Integrated transmitter (up-converter) including frequency synthesized local oscillator

e. Low noise amplifier (LNA) at 20 and 30 GHz

The most significant impact of a space qualified 30 GHz LNA would be a greatly improved G/T at the satellite. Not only is this important for the overall system capacity, but also for the compensation of large RF losses within the multibeam antenna system.

f. Frequency synthesizer

Frequency synthesizer technology for effective high RF frequency generation requires 1 or 2 GHz direct digital circuitry for dividers and multipliers. This technology needs to be developed.

Technology Advancement Potential

The following is an identification and status assessment of specific technologies that when applied to system subassemblies may have significant advancement potential:

a. Solid state power amplifier technology

Solid state power amplifiers are currently built with GASFET device technology, Impatt devices (Si or GaAs material), or transfer electron device (TED) technology (GaAs or indium phosphate material).

The best projected performance of a single GASFET device operating at 30 GHz is 0.25-0.3 W of RF power per module by 1983 to 1985 and approximately 2 W total if 8 or 10 single modules are power combined. In our opinion, while GASFET amplifiers at 20 GHz (for space applications) are feasible, their use in ground terminals operating at 30 GHz may not be cost effective (due to the low gain per stage).

Impatt diode high power amplifiers and related technologies (both Si and GaAs) are well developed, and have made steady progress both in frequency and power performance in the last five years.

During the 1970s, 1 or 2 W Impatt RF power amplifiers at X-band were considered a great achievement. Today, 1 W and 2 W power

modules at 44 GHz have been demonstrated. In addition, 5 to 10 W K-band power amplifiers are being bread-boarded by several manufacturers. TEDs (similar to Impatt devices) have potentially wider bandwidths than Impatt devices, but have a lower output powor (0.5-1 W).

b. Medium power terminal TWT development

The tube technology being pushed for medium power requirements is the helix type TWT which promises significantly lower costs with uncompromised performance. At this time, no U.S. manufacturer has a 30 GHz TWT in production that provides more than 1 W of RF power. However, several design efforts (Varian and Hughes) are aimed at 10 or 15 W CW RF power at 30 GHz with over 2 GHz of bandwidth. Space-qualified helix TWTs with 20 W of power at 20 GHz are no longer a novelty. However, for tubes with higher power and linear wide bandwidths to become a reality, a larger R&D effort is needed in this area.

Designing and using these tubes at power levels below 10 W will not have a major impact on their design or cost. However, designs requiring over 25 W of RF power are no longer achievable from this relatively low cost helix technology due to limitations of thermal dissipation.

c. Monolithic microwave integrated circuit (MMIC) technology

This technology, unlike hybrid integration, does not use discrete devices (e.g., diodes, transistors) but integrates the complete circuit with a device substrate material such as GaAs or Si. The advantage of this technique is the low-cost, mass-production potential of complete subsystems. Several circuits and their functions can be combined into a small area without human operator involvement.

Many successful subassemblies with various functions at C and X band have been built in the United States and in Europe using this technology. Based on the results achieved for the construction of low cost receiver front end operating at 11/12 GHz, this technology appears to be very promising; it needs to be pursued more vigorously as one of the fabrication alternatives for a low cost K-band up-and-down converter and perhaps a low cost 1 W solid state HPA. As an example, Texas Instruments Co. developed an MMIC GASFET amplifier that operates from 7 to 10 GHz and delivers 1 W of RF power. A low noise receiver front end (including the LNA) with MMIC has been developed by Hughes for the 11/12 GHz band. This receiver is expected to be in production by 1982. A complete low noise receiver chip at 20 GHz for low cost terminals can be designed and built with

a 3 to 5 year R&D effort. However, when the production quantity is less than 10,000, the MMIC hybrid technology might not be the preferred fabrication technique.

d. Low noise GASFET amplifiers

Devices with 0.5μ gate width and amplifers at 18 GHz are available today. So far the best result measured on a low noise GASFET amplifier is 2.5 dB NF for a single stage 8 dB gain at 18 GHz. Overall receiver noise figures are expected to be around 5-6 dB for the terminal. However, for space applications 0.25μ gate width devices at 30 GHz might be a real challenge. This technology requires several years of extensive R&D efforts.

20/30 GHz Technology Status Projections

The following are status projections of 20/30 GHz technologies for the 1982-1987 time periods with and without NASA funding:

a. Antenna systems

Antenna design efforts for small terminal applications are well underway with the exception of dual 30/20 GHz feed systems. According to some industry experts, a one-year effort could produce a cost effective antenna system without tracking (a two-year effort is needed if a low cost tracking system is included).

b. Solid state and TWT power amplifiers

Several R&D efforts are currently underway for the development of 20 GHz solid state power amplifiers with 0.5-1.0 W of power/module for space applications. However, no R&D design effort is reported for the design of solid state power amplifiers operating at 30 GHz. Technology advances seem to be fairly promising for 2-5 W amplifiers. However, without NASA funding, industry will not pursue any one of these areas due to the high risk involved. Similar comments can be made about TWT amplifiers. The required effort for the solid state amplifier, and the helix type TWT with 5-10 W of power is about 2 to 3 years of extenstive R&D work in both areas.

c. Low noise amplifier and receiver at 20 GHz

This area is in far better shape than other subsystems. Several companies are pursuing it with an in-house effort due to the commonality of the military SATCOM band. A 20 GHz low noise amplifier can be built with a one-year effort. The complete integrated receiver front end will require about three years of R&D

effort. Again, this type of effort will not be supported by the manufacturing companies due to the high risk involved and the uncertain market potential.

d. Frequency synthesizers

This technology is the most developed up to at least 18 GHz.Work needs to be done in the area of application of LSI technology to the existing designs for cost reductions. Substantial work and R&D funding is needed to extend the present operating frequency to 30 GHz in a cost effective way. Since there is a potentially large market and low risk involved, industry will most likely share the cost of development with NASA.

System Performance Impact

The following is an assessment of the impact of these technologies on system performance:

a. Antenna systems

The use of low cost wire-mesh fiberglass antenna systems (up to 3 m) at 20 or 30 GHz does not require any sacrifice in performance. Their surface tolerances (0.010 - 0.015 rms) are acceptable and do not represent any significant RF losses.

b. Transmitters

Solid state transmitters, in comparison to TWT high power amplifers, require a simpler power supply and have a longer lifetime with a graceful degradation in performance. However, solid state amplifiers are power limited to $\approx$ 10 W at 30 GHz (1-2 W per module). Also, if the module is not a GASFET transistor but an Impatt device, the noise-power characteristics (AM and FM) of the device will be increased relative to that of the TWTs. This may affect the system performance depending on the mode of operation (FDMA or TDMA and peak or CW power). Solid state amplifiers are not always inherently stable and spurious oscillations can occur at undesired frequencies. The likelihood of this is very small, however, due the 40 dB of isolation between stages found in well designed systems.

c. Integrated front-end receiver and transmitter

This type of technology is fairly new and has a high degree of risk. Even when individual circuit functions are tested and found to be within specifications, a fully integrated multifunction chip can be lossy, and may have poor performance due to unexpected events. Trouble-shooting individual circuits and malfunctions after

integration is impossible and the chip must be replaced. However, the promise of low cost chips ($40-$100) could dramatically change terminal economics.

d. LNA

The LNA development at 20 GHz has very little risk involved, and the impact of this would be a 1.5-2.0 times increase in system capacity or the equivalent in savings of satellite DC and RF power.

A 30 GHz satellite LNA development would greatly enhance satellite G/T and consequently reduce terminal RF power requirements accordingly. The expected 2 to 3 dB improvement in the satellite receiver NF will provide either increased system capacity or lower cost terminals. The development of a 30 GHz LNA is a high risk effort because it requires 0.25μ wide gate GASFET device development prior to any circuit design. Even after the device is made available, if it requires a fairly complex matching structure and is lossy with a low gain, it will not improve the overall NF beyond what is achievable with low noise image-terminated mixers.

e. Synthesizers

A new synthesizer technique with digitally controlled logic is being developed. Digital rather than analog circuit design has little risk if any. A high resolution and fast switching frequency source can improve the performance of an FDMA system. However, for TDMA applications, the high resolution is far less important.

SWITCHING AND SAW FILTERING

The FDMA satellite system can route signals among the 31 beams set up to satisfy Traffic Model A with very little switching. The switching required is used to readjust the network for growth in traffic to some centers accompanied by a compensatory decline in traffic to others. For this, switching of blocks of bandwidth at an intermediate frequency of 3 GHz among beams will do. Thus, a small, low-power microwave matrix switch with a slow switching speed (i.e., a scaled-down version of the switch advocated in a previous MITRE report (Katz, et al., 1979)) can serve this purpose.

There had been discussion of slicing the traffic in a beam down to narrower bands for much more detailed routing (GE, 1980). A second intermediate frequency in the 10 to 30 MHz range would have been used and the number of bandwidth paths through the satellite would have increased enormously. This step, as noted above, is not necessary. However, prior to proving this fact by actually devising

FDMA systems, investigations were made by MITRE of the switching and filtering capability currently existing for supporting such an approach. That material is summarized in two appendixes at the end of this report, Appendix D on SAW filtering, and Appendix E on LSI switching.

SATELLITE AND TERMINAL FREQUENCY SYNTHESIZERS

Several satellite frequency synthesizers supply the local oscillator (LO) frequencies to the regional RF downconverters and over 100 LO frequencies to the IF converters, and frequency shift mixers. In addition, they also provide RF signals to the 32 upconverters for the downlink beams. The direct synthesizer output frequency could be in the 1-2 GHz range and multiplied to the appropriate discrete frequency according to the regional frequency plan. The 100 MHz reference source is assumed to be phase locked to a high quality 5 MHz atomic standard. The 100 or 110 MHz reference source can be applied to generate the large number of IF frequencies either by a multiplier technique or an upconversion technique through the synthesizer 1-2 GHz output frequency. An alternate approach would be to divide and mix the 2 GHz synthesized signal by a large number of individual smaller synthesizers. However, this approach would increase the close-carrier phase noise product. The narrowband filters within the IF multiplexers (tuned at 2-4 GHz) could have as small as a 7-10 MHz 3 dB bandwidth (derived from the traffic matrix). Therefore, a 0.1% resolution has been selected for the satellite IF frequency synthesizer (10 kHz).

The reference frequency standard stability was chosen to be better than 5×10^{-9} per day. The synthesizer settling time should be less than 10 ms. Future LSI and high speed digital technology might make it possible to use higher output frequency direct synthesizers in the 2 or 4 GHz range without multipliers. Space qualified synthesizers require an R&D effort.

Digitally controlled direct synthesizers for ground terminal applications are currently available with 2 GHz outputs. They operate without multipliers, have very low phase noise and can have a frequency resolution of 50 kHz.

A dedicated coarse synthesizer is needed in the terminal for each up and downconverter (one per carrier frequency). Each coarse synthesizer is driven by a processor-controlled digitally-programmable common synthesized fine source at some VHF or UHF frequency. The synthesizer for both the uplink and downlink needs a < 100 kHz resolution, a minimum phase noise, and a better than 5×10^{-9} per day frequency stability.

Single sideband phase noise characteristics that are better than -90 dBc/Hz at 10 kHz from the carrier are common for low cost satellite terminal synthesizers available today. This type of synthesizer cost less than $5000.

EXPERIMENT FOR DEMONSTRATING FDMA SYSTEM

The MITRE Corporation has proposed that a method of combining an FDMA experiment with NASA's planned TDMA satellite demonstration be implemented. The following illustration of the plan is based on a description of the TDMA Flight B demonstration furnished to NASA by TRW (TRW, 1980). The MITRE plan uses the TRW description only to show the method of adding the FDMA experiment. The method will work as well with other proposed versions of the TDMA demonstration and the use of a particular illustration is not to be construed as an endorsement.

Figure 9-6 is a representation of the TRW frequency plan for Flight B. This plan shows six 500 MHz bands in beams to six population centers; these beams are assigned partly to support FDM experiments. The communications payload proposed in support of this plan is given in figure 9-7. As illustrated in figure 9-7, the communications payload shown consists of three main parts:

1. Antennas for uplink beams, some antenna switching and low noise amplifiers.

2. Down converters to intermediate frequency bands plus equipment for switching or processing TDMA traffic.

3. Upconverters from intermediate frequency bands to the downlink frequencies, TWT amplifiers, redundancy switches, and downlink antennas.

The MITRE plan for demonstrating the operation of FDMA will make use of parts 1 and 3 of the communications payload but will switch in an FDM processing section to replace part 2 which, as shown in figure 9-7, processes TDM. Thus, on the operation of switches, the satellite is reconfigured from TDM to FDM operation and, when desired, back again to TDM. An illustration of this plan is given in figure 9-8. At the left of figure 9-8 is a box representing part 1 containing the antennas and amplifiers. These will be used as before. There follows next a box containing transfer switches which are to be added so that signals from the antennas may be presented to either the TDMA or the FDMA processing packages. These packages are followed by a second box representing more transfer switches that connect the upconverters and TWTs to

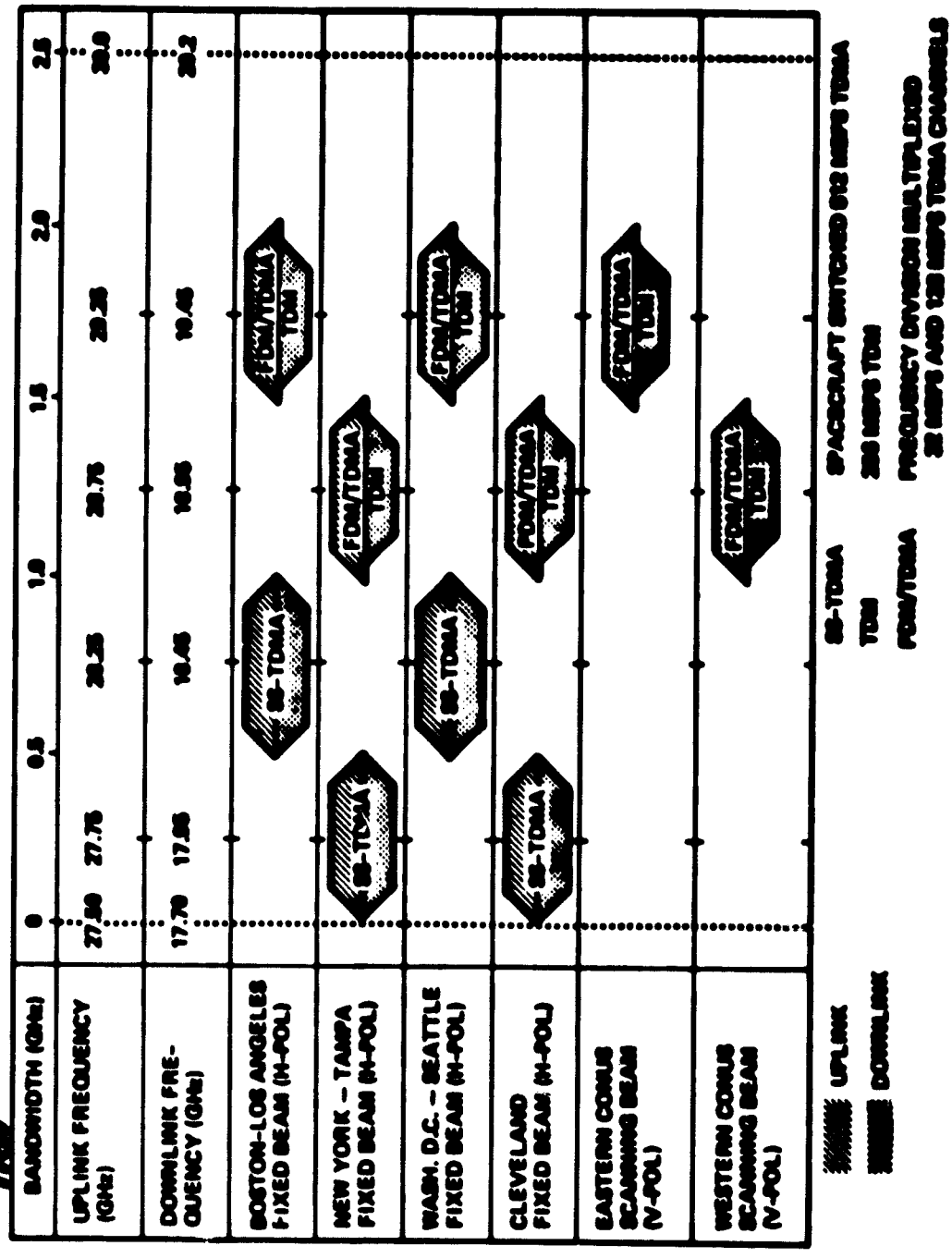

Figure 9-6. TRW Frequency Plan - Flight B

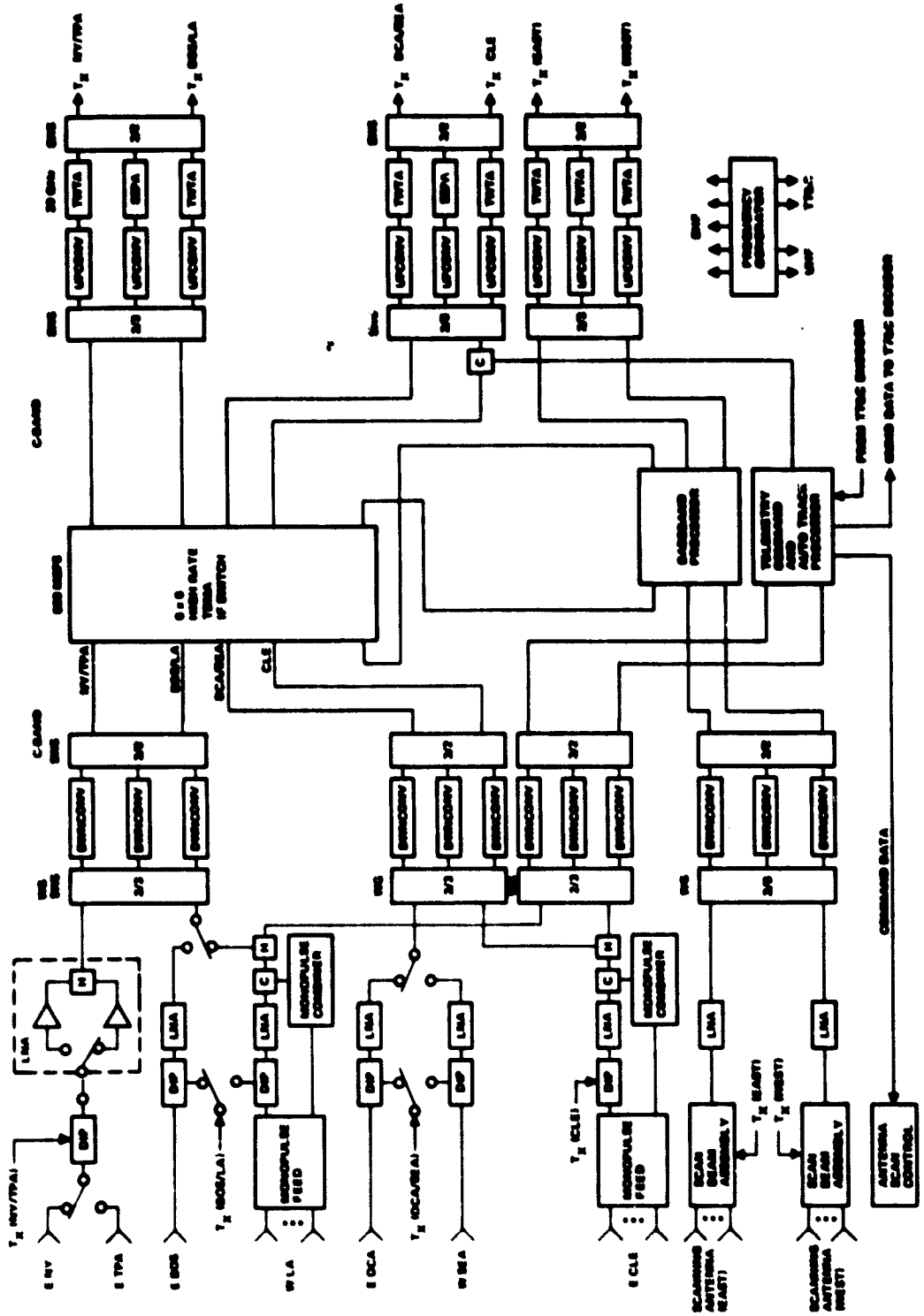

Figure 9-7. TRW Plan B TDMA Communications Payload for Demonstrating TDMA

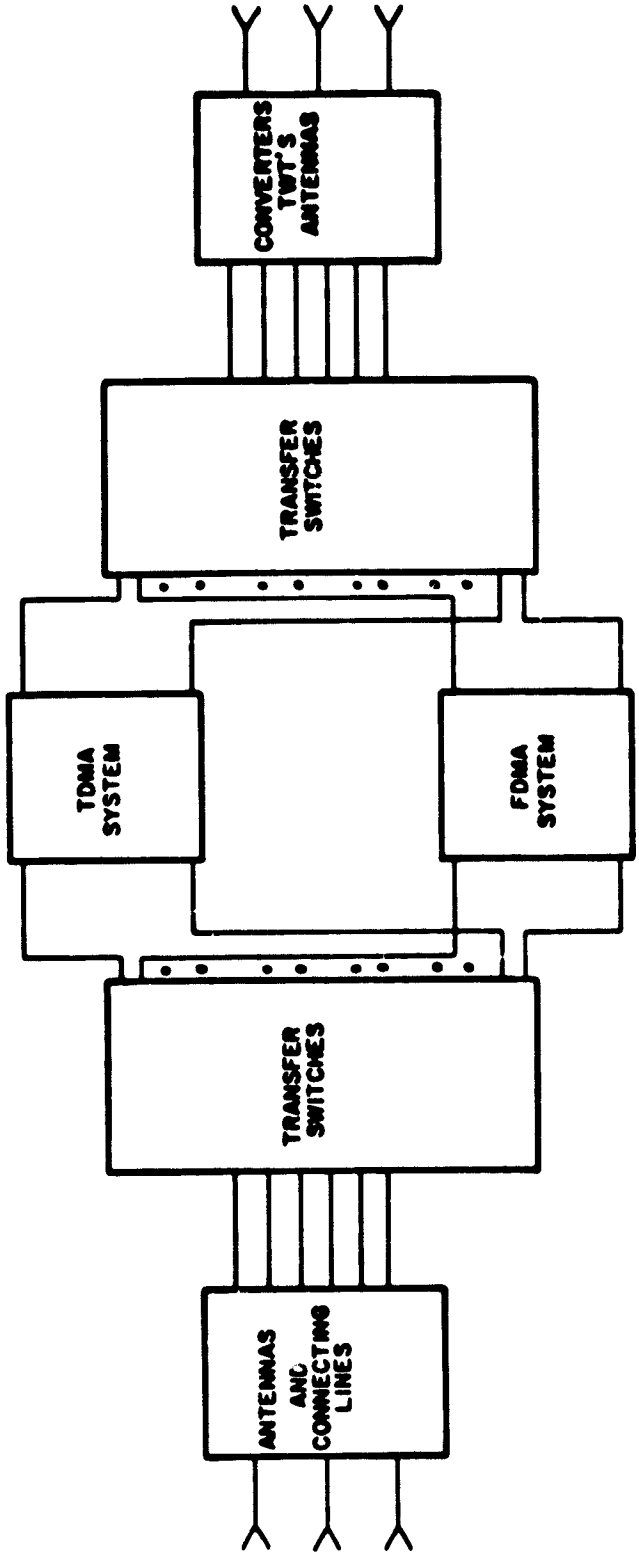

Figure 9-8. Principle for Adding an FDMA Experiment to a TDMA Experiment

whichever system is operating. The switches are followed by the upconverters, TWTs, and antennas of part 3. These too will be used as before.

The plan has the following advantages:

1. Maximum use is made of equipment already in the satellite for TDMA.

2. Minimal changes are required of the TDMA experiment.

3. Minimum equipment necessary for demonstrating FDMA is added.

4. Operating switches can conveniently convert the system from TDMA to FDMA and back again.

The satellite control system must respond to a command to throw the switches. It will also be necessary to apply electric power to the FDMA system when it is selected for use. Shutting off power to some parts of the TDMA system may be desirable or advisable at this time.

A more detailed picture of the FDMA portion and its relationship to parts 1 and 3 of the satellite is given in figure 9-9. The FDMA equipment shown is arranged to demonstrate the "regional" FDMA design. This design aims at using fewer analog RF components in the FDMA processing equipment. The regional approach is described in detail in section 11 of this report. The regional concept FDM processor to be substituted for the TDMA is shown in figure 9-9.

Starting from the left, figure 9-9 shows the antenna and low noise amplifiers that service beams from New York, Boston, Los Angeles, Washington DC, Seattle, and Cleveland. The monopulse functions served by beams from Los Angeles and Cleveland are not disturbed. The output lines from the low noise amplifiers are brought to waveguide transfer switches as shown in figure 9-9. These switches have a stationary housing and a rotating cylindrical armature. The armature contains two waveguides, each bent in an arc making a 90° change in direction. Motion of the armature is bidirectional over a 90° arc. Viewed from the top of the armature, the paths of the waveguides, if they were visible, would resemble the stitching on a baseball and so these switches are referred to as "baseball switches."

The armatures are shown in figure 9-9 in the position where one of the waveguide arcs connects the amplifier outputs to the FDM

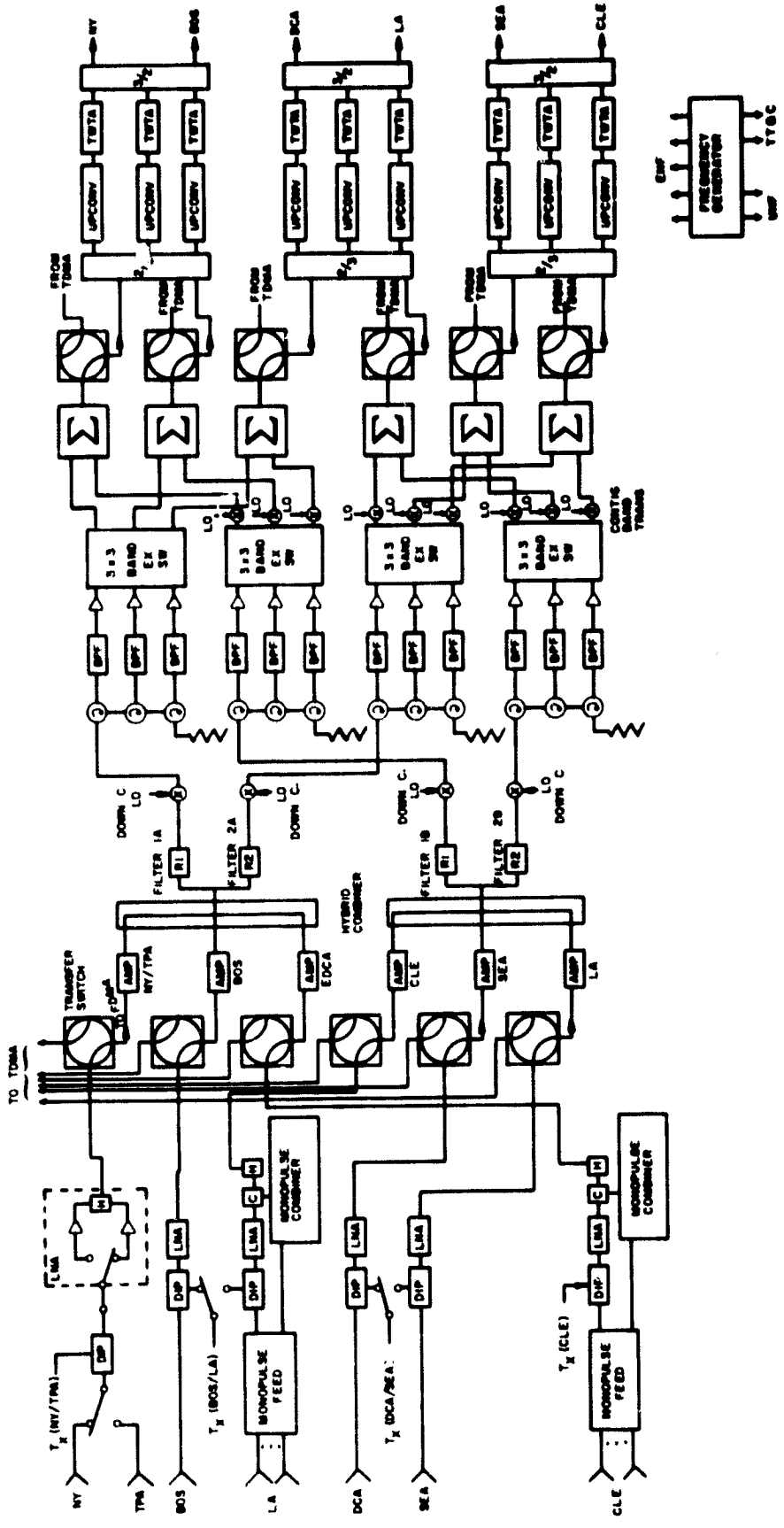

Figure 9-9. Connection of FDM Processor in Plan B

regional system. Lines are shown going up from the switches to the TDM system which is not shown. If the armatures were to rotate 90 counter-clockwise, then the amplifier outputs would be connected to the TDM system. When the signals enter the FDM system, they first encounter a second set of broadband 30 GHz amplifiers. These amplifiers provide additional gain to make up the loss encountered in hybrid, adding the beam channels in groups of three to form two regions. Region 1, the "Eastern" region, consists of the beams from New York, Boston, and Washington. Region 2, the "Western" region, will consist of Seattle, Los Angeles, and Cleveland.

The regions are employed so that a group of three cities may share filters and frequency converters in common. Regions are limited in number of members to prevent beam interferences. Within a region, no channel bandwidth may be used more than once; thus, there is no frequency reuse within a regional grouping. The second region operates in a different band from the first. If there are more than two regions, then regions with sufficient geographical separation may reuse the same bandwidth.

After being combined in a three-beam region, the combined signal in each region is diplexed according to regional destinations. The regional destination signals are then sent to a bank of filters which sort the regional signals by beams within the region. Circulators are employed with the beam filter bank. It is assumed that traffic capacity for the three beams in each region will be different and that three different filter bandwidths will be used. A 3 x 3 switch will be used so that bandwidths can be exchanged between cities and the capability to accommodate decline in traffic to some cities and growth in traffic to others can be demonstrated. Two banks of beam filters are used in each region, one for traffic originating in the region, the other for traffic destined for it from the other region. Hence, each beam is preceded by a hybrid combiner to add the traffic from these two sources. Bandwidth is minimized in the combined signal by using translating mixers before the combiners to render contributions to a downlink beam from the two uplink regions contiguous in frequency. The combiners are followed by baseball switches which accept either the FDMA signals or the signals from the TDM processor before passing them to the upconverters, TWTs, and antennas of the original part 3 of the satellite.

As can be seen, the arrangement described will permit the demonstration of FDMA and TDMA operation from the same satellite. Table 9-3 lists the components which are needed to add the FDMA system and the switching capability. It is estimated that the additional signal components will weigh 121.5 lb and consume 213.9 W of power. From this total weight, 12 lb are assigned to RF electro-

Table 9-3

Two Region Demonstration Satellite Weight and Power

	QUANTITY	WEIGHT/UNIT	TOTAL W. (lb)	POWER/6 (W)	TOT P. (W)
RF Switches					
input	6	1.0 lb	6.0	12	72
Output	6	1.0 lb	6.0	12	
LNA (NF = 6.0 dB) (6 = 10.0 dB)	6	8 oz	3.0	0.9	5.4
RF Hybrid Comb.	2	1 0 lb	5.0		
RF B.P. Filter	4	12 oz			
RF Down Conv.	4	1.0 lb	4.0		
IF CIRC (4-6 GHz)	12	4 oz	3.0		
IF B.P. Filter	12	6 oz	4.5		
IF Ampl. (4-6 GHz)	12	6 oz	4.5	0.9	10.8
IF Freq Shifter	10	4 oz	2.5		
3 x 3 IF Sw. Matrix	4	6 oz	1.5	0.3	1.2
IF Hybrid Comb.	6	12 oz	4.5		
IF Driver Amp.	6	8 oz	3.0	0.9	4.5
RF Step Att.	6	24 oz	9.0		
Freq. Synth.	1	65.0 lb	65.0		120.0
		TOTAL	121.5	TOTAL	213.9

mechanical switches and 65 lb for the frequency synthesizer. The arrangement proposed will have an impact on the satellite but will allow the evaluation of both TDMA and FDMA systems.

LIST OF REFERENCES

(GE, 1980) "Study of Advanced Communications Satellite Systems Based on SS FDMA," Doc. No. 80SDS4217, Philadelphia, PA: GE Space Division, May 1980.

(Katz, et al., 1979) J. L. Katz, et al., "Application of Advanced On-Board Processing Concepts to Future Satellite Communications Systems," MTR-3787 Vol. I, Bedford, MA: The MITRE Corporation, June 1979.

(Silver, 1942) S. Silver, Microwave Antenna Theory and Design, NY: McGraw Hill, 1948, p. 488.

(TRW, 1980) "30-20 GHz Communications System, Preliminary Development Plan for Baseline System," Vol. 1, Task 1 Report, Redondo Beach, CA: TRW, 16 June 1980, p. 3-52.

SECTION 10

SYSTEM DESIGN CONSIDERATIONS

Detailed link budget and beam plans are discussed under constraints of available spacecraft power. The terminal and spacecraft cost models used are described.

PRELIMINARY DESIGN EFFORTS

The number of shaped beams N_B and the number of cells N_C should be minimized under the constraints of the NASA traffic models to simplify the design of the satellite multibeam antenna (MBA). Beginning with the 40 metropolitan areas of the initial model, each area is encircled with a single beam cell until the entire CONUS is covered with uniformly-sized contiguous cells. These cells are approximately 500 km in diameter, corresponding to a 0.7° half-power beamwidth (HPBW) on an earth projection from geostationary orbit.

The result is an $N_C = 49$ cell coverage of CONUS (field of view (FOV) $\cong$ 3° x 6°). A geostationary satellite at 100° W longitude guarantees terminal elevation angles of at least 30°. The approximate length of the footprint is 4900 km east-west and 2500 km north-south. A simple antenna system over the same FOV would provide approximately 29 dBi gain of nearly uniform illumination. The multibeam plan mentioned above would achieve a minimum gain of 39 to 44 dBi. The resulting complexity of a 49-beam antenna and feed system or variable beam forming network (VBFN) implies an ambitious design approach. However, since large areas of CONUS have no traffic requirements, many cells may be eliminated from the beam plan to reduce the spacecraft antenna complexity.

Since the link budgets of table 10-1 suggest that 0.7° beam cells may not fully support the small (2 m) terminal traffic, smaller beam cells are highly desirable. A 0.5° beam cell would increase the received signal by approximately 2.5 dB. However, the MBA would require almost 100 single 0.5° cells over CONUS for complete coverage (Foldes, 1980). Support of 100 such beam cells would require at least 100 feed horns and transponders and a few hundred variable power dividers (VPDs) and phase shifters. The reduced coverage design described below is better matched to Traffic Model A and provides an alternative solution.

This design handles the non-uniform traffic with three MBAs. Each antenna covers a different portion of CONUS. The MBA used for

Table 10-1

Sample Power Budgets for 0.8° Beam Cells

a. Uplink (≈ 30 GHz)

TERMINAL				
RATE R (Mb/s, dB-Hz)	33.8; 75.3	5.56; 67.5		0.88; 59.4
TRANSMITTER POWER (W, dBW)	1000; (30.0)	166; (22.2)		115; (20.6)
ANTENNA				
Diameter (m), Gain (dB)	4.5; (60.0)	4.5; (60.0)		2.0; (53.5)
Half-Power Beamwidth (°)	0.15	0.15		0.35
EIRP (dBW)	90.0	82.2		74.1
LOSSES L				
Antenna Pointing (dB)		1.5	4.0	
Waveguide (dB)		2.5		
UPLINK LOSSES L_u				
PATH (dB)		213.0	226.1	
RAIN (dB)		6.0		
ATMOSPHERIC (dB)		1.1		
INTERMODULATION, POLARIZATION, etc. (dB)		6.0		
SATELLITE				
ANTENNA				
Diameter (m), Gain (dB)		0.9; (46.0)		
Half-Power Beamwidth (°)		0.8		
Minimum Gain (Cell Boundary) (dB)		(42.0)		
VARIABLE BEAM FORMING LOSS (dB)		(2.0)		
SYSTEM TEMPERATURE (Parametric Amplifier) T (°K, dB - K)		850; (29.3)		
EFFECTIVE GAIN (MINIMUM)/SYSTEM TEMPERATURE G/T (dB/°K)		10.7		
RECEIVER IMPLEMENTATION LOSS L_I (dB)		2.5		
CARRIER POWER/NOISE ENERGY				
C/kT = EIRP - L - L_u + G/T - L_I - k (dB-Hz)	(96.7)	(88.9)		(80.8)
Boltzmann Constant (dBJ/°K)				
k = 1.38 x 10^{-23} (J/°K)		-228.6		
CARRIER POWER/NOISE POWER				
C/N = C/N R = C/kTR (dB)		21.4		
E_b/N_0 = C/N - M_I (BER = 10^{-6}) (dB)		10.4		
UPLINK MARGIN M_I (dB)		11.0		
EQUIPMENT AGING MARGIN (dB)		2.0		
NET MARGIN (dB)		9.0		

Table 10-1

Sample Power Budgets for 0.8° Beam Cells

b. Downlink (≈20 GHz)

SATELLITE				
TRANSMITTER POWER (W; dBW)	43.7; (16.4)	12.3; (10.9)		9.5; (9.8)
AFTER BACK-OFF (dB)	(7.0)	(5.0)		(5.0)
ANTENNA				
Diameter (m); Gain (dB)		1.2; (46.0)		
Half-Power Beamwidth (°)		0.8		
EIRP (dBW)	62.4	56.9		55.8
LOSSES L_S				
Variable Beam Forming (dB)		2.0		
Contour (dB)		4.0	7.3	
Pointing (±0.1°) (dB)		1.3		
DOWNLINK LOSSES L_D				
PATH (dB)		210.0		
RAIN (dB)		5.0	222.0	
ATMOSPHERIC (dB)		1.0		
INTERMODULATION, POLARIZATION (dB)		6.0		
TERMINAL				
ANTENNA				
Diameter (m); Gain (dB)	4.5; (57.0)	4.5; (57.0)		2.0; (50)
Half-Power Beamwidth (°)	0.23	0.23		0.52
LOSSES L_T				
Antenna Pointing (dB)		0.5	1.5	
Waveguide (dB)		1.0		
SYSTEM TEMPERATURE (°K; dB - °K)	500; (27.0) (Paramp)	850; (29.3) (GaAs FET)		850; (29.3) (GaAs FET)
EFFECTIVE GAIN/SYSTEM TEMPERATURE G/T (dB/°K)	30.0	27.7		20.7
RECEIVER IMPLEMENTATION LOSS L_I (dB)		2.5		
CARRIER POWER/NOISE ENERGY				
C/kT = EIRP - L_S - L_D - L_T + G/T - L_I - k (dB-Hz)	87.7	79.9		71.8
Rate R (Mb/s; dB-Hz)	33.8; 75.3	5.56; 67.5		0.88; 59.4
CARRIER POWER/NOISE POWER				
C/N = C/kTR (dB)		12.4		
E_b/N_o = C/N - M_D (dB)		10.4		
DOWNLINK MARGIN M_D (dB)		2.0		
EQUIPMENT AGING MARGIN (dB)		2.0		
NET MARGIN (dB)		0.0		

the eastern U.S. provides fixed, reshapable, reconfigurable beams formed by clustering varying numbers of component beam cells. A second MBA requiring fewer beams covers the western U.S. and a third MBA using other fixed or movable beams handles the Mid-West's moderate-to-light traffic. The movable beam concept can be extended to the western or eastern MBAs if desired. It may allow the use of TDMA scanning beam operations within a TDMA-FDMA hybrid mode as suggested by Bell Laboratories (Acampora, et al., 1979) and others.

Beam plan 1 utilizes 0.7° cells exclusively for the eastern and western MBAs. As shown in the beam plan 1 option of figure 10-1, two or more cities may be serviced by a single cell. After the traffic volume and number of terminals have been determined for each cell, various beam topologies can be examined for reducing the number of VBFNs. Improvements are sought by considering several combinations (clustering) of cells: triplets (a shaped beam of 3 cells using 3 feed horns), quadruplets (rhombic) (4 cells requiring 4 feeds), shown in figure 10-1, and sextuplets (6 cells with 6 feeds) (Foldes, 1980).

Each shaped beam employs a single polarization and a single frequency band. Polarization and frequency bands can vary among the shaped beam clusters (Fuenzalida, 1971). Each frequency band within a cluster can be further subdivided according to beam frequency allocations. Each shaped beam is served by one VBFN network. Therefore, the required number of VBFNs is defined by the optimum combination of single cells and the desired shaped beam contour gain level. Initially a 6-dB down gain contour was selected for computing link budgets.

Next, the number of required transponders, using traveling wave tube (TWT) high power amplifiers (HPAs), and transponder capacities needs to be defined. A standard FDMA transponder with a capacity of 32 Mb/s in a 40 MHz bandwidth has been selected. The question is how many of these transponders per beam cell are required? If possible, only one transponder per beam cell is desired so that the number of transponders equals the number of cells. However, neither the traffic nor the power limitations of present or projected TWT amplifiers offer much hope for the use of only one TWT per beam cell. The number of standard 40 MHz bandwidth transponders required, based on a 32 Mb/s capacity transponder, is indicated in each shaped beam of figures 10-1 to 10-3.

Roman numerals index the different shaped beams. The total traffic in each shaped beam is approximately 32 Mb/s times the number of transponders indicated. By using different topologies the number of shaped beams can be N_B = 8, 6, or 4 for the eastern U.S. Unfortunately, the traffic within the 0.7° cells is so heavy that

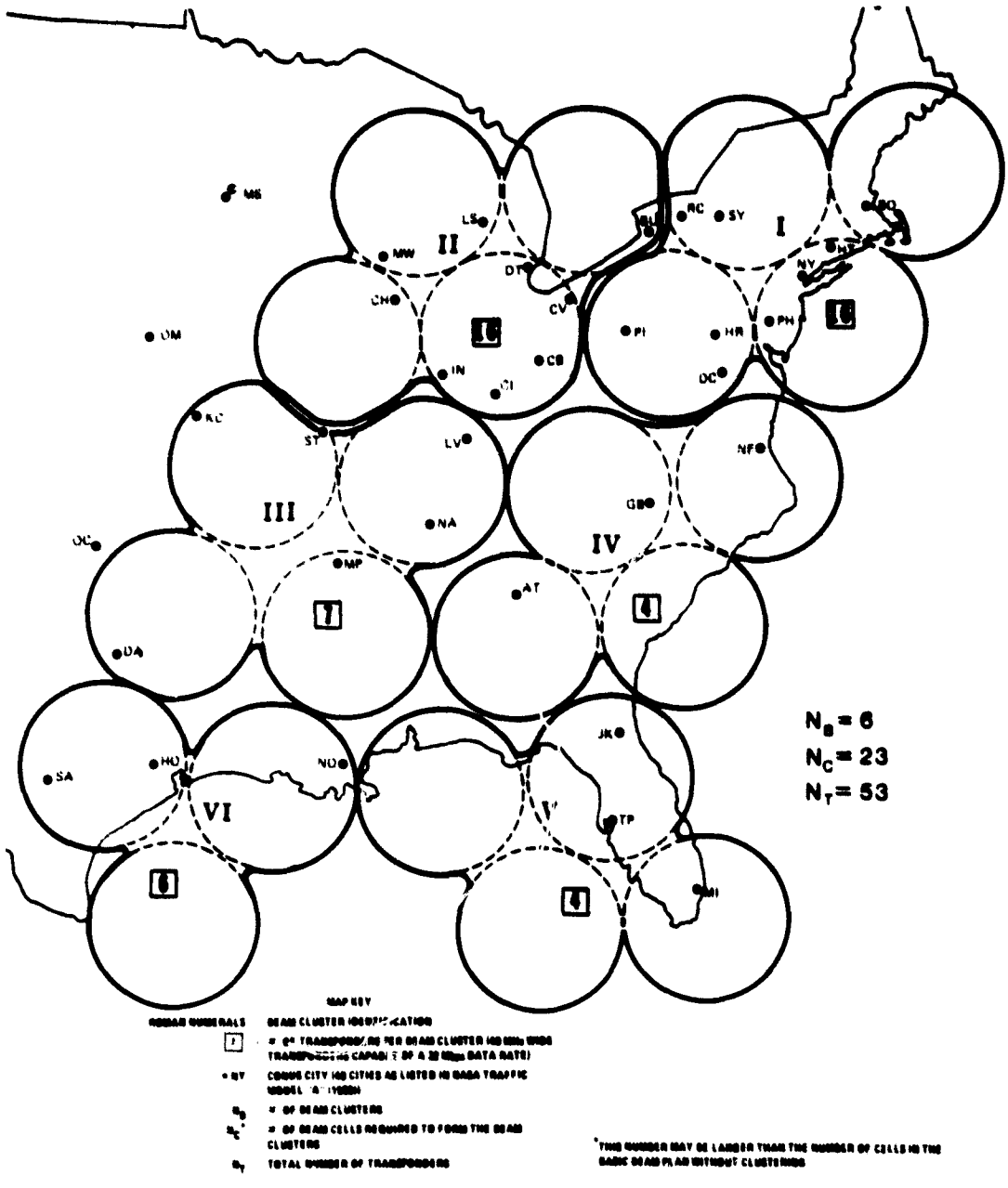

Figure 10-1. Beam Plan 1 (Beam Cell Size = 0.7° HPBW), Rhombic Beam Clusters for Coverage of the Eastern Portion of CONUS

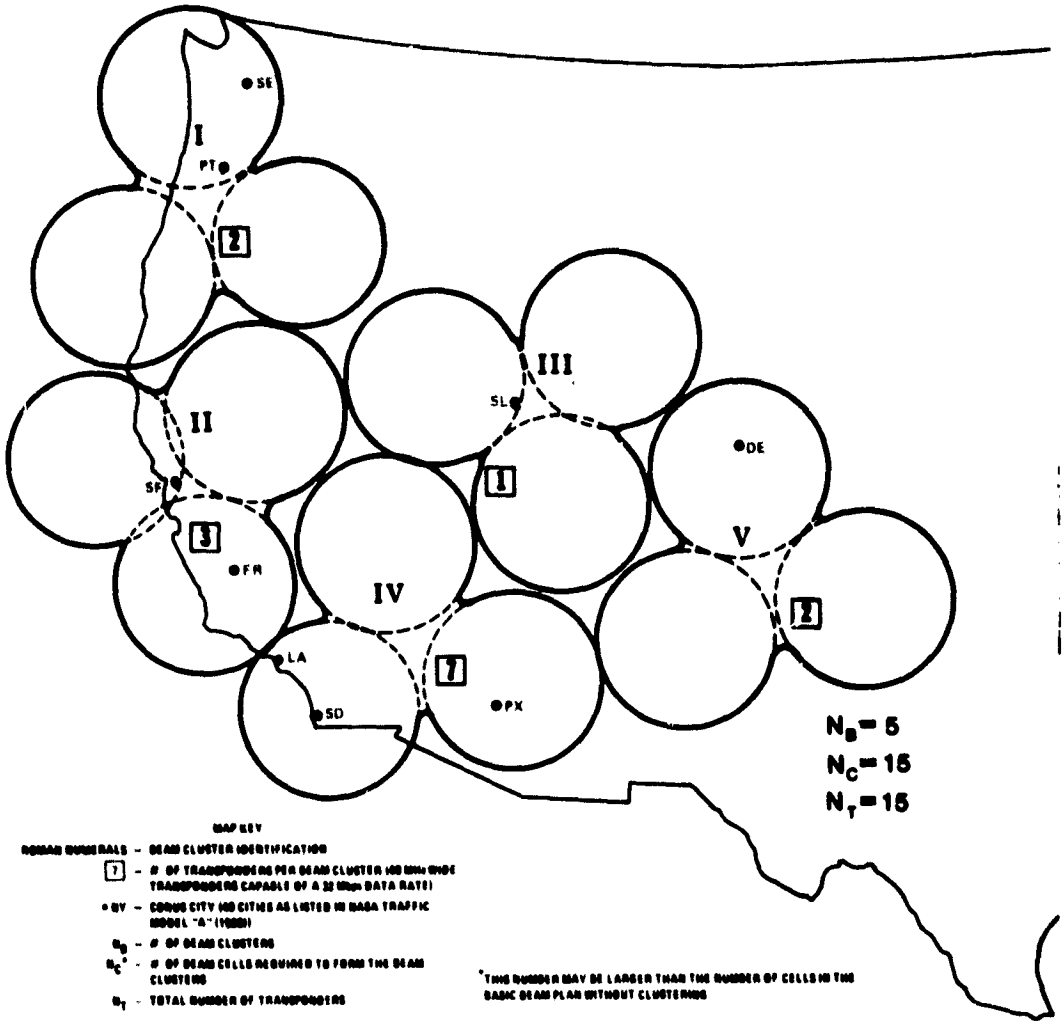

Figure 10-2. Beam Plan 2 (Beam Cell Size = 0.7° HPBW (Western CONUS) and 0.5° HPBW (Eastern CONUS)), Triplet Beam Clusters for Coverage of the Western Portion of the CONUS

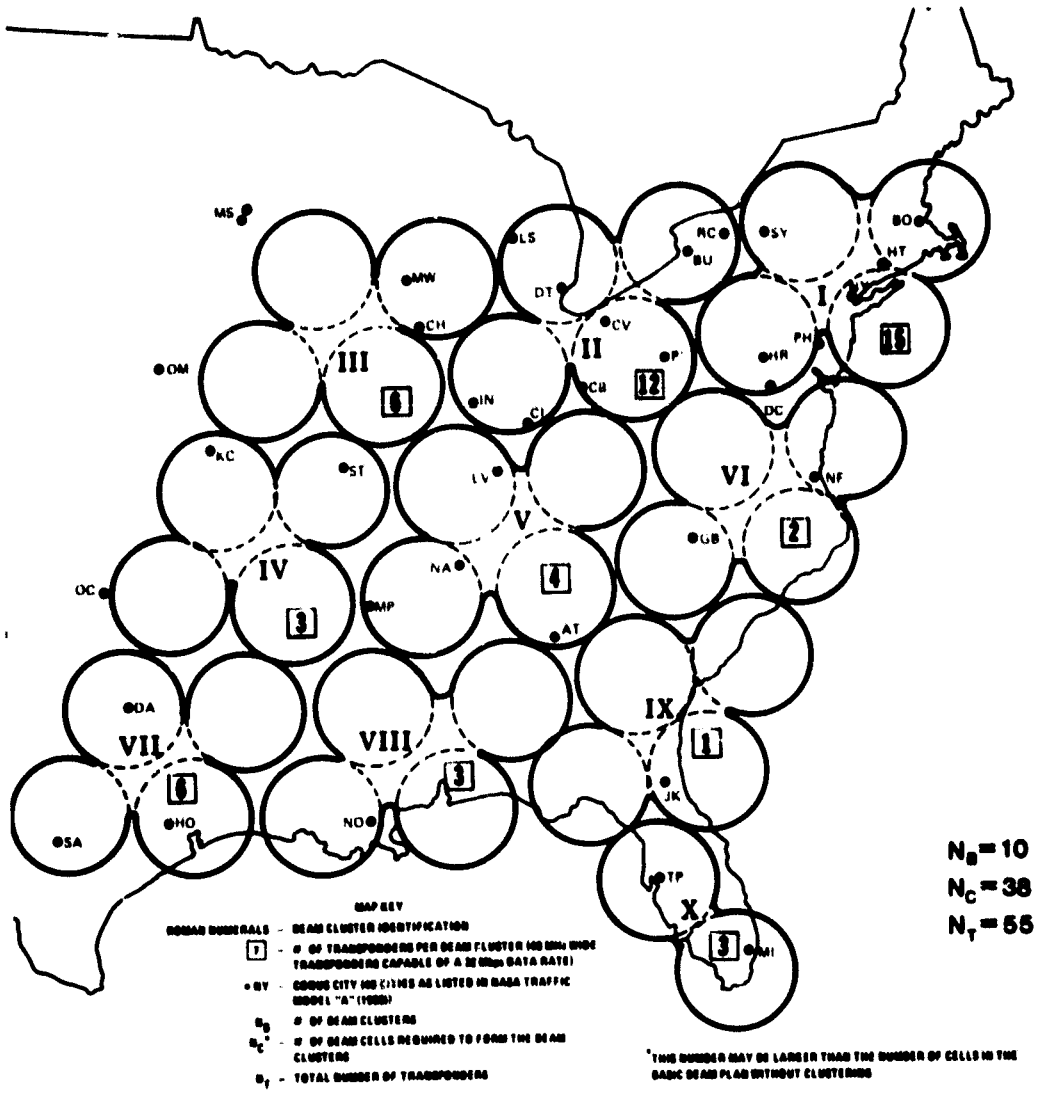

Figure 10-3. Beam Plan 3 (Beam Cell Size = 0.7° HPBW (Western CONUS) and 0.5° HPBW (Eastern CONUS)), Rhombic Beam Clusters for Coverage of the Eastern Portion of the CONUS

smaller cells with less traffic and more antenna gain are necessary. Western coverage with a triplet option is shown in figure 10-2.

In beam plan 2, the cell size is changed from 0.7° to 0.5° only for the eastern U.S. The same process is reapplied using triplet and rhombic quadruplet combinations of the 0.5° cells. Due to the smaller cell sizes, N_B now ranges from 8 to 11; the total number of single cells with required traffic in the eastern U.S. has increased to 33 from 23. In beam plans 1 and 2 some shaped beam clusters contain cells that support no traffic. They are viewed as spare beam cells that could be used for rain margins, traffic fluctuations, and redundancy.

Beam plan 3 of figure 10-3 is very similar to beam plan 2. This time traffic from Texas, Oklahoma, and Kansas is included as part of the eastern U.S. coverage plan. The total number of shaped beams ranges from 7 to 12 and the number of cells increases from 33 to 38. Observe that beam plan 3 has increased traffic efficiency (less traffic per beam cell).

For 0.7° cells, downlink power budgets computed with 5-dB rain margins, for 100 W TWTs (without the necessary -3 dB, or even -6 dB backoff for reducing IM interference) are required. However, for the 0.5° beam size, 50 W TWT HPA transponders can be applied. In addition, for the same traffic density, the number of transponders can be halved, thereby reducing the size and weight of the satellite HPAs by a factor of four. For the smaller 0.88 Mb/s terminals, the required satellite EIRP is 41 dBW per terminal and the TWT power to data rate efficiency is 1 W per Mb/s. The 32 Mb/s TWT HPA then requires about 62 W of power (with 3-dB backoff). An additional 3-dB TWT backoff (6-dB backoff from saturation level) within the HPA still might be desirable. Future intermodulation calculations are needed to determine if this is necessary.

As indicated above, 0.7° cells imply four times the downlink power. Even with beam plan 4 which employs only 0.5° cells, the number of transponders and TWTs approaches approximately 100 (including a 30% redundancy). Limited solar cell power and weight considerations strongly suggest a reduction in this number, if possible.

Based on these beam plans, the ratio of transponders to beam cells for a 0.5° cell size is approximately 1.5 for traffic model A. The ratio for 0.7° cells is approximately 4.5 within the heavier traffic areas of the eastern U.S. and approximately 2.0 for regions of lighter traffic in the western U.S. The 0.5° cells are more desirable in that they permit a smaller number of transponders and a reasonable number of cells. Nevertheless, it appears that the

traffic model is at least four times larger than can be supported by a 0.5° cell FDMA satellite system using current technology.

Beam plan 4 uses 0.5° fixed beams in the western U.S., scanning 0.5° beam cells in the Mid-West, and fixed 0.5° beam cells in the eastern U.S. Within this beam plan, 26 cells support the traffic in the East while only eight cells support traffic in the West. A total of 34 cells are required to serve the 40 city plan covering CONUS. The total number of transponders required in the satellite is 71 to 76. With the above 62 W 40 MHz bandwidth RF TWT specification and a 25% conversion efficiency, the required DC power is approximately 75 x 62 W x 4 = 18,600 W. This agrees with the DC power requirements of the 64-68 beam GE system (Kiesling, 1980).

MITRE Beam Plan 5, an early attempt to avoid cell sizes that were too small in terms of satellite antenna implementation, resulted in 0.8 degree cell sizes and a close-packed arrangement of 17 cells covering the eastern United States. A more scattered collection of six cells would cover the western United States. Although complete coverage of CONUS is not required, an additional option could include a much larger single beam cell to cover midwestern regions for lower data rate users. Thus, a possible implementation of CPS to CPS Traffic Model A would be 23 spot beams and one area coverage beam.

The most difficult design problem arises in the northeastern portion of the United States encompassing megalopolis areas. The 17-beam pattern for the eastern United States is shown in figure 10-4. Beam designations and cities within each beam are listed in the legend. Based on the traffic model, it is observed that five of the beams carry much more traffic. For this reason, two sub-bands are allocated to these five beams. The extra sub-bands were derived in an optimum fashion to provide maximum interbeam isolation and minimum crosstalk between adjacent sub-bands. Since the sub-bands are shown to be equal in bandwidth, the possibility of wasted bandwidth exists within the lower density traffic cells. As shown in section 5, if such cells are in rainy regions this extra bandwidth may allow higher availability.

For completeness, link budgets for the 0.8° cell sizes are included in tables 10-1a and 10-1b.

SATELLITE RF POWER GENERATION

The 18.6 kW DC power requirement mentioned above is probably too large for a 1990 satellite even with the optimistic expectations of GaAs solar cell efficiencies. The current silicon solar cell

efficiency is approximately 100 W/m^2 and the efficiency projected for 1985 is about 130 to 150 W/m^2 (Staelin, Harvey, 1979). In the subsequent discussion, a 5 kW DC power satellite at beginning of life (BOL) is assumed. This implies the need for about 34 to 39 m^2 of solar cells. For comparison, the INTELSAT-V satellite has a solar cell area of about 13 m^2 and a primary power of 1475 W BOL (Martin, 1979; FACC, 1979).

The overall total DC to RF output power conversion efficiency has risen from about 10% five years ago to 14% to 15% for the more recent satellites. Five years from now this overall efficiency may reach 19% or 20%. More detailed estimates of the individual factors included in this conversion are listed in table 10-2.

If a 75 W output power for a saturated TWT and a 5-dB BO is assumed, approximately 23.7 W of useful RF output power is available from each satellite TWT. From the total available RF output power listed in table 10-2, this implies that the number of 250 MHz bandwidth TWTs which can be supported is 32 to 34. In other words, at least 32 downlink beams, with about 25 W of power per beam and 30% efficiency, are feasible with a 5000 W DC power satellite in 1985.

TRUNKING TRAFFIC POWER LOAD

The goal is to attempt to serve both trunking and CPS users on the same satellite. Although it may be desirable or even necessary to use a separate satellite for trunking traffic, it is assumed here that all traffic is handled by a single satellite. This raises the issue of the amount of DC power required to support the trunking traffic. In order to provide this estimate, a cursory design of the pure trunking portion of the system was necessary.

According to the NASA supplied traffic model, there are 39 trunking terminals distributed among 18 beam areas. The terminal types and numbers are listed in table 10-3 along with estimated downlink RF output powers to these terminals based on reasonable downlink power budgets for each trunking terminal type.

In contrast to CPS traffic, busy hour trunking traffic must be supported with a 100% duty factor. Assuming an overall DC to RF output power conversion efficiency of 16%, approximately 616 W of the satellite DC power are required for trunking (see table 10-3). If this amount is subtracted from the 5000 W total available satellite DC power, 4384 W of DC power can be devoted to CPS traffic. With the same 16% conversion efficiency, this leaves 701 W of total downlink CPS power or about 22.6 W per beam for a 31-beam

Table 10-2

Estimated Power Conversion Efficiencies for a 5000 W DC Power Satellite

Total DC Power Available	5000 W
Fraction of DC Power Allocated for Communications	η_{DC} = 60 to 65%
DC Power Available for Communications	3000 to 3250 W
Power Supply Efficiency	η_{PS} = 85%
DC Power Input to TWTs	2550 to 2763 W
HPA (2-collector) TWT Efficiency at Saturation	η_{SA} = 40%
Efficiency at 5-dB Backoff (BO)	η_{BO} = 30%
Available RF Output Power	5000 W x η = 765 to 829 W
where $\eta = \eta_{DC}\ \eta_{PS}\ \eta_{BO}$ = 15.3 to 16.6%	

Table 10-3

Trunking Terminal Downlink Power Allocation

Terminal Type	Data Rate (Mb/s)	G/T (dB/°K)	Downlink Power per Terminal (W)	Number of Terminals	Total Downlink Power (W)
A	548	37.9*	7.4	4	29.6
B	274	37.9*	3.7	11	40.7
C	87.5	37.9*	1.2	18	21.6
D	12.6	29.2†	1.1	6	6.6
				Total:	98.5 W

* 10 m Antenna and 200°K System Noise Temperature

† 4.5 m Antenna and 300°K System Noise Temperature

55% Antenna Efficiency

3-dB Beam Edge Reduction Included

CPS system. If 25 W per beam are required for CPS traffic in a 31-beam CPS system, then 5513 W of DC power are required rather than 5000 W. The additional 513 W could be obtained with 3.4 to 3.9 m^2 of additional solar cell area. The actual detailed computation for the total required power in the final system design recommended in section 11 is consistent with this model which uses a fixed average power per beam.

The next step is to estimate what total downlink power is required to service the CPS terminals of the traffic model. If this power exceeds the useful output power available for CPS traffic, then either more DC power is required on the satellite, or only a fraction of the postulated CPS traffic can be handled by a 5000 W satellite.

The estimated downlink power budgets for the three CPS terminal types of Traffic Model A are given in table 10-4. The same format as table 10-1 is employed. Many of the parameter values are the same, particularly the losses, including an assumed 5-dB loss for rain, etc., (Crane, 1979; Berk, 1979; Lin, et al., 1980). The main difference is that 0.33° beams are used in table 10-4. An 8-m dish is also recommended for the 33 Mb/s CPS terminal. The downlink powers devoted to each terminal are sufficient to provide at least a 1-dB margin in addition to the 5-dB rain loss so that the overall downlink margin in the absence of rain is at least 6 dB.

If half the CPS terminals are active, the total downlink power required is approximately

$$(1.6 \times 80 + 1.8 \times 300 + 0.3 \times 1824)\ 0.5\ W = 608\ W$$

with the powers and numbers of terminals data in table 10-4. This is 93 W less than the 701 W that are available for CPS downlink power with a 5 kW satellite, as computed previously. Thus, if the traffic were distributed uniformly in the 31 beams, the traffic model would be satisfiable with an extra 0.6 dB of margin. Alternatively, less intermodulation interference could be suffered by backing off the satellite TWTs another 0.6 dB.

Since the traffic model is highly non-uniform, the beams containing the heavier traffic loads would require more than one of the nominally 22.6 W TWTs. If all the TWTs are identical, there are four extra TWTs to cover diophantine problems of matching the required power within every beam. It appears that the traffic will not be handled to the extent that too much excess power is

Table 10-4

Downlink Power Budgets for System A CPS Terminals (cf., Table 10-1)

SATELLITE			
TRANSMITTER POWER (W;dBW)	1.6;(2.0)	1.8;(2.6)	0.3;(-5.2)
AFTER BACKOFF (dB)		(5.0)	
ANTENNA			
Diameter (m); Gain (dB)		3.5;(53.7)	
Half-Power Beamwidth (°)		0.33	
EIRP (dBW)	55.7	56.3	48.5
LOSSES L_S		7.3	
DOWNLINK LOSSES L_D		222.0	
TERMINAL			
NUMBER*	80	300	1824
ANTENNA			
Diameter (m); Gain (dB)	8.0;(62.0)	4.5;(57.0)	4.5;(57.0)
Half-Power Beamwidth (°)	0.13	0.23	0.23
LOSSES L_T		1.5	
SYSTEM TEMPERATURE (°K; dB - °K)	400;(26.0)	850;(29.3)	850;(29.3)
G/T (dB/°K)	36.0	27.7	27.7
RECEIVER LOSS L_I(dB)		2.5	
C/kT (dB-Hz)	87.0	79.3	71.5
RATE R (Mb/s; dB-Hz)	33.8;75.3	5.56;67.5	0.88;(59.4)
C/N (dB)	11.7	11.8	12.1
E_b/N_o = C/N - M_D (dB)		10.4	
DOWNLINK MARGIN M_D (dB)	1.3	1.4	1.7

*The number of CPS terminals of each type is based on the revised traffic model supplied by NASA/LeRC in the Dec. 1980 RFP for an SS-FDMA System Study.

squandered on lighter traffic beams demanding less output power than one TWT provides.

TERMINAL COST MODEL

The methodology for estimating terminal costs is explained in this subsection. The principal components of a generic terminal are identified as physical operational modules. Whenever possible, hardware cost estimating relationships based on technical operating characteristics are proposed for each module. Otherwise, cost data supplied by manufacturers is used directly. All costs in this report are given in terms of 1980 dollars.

A terminal is functionally described in terms of its overall parameters of operating frequency, transmitter power rating, and antenna aperture size. Values are assigned to these parameters to meet the required uplink power budget. Basic cost model formulas are then applied to these technical parameters to yield a hardware cost for the antenna and transmitter modules. Then total terminal development and production costs are derived.

The methodology yields cost information for three separate phases of a new-product cycle. The first research and development (R&D) phase costs include the non-recurring costs of designing and developing a new terminal and the production cost of a small quantity (e.g., five) of advanced engineering development models. The latter entails both hardware costs and recurring engineering, program management, data, testing, general and administrative (G&A) costs, and profit. In the second low rate production (LRP) phase, a moderate quantity (e.g., twenty-five) of terminals is produced using prototypes, final drawings, and special tooling if required. The third phase is for the full scale production (FSP) of a large number of terminals. The LRP phase is appropriate for large terminals since only relatively small quantities may be deployed. The FSP phase is appropriate for smaller terminals.

In each of the three phases, the cost of the first terminal is calculated from the basic hardware module cost and k-factors (described below) which are useful in estimating other costs. Then a well-known and accepted learning curve method is applied to obtain the total average production cost for an arbitrary number of terminals.

The terms and equations used are defined below for first terminal cost for each of the three production phases. The cost estimates are based on key RF hardware costs associated with the following modules of a generic terminal:

TRX - transmitter

ANT - antenna (dish, pedestal, mount, step-tracking system)

MOD - modem

SYN - frequency synthesizer

UPD - up/down converters

STD - frequency standard

LNA - low noise amplifier.

The cost (in $K) of each item is represented by a name formed by placing a C before the above variable name abbreviations. All modules but the antenna, frequency standard, transmitter, and modem are dual redundant to provide a 99.9% terminal reliability. CTRX can be computed as a function of frequency f(GHz) and transmit power P(W), and CANT as a function of frequency and dish size D(m), as outlined below.

Let RDF and PRF be R&D and production scaling factors that are defined as follows:

$$\text{RDF} = \begin{cases} 1.15, & \text{R\&D phase} \\ 1.00, & \text{production phases} \end{cases} \qquad (10.1)$$

$$\text{PRF} = 3.0, \quad \text{FSP phase}$$

Then the transmitter and step-tracking antenna hardware costs are given by

$$\text{CTRX} = \left\{ \begin{array}{l} 13\ P^{0.25}\ f^{0.33}\ \text{RDF}, \quad P > 50\ \text{W} \\ 7\ P^{0.25}\ f^{0.33}\ \text{RDF}, \quad P \leq 50\ \text{W} \end{array} \right\} \quad f > 20\ \text{GHz} \qquad (10.2)$$

and

$$\text{CANT} = 9.2\ D^{0.75}\text{PRF}, \quad f > 15\ \text{GHz}. \qquad (10.3)$$

The total hardware (HDW) cost, CHDW, is the weighted sum of the module costs

$$CHDW = 1.15\ (CANT + CSTP\ \ ?\ (CTRX + CMOD + CSYN + CUPD + CLNA)). \quad (10.4)$$

The 1.15 factor is a fixed value, frequency independent, that is supported by the historical cost experience of manufacturers. The factor of 2 accounts for the dual-redundancy modules.

The hardware cost is then used in a series of equations to calculate the first unit terminal cost

$$C_1 = CHDW + CBTE + CASS + CINT + CTST + CDAT + CPEC + CENG + CPMG + CGAA + CFEE \quad (10.5)$$

The variables in equation (10.5) are defined as follows:

CBTE -- built-in test equipment cost

$$CBTE = 0.1\ CHDW \quad (10.6)$$

CASS -- assembly cost

$$CASS = k_1(CHDW + CBTE) \quad (10.7)$$

CINT -- integration of subsystems cost

$$CINT = k_2(CHDW + CBTE) \quad (10.8)$$

CTST -- system testing

$$CTST = k_3(CHDW + CBTE + CASS + CINT) \quad (10.9)$$

CDAT -- documentation of test data

$$CDAT = k_4(CHDW + CBTE + CASS + CINT) \quad (10.10)$$

CPEC -- peculiar equipment costs

$$CPEC = k_5(CHDW + CBTE + CASS + CINT) \quad (10.11)$$

CENG -- engineering and tooling and quality control costs

$$CENT = k_6(CHDW + CBTE + CASS + CINT) \quad (10.12)$$

CPMG -- program management cost

$$CPMG = k_7(CHDW + CBTE + CASS + CINT) \quad (10.13)$$

CGAA -- general and administrative costs of the production facility

$$CGAA = k_8(CHDW + CBTE + CASS + CINT + CTST + CDAT + CPEC + CENG + CPMG) \quad (10.14)$$

CFEE -- profit

$$CFEE = k_9(CGAA + CHDW + CBTE + CASS + CINT + CTST + CDAT + CPEC + CENT + CPMG). \quad (10.15)$$

The values of the k factors appearing in the above equations depend on the operating frequency of the terminal and the production phase considered. The various k-factors used in the cost estimates are given in table 10-5.

Table 10-5

k-Factors Used in the Cost Estimates of Each Phase

	Factor								
	k_1	k_2	k_3	k_4	k_5	k_6	k_7	k_8	k_9
R&D	0.28	0.11	0.27	0.05	0.12	0.31	0.22	0.16	0.10
LRP	0.19	0.11	0.10	0.08	0.16	0.40	0.12	0.16	0.10
FSP	0.10	0.11	0.08	0.05	0.02	0.12	0.06	0.16	0.10

Now that the first unit terminal cost (C_1) is available from equation (10.5), the average cost of a terminal for each of the three phases can be computed as follows. Let L = 0.95 be the learning curve factor for K_a-band. Then the nth-unit terminal cost in any phase is given by

$$C_n = C_1 L^{\log_2 n} \quad (10.16)$$

The total and average terminal cost for N terminals can be expressed as

$$C(N) = \sum_{n=1}^{N} C_n = C_1 \sum_{n=1}^{N} L^{\log_2 n} \quad (10.17)$$

$$\overline{C(N)} = C(N)/N. \tag{10.18}$$

Unfortunately, C(N) cannot be expressed in closed form. A good approximation to the total terminal cost derived by Cho and Schmidt of MITRE (Cho, Schmidt, 1980) is

$$C(N) \approx C_1\left(N^{\log_2 L}\left(\frac{N}{1+\log_2 L} + .5 + \frac{\log_2 L}{12N}\right) - \frac{1}{1+\log_2 L} + .5 - \frac{\log_2 L}{12}\right) \tag{10.19}$$

$$\approx 1.08\ C_1 N^{0.926}, \text{ for } L = 0.95 \text{ and large } N$$

Using this approximation, the average terminal cost becomes

$$C(N)/N \approx 1.08\ C_1 N^{\log_2 L} \approx 1.08\ C_1 N^{-0.074} \tag{10.20}$$

Let NRF be a non-recurring engineering cost factor that is supported by a cost history data base of manufacturers for various frequency bands:

$$NRF = \begin{cases} 4.0, & 7/8 \text{ GHz} \\ 5.0, & 30/20 \text{ GHz} \\ 5.6, & 44/20 \text{ GHz} \end{cases} \tag{10.21}$$

Then the total cost of the R&D phase is

$$C_{R\&D} = C(N) + NRF.C_1$$

$$\approx C_1\ (1.08\ N^{0.926} + 5), \text{ for } N \geq 5 \tag{10.22}$$

using equations (10.19) and (10.21). Equations (10.19) and (10.20) are used to calculate the total and average costs of the LRP and FSP phases.

SATELLITE COST MODEL

The SAMSO spacecraft cost model (DCA/MSO, 1976; Katz, et al., 1979) which requires only communications payload weight W_c(in lb) as an input is used in this report. The non-recurring engineering and first unit spacecraft costs (in \$M), CNRE and CFUS, respectively, are given by

$$\text{CNRE} = 0.016\, W_c^{1.16} \tag{10.23}$$

$$\text{CFUS} = 0.031\, W_c^{0.93}, \text{ first spacecraft.} \tag{10.24}$$

Additional satellites are assumed to cost approximately 0.9 CFUS each. Launch costs and the cost of an apogee-perigee engine are estimated separately.

REFERENCES

(Acampora, et al., 1979) A. S. Acampora, et al., "A Satellite System with Limited-Scan Spot Beams," IEEE Trans. Commun. Vol. COM-27, No. 10, October 1979, 1406-1415.)

(Berk 1979) G. Berk, "The Effect of Excessive Rain Attenuation on Satellite Link Availability," WP-22125, Air Force Contract No. F19628-80-C-0001, Bedford, MA: The MITRE Corporation, December 1979.

(Cho, Schmidt) C. C. Cho and B. K. Schmidt, "Learning Curves and Total Production Cost: A Closed Form Approximation," WP-22862, Air Force Contract No. F19628-80-C-0001, Bedford, MA: The MITRE Corporation, June 1980.

(Crane, 1979) R. K. Crane, "Prediction of Attenuation by Rain," Concord, MA: Environmental Research and Technology, Inc., August 1979.

(DCA/MSO, 1976) "MILSATCOM Systems Architectures, Annex G, 'Cost Models'," Washington, DC: Defense Communications Agency, MILSATCOM Systems Office, March 1976.

(FACC, 1979) "Concepts for 18/30 GHz Satellite Communication System Study," Volume 1 - Final Report, WDL-TR8457 (CR 159625), Contract No. NAS 3-21362, Palo Alto, CA: Ford Aerospace & Communications Corporation/Western Development Laboratories Division, 1 November 1979, p. 3.2-19.

(Foldes, 1980) P. Foldes, "Ka Band, Multibeam Contiguous Coverage Satellite Antenna for the USA," AIAA 8th Communications Satellite Systems Conference, Orlando, Florida, April 20-24 1980, pp. 490-499.

(Fuenzalida, 1971) J. C. Fuenzalida and E. Podraczky, "Reuse of the Frequency Spectrum at the Satellite," Communication Satellites for the 70's: Systems, Feldman and Kelley, eds., Progress in Astronautics and Aeronautics, Vol. 26, Cambridge, MA: MIT Press, 1971.

(Katz, et al., 1979) J. L. Katz, et al., "Application of Advanced On-Board Processing Concepts to Future Satellite Communication Systems," Final Report, MTR-3787, Vol. 1, Contract No. F19628-79-C-0001 for NASA/Lewis Research Center, Bedford, MA: The MITRE Corporation, June 1979.

(Kiesling, 1980) J. D. Kiesling, "A Study of Advanced Communications Satellite Systems Based on SS-FDMA," Document No. 805DS4217, Contract No. NAS 3-21745, Valley Forge Space Center, Philadelphia, PA: General Electric/Space Division, May 1980.

S. H. Lin, H. J. Bergman, and M. V. Pursley, "Rain Attenuation on Earth Satellite Path - Summary of 10 Year Experiments and Studies," The Bell System Technical Journal, Vol. 59, No. 2, February 1980, pp. 183-228.

(Martin, 1979) D. H. Martin, "Communications Satellites, 1958 to 1982," Interim Report, SAMSO-TR-79-078, AD A078051, El Segundo, CA: The Aerospace Corporation, 10 September 1979, p. 4-37.

(Staelin, Harvey, 1979) D. H. Staelin and R. Harvey, "Future Large Broadband Switched Satellite Communications Networks," Final Technical Report, Contract No. NAS-5-25091, Cambridge, MA: MIT Research Laboratory of Electronics, December 1978, pp. 98-128.

SECTION 11

EXEMPLAR SYSTEM DESIGNS

Three exemplar system designs are presented and evaluated in terms of system performance and cost. Two designs (a six-region and a four-region network) are based on Traffic Model A, and the third (a five-region network) is based on Model B. A unique feature of these designs is the organization of traffic on a regional basis. The regional concept greatly simplifies the satellite design as will be shown later.

VERSION A

The satellite systems designed to handle Traffic Model A serve 45 major CONUS cities. In an effort to conserve downlink satellite RF power, only these cities and their immediate surrounding areas are illuminated; continuous coverage of CONUS is not provided in Version A. Thirty-two beams of 0.33° cover the specified 45 cities. The half-power beamwidth of 0.33° is chosen because it is approximately the smallest beam size feasible with the state-of-the-art satellite pointing accuracy of 0.05°. This degree of pointing accuracy requires monopulse tracking. Small beam cells allow frequency reuse and help achieve the necessary link margins.

Several technology constraints and NASA specified parameters led to the regional routing concept:

1. Direct access to the satellite is permitted for up to several thousand multichannel terminals.

2. Individual routing of a user's call is required.

3. Channel assignments are made dynamically under the direction of a central control center.

4. The specified traffic is distributed among the traffic centers in a non-uniform manner.

5. The system is bandwidth and power limited. The bandwidth is limited to the 2.5 GHz available in the 20/30 GHz frequency bands. The available DC power is limited by the solar array technology constraints.

6. The satellite needs to be simple if it is not to exceed the 5000 lb weight limitation. (This weight constraint is due to launch vehicle limitations.)

The regional routing satellite system concept is described in more detail in the remaining sections.

Regional Concept

A region is a geographical area containing a collection of beams. The total CPS and cross-traffic supported should be approximately the same in all regions. An even distribution of traffic among the regions is important for two reasons: (1) to ease the satellite multiplexer specifications, and (2) to ensure efficient use of the allocated bandwidth. Since the beams carry non-uniform amounts of traffic, regions may contain unequal numbers of beams. The number of regions implemented depends on the total specified traffic, the available bandwidth, beam locations, and so on. Designing for the minimum number of regions is desirable. Using too many regions provides no additional improvements and only serves to complicate the satellite and the frequency plan.

The satellite must provide full connectivity between all uplink and downlink beams. In a 32-beam system ($N_B = 32$) every receive horn must have connectivity to all 32 transmit horns. In an FDMA system this connectivity is provided by bandpass filters. Therefore, every receive horn must be connected to a multiplexer consisting of 32 filters. The number of such multiplexers equals the number of receive horns, $N_B = 32$, and the total number of filters equals $N_B^2 = 32^2 = 1024$.

In a satellite which uses the regional concept, the receive horns of a region are connected to a common output; therefore, the number of multiplexers equals the number of regions, N_R. In a six-region system the number of multiplexers is $N = 6$ and the total number of bandpass filters is $N_R \times N_B = 6 \times 32 = 192$. Thus, the regional concept greatly reduces the number of filters in the satellite. Each filter is connected to IF amplifiers and frequency converters, and as the number of filters is reduced, so is the number of these components. In addition, the regional routing scheme reduces the number of down-converters from N_B to N_R (32 to 6). This reduction in satellite complexity signficantly reduces the satellite weight and power consumption.

Figure 11-1 shows a view of CONUS as seen from a satellite in a geostationary orbit over 90° west longitude. The 32 beams and the cities they serve are identified. In addition, the regional boundaries for a four-region system are shown.

VG-55,819

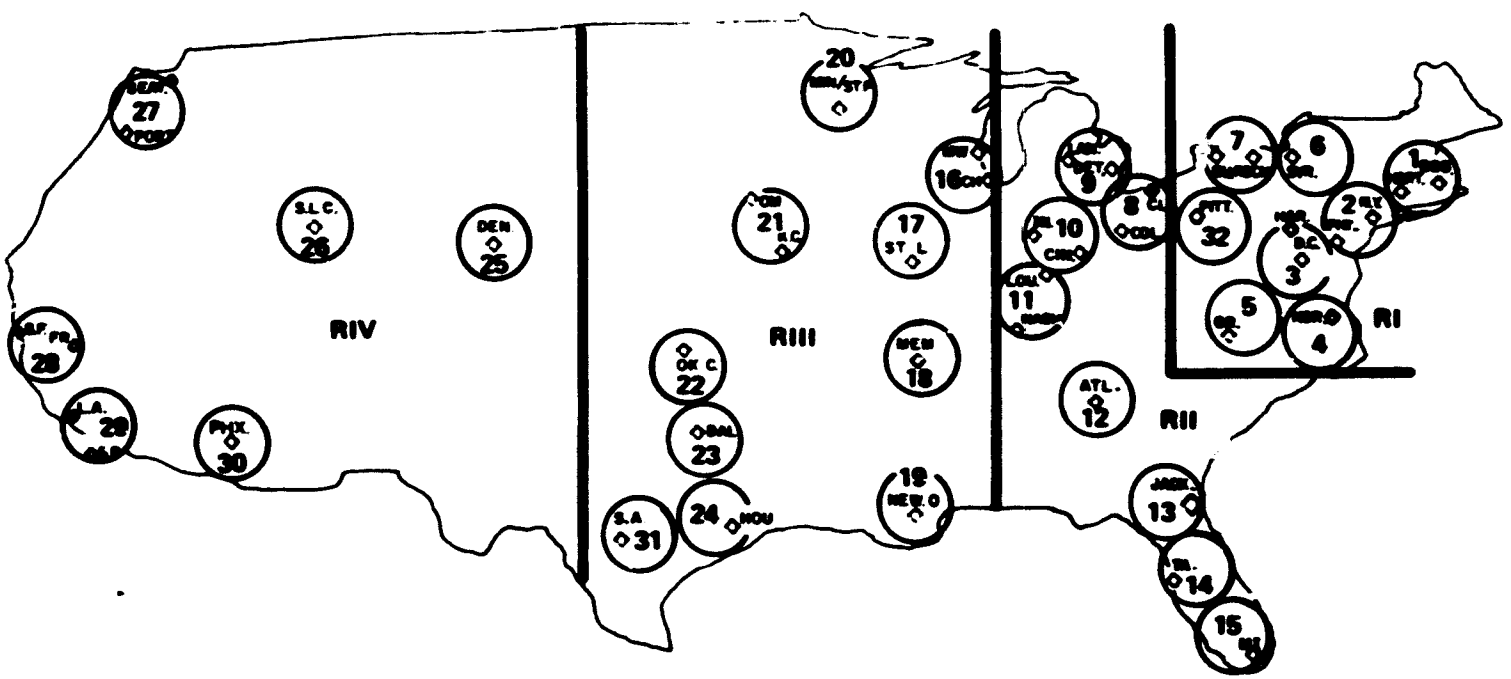

Figure 11-1. A Four-Region Beam Plan (CONUS as seen from 90° West Longitude)

Frequency Organization

The total available uplink (downlink) bandwidth of 2.5 GHz is divided into four bands. Bands $U_1(D_1)$ and $U_2(D_2)$ are each 850 MHz wide, and bands $U_3(D_3)$ and $U_4(D_4)$ are each 400 MHz wide, as shown in figures 11-2 and 11-3 for a four-region network.

A bandwidth of 850 MHz is assigned to each region for CPS traffic. Using 850 MHz, for each CPS band provides a reasonable balance between the needs of the CPS users and trunking users. (Under different system specifications, other bandwidth allocations for the CPS bands may be more desirable.) The selection of CPS/trunking bands must be made carefully to ensure sufficient resources for all users.

Band U_1 is used for CPS traffic in regions 1 and 3. Similarly, band U_2 is used for CPS traffic in regions 2 and 4. This ensures interference-free operation for the CPS traffic, because beams that use the same frequency band are sufficiently separated (see section 4). In region 1, band U_2 may be used for trunking traffic in those beams that are sufficiently separated from beams in region 2 (for example, beams 1 and 2 in figure 11-1). In region 2, band U_1 may be used for trunking traffic in those beams that are sufficiently separated from beams in regions 1 and 3. Beams that carry trunking traffic and lie close to beams of adjacent regions employ band U_3 and/or band U_4 (for example beams 3 and 32 in figure 11-1). Bands U_3 and U_4 are used exclusively for trunking traffic.

Allowing the trunking terminals to use frequency bands allocated for CPS terminals in other regions provides a single satellite system with additional bandwidth. In some regions, the entire 2.5 GHz bandwidth can be used to support both trunking and CPS traffic. If frequency bands were preassigned to each traffic type, the full 2.5 GHz would not be available to any region, thereby reducing the total system capacity. However, allowing the trunking stations and the CPS stations to use common frequency bands requires careful frequency planning. Also, the use of these common frequency bands for trunking traffic is not permitted in every beam due to interference problems (see section 4).

In summary, every region has 850 MHz of bandwidth available for CPS traffic and may have as much as 1650 MHz of bandwidth available for trunking traffic. Figure 11-4 shows the frequency band assignments for each beam in a four-region network using the frequency organization described above. In addition, the polarization (either vertical or horizontal) assigned to each band within a beam is identified. Polarization is assigned to increase each beam's isolation from interference (see section 4).

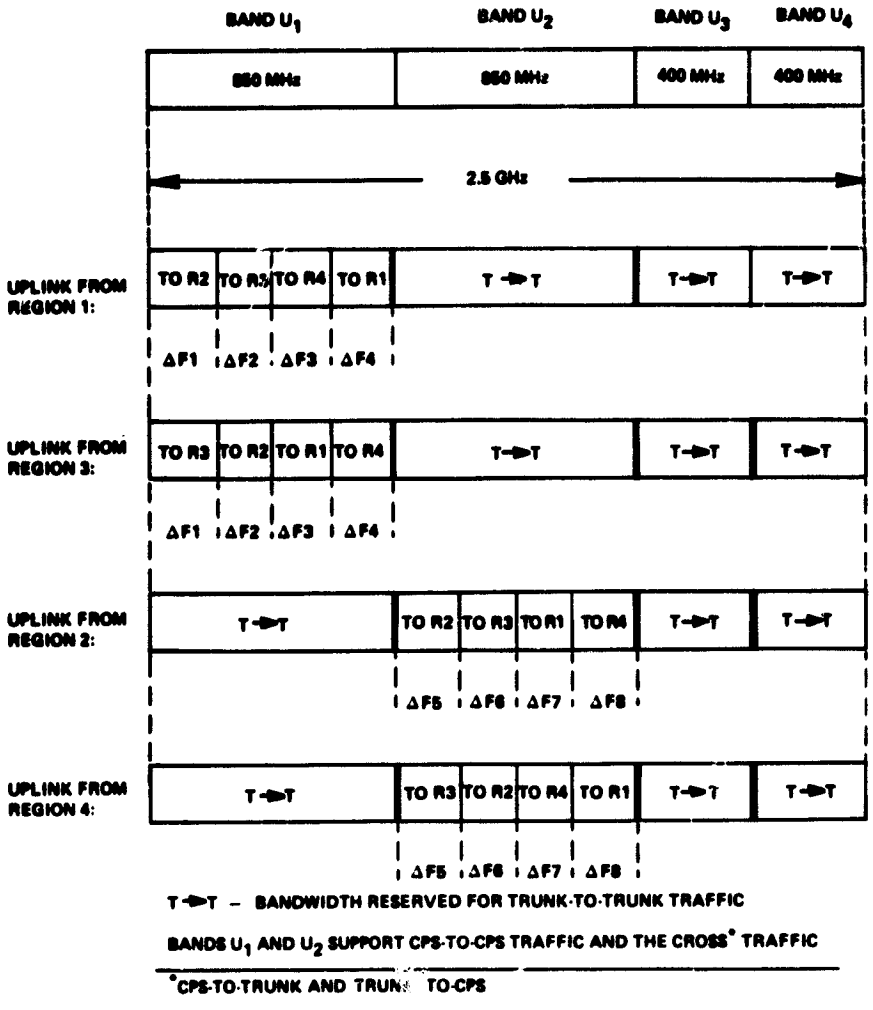

Figure 11-2. Uplink Frequency Plan for a Four-Region Network

C-3

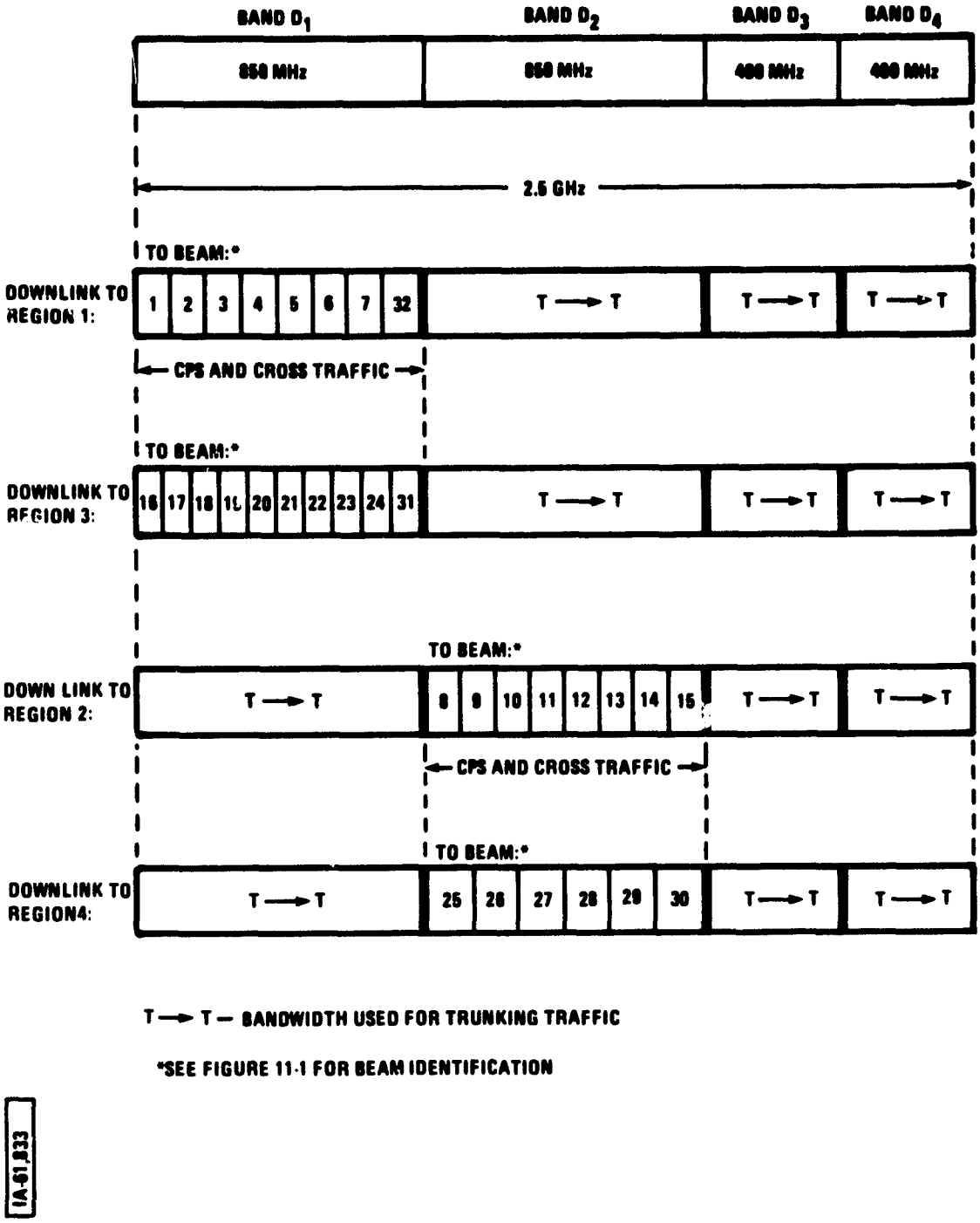

Figure 11-3. Downlink Frequency Plan for a Four-Region Network

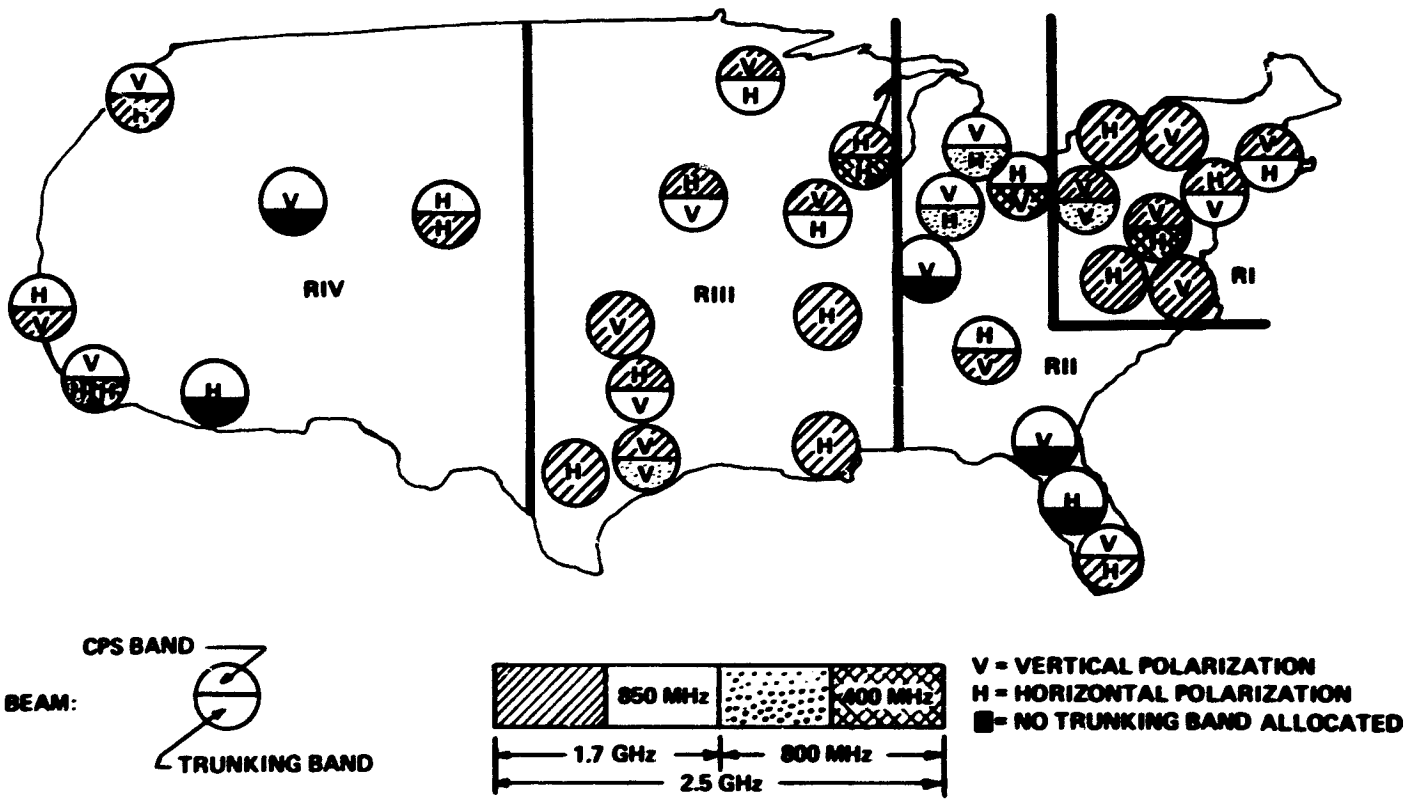

Figure 11-4. A Four-Region Frequency and Beam Plan as Seen From 90° West Longitude

In every region, the uplink CPS band is organized according to destination. The band is first divided into sub-bands, one for each regional destination. Next, each sub-band is divided into beam sub-bands, one for every beam within the addressed region. These sub-bands are non-uniform in width because they vary according to the amount of traffic destined for the individual beams.

The beam sub-bands contain channels for individual users. These channels are transparent to the satellite. (The smallest frequency bands routed on-board the satellite are the beam sub-bands.) Unlike the regional sub-bands and the beam sub-bands that have fixed widths and frequency allocations, the channel assignments change dynamically. As users start and finish their transmissions, individual channel assignments vary with time. Users within the same region are never assigned the same instantaneous channel bandwidths. Frequency reuse occurs only among the regions and not within a region.

A six-region network is designed in parallel with the four-region network previously presented. Figure 11-5 shows the six regional boundaries, the frequency band assignments, and the assigned polarizations. The two parallel designs allow a comparison of costs, performance, and trade-offs for various configurations.

Transponder Architecture

A simplified block diagram of the transponder for a six-region system is shown in figure 11-6. The operation of the transponder is explained with reference to figure 11-7.

Since frequency reuse is not permitted within a region, the receive horns of a region can be combined in groups. In region 1, four horns (H_1 through H_4) are combined; in region 2, eight horns are combined, and so on. The instantaneous channel frequencies received by H_1, H_2, H_3, and H_4, are shown in figure 11-7A.

The signals received by the horns are amplified by low-noise preamplifiers, (A_1 through A_4) and then fed into antenna combiners (C_1 through C_6) that connect the receive horns of a region. The frequency bands at the outputs of these combiners are shown in figure 11-7B.

The combiners feed RF multiplexers (MUX 1 through MUX 6) which split the uplink bands into six destination sub-bands; the sub-bands destined for region 1 are indicated in figure 11-7C.

The union of sub-bands from regions 1, 3, and 5 that are destined for downlink region 1 is formed by a hybrid combiner, C_7;

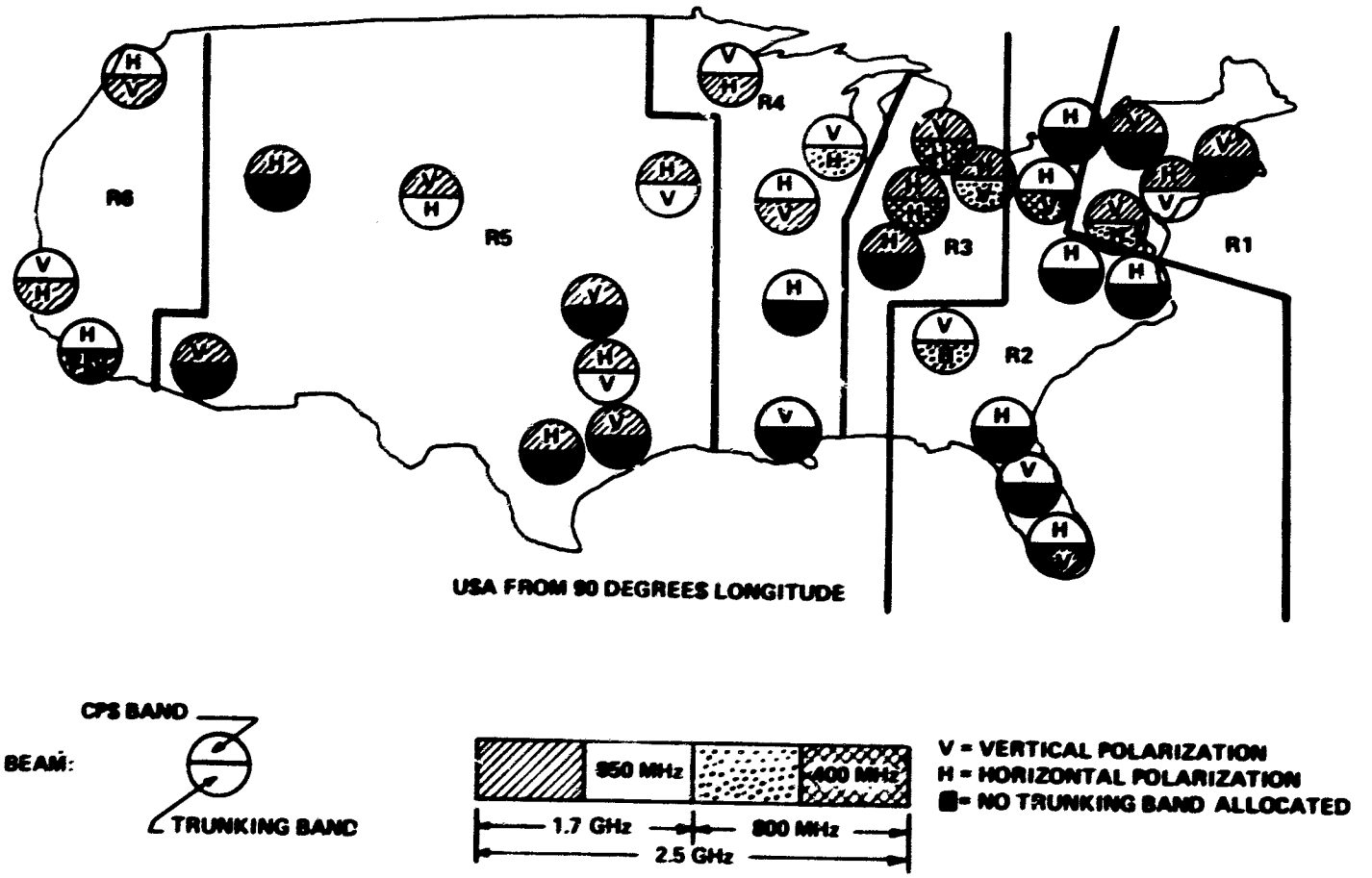

Figure 11-5. Beam and Frequency Plans for a Six Region CPS and Trunking FDMA Satellite System

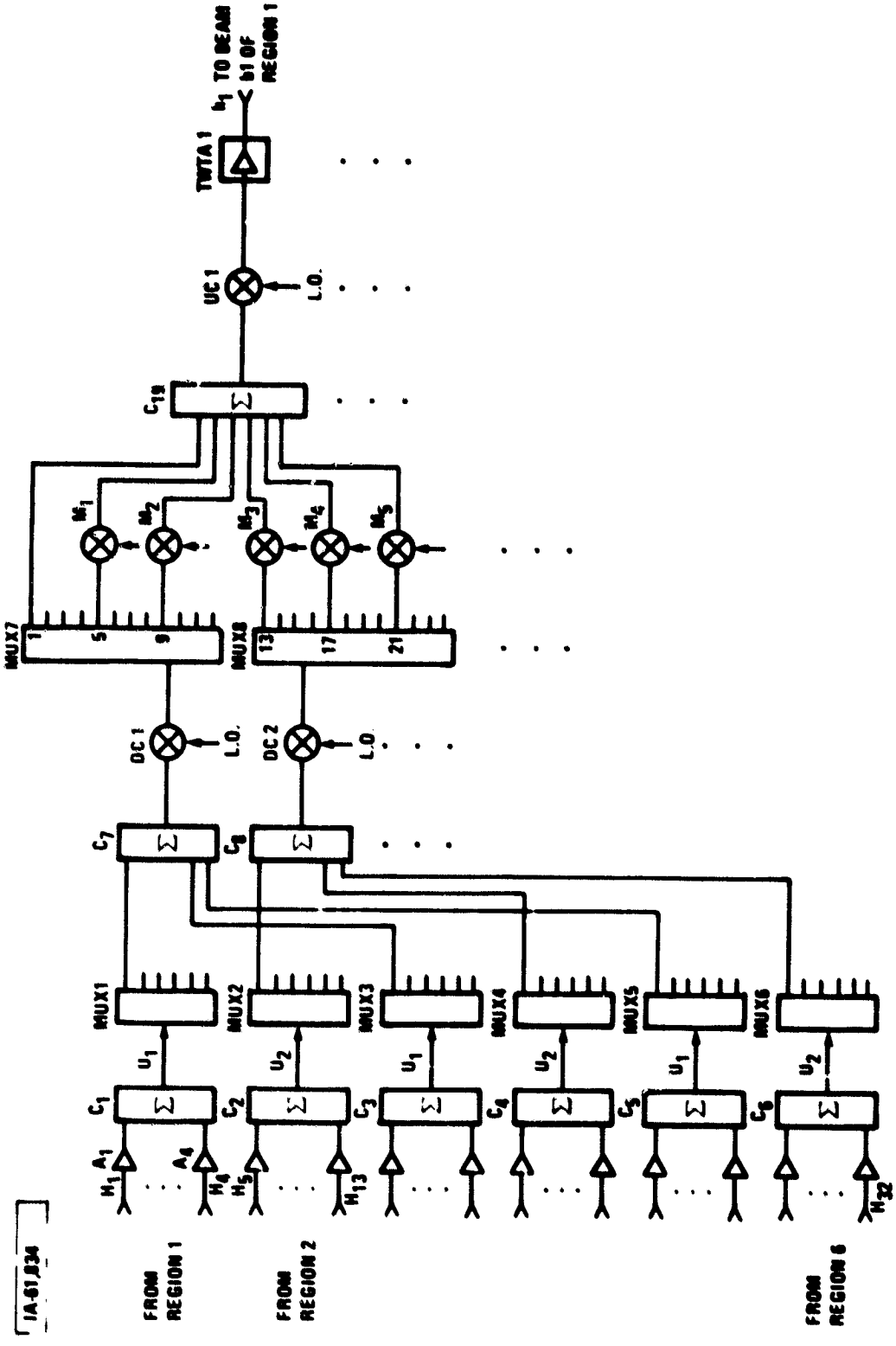

Figure 11-6. A Simplified Block Diagram of an FDMA Satellite Transponder for a Six-Region Network

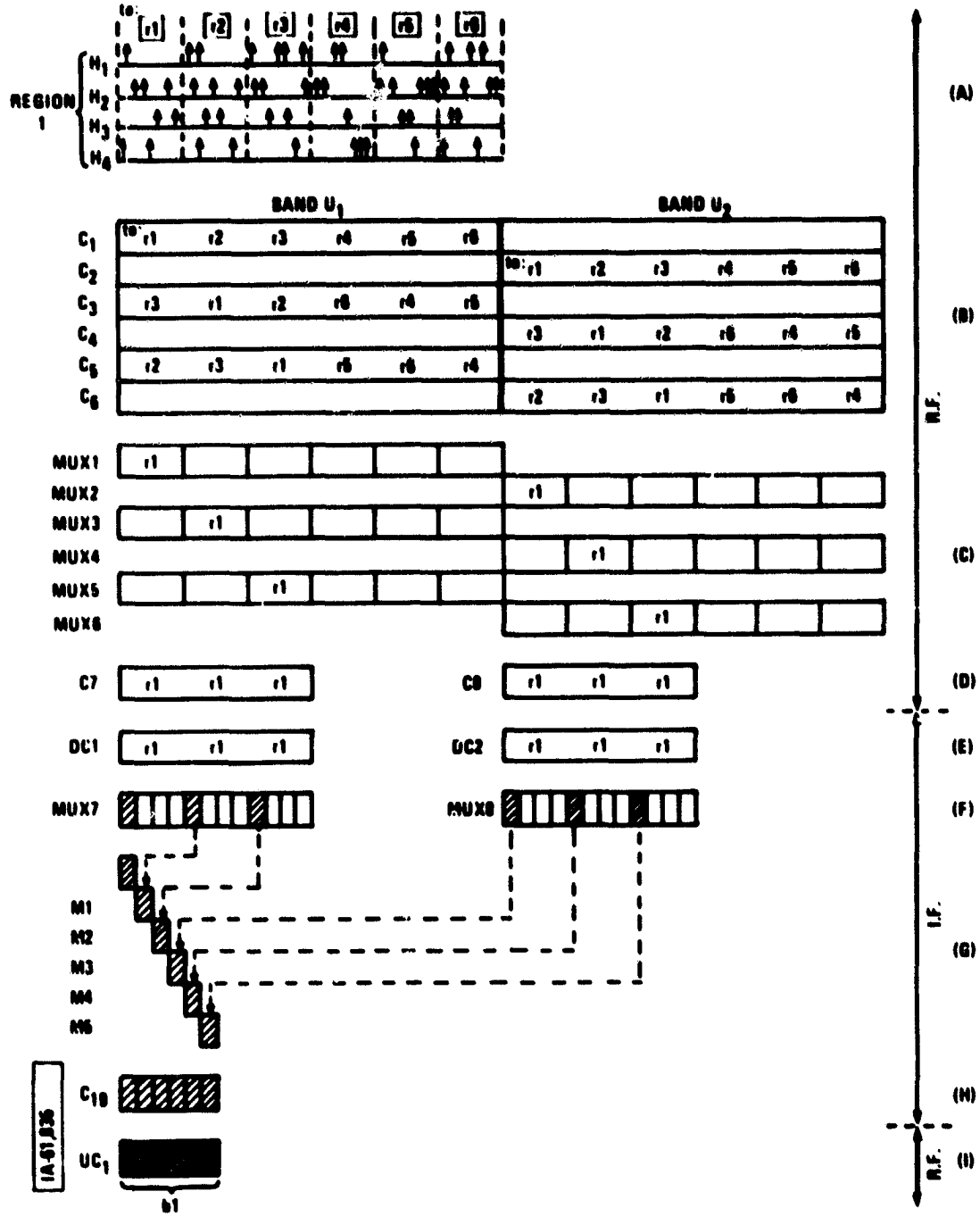

Figure 11-7. The Frequency Bands at the Outputs of Various Transponder Devices (As Identified in Figure 11-6); This Example Shows the Routing of Traffic to Beam 1 of Region 1

the union of sub-bands from regions 2, 4, and 6 that are also destined for region 1 is formed by another combiner, C_8. (Similar combiner pairs are needed for the remaining downlink regions.)

The combined bandwidths are then downconverted, by means of downconverters DC1 and DC2, to a convenient intermediate frequency, e.g., 4 GHz. A lower frequency permits the realization of the IF multiplexer pairs (MUX 7, MUX 8, through MUX 17, MUX 18) which are composed of narrowband filters. The passbands of these filters are tailored to the traffic and are therefore unequal. MUX 7 and MUX 8 channelize region 1 traffic into downlink beam traffic. The sub-bands of downlink b_1 are shown shaded in figure 11-7F.

Intermediate frequency mixers, M_1 through M_5, align the disjoint sub-bands into a contiguous beam bandwidth as shown in figure 11-7G.

Combiner C_{19} collects these sub-bands. Downlink beam b now occupies a contiguous frequency band. (Continuous downlink bands are desirable because they ease the specifications on the satellite power amplifiers and the ground terminals.)

An upconversion to microwave frequencies is provided by the upconverter UC_1. The signal is then amplified by a TWT and sent to transmit horn h_1.

Switching

Although virtually all the traffic is routed through the satellite and not switched, two types of on-board switching may be needed. The first type involves switching spare satellite components to replace degraded on-line units. This switching allows hardware redundancy for active elements that might fail. The switches are electromechanical, and are activated only if needed so as not to drain the DC power required to run the communications package.

The second type involves switching bandwidth among beams. This allows the hardwired satellite systems previously described to become more flexible. As traffic patterns change with time, the system can adjust dynamically on a daily, monthly, or yearly basis. The switching network allows a beam with reduced traffic demands to exchange its bandwidth with a beam that has an increased traffic demand. Thus, the total system bandwidth is more efficiently utilized.

Bandwidth swapping requires the network control center to carry out three operations. First, all the users communicating with the

beams swapping bandwidths must be given new transmit frequencies. Second, the control center must issue update commands to the satellite for the reconfiguration of the on-board switch. Third, all the users in the beams being altered must be given new receive frequencies.

Figure 11-8 shows a simplified block diagram of a conceptual four-region satellite with a bandwidth switching system included. The addition of the switching equipment does not change the basic architecture of the regional-routing satellite. Using figure 11-8 and figure 11-9 the bandwidth swapping operation can be explained. In figure 11-9(A) the initial downlink frequency organization is shown for Region 1. Under the initial conditions, the satellite is configured according to a predefined traffic matrix. With time, this traffic matrix (based on a traffic model) may change due to traffic growth or reduction in individual beams. Beams with small traffic capacity may vary in bandwidth by as much as $\pm 50\%$ of their original capacity. Large beams, on the other hand, may vary up to $\pm 30\%$ in their bandwidth requirements. In this example, the traffic in Beam 1 has been reduced by $\sim 50\%$ while the traffic in Beam 7 has increased by $\sim 50\%$. Since they are both in the same region, their current bandwidths can be swapped to accommodate these changes in traffic distributions. As shown in figure 11-8, the total downlink of Beam 1 is the sum of the bandwidths of bandpass filters BPF1, BPF9, BPF17, and BPF25. A bandpass filter carries all the traffic from all the beams in one region destined to an individual downlink beam. The users' transmit frequencies route the signals to the proper bandpass filters. Therefore, in order to swap bandwidth capacity, the users must first exchange their transmit frequencies. In this example, users wishing to communicate with users in Beam 1 must now use transmit frequencies that will route their signals to bandpass filters BPF7, BPF15, BPF23, and BPF31. The output of these filters must now be sent to Beam 1. This is the function of the switch. In the initial phase of operation, the outputs from BPF1, BPF9, BPF17, and BPF25 are routed to the switch outputs (1, 9, 17, and 25) that service Beam 1. After the switch is reconfigured, the outputs of BPF7, BPF9, BPF17, and BPF25 are routed to these switch outputs. Figure 11-9(B) shows the downlink frequency organization of Region 1 after the swap has taken place. As indicated in the diagram, the locations of the beam bands within the frequency spectrum have shifted, thereby requiring all users in Beams 1 and 7 to change their receive frequencies.

In figure 11-8, only one switching matrix is shown for simplicity. However, the number of switching matrices (N_S) is equal to the number of regions (N_R). The number of input/output ports (N_{P_i}) for each switch is $N_R \cdot N_{BR_i}$ where N_{BR_i} is the number of beams in region i. Due to the required exchange of frequency bands during

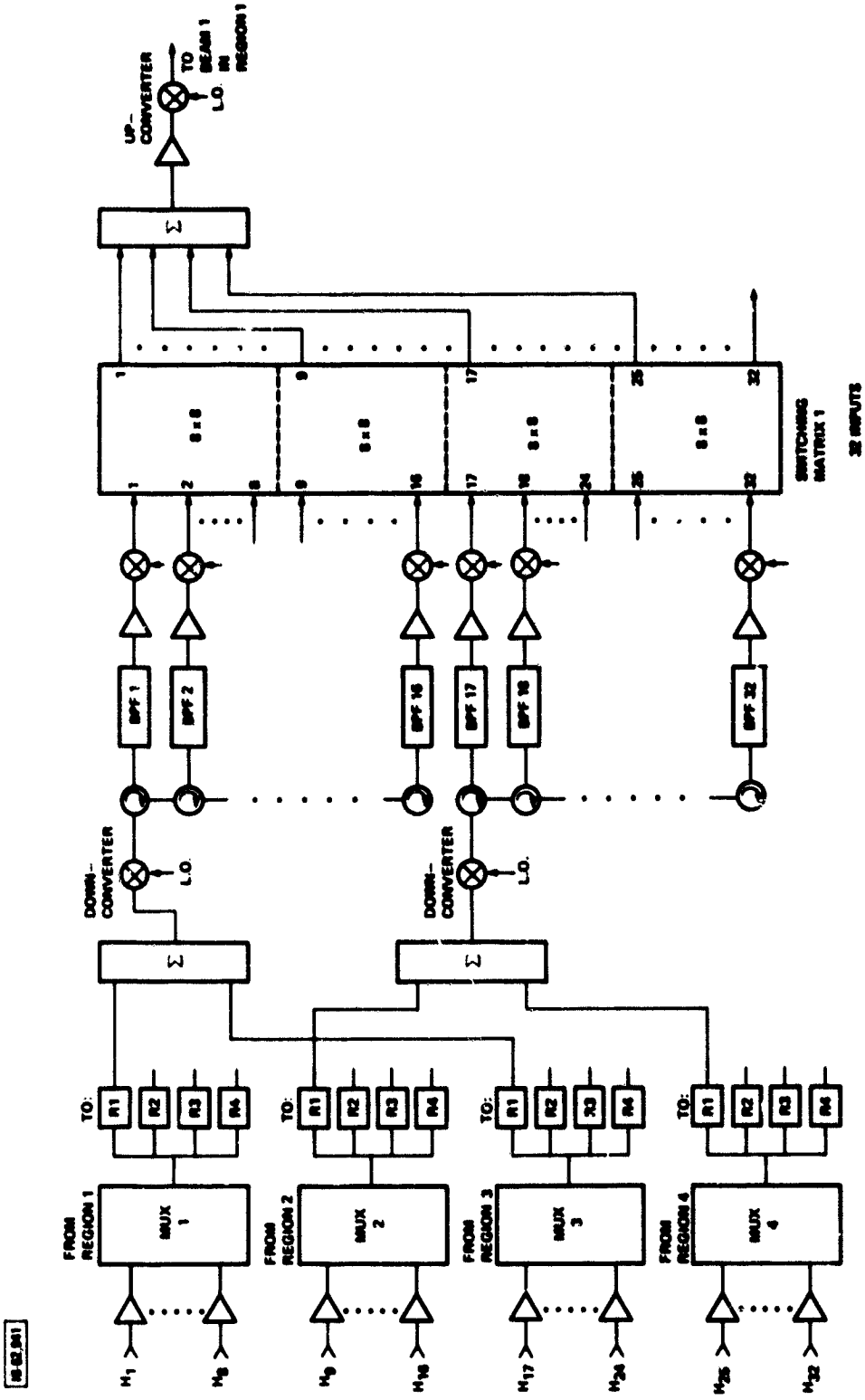

Figure 11-8. A Simplified Block Diagram of a Conceptual Four-Region FDMA Satellite (With a Bandwidth Swapping System Included)

IA-62,948

CPS DOWNLINK TO REGION 1

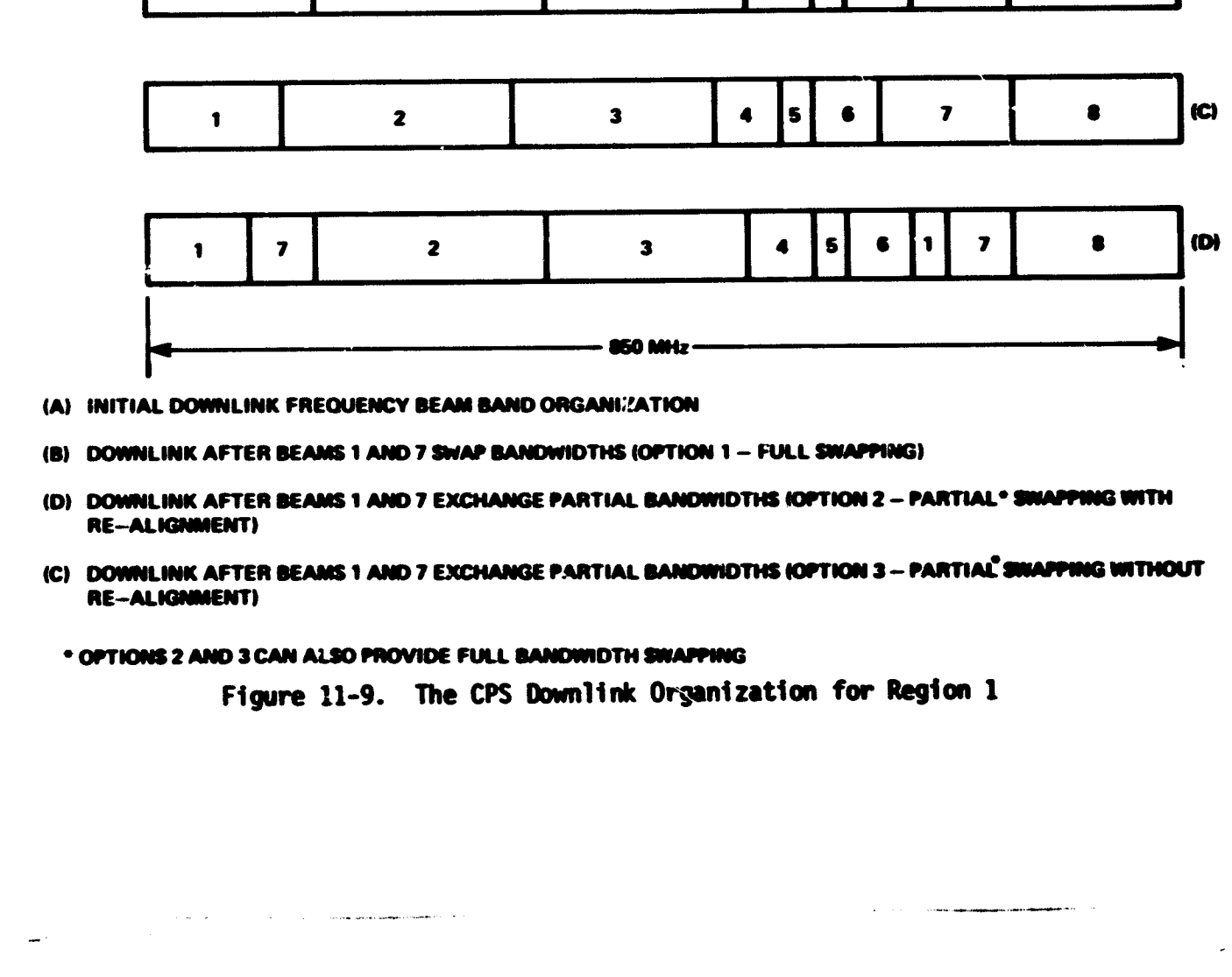

(A) INITIAL DOWNLINK FREQUENCY BEAM BAND ORGANIZATION

(B) DOWNLINK AFTER BEAMS 1 AND 7 SWAP BANDWIDTHS (OPTION 1 – FULL SWAPPING)

(D) DOWNLINK AFTER BEAMS 1 AND 7 EXCHANGE PARTIAL BANDWIDTHS (OPTION 2 – PARTIAL* SWAPPING WITH RE–ALIGNMENT)

(C) DOWNLINK AFTER BEAMS 1 AND 7 EXCHANGE PARTIAL BANDWIDTHS (OPTION 3 – PARTIAL* SWAPPING WITHOUT RE–ALIGNMENT)

* OPTIONS 2 AND 3 CAN ALSO PROVIDE FULL BANDWIDTH SWAPPING

Figure 11-9. The CPS Downlink Organization for Region 1

a bandwidth swapping procedure, bandwidth swapping is permitted only within each region to avoid interference between the regions. Thus, the maximum number of crosspoints (N_{c_i}) needed to allow any beam to swap its bandwidth with another beam in region i is $N_R \cdot (N_{BR_i})^2$. The DC power (P_S) consumed by the N_S switching matrices is about (5 mA x 6 V)/crosspoint $\cdot \left[\sum_{i=1}^{N_R} N_{c_i}\right]$ crosspoints. The weight of the switching system (W_S) is estimated to be [(2 lb/switch) · 1 switch/region) + (2 lb/driver) · (1 driver/region)] · N_R regions. In summary:

	General	4-Region System	6-Region System
No. Switching Matrices (N_S) =	N_R	4	6
No. I/O Ports (N_{p_i}) =	$N_R \cdot N_{BR_i}$	32/switch	24, 48, 24, 30, 48, 18
No. Crosspoints $(N_{c_i})_{max}$ =	$N_R \cdot (N_{BR_i})^2$	256	96, 384, 96, 150, 384, 54
DC Power (P_S)	$30\left[\sum_{i=1}^{N_R} N_{c_i}\right]$ mW	31 W	35 W
Weight (W_S)	$4N_R$ lb	16 lb	24 lb

The system as described above swaps only entire bandwidths between beams. This system is based on the assumption that a reduction or increase in a beam's capacity is proportional to its total traffic distribution. This system cannot handle situations where the traffic volume between two regions changes while the other distributions remain constant. Figure 11-9(C) shows the downlink frequency organization of Region 1 after Beams 1 and 7 swap only part of their bandwidth by exchanging only one or two (but not all four) bandpass filters. Thus, if the traffic capacity of these beams changes due to varying traffic demans in some regions, the appropriate filter(s) can be swapped. In this system, users are not required to swap their receive frequencies. The transmit frequencies and the switch configurations must be changed as described earlier. In addition, to align the downlink bands as shown in figure 11-9(C), the local oscillator (LO) frequencies of many IF frequency converters and the up-converters must be changed. In this system, users not involved in the bandwidth swapping may be affected by the swap (in this example, Beams 2, 3, 4, 5 and 6 are forced to change their receive frequency bands). Figure 11-9(D) shows another downlink frequency organization of Region 1 after a

partial bandwidth swap has taken place between Beams 1 and 7. This third option provides partial bandwidth swapping without the need for LO frequency changes. However, this system is not free from drawbacks. Both the satellite TWTAs and the earth terminal receivers are forced to operate over a wider band because these beam bands are no longer continuous.

Bandwidth swapping in a regional-routing satellite system offers a small to moderate amount of flexibility. The limitations arise from several constraints placed on this FDMA system. Bandwidth swapping is useful on a beam basis, but there cannot be a growth in total system capacity since the system is initially designed for maximum capacity. Also, due to the regional frequency organization needed to avoid interference, bandwidth swapping is limited to only beams in the same region. Therefore, there can be no swapping of bandwidths to accommodate any growth (reduction) in the size of the largest (smallest) capacity beam of a region. Thus, a region with a small number of beams is limited in its flexibility (e.g., Region 6 has only three beams in the six-region system).

The traffic density is assumed to be proportional to the population density. Therefore, any shifts in the population density will be reflected in changes in the traffic density. Since bandwidth swapping is conducted on a regional-beam basis, shifts in the population density that cross regional boundaries can not be handled by this system. The regions in the four-region and six-region systems described earlier divide CONUS vertically. Thus, if the population density shifts towards the south (as some people project it will) the northern beams of a region can exchange their larger bandwidths for those of the smaller southern beams in their regions. However, should the populaton density move in a easterly or westerly direction across regional boundaries, the regional bandwidths could not be reapportioned to help the expanding region(s).

The level of flexibility required for any bandwidth switching technique impacts the design, cost, and performance of the satellite, network control, and earth terminals. Option 1 as shown in figure 11-9(B) is fairly straight-forward but lacks some flexibility since it does not support partial swapping. Option 2, on the other hand, supports partial swapping, but is quite complex to implement. Option 3 provides partial swapping and is not as complex as Option 2 but may be difficult and/or expensive to implement. All these trade-offs must be considered before a bandwidth swapping system is selected for a regional FDMA satellite system.

Traffic Capacity

The total specified CPS and cross-traffic is approximately 3.8 Gb/s. The total trunking traffic is specified as 6.1 Gb/s. In the CPS frequency bands, the bandwidth occupied may equal 1.728 times the traffic rate (R). This bandwidth expansion factor is the product of three factors: a factor of 1.2 for coding that allows up to 20% of the users to adaptively use a rate 1/2 code to combat fading, a factor of 1.2 for modulation (see section 5), and a factor of 1.2 for guard bands and/or blocking (see section 7).

Table 11-1 contains the regional CPS traffic, bandwidth requirements, and actual supportable bandwidth for both the four-region and the six-region systems. As shown in table 11-1, the total traffic in each region is roughly the same. The four-region system is capable of handling 52.1% of the total CPS traffic when a bandwidth expansion factor of 1.728 is assumed. However, the six-region system is capable of supporting 73.5% of the CPS traffic for the same bandwidth expansion factor. The six-region system carries an additional 21.4% of the total CPS traffic. Therefore, the six-region system is preferred over the four-region system for CPS traffic.

As mentioned earlier, the spacecraft is downlink power limited. This problem has reduced the capacity of the system by 25%, overall. This prevents the network from carrying more than 75% of the total specified CPS traffic. The remaining reduction in capacity is due to bandwidth limitations. Compounding the bandwidth problem is the expansion factor of 1.728. This factor may be seen as too large and on the pessimistic side. A factor of 1.44 or 1.50 is also under consideration if blocking and filter design problems can be solved. If the power problem is eliminated and a bandwidth expansion factor of 1.44 is used, both the four-region and the six-region system can enjoy improved capacity. In this case, the four-region system can handle 62.5% of the CPS traffic while the six-region system can support 92.7% of the total CPS traffic.

On a regional level, most regions fare quite well and suffer no large reductions in traffic. However, one region, the region serving the northeast corridor, suffers a large reduction in traffic. This area is densely populated and needs special attention during planning phases. More work is required to ensure that this region has adequate power and bandwidth resources.

Table 11-2 contains a summary of the trunking traffic requirements for the four-region and the six-region systems. The bandwidth expansion factor of 1.2 used for trunking is required for guard bands and/or blocking. Trunking terminals use site diversity

Table 11-1

CPS Traffic and Bandwidth Specifications for a Four-Region and a Six-Region System Using a Bandwidth Expansion Factor of 1.728

IA-61,276

REGION	TRAFFIC RATE (Mbps)	BANDWIDTH* (MHz)	SUPPORTABLE BANDWIDTH (MHz)	% OF TOTAL REGIONAL TRAFFIC
I	1108.3	1915.2	850.0	44.4%
II	843.0	1456.7	850.0	58.4%
III	913.8	1579.1	850.0	53.8%
IV	911.0	1574.2	850.0	54.0%
	3776.1	6525.2	3400.0	
52.1% OF THE CPS TRAFFIC IS SUPPORTABLE.▲				
①	729.5	1260.6	850.0	67.4%
②	656.4	1134.3	850.0	74.9%
③	565.4	977.0	732.8	75.0%
④	573.0	990.1	742.6	75.0%
⑤	629.6	1087.9	816.0	75.0%
⑥	622.2	1075.2	806.4	75.0%
	3776.1	6525.2	4797.8	
73.5% OF THE CPS TRAFFIC IS SUPPORTABLE.▲				

*BANDWIDTH = 1.2 x 1.2 x 1.2 x R = 1.728 R

FOR CODING — FOR MODULATION — FOR GUARD BANDS — TRAFFIC RATE

▲ 25% OF THE OVER-ALL REDUCTION IN TRAFFIC IS DUE TO THE D.C. POWER LIMITATIONS ON-BOARD THE SATELLITE.

Table 11-2

Trunking Traffic and Bandwidth Specifications for a Four-Region and a Six-Region System with a Bandwidth Expansion Factor of 1.2

IA-61,274

REGION	TRAFFIC RATE (Mbps)	BANDWIDTH* (MHz)	SUPPORTABLE BANDWIDTH (MHz)	% OF TOTAL REGIONAL TRAFFIC
I	2246.0	2694.0	1650.0	61.2%
II	1112.0	1334.4	1000.8	75.0%
III	1452.0	1742.4	1202.8	69.0%
IV	1244.0	1492.8	1119.6	75.0%
	6053.0	7263.6	4973.2	

68.5% OF THE TRUNKING TRAFFIC IS SUPPORTABLE.▲

①	2091.0	2509.2	1650.0	65.8%
②	462.0	554.4	415.8	75.0%
③	804.0	964.8	723.6	75.0%
④	868.0	1041.6	677.2	65.0%
⑤	684.0	820.8	615.6	75.0%
⑥	1144.0	1372.8	1029.6	75.0%
	6053.0	7263.6	5111.8	

70.4% OF THE TRUNKING TRAFFIC IS SUPPORTABLE.▲

*BANDWIDTH = 1.2 R ← TRAFFIC RATE

↑ BANDWIDTH EXPANSION FOR GUARD BANDS

▲ 25% OF THE OVER-ALL REDUCTION IN TRAFFIC IS DUE TO THE D.C. POWER LIMITATIONS ON-BOARD THE SATELLITE.

to combat rain fading; they do not use adaptive coding. Therefore, no bandwidth expansion factor is needed for coding. It is assumed that the modulation used for trunking traffic ensures at least 1(b/s) Hz which results in no bandwidth expansion.

As shown in table 11-2, the four-region system is capable of handling 68.5% of the total trunking traffic; the six-region system can support 70.4%. This is not a significant increase in trunking capacity for the six-region system compared to the four-region system. However, since the six-region system is selected to support the CPS traffic, it must be used for the trunking as well. Since both traffic types share portions of the same bandwidth, they are forced to use the same regional divisions to ensure interference-free operation as provided by the regional frequency plan. However, if the trunking traffic uses only dedicated frequency bands, it can use a regional plan that differs from that of the CPS system.

In order to achieve the large traffic capacities described above, the system employs frequency reuse. In the four-region system (including trunking), Bands U_1 and U_2 are reused ~3 times, and Bands U_3 and U_4 ~4 times each. This level of frequency reuse generates almost 8500 MHz of total system bandwidth. In the six-region network (including trunking), Band U_1 is reused ~5 times, Band U_2 ~ 4 times, and Bands U_3 and U_4 ~5 times each. This yields a total system bandwidth of about 10,000 MHz.

Satellite Weight and Power

A block diagram of the six-region satellite is shown in figure 11-10. The weight and size of this satellite are limited by the launch vehicles. The Space Shuttle places the satellite into a temporary orbit from which an interim upper stage (IUS) rocket carries it to a geostationary orbit. Therefore, the satellite must weigh no more than 5000 lb because of IUS rocket capacity and must fit inside the Shuttle's cargo bay.

The predominant element that determines the weight of the spacecraft is the transponder. The transponder components include the TWT amplifier and its driver stage, switches for spare units, upconverters, the receiver front end, and downconverters. The IF multiplexers and IF amplifiers are not included in the transponder weight because their numbers vary with each regional design. (The number of transponders remains constant for a fixed number of beams regardless of the regional beam distribution.)

Table 11-3 contains the estimated CPS (no trunking) satellite weight and power budget for the four-region and six-region systems. The total weight of a single transponder is calculated to be

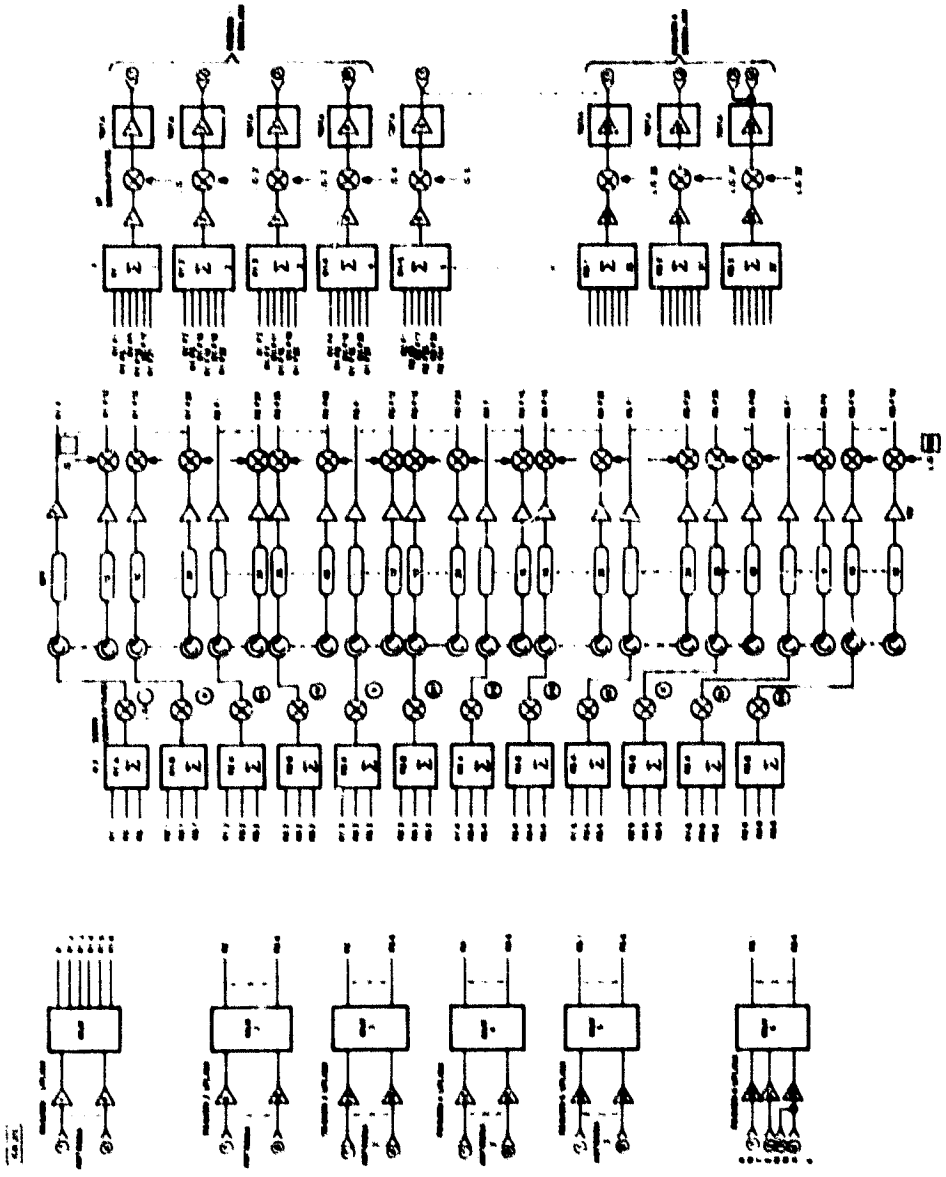

Figure 11-10. A Block Diagram of a Six-Region FDMA Satellite Transponder

Table 11-3

The Estimated CPS* Satellite Weight and Power Budget for the Four-Region and Six-Region Systems (Traffic Model A)

Components or Subsystem	4 Region Satellite System			6 Region Satellite System		
	Weight/UNIT lb	Weight/TOTAL lb	Power TOTAL W	Weight/UNIT lb	Weight TOTAL lb	Power TOTAL W
Ant. System	55	220	-	55	220	-
RF Mux	2.5	10	36	2.5	15	36
IF Mux	10 oz	92	144	10 oz	138	173
Transponder	41.5	1660	3000	41.5	1660	3000
Other El. & Battery		240 -	300 250		300 -	375 250
T.T. & Contr.		40	300		40	300
Structure Mech. Therm.		200	-		200	-
Solar Array		312	196		312	196
Allowance EOL			800			800
Comm Payload		2774	5026		2885	5130
Liquid Fuel		300			300	
ap. - Per Eng.		2000			2000	
	TOTALS:	5074 lb	5026 W		5185 lb	5130 W

* No trunking service.

41.5 lb. This weight includes the components required for 25% redundancy of each active element. The weight of the transponders can be used to estimate the total spacecraft weight. If the number of transponders (TRSPDRS) is N, the approximate weight of the spacecraft (S/C) obeys the rule-of-thumb:

$$(S/C)_W = TRSPDR_W \times N \times F$$

where F is a multiplication factor in the range of 2 to 3. The total weight of both spacecraft is independently estimated to be just over 5000 lb. Since the spacecraft total weight was calculated to be about 5000 lb and the 40 (32 active and 8 spare) transponders were calculated to weigh about 41.5 lb each, F is found to be roughly equal to 3. As shown in table 11-3, the number of regions plays only a minor role in the in the overall weight of the spacecraft.

Both spacecraft consume about 5000 W of DC power. This meets the constraints placed on the size and capacity of the projected solar array. Table 11-4 compares the capacities of a 2500 W, a 5000 W, and a 10,000 W solar array in order to provide additional information about the impact of solar array technology on the system design.

A final comment on the weight and power of the satellite should be made concerning the trunking traffic. As mentioned earlier, the estimates include only the CPS system and do not include the trunking system. Since the spacecraft has reached its limits, one must conclude that a separate trunking satellite is needed to support the specified traffic model. A single CPS/trunking satellite may be possible if the traffic requirements are reduced or if more power is available.

Terminal Design

Figure 11-11 contains a block diagram of an F type CPS terminal. The F terminal is the average size CPS terminal. This earth station requires a 4.5 m dual feed antenna system with step-tracking. The station contains redundant units for the LNA, TWTA, frequency synthesizer and modems. The LNA operates with a 400°K noise temperature. The TWT amplifier with an output range of 10 W to 50 W saturated power operates in a 5-dB backed-off mode. The terminals are microprocessor controlled and are connected to the network control center via an orderwire.

Table 11-5 contains the link margins for the CPS terminals. A more detailed list of losses is presented in table 11-6.

Table 11-4

Various Solar Array Capacities and their Impact on System Capacity (Beam Cell Size = 0.3°)

SOLAR ARRAY (W)	2,500	5,000	10,000
COMMUNICATIONS PAYLOAD (AVERAGE POWER) (W)	1,200	2,500	5,000
TT&C (W)	50	50	50
BOL (W)	3,250	5,025	10,250
EOL (W)	2,437	3,768	7,687
RF POWER AVG (W)	382	766	1,176
64 kb CAPACITY (# OF CHANNELS)	20,017	40,343	62,100
TOTAL CAPACITY (Mb/S)	1,291	2,582	3,974
ARRAY SIZE (ft^2)	10	15	18
TOTAL ARRAY (ft^2)	325	355	569
$(m)^2$	36	37	63

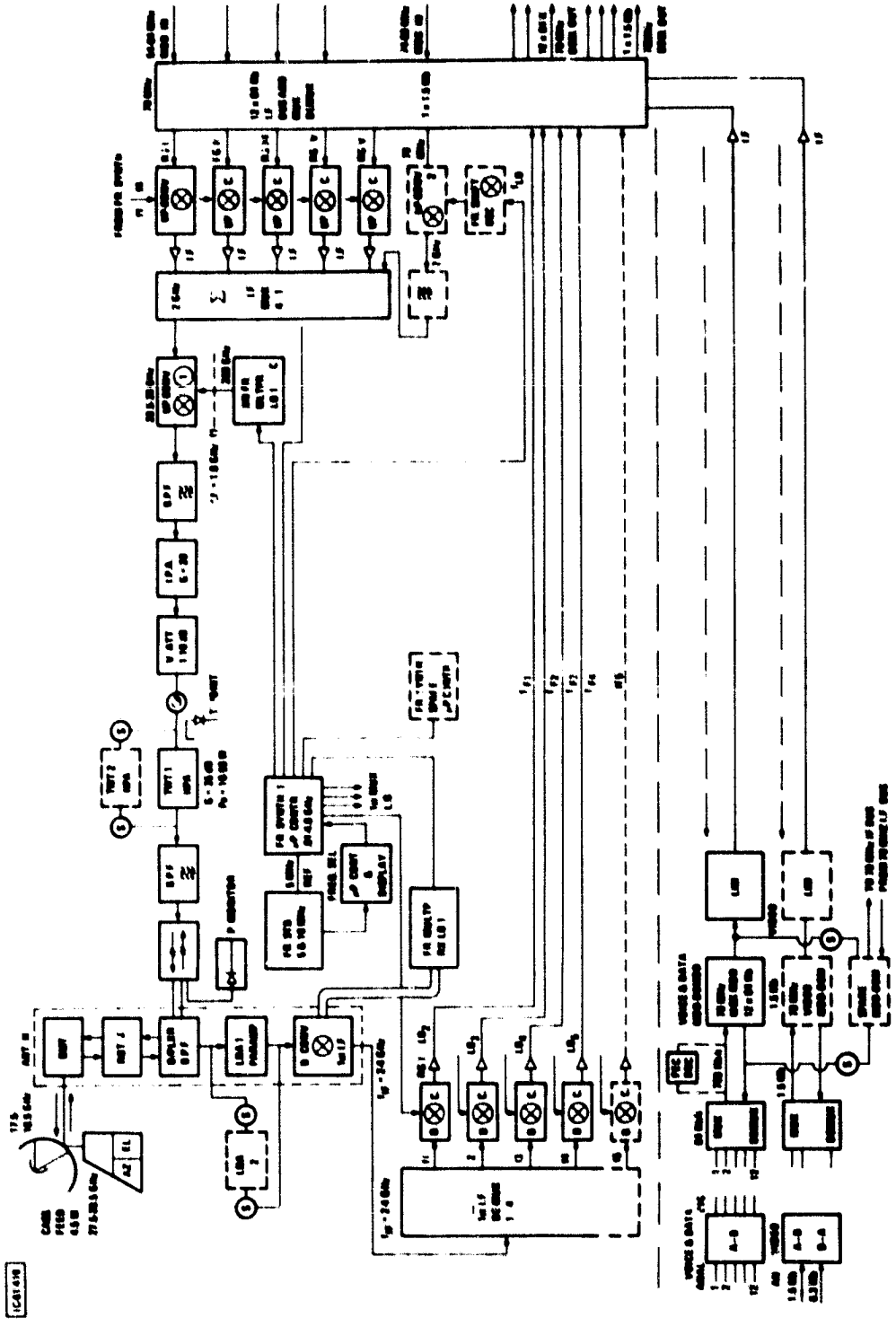

Figure 11-11. A Block Diagram of an F-Type CPS Terminal for Traffic Model A

Table 11-5

Link Budgets for the Model A CPS Terminals

Parameter	Terminal Type and Data Rate E 33.Mb/s	F 5.5Mb/s	G 0.8Mb/s
Uplink @ 30 GHz			
Ant. Size (m)	8.0	4.5	4.5
Gain (dB)	65.5	60.5	60.5
Terminal $EIRP_{eff}$ (dBW)	76.2	68.5	60.5
Path Loss (dB)	-213.0	-213.0	-213.0
Rain Loss (dB)	- 10.0	- 10.0	- 10.0
Misc. RF Losses (dB)	- 5.0	- 5.0	- 5.0
S/C Ant. $Gain_{eff}$ (dB)	48.0	48.0	48.0
S/C Noise $T_{S/C}$ (°K)	1150.0	1150.0	1150.0
S/C $(G/T)_{eff}$ (dB/°K)	17.4	17.4	17.4
$(C/kT)_{U.L.}$ (dB-Hz)	94.2	86.5	78.5
Margin (dB)	16.0	16.0	16.0
Downlink @ 20 GHz			
S/C Ant. $Gain_{eff}$ (dB)	48.0	48.0	48.0
S/C $EIRP_{eff}$ (dBW)	49.0	49.6	41.6
Rain Loss (dB)	- 4.0	- 4.0	- 4.0
Misc. RF Losses (dB)	- 5.5	- 5.5	- 5.5
Path Loss (dB)	-210.0	-210.0	-210.0
Term. Noise T_{ET} (°K)	400.0	850.0	850.0
$(G/T_{ET})_{eff}$ (dB/°K)	36.0	27.7	27.7
$(C/kT)_{D.L.}$ (dB-Hz)	94.1	86.4	78.4
Margin (dB)	10.0	10.0	10.0
Overall C/kT (dB-Hz)	91.1	83.1	75.1
$(E_b/N_o)_{eff}$ (dB)	16.0	16.0	16.0
Net Link Margin (dB)	3.0	3.0	3.0

Table 11-6

Summary of the RF Path Losses for the Model A Earth Stations and Spacecraft

TERMINAL	E	F	G
TRANSMIT POWER (dBW-W)	14.3(30)	11.0(12W)	3.0(2W)
FEED LOSS (dB)	-0.5	-0.5	-0.5
ANT GAIN (dB)	65.5	60.5	60.5
EFF RAD POWER (EIRP) (dBW)	76.2	68.5	60.5
ANT POINTING ERR (dB)	-1.0	SAME	SAME
PROPAGATION LOSS (dB)	-213.0	SAME	SAME
ATMOSPHERIC LOSS (dB)	-1.0	SAME	SAME
POLARIZATION LOSS (dB)	-2.5	SAME	SAME
TOTAL LOSS (dB)	-5.0	SAME	SAME
MARGIN (dB)	+3.0	+3.0	+3.0
SPACECRAFT			
FEED LOSS (dB) +W. G. LOSS	-2.0	SAME	SAME
ANT GAIN (dB) min at edge (-4 dB)	50.5	SAME	SAME
ANT POINTING ERR (dB) $\pm$ 0.1°	-1.5	SAME	SAME
REC CARRIER POWER (dBW)	-103.8	-112.0	-119.5

System Costs

The total costs of the terminals and the satellites are presented in table 11-7. The satellite cost is based on the SAMSO model. The terminal costs are calculated by a MITRE computer model (see section 10). The space segment cost is based on the assumption of four satellites: two operational units (one CPS and one trunking) and two spare units. The spacecraft are based on a four-region system. Since the six-region satellite weighs about the same as the four-region satellite, its cost is expected to be only slightly higher (~4%) (see section 10). The total cost of the satellites is $360M (1980 dollars). The CPS terminal ground segment is $1,176M (1980 dollars). A more detailed cost estimate for the individual terminals is given in table 11-8. The total system cost is $1,536M. The ground segment is the dominant factor in the system costs. This has been traditionally the case whenever the number of ground terminals exceeds several hundred. Here there are several thousand. A major effort to reduce terminal cost is indicated.

VERSION B

The satellite system designed to handle Traffic Model B serves about 280 standard metropolitan statistical areas (SMSAs). Over 10,000 CPS terminals are distributed among the SMSAs according to CONUS population. Table 11-9 shows the distribution of these CPS terminals among the population centers identified in Traffic Model B. Figure 11-12 shows the beam plan for this satellite system. Version B provides more CONUS coverage than Version A. Heavy traffic areas are supported by twenty-four 0.33° HPBW beams. Light traffic areas are covered by twenty-one 0.7° HPBW beams. The 0.7° beams provide less gain, but cover more area than the 0.33° beams. Due to the loss in gain, most of the 0.7° beams carry less than 30 Mb/s of traffic.

An alternative beam plan is given in figure 11-13. This plan provides additional CONUS coverage and beams for expansion. The system requires twenty-four 0.33° beams for large traffic centers and twenty-six 0.7° beams for the less populated areas. Table 11-10 shows the traffic distribution among the twenty-four 0.33° beams. Table 11-11 lists the traffic found in each 0.7° beam.

Version B also uses the regional routing concept. In this system, CONUS is divided into five-regions. Again, each region contains almost equal amounts of traffic.

As with the previous systems, the satellite for this system is also downlink power limited. Consequently, the satellite carries

Table 11-7

Estimated System Costs for the CPS Terminals and Four-Region Satellites (Model A)

CPS TERMINAL COST SUMMARY

Terminal Type	E	F	G
Cost/Unit (Q=100)	$1,535K	$ $735K	$ $576.8K
(Q=1000)	--	$ $622K	$ $475.0K
Number of Sat. Term :	80	300	1824
Total Terminal Cost :	$122.80 M	$186.81 M	$866.40M
Total Ground Segment :	$ 1,176M		

CPS SATELLITE COST ESTIMATE (4 Regions)

Total Sat. Weight :	5074 lb	2283.3 kg
Transponder Weight :	44.5 lb	20.0 kg
Power DC Total :	5026 W	
Comm. Payload Weight :	2800 lb	1260.0 kg
Sat. Cost		
NRE:	$146M	
RE:	$ 49M	
Total Sat. System Cost:	Sat. Cost + Launching (two only)	
No. of Satellites (4) :	(3 x $45) + $49M + $30M =	$214M
NRE:		$146M
Terminal Gr. Segment :		$1176M
TOTAL SYSTEM COST :		$1536M

Table 11-8

CPS Terminal Hardware and Production Cost Estimations Based on Traffic Model A

TERMINAL TYPE	G	F	E
ITEM	COST (x 1000)		
ANTENNA SYSTEM (dish size)	$85.2 (4.5m)	$85.2 (4.5m)	$131.3 (8.0m)
TRANSMITTER (RF power output)	$38.2 (10W)	$38.2 (10W)	$106.2 (50W)
LNA (noise temperature)	$15.0 (850°K)	$15.0 (850°K)	$15.0 (850°K)
UP/DOWN CONVERTERS	$52.0	$52.0	$52.0
FREQUENCY SYNTHESIZER	$20.0	$20.0	$20.0
FREQUENCY STANDARD (5 MHz)	$10.0	$10.0	$10.0
MODEM	$40.0	$120.0	$160.0
MULTIPLEXER	$15.0	$15.0	$60.0
PRODUCTION MANAGEMENT	$26.0	$28.0	$85.0
GENERAL AND ADMINISTRATION	$90.5	$97.5	$294.0
PROFIT	$66.7	$72.0	$217.3
TOTAL COST (1st ITEM)	$733.6	$958.0	$2,005.0
AVERAGE COST (100 TERMINALS)	$576.8	$735.0	$1,535.0
AVERAGE COST (1000 TERMINALS)	$475.0	$622.0	N/A

Table 11-9

Distribution of Model B CPS to CPS Traffic
Among Population Centers

Population	Number of Centers	Number of Terminals per Center by Type E	F	G	H	I	J	Total CPS Traffic per Center (Mb/s)*
0 to 200k	115	0	0	1	1	2	3	0.98
200k to 400k	66	0	1	3	3	4	6	3.52
400k to 800k	47	0	2	6	6	9	13	7.25
800k to 1.6M	28	2	4	11	11	17	26	23.7
1.6M to 3.2M	14	5	9	23	23	34	51	53.9
3.9M (Boston)	1	8	26	40	40	61	93	83.1
4.8M (Detroit, Philadelphia)	2	9	29	44	44	68	103	92.7
7.0M (Chicago, Los Angeles)	2	14	37	65	65	100	152	141
9.4M (New York)	1	20	45	88	88	134	203	170

*50% of Terminals Active

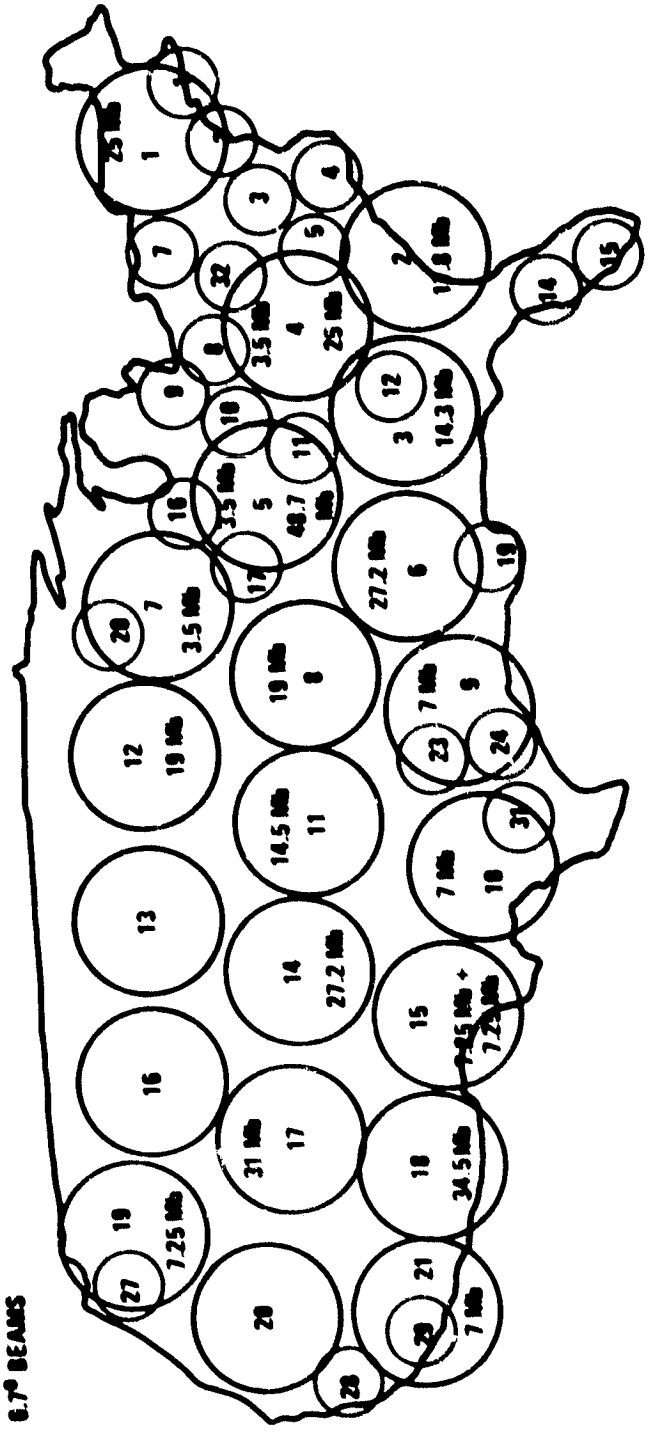

Figure 11-12. A Beam Plan for Traffic Model B. (CONUS as Seen From 90° West Longitude)

VG-55,802

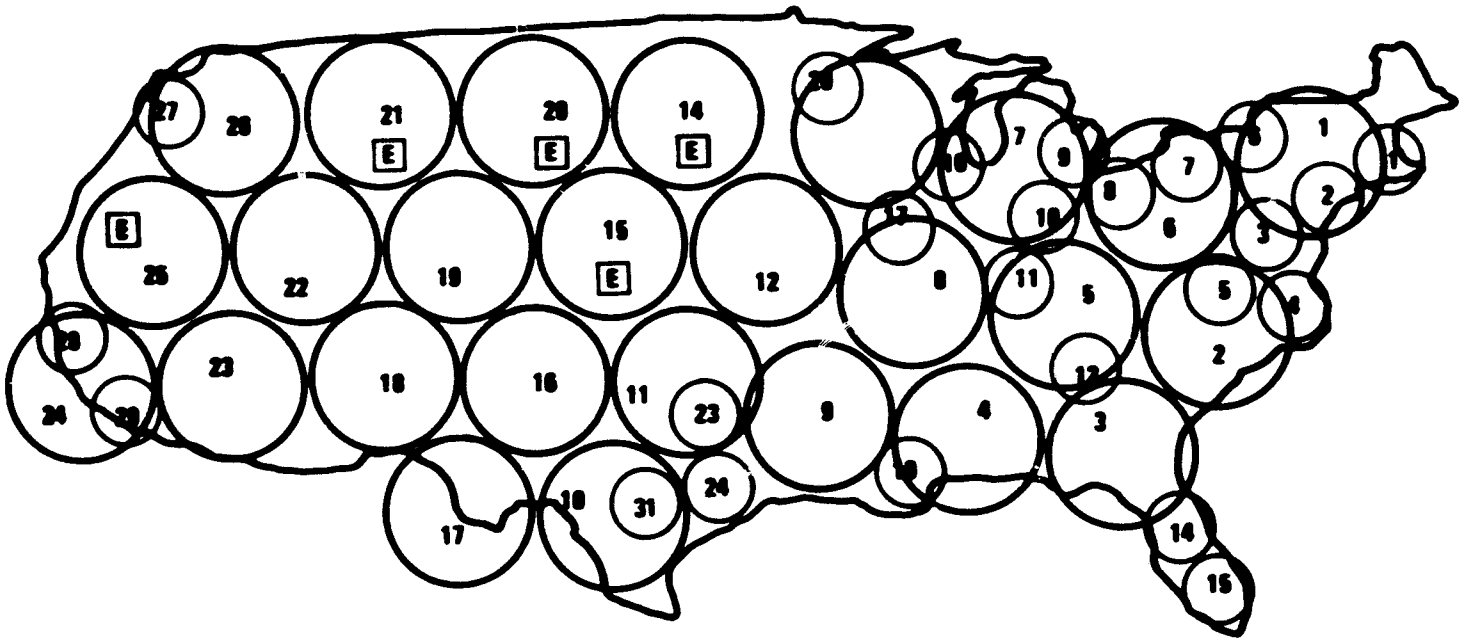

Figure 11-13. An Alternative Beam Plan for Traffic Model B (CONUS as Seen from 90° West Longitude)

Table 11-10

Distribution of Model B CPS-to-CPS Traffic Among the 0.33° Beams

Beam	Major Cities	Traffic (Mb/s) 50% CPS
1	Boston, Hartford	193.76
2	New York, Philadelphia	441.23
3	Harrisburg, Washington D.C.	118.57
4	Norfolk	34.47
5	Greensboro	25.27
6	Syracuse, Rochester	34.47
7	Buffalo, Pittsburgh	81.12
8	Cleveland, Columbus	113.64
9	Lansing, Detroit	118.11
10	Indianapolis, Cincinnati	78.14
11	Louisville, Nashville	34.47
12	Atlanta	57.42
13	-	- (used in Model "A" only)
14	Tampa	41.51
15	Miami	54.65
16	Milwaukee, Chicago	186.03
17	St. Louis	53.90
18	-	- (used in Model "A" only)
19	New Orleans	30.95
20	Minneapolis, St. Paul	53.90
21	-	- (used in Model "A" only)
22	-	- (used in Model "A" only)
23	Dallas	53.90
24	Houston	57.42
25	-	- (used in Model "A" only)
26	-	- (used in Model "A" only)
27	Seattle, Portland	58.17
28	San Francisco, Fresno	126.15
29	Los Angeles, San Diego	279.75
30	-	- (used in Model "A" only)
31	San Antonio	34.47
		2361.47 Mb/s [Total "city" Traffic]

Beams 1-31 : 0.33° HPBW Cells

Table 11-11

Distribution of Model B CPS-to-CPS Traffic Among the 0.7° Beams

Beam	Major Cities	Traffic (Mb/s) 50% CPS
①	Albany, Springfield	10.77
②	Greensville, Columbia	25.06
③	Jacksonville, Savanna	17.81
④	Pensacola, Mobile	14.29
⑤	Birmingham, Chattanooga	48.76
⑥	Johnstown	3.52
⑦	Appleton	3.52
⑧	Memphis	27.22
⑨	Little Rock, Shreveport	7.04
⑩	McAllen, Corpus Christi	7.04
⑪	Ok City, Tulsa	14.50
⑫	Omaha, Kansas City	37.99
⑬	Duluth	3.52
⑭	-	- (available for expansion)
⑮	-	- (available for expansion)
⑯	Lubbock	3.52
⑰	El Paso	7.25
⑱	Albuquerque	7.25
⑲	Denver	27.22
⑳	-	- (available for expansion)
㉑	-	- (available for expansion)
㉒	Salt Lake City	30.95
㉓	Phoenix	34.47
㉔	Bakersfield	7.04
㉕	-	- (available for expansion)
㉖	Spokane, Eugene	7.25
		345.99
	Small Regional Traffic Areas⊙	112.70
		458.69 Mb/s [Total "Regional" Traffic]

Beams 1 - 26 : 0.7° HPBW Cells

⊙ cities and counties too small and too numerous to identify or locate within the beam cells for this conceptual design.

only 32 active transponders. (Eight spare units are also on-board to provide redundancy.) Since there are more than 32 beams, some transponders must serve more than one beam. This is accomplished by combining the 0.7° beam cells in clusters of three. Each triplet beam cluster is supported by one transponder. A variable beam forming network (VBFN) is shown in figure 11-14. In addition to the transponder problem, the power shortage also affects the traffic capacity of the system. This system is limited to carrying about 75% of the specified total traffic (which is the same for both traffic models). However, if a 3-dB BO rather than a 5-dB BO in the satellite TWTs is tolerable for downlink performance in the 0.7° beams, then 100% of the specified total traffic can be supported. This reduced BO should be acceptable since these beams service mostly voice traffic where BERs of 10^{-3} are adequate.

Satellite Weight and Power

Table 11-12 contains the weight and power budget for a five-region CPS satellite. The spacecraft weighs 5273 lb and must generate 5112 W of DC power. As shown in table 11-12, a 0.3° beam transponder weighs less than a 0.7° transponder (41.5 lb vs. 42.0 lb). This difference in weight is due to the VBFN hardware used in the 0.7° transponders to form the triplet beam clusters.

The weight of the five-region satellite is about the same as the four-region and six-region satellites. The number of transponders appears to determine the weight of a given satellite, not the number of beams or the number of regions.

The weight and power budget for the five-region satellite does not include trunking to trunking service. Since this CPS-only satellite is also at its limits (5000 lb and 5000 W), the trunking traffic again requires a second, separate satellite.

Terminal Design

The CPS terminals defined by Traffic Model B are, on the average, much smaller in capacity than those CPS terminals defined by Traffic Model A. Since the terminal capacities are lower, the terminal designs are simpler and require less built-in redundancy. However, the antenna sizes are still quite large for CPS stations (2.0 - 4.5 m in range). The block diagram of an average size CPS terminal (type H) is presented in figure 11-15.

A link budget for each CPS terminal is given in table 11-13. The rain margins are the same as those specified in Traffic Model A.

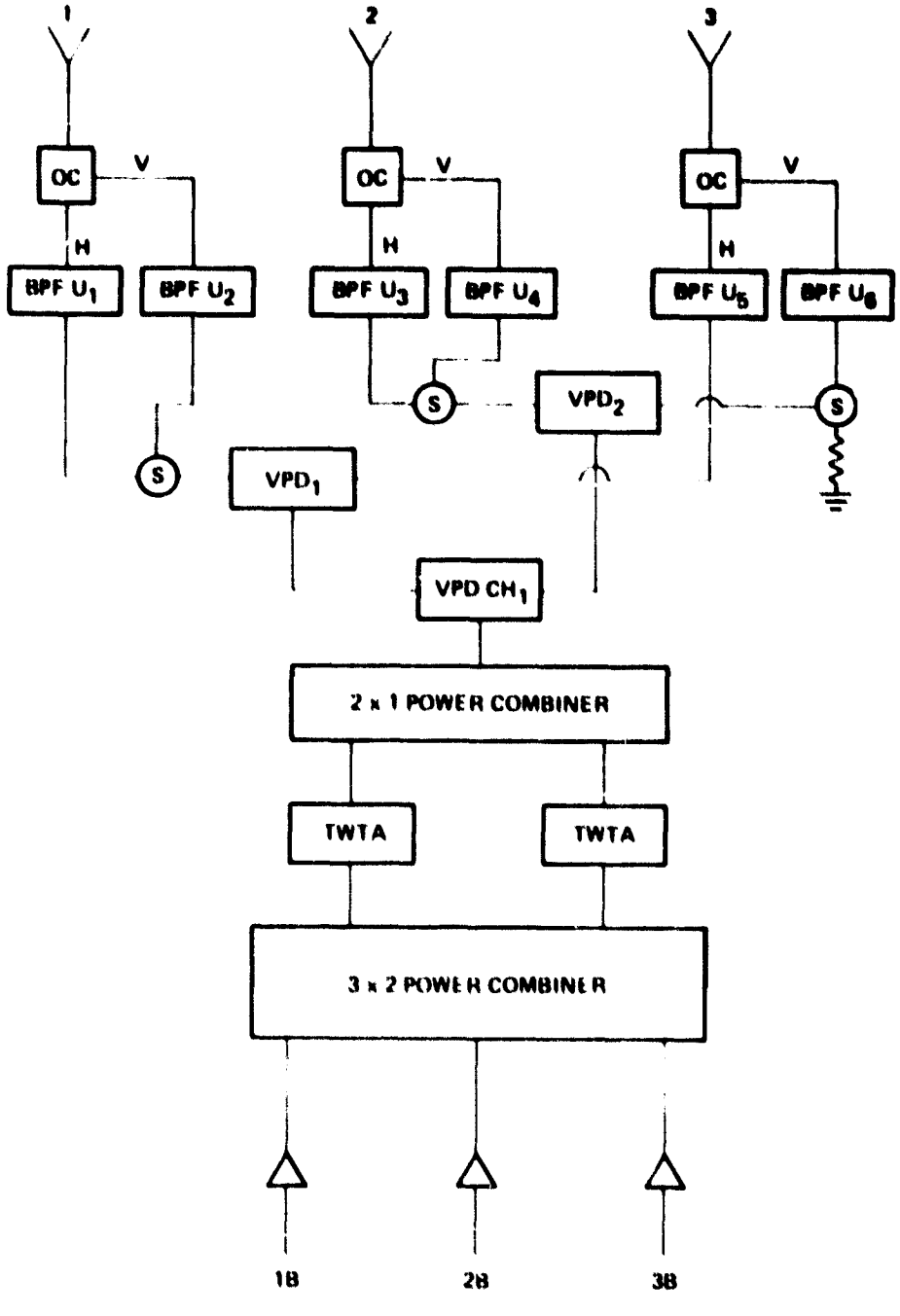

Figure 11-14. A Variable Beam Forming Network (VBFN) Antenna System for a Triplet Beam Cluster

Table 11-12

The Estimated CPS Satellite Weight and Power Budget for the Five-Region System (Traffic Model B)

COMPONENTS OR SUBSYSTEM	WEIGHT PER UNIT (lb)	TOTAL WEIGHT (lb)	TOTAL POWER (W)
ANTENNA SYSTEM:			
UP/DOWN (0.3°)	55.0*	174.0	
UP (0.7°)	15.7*	36.45	
DOWN (0.7°)	22.0*	49.0	
TOTAL (INCLUDES HORNS)		259.4	--
RF MUX	2.5	12.5	55.5
IF MUX	10.0 oz	145.0	181.0
TRANSPONDER (0.3°)	41.5	1172.5	
TRANSPONDER (0.7°)	42.0	531.5	
		1704.0	3188.5
OTHER ELECTRONICS & BATTERY		300.0	
T.T. & CONTROL		40.0	300.0
STRUCTURE MECH. THERM.		200.0	--
SOLAR ARRAY		312.0	-212.0
ALLOWANCE EOL			800.0
COMM. PAYLOAD (DRY)		2973.0	5112.0
LIQUID FUEL		300.0	--
AP-PER ENGINE		2000.0	--
TOTAL		5273.0	5112.0

*Unit weight does not include horn weight.

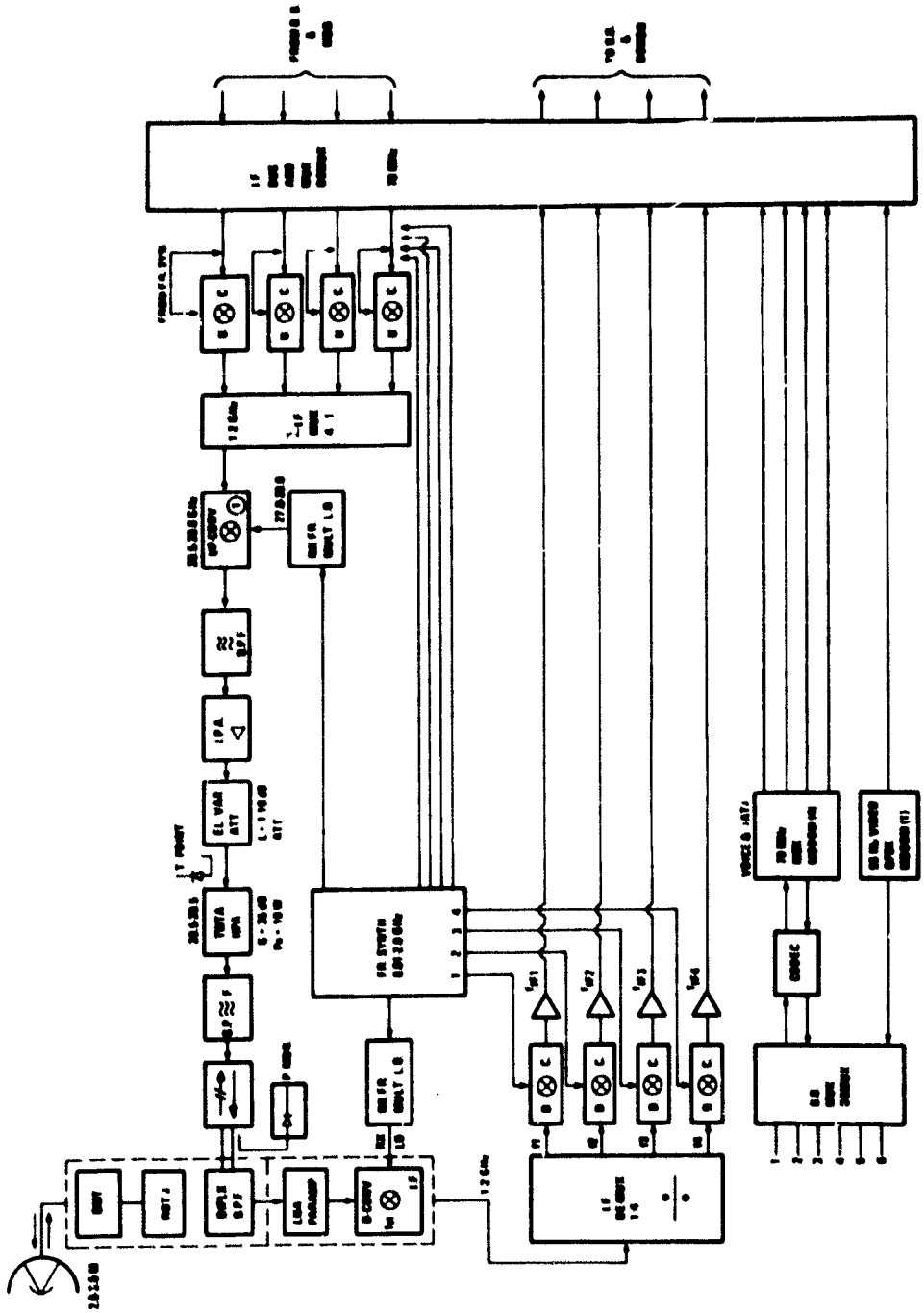

Figure 11-15. A Block Diagram of an H-Type CPS Terminal for Traffic Model B

Table 11-13

Link Budgets for the Model B CPS Terminals

PARAMETER	"G" 0.696 Mb	"H" 0.432 Mb	"I" 0.32 Mb/s	"J" 0.064 Mb/s
UP-LINK -30 GHz				
ANT. SIZE (m)	4.5	4.5	4.5	2.0
GAIN (dB)	60.5	60.5	60.5	53.5
GR. TERMINAL $EIRP_{eff}$(dBW)	66.0	64.0	62.5	55.5
PATH LOSS (dB)	-213.0	-213.0	-213.0	-213.0
RAIN LOSS (dB)	-10.0	- 10.0	- 10.0	- 10.0
MISC. RF LOSS (dB)	- 5.0	- 5.0	- 5.0	- 5.0
S/C ANT. $G_{s_{eff}}$ (dB)	48.0	48.0	48.0	48.0
S/C Tsys. NOISE °K	1150.0	1150.0	1150.0	1150.0
S/C $(G/T)_{eff}$ dB/°K	16.5	16.5	16.5	16.5
$(C/kT)_{UP-L}$ dB-Hz	77.6	75.6	74.0	67.0
MARGIN	+16.1	16.3	16.0	16.0
DOWN LINK -20 GHz				
S/C ANT. $GAIN_{eff}$(dB)	48.0	48.0	48.0	48.0
S/C $EIRP_{eff}$ (dBW)	40.6	38.6	34.7	36.5
RAIN LOSS (dB)	-4.0	-4.0	-4.0	-4.0
MISC. RF LOSS (dB)	-5.5	-5.5	-5.5	-5.5
PATH LOSS (dB)	210.0	-210.0	-210.0	-210.0
TERM. NOISE T_{ET} °K	850.0	850.0	500.0	500.00
$(G/Tsys)_{eff}$(dB°K)	27.7	27.7	30.2	21.5
$(C/kT)_{D.L.}$ dB-Hz	77.4	75.4	74.0	67.1
MARGIN (dB)	10.0	10.0	10.0	10.0
OVERALL C/kT (dB-Hz)	74.5	72.5	71.0	64.0
$(E_b/N_o)_{eff}$ (dB)	16.0	16.0	16.0	16.0
LINK MARGIN (dB)	3.0	3.0	3.0	3.0

System Costs

The total costs of the terminals and the five-region satellite are shown in table 11-14. The space segment cost is based on the assumption of four satellites: two operational units (one for CPS and one for trunking) and two spare spacecraft. The launching cost ($30M) includes launching the two operational spacecraft but not the spare units. The total satellite cost is $345M (1980 dollars). The total ground segment cost is $3,933M (1980 dollars). The total system cost is $4,278M. This cost is prohibitively high and must be reduced if an operational system is ever to be realized. The bulk of the cost is due to the 10,000 CPS earth stations. Vast improvement in terminal technology is needed if a large network is to become economically feasible.

Table 11-14

Estimated System Costs for the CPS Terminals and Five-Region Satellites

TERMINAL TYPE:	H_{xK}	I_{xK}	J_{xK}	G_{xK}
COST/UNIT (Q = 100)	$576.8	$556.8	$435.0	$576.8
(Q = 1000)	$475.0	$455.0	$367.7	$475.0
NO. OF SAT. TERMINAL:	1600	2400	3600	1600
TOTAL TERMINAL COST:	$760.M	$1,092M	$1,321M	$760.0M
TOTAL GROUND S. COST:	$3,933M			

CPS SATELLITE COST ESTIMATE

TOTAL SAT. WEIGHT (lb):	5239.0
TRANSPONDER WEIGHT (lb):	44.0
POWER DC TOT. (W):	5200
COMM. PAYLOAD WEIGHT:	2939.0
SAT. COST	
NRE:	$156.0M
RE:	$ 52.0M
NO.OF SATELLITE:	4
SAT. TOTAL COST:	$345M

TOTAL SYSTEM COST: $4,278M

SECTION 12

CONCLUSIONS AND RECOMMENDATIONS

The major conclusions and recommendations of this study are presented here in summarized form. Quantitative data supporting most of these remarks can be found elsewhere in this report. Other statements may not be substantiated in sufficient detail in this document. However, they do represent important observations generated during the study which appear to be worthy of more in-depth analysis.

1. Satellite routed (SR)-FDMA is technically feasible and can be competitive with satellite switched (SS)-TDMA for customer premises service (CPS) in the 30/20 GHz frequency bands, even for very ambitious traffic models involving thousands of multichannel, high capacity earth terminals distributed non-uniformly.

   This has been demonstrated theoretically by developing practical multiple beam frequency plans for FDMA with a methodology that can be applied to any traffic model. Performance flexibility is achieved by adaptable transmitter power diversity and frequency assignments implemented at the earth terminals on a demand basis under centralized network control facilities. FDMA and TDMA are contrasted and compared by interchanging frequency and time. The technology at 30/20 GHz is much the same, but there are some differences in corresponding subsystems or components.

FDMA	TDMA
wideband filters	fast switches
agile frequency synthesizers	high burst rate modems
stable frequency standards	accurate time synthesizers
backed-off high power amplifiers	higher peak power transmitters

2. The regional concept of organizing the non-uniformly distributed traffic into several groups of beams of approximately equal total traffic is recommended for simplifying the satellite design.

   Traffic from beams in the same region can be combined directly in the satellite with a tolerable level of interchannel interference (crosstalk) if no two users of a region are assigned the same frequency channel. Frequency reuse is attained by allocating the same frequency band to more than one region.

   Only filtering and frequency translation of large segments of bandwidth containing many channels is required in the satellite. Fundamentally, there is no need for short-term switching on an SR-FDMA satellite. However, subswitches with several input ports from filters of different bandwidths, and a number of output ports proportional to the number of downlink antenna beams may be useful for redistributing traffic on a daily or longer-term basis.

3. Approximately 75% of the 3.8 Gb/s of CPS traffic and 70% of the 6.1 Gb/s trunking traffic can be satisfied with a single satellite generating slightly more than 5 kW of DC power and weighing about 6000 lb. This is about 1000 lb too heavy for the interim upper stage (IUS) capability of the Space Shuttle.

   This results from realistic link budget and power conversion efficiency calculations involving thirty-two 0.33 beams on both the uplinks and downlinks for one traffic model and twenty-four such beams plus twenty-one 0.7 beams for another traffic model. Margins of at least 15 dB on the uplink and at least 6 dB on the downlink in the absence of rain are included in the designs. Minimum shift keying (MSK) modulation or a more bandwidth and power efficient scheme is assumed to achieve average (b/s)/Hz ratios of about 1/1.2 for CPS terminals and 1 for trunking terminals. All CPS terminals utilize a rate 1/2 code when experiencing rain fades.

4. A separate satellite should be used for trunking to trunking traffic.

   This would reduce the weight of the CPS satellite to 5000 lb or less which is within the capability of the IUS. An orbital separation of the trunking and CPS satellites that exceeds the beamwidths of the earth terminal antennas

would permit more non-interfering bandwidth for both types of service. This especially eases the downlink power limitation on the CPS satellite. CPS-trunking cross-traffic can be handled by colocated CPS terminals at each trunking station or ground network interconnects.

Employing two separate satellites to handle the specified traffic does contradict the objective of orbital arc conservation. However, technology limitations force the use of two spacecraft to meet with the traffic models. The primary technology constraint is the amount of satellite DC power available for the communications payload. This problem will limit system capacity regardless of the access mode used. Therefore, there will always be a trade-off between system capacity and orbital arc conservation. As technology improves, the capacity of single satellite systems will increase, thereby reducing the impact of this trade-off.

5. If trunking and CPS traffic are carried by the same satellite, the cross-traffic should be accomplished on the ground by providing each trunking terminal with an IF/baseband interface for the various CPS channel types rather than colocating a full CPS terminal or cross-strapping in the satellite.

6. SR-FDMA concepts should be demonstrated on an experimental satellite.

   A feasibility demonstration of the SR-FDMA regional approach could be accomplished with the addition of 210 W and 120 lb to a SS-TDMA experimental satellite. This would provide the opportunity for a fair comparison of the two satellite architectures. The FDMA portion would also permit direct access by smaller users.

7. CPS terminal costs estimated for the 30/20 GHz bands must be reduced drastically regardless of the access scheme.

   The constraint of a single satellite for trunking and CPS users in conjunction with the large (~10 Gb/s) traffic model results in system designs where the ground segment cost is much too large compared to the cost of the spacecraft. For FDMA, it is estimated that even the smallest CPS terminal with a 2 m dish without step-tracking, a 10 W transmitter, and a single 64 kb/s channel, has an average cost of about $250K in quantities of 1000. TDMA terminals will tend to cost more than FDMA

terminals because of higher burst rate, higher power, and more stringent synchronization requirements. Solid state amplifiers in the 1 W category and GaAs FET low noise amplifiers would help lower terminal costs. Concentrated low cost technology developments of inexpensive up/down converters, modems, frequency synthesizers, etc., are warranted.

Space segment innovations that ease the burden on earth terminals should be investigated. This includes larger satellite antennas and/or multiple satellites that handle different segments of the traffic divided by service type and/or geographical region. Crosslinks, movable beams, or interconnection via terrestrial networks should be considered.

Traffic model expectations for CPS could be modified downward, e.g., lower data rates, fewer channels, and more exchange of data and voice for video traffic. FDMA with or without on-board baseband processing should receive greater emphasis toward achieving lower cost terminals.

APPENDIX A

COMPARISON OF FDMA AND TDMA

The fundamental concepts used for comparing SR-FDMA and SS-TDMA are presented in figures A-1 and A-2, respectively. In both concepts there are two coverage areas, covered by beams A and B on the uplinks and beams a and b on the downlinks.

In FDMA, individual user channels are routed without switching in the satellite by selecting a carrier frequency that falls within the appropriate RF path bandwidth. For example, in figure A-1, channels destined for the same coverage area use bands 1 or 3, while channels between areas use bands 2 or 4. Given the channel bandwidths, the carrier frequencies of signals intended for the same downlink beam are chosen for non-interference. Generally, for maximum flexibility in frequency assignment, this implies that the bands routed to the same downlink beam are disjoint. Similarly, bands routed from the same uplink beam are disjoint to avoid ambiguity in the destination of signals with certain carrier frequencies. In other words, all four bands are disjoint in figure A-1.

The absence of switching in the satellite is achieved by frequency agility on the ground. Network control stations must assign carrier frequencies for individual channels of each terminal which, therefore, must employ a frequency synthesizer for independently generating the carrier frequency of each channel. In effect, switching is accomplished on the ground by channel frequency selection.

In TDMA, individual user channels can only be routed with switching in the satellite by selecting a transmission time that falls within the appropriate time interval. For example, in figure A-2, channels destined for the same coverage areas use intervals 1 or 3, while channels between areas use intervals 2 or 4. Given the signal durations, the transmission times of signals intended for the same downlink beam are chosen for non-interference. Generally, for maximum flexibility in time assignment, this implies that the intervals associated with the same downlink beam are disjoint. Similarly, intervals associated with the same uplink beam are disjoint to avoid ambiguity in the destination of signals with certain transmission times. In other words, all four intervals are disjoint in figure A-2.

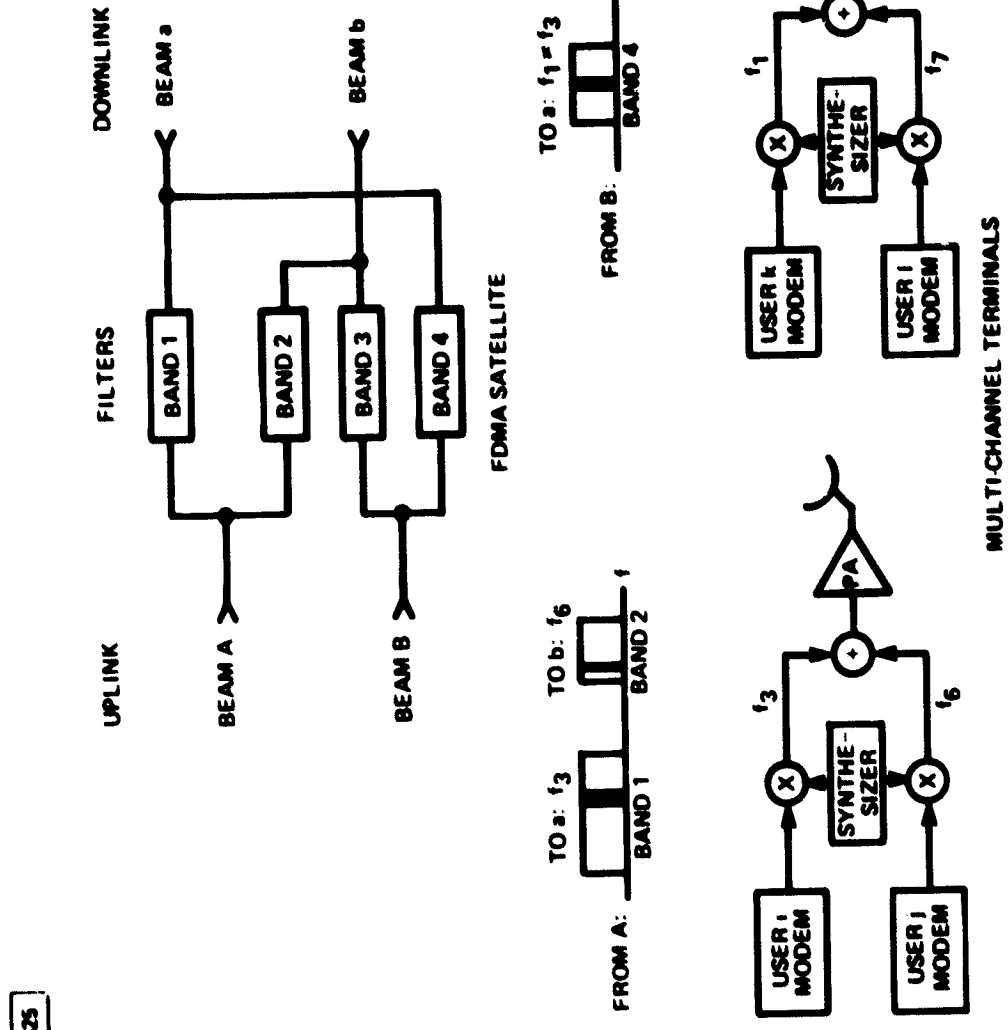

Figure A-1. Fundamental SR-FDMA Concept

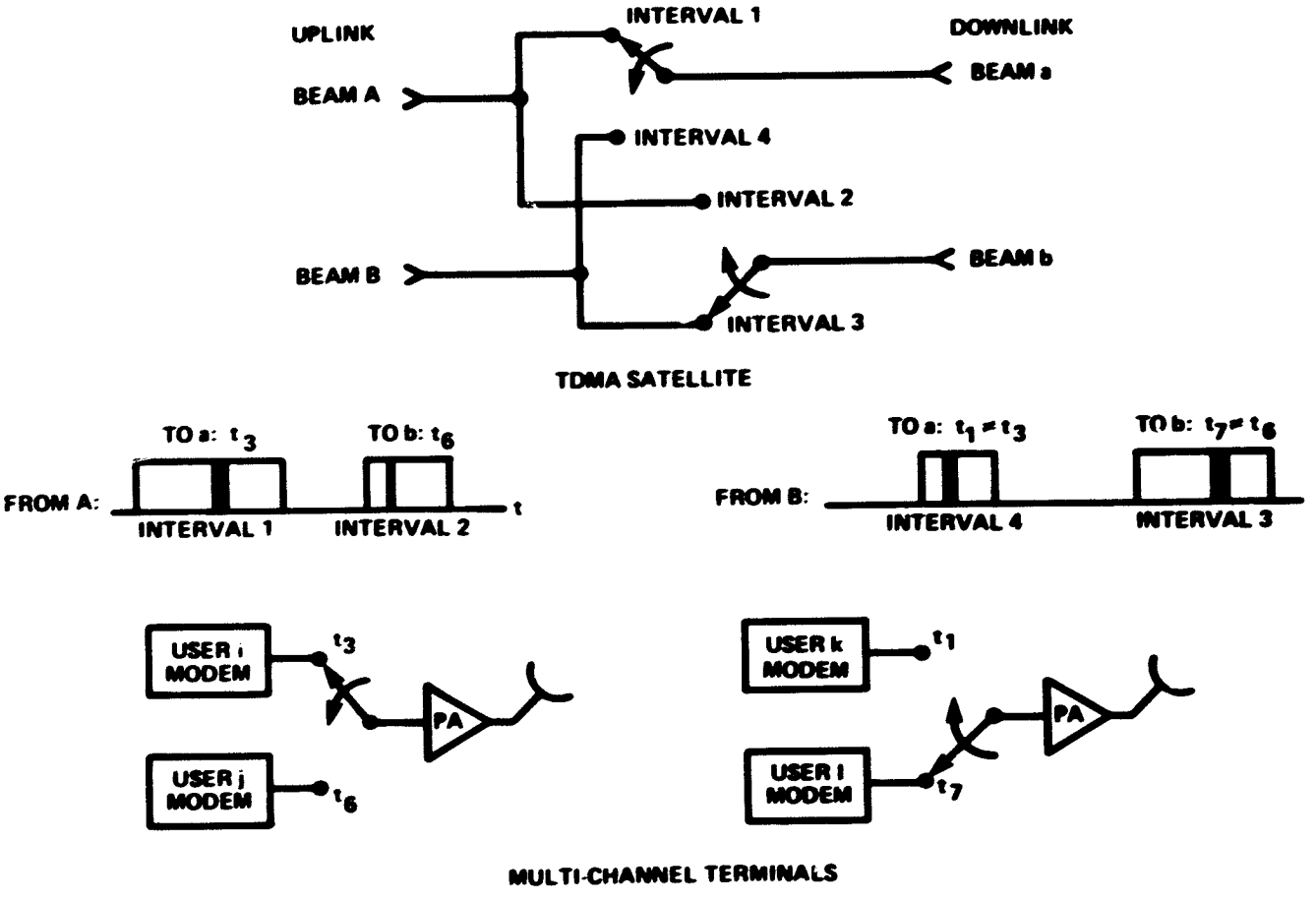

Figure A-2. Fundamental SS-TDMA Concept

The presence of switching in the satellite must be accompanied by switching on the ground. Network control stations must assign transmission times for individual channels of each terminal. Note that whereas in FDMA all carrier frequencies could coexist at the same time, in TDMA all transmission times could involve the same carrier frequency.

It should be apparent that FDMA and TDMA can be compared by interchanging frequency and time. FDMA requires filters and frequency synthesizers; TDMA requires switches and synchronizers. Both schemes demand roughly the same total bandwidth for equivalent traffic. In FDMA, there are frequency parallel channels at lower channel burst rates and varying carrier frequency spacings. In TDMA, there are time serial channels at higher channel burst rates but with varying instantaneous bandwidths. The attractiveness of one scheme over the other depends on the relative cost of filters, frequency synthesizers, and crosstalk or IM interference with FDMA, compared to switches, synchronizers, and guard times or intersymbol interference with TDMA. In FDMA, a reduction in IM interference requires more power amplifier backoff, while in TDMA more power per channel is required to maintain the same signal energy to noise contrast ratio. Thus, qualitatively, at least, both schemes result in roughly the same satellite power requirements.

If individual channels of any terminal are to be routed independently, then they must be assigned separate carrier frequencies in FDMA and separate transmission times in TDMA. It is not apropos to consider bundles of channels from one terminal all going to the same destination. That is a special case that begs the question of pure FDM versus pure TDM. This follows because in that case, channels from a given terminal could be arranged in a TDM format on one carrier frequency in the FDMA approach (TDM/FDMA), while the same channels could be arranged in an FDM format for one transmission time in the TDMA approach (FDM/TDMA). Hence, the purity of independent channel destinations must be maintained for a fair comparison of SS-TDMA with SR-FDMA, i.e., FDM/FDMA.

If all the channels of a given terminal were destined for the same location, then that terminal would be a trunking terminal. Here the focus is on CPS terminals where each channel can be routed independently. The usual view of TDMA with multichannel terminals is FDM/TDMA, where the channels of one terminal are frequency division multiplexed and time division applies only to the terminal access to the satellite. As such, the burst rate and power increases required at a terminal equal the number of terminals in the same beam. In this TDMA architecture, the trunking terminal designation is unavoidable without satellite baseband processing or processing which uses frequency division techniques to separate

channels from the same terminal. Hence, this would really be a hybrid FDM/TDM satellite architecture.

BURST RATES

The most dramatic feature of the TDMA approach is the increased burst rate required for a typical terminal channel compared to the FDMA approach. The power increase factor for a given terminal is reduced by the number of channels in the terminal if a single high power amplifier is employed, as is usually the case.

In the most direct comparison between FDM/FDMA and TDM/TDMA with independent channel destinations, all channels occupy the same duration T in FDM/FDMA, and the same bandwidth W in TDM/TDMA. Therefore, from conservation of the number of bits transmitted in FDM/FDMA, the bandwidth of channel i of terminal j, W_{ij}, times T, must equal the product of W and the burst duration of channel i of terminal j, T_{ij}, in TDM/TDMA. Here it is assumed that the bandwidth per data rate ratio is the same in both cases. This product also indicates the buffer memory requirements for TDM/TDMA. In addition, each link of the TDM/TDMA system must be synchronized to a fraction of the interval 1/W. The burst rate increase factor is W/W_{ij}.

Typical burst rate and power increases are shown in table A-1 for a W = 250 MHz beam bandwidth, when the data rate $R_{ij} = W_{ij}$. The realization of burst rate increases of more than 20 dB and power increases of more than 10 dB could be formidable tasks, especially if lower cost terminals are necessary. This suggests that TDM/TDMA is not practical for CPS.

The situation is even worse if the cases of equal burst durations and equal burst rate increases are examined. Let n_i be the number of channels in a terminal of the ith type, and let m_{ij} be the number of active terminals of the ith type in the jth beam. Then the burst rate increase factor for TDM/TDMA relative to FDM/FDMA in that beam is

$$l_j = \sum_i m_{ij} n_i. \qquad (A.1)$$

In other words, the burst rate of each channel must be increased by a factor equal to the total number of channels in the beam because only one channel can be active at a time in TDM/TDMA. Here active means that there is a signal presently being transmitted over a particular terminal channel. In FDM/FDMA, all channels are active simultaneously.

Table A-1

Terminal Burst Rate and Power Increases in Beam Bandwidth of W = 250 MHz
Assuming $W_{ij} = R_{ij}$ and Independent Channel Destinations

R_{ij} (Mb/s)	Burst Rate Increase W/W_{ij}	Power Increase $W/W_{ij}.N$ Number of Channels per Terminal N = 14	68	278
6.3	39.7 = 16.0 dB	2.83 = 4.5 dB	-	-
1.5	167 = 22.2 dB	11.9 = 10.8 dB	2.45 = 3.89 dB	-
0.064	3906 = 35.9 dB	279 = 24.5 dB	57.4 = 17.6 dB	14.1 = 11.5 dB
0.056	4464 = 36.5 dB	319 = 25.0 dB	65.7 = 18.2 dB	16.1 = 12.1 dB

Typical burst rate increase factors for equal burst durations are given in table A-2 for several examples selected from traffic models A and B involving only CPS terminals. The striking fact is that TDM/TDMA usually requires more than a thousand-fold increase in burst rate compared to FDM/FDMA. Therefore, more than a 30 dB increase in channel power is necessary to maintain the same individual channel carrier to noise ratio. Thus, whereas multiwatts to watts may be adequate for FDM/FDMA channels, watts to kilowatts are required for TDM/TDMA. Furthermore, channel data rates of kilobits to megabits per second at FDM/FDMA become burst rates of megabits to gigabits per second with TDM/TDMA. It is apparent that these TDM/TDMA powers and burst rates may be difficult to achieve for some of the higher data rate channels, especially at reasonable terminal costs. The use of bandwidth expansive coding to enhance performance would accentuate the burst rate problem.

If it is assumed that a single power amplifier is used in a terminal, and that the backoff factor is the same, the total terminal power increase of TDM/TDMA over FDM/FDMA for a terminal of type i in beam j is

$$k_{ij} = l_j/n_i \ . \qquad \text{(A.2)}$$

If FDMA requires more terminal backoff, then the factor of equation (A.2) would be reduced by the ratio of the two backoff factors. Various k_{ij}'s can be computed by using table A-2.

Table A-2

Increased Burst Rate Factors (l_j) per Beam for Equal Burst Durations and TDM/TDMA Relative to FDM/FDMA for CPS Terminals Only and Beam Plan of Section 7.

a. Traffic Model A ($n_E = 278$, $n_F = 68$, $n_G = 14$)

Beam	j	m_{ij}			l_j	dB
		i=E	F	G		
New York/Philadelphia	2	4	18	215	5346	37.3
Cleveland/Columbus	8	2	9	52	1896	32.8
Boston/Hartford	1	1	11	65	1936	32.9
San Diego/Los Angeles	29	9	14	120	5134	37.1
Phoenix	30	5	7	40	2426	33.8
Portland/Seattle	27	5	12	64	3102	34.9
Norfolk	4	0	9	20	892	29.5
Memphis	18	0	4	32	720	28.6
Washington, D.C./Harrisburg	3	4	12	115	3538	35.5
Chicago/Milwaukee	16	10	18	124	5740	37.6

b. Traffic Model B ($n_E = 36$, $n_F = 9$, $n_G = 11$, $n_H = 7$, $n_I = 5$, $n_J = 1$)

Beam	j	m_{ij}						l_j	dB
		I=E	F	G	H	I	J		
New York/Philadelphia	2	10	30	96	96	283	424	4197	36.2
Cleveland/Columbus	8	5	15	48	48	68	103	1622	32.1
Boston/Hartford	1	3	8	37	37	66	99	1275	31.1
San Diego/Los Angeles	29	23	66	75	75	158	237	3799	35.8
Phoenix	30	13	38	37	37	53	79	1820	32.6
Portland/Seattle	27	13	38	64	64	84	126	2508	34.0
Norfolk	4	0	0	48	48	26	39	1033	30.1
Memphis	18	0	0	21	21	42	63	651	28.1
Washington D.C./Harrisburg	3	10	30	64	64	151	227	2764	34.4
Chicago/Milwaukee	16	25	75	96	96	163	245	4363	36.4

APPENDIX B

INTERCONNECTION OF CPS AND TRUNKING USERS

The SR-FDMA system approach defines two transponders, one for trunking (T) traffic and one for customer premises service (CPS) traffic. This distinction permits independent optimization of the trunking links and the CPS links for best performance and cost. Combining the two capabilities (i.e., trunking and CPS) into one transponder type would result in a less effective satellite system design, since either the CPS terminals or the satellite transponder would be required to be larger (EIRP and G/T) and therefore significantly more expensive.

Figure B-1 illustrates the RF bandwidth available within a typical region of the six-region design. The first 850 MHz of bandwidth is dedicated to trunking, the second 850 MHz band is shared between CPS and trunking traffic as system demand dictates, and the two 400 MHz bands are dedicated to trunking users. In other regions, the functions of the two 850 MHz bandwidths may be interchanged.

It is desirable to interconnect CPS users with trunking users in order to provide a connection to terrestrial communications systems. This connection could be made in two generic ways: (1) cross-strapping of "bands" in the satellite transponder, or (2) use of interfaces at the ground terminal locations.

The first approach, cross-strapping, appears attractive at first glance since there is an implication that terminals would not be affected. In this case (option 1), the trunking to CPS (T→CPS) uplink would usurp trunking bandwidth as shown in the trunking to trunking (T→T) portion of figure B-1. The corresponding downlink would be in the shared CPS/T portion of the CPS transponder. The interconnection or satellite routing between the trunking transponder uplink and CPS transponder downlink would be accomplished by additional frequency translation, perhaps using a satellite switch. Similarly, the CPS to trunking uplink would access the CPS/T 850 MHz portion of the CPS transponder and be frequency translated into an appropriate portion of the trunking transponder downlink.

Either the traffic being transmitted between CPS and trunking users preempts trunking channel capacity, or additional capacity at the trunking terminal will be required. Since it is desirable that

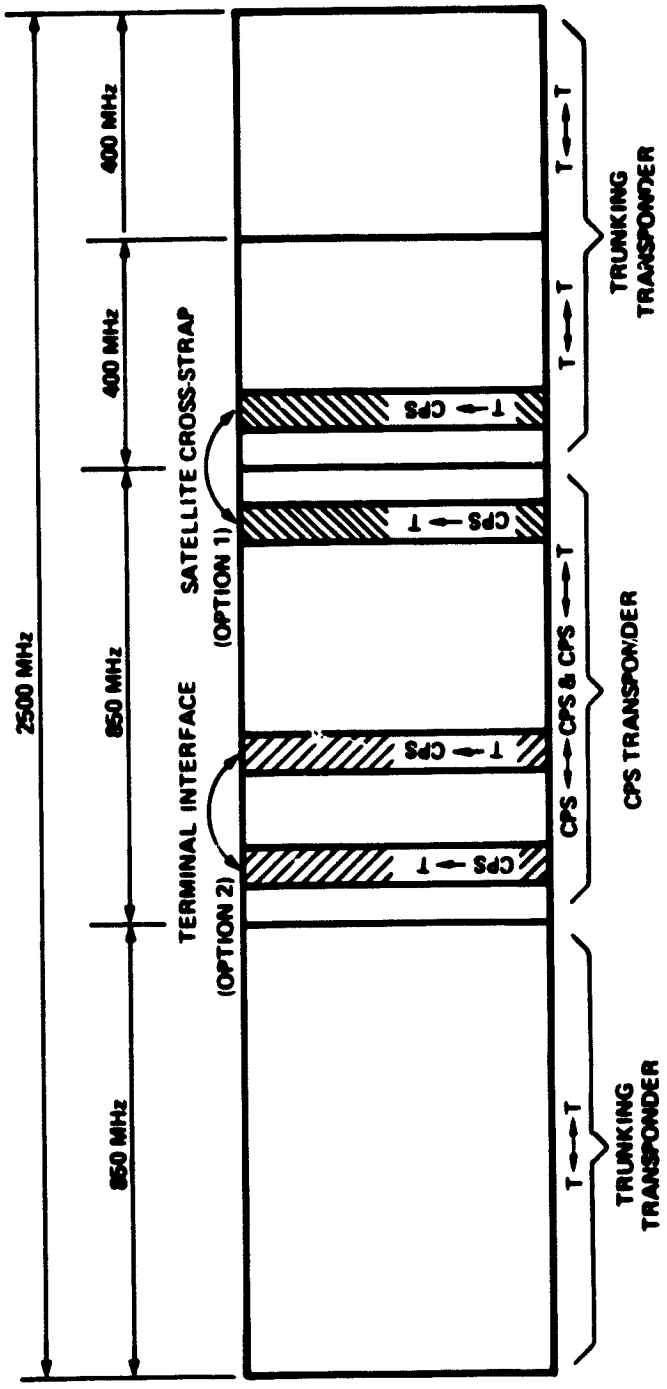

Figure B-1. RF Bandwidth Allocation for CPS and Trunking Users (One Typical Region of Six Region Plan)

the trunking bandwidth (i.e., capacity) not be changed or reduced, one alternative is to provide additional channels at the trunking terminal. These channels must come from the CPS/T allocation. Consequently, the trunking terminal must add additional up/down converters and baseband equipment to handle CPS to trunking and trunking to CPS traffic. Thus, the objective of an unchanged terminal segment is not achieved unless a reduction in T→T traffic is acceptable. Since this is unlikely, the trunking terminal segment must be modified. Moreover, there is the added cost and complexity of the trunking to CPS cross-strap in the satellite. Therefore, this option seems to be without merit.

Interconnection at the trunking terminal without cross-strapping in the satellite (option 2) seems to be a reasonable approach since the number of terminals affected is relatively small. The terrestrial net interface exists at the trunking terminals. The nature of the SR-FDMA RF system design permits the trunking terminal to operate in either the trunking bands or "shared" CPS/T bands. When the trunking terminal is operating in the shared bands, its EIRP is adjusted downward to match that of the CPS terminals. This is required for reasons of power balance (always a concern with non-processing FDMA systems).

One approach to interconnection would be to colocate a CPS terminal at each trunking terminal site. However, that seems an unnecessary expense for a single CPS/T satellite. The RF bandwidth of the trunking terminal easily permits the addition of the CPS terminal up/down converters and baseband equipment to provide the same capability as a separate CPS terminal. The only potential concern for combining RF equipment would be the possibility of intermodulation or cross interference between CPS and trunking signals in the shared front end. This should be a minor problem easily contained by filtering. Thus, the modified trunking terminal acts like a trunking terminal and a pseudo-CPS terminal. The CPS to trunking uplinks and the trunking to CPS uplinks are in the CPS/T shared portion of the CPS transponder. The pseudo-CPS portion of the trunking terminal is used for the cross-traffic. Full interconnection between trunking and CPS users is provided. Equipment changes, which are the key system cost consideration, are not required at the CPS terminals. The additional up/down converter and baseband equipment required at the limited number of trunking terminals results in a modest increment to system cost. This is of small consequence since the trunking to trunking traffic capacity is not reduced. In addition, satellite design remains simplified.

Therefore, the best approach for CPS/T user interconnect appears to be at the trunking terminal through the use of additional CPS IF or RF converter and baseband equipment.

APPENDIX C

AN ALTERNATIVE FDMA SYSTEM

Color Assignment

The use of a polarized reflecting screen imposes the condition that about half the beams be vertically and half horizontally polarized. Polarization is also expected to help reduce beam interferences. The question of whether both purposes can be served at the same time is now addressed. Figure C-1 shows that the beam plan has a group of beams very close together on the east coast. This pattern is repeated near the Great Lakes, in Florida, and in Texas. In this discussion, five 500 MHz bands will be used to prevent interferences between these and other beams. Adjacent beams will use different bands and different polarizations. The situation is similar to using several colors on a map to distinguish different countries. There are 10 "colors" available in this process consisting of bands numbered from 1 to 5, each available with either polarization. Beams can interfere via their sidelobes even if they do not touch at their -3 dB contours, so "color" assignment is necessary.

While the use of 500 MHz bands does not coincide with the bandwidth and traffic plans of all FDM processors in the range of FDM multibeam systems, the antenna principles described here apply to all the processors. Since the band is 2.5 GHz wide and five bands are planned, it is natural to make each band 500 MHz wide.

The next step is to determine the beam separations for every pair of beams on the map. These are arranged in the matrix form of figure C-2. Because the matrix is symmetrical, only 435 independent values need be entered. The figure has rows and columns which stand for the numbered cities on the map of figure C-1. The intersection of any row and column gives the angular separation in degrees between the peaks of the beams for those traffic areas. For example, the intersection of row 7 and column 18 yields 1.5°. As can be deduced from the names alongside the rows, this is the separation of the beams for Buffalo/Pittsburgh and Memphis.

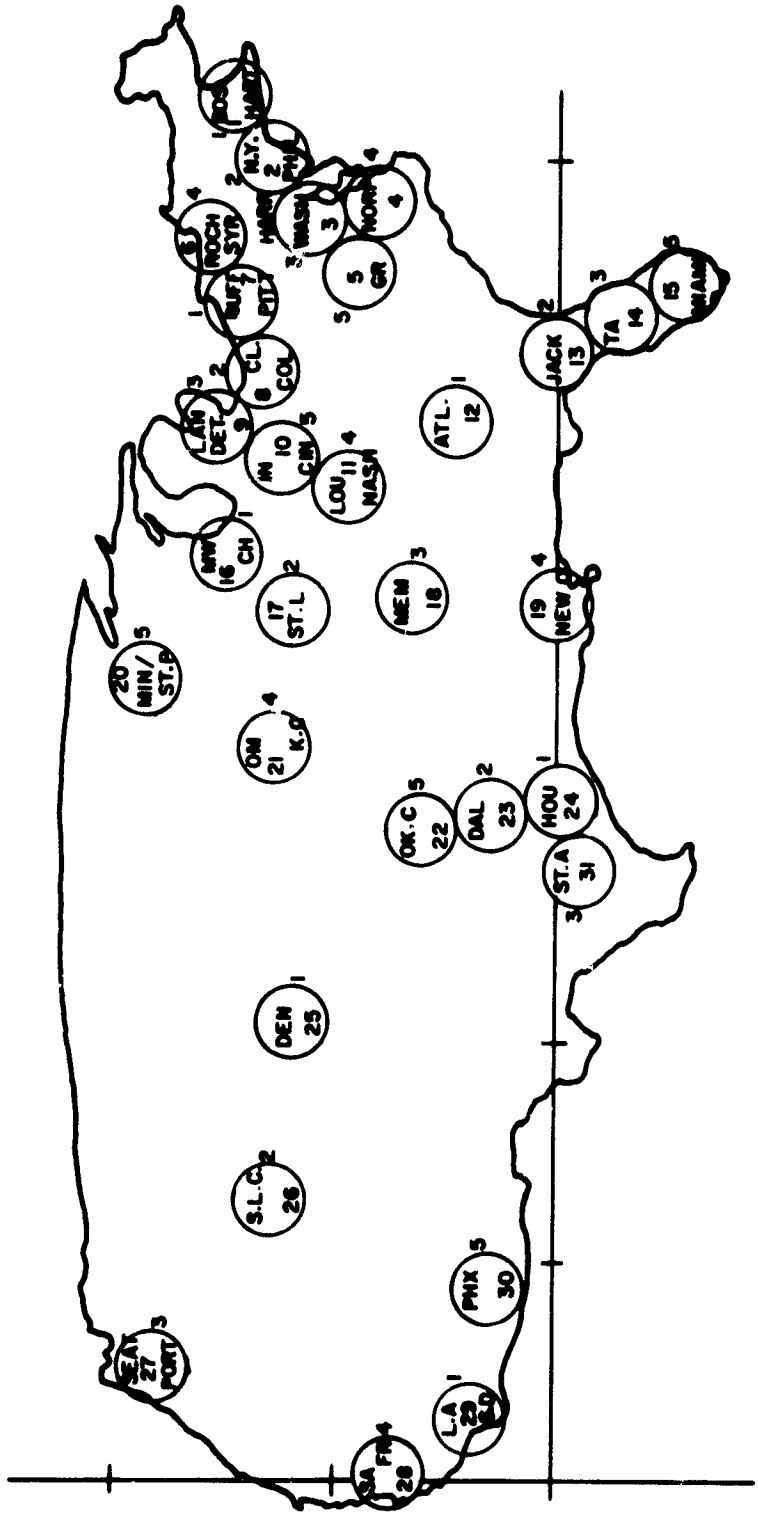

MIN PHI	-4.14
MAX PHI	2.67
RANGE PHI	6.81
PHI INTERCEPT	-4.00

MIN THETA	4.26
MAX THETA	7.25
RANGE THETA	2.99
THETA INTERCEPT	5.00

Figure C-1. Beam Plan for Traffic Model A

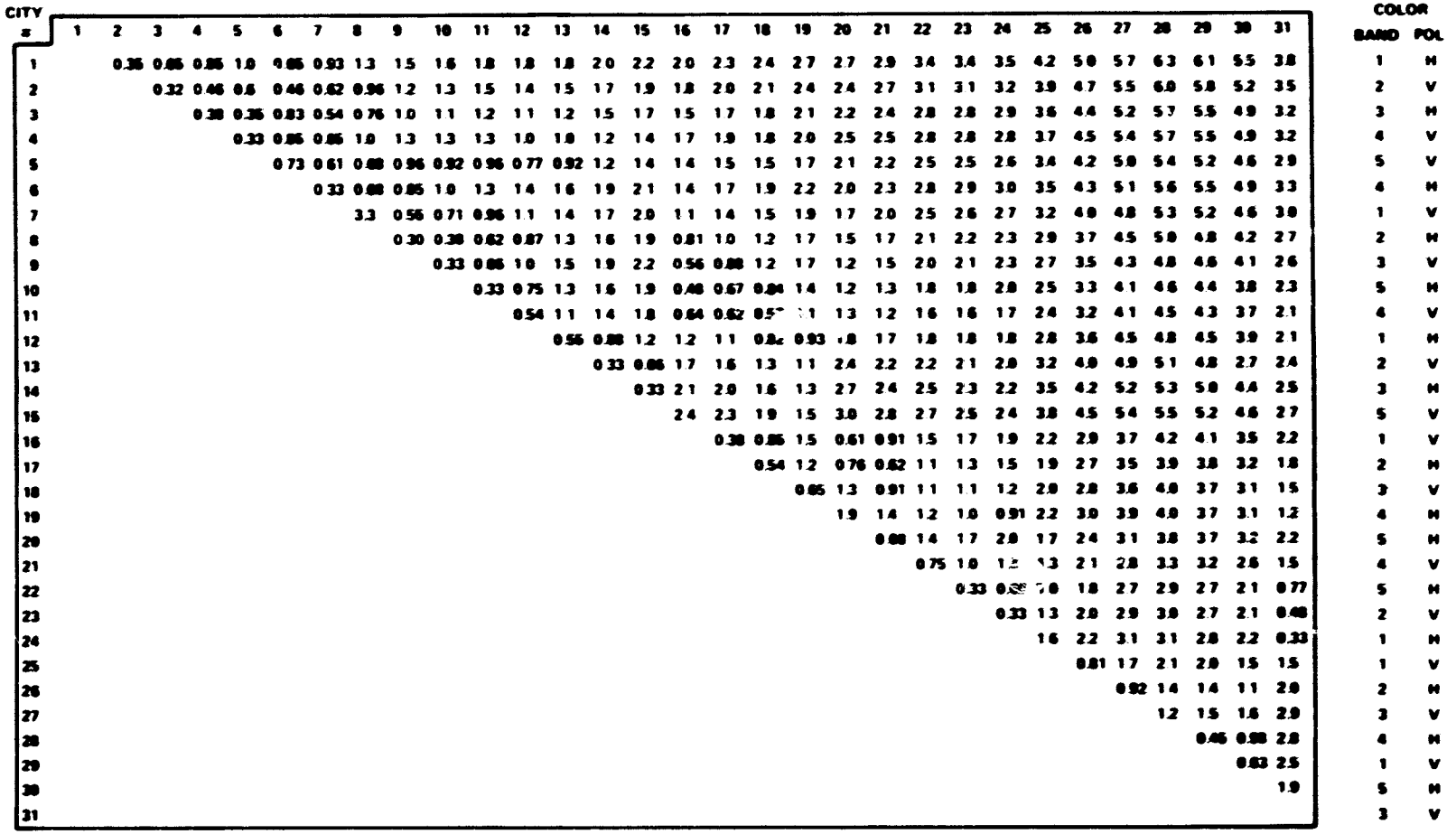

CITY #	1	2	3	4	5	6	7	8	9	10	11	12	13	14	15	16	17	18	19	20	21	22	23	24	25	26	27	28	29	30	31	COLOR BAND	COLOR POL
1		0.35	0.85	0.85	1.0	0.85	0.93	1.3	1.5	1.6	1.8	1.8	1.8	2.0	2.2	2.0	2.3	2.4	2.7	2.7	2.9	3.4	3.4	3.5	4.2	5.0	5.7	6.3	6.1	5.5	3.8	1	H
2			0.32	0.46	0.6	0.46	0.62	0.96	1.2	1.3	1.5	1.4	1.5	1.7	1.9	1.8	2.0	2.1	2.4	2.4	2.7	3.1	3.1	3.2	3.9	4.7	5.5	6.0	5.8	5.2	3.5	2	V
3				0.38	0.35	0.83	0.54	0.76	1.0	1.1	1.2	1.1	1.2	1.5	1.7	1.5	1.7	1.8	2.1	2.2	2.4	2.8	2.8	2.9	3.6	4.4	5.2	5.7	5.5	4.9	3.2	3	H
4					0.33	0.85	0.85	1.0	1.3	1.3	1.3	1.0	1.0	1.2	1.4	1.7	1.9	1.8	2.0	2.5	2.5	2.8	2.8	2.8	3.7	4.5	5.4	5.7	5.5	4.9	3.2	4	V
5						0.73	0.61	0.88	0.96	0.92	0.96	0.77	0.92	1.2	1.4	1.4	1.5	1.5	1.7	2.1	2.2	2.5	2.5	2.6	3.4	4.2	5.0	5.4	5.2	4.6	2.9	5	V
6							0.33	0.88	0.85	1.0	1.3	1.4	1.6	1.9	2.1	1.4	1.7	1.9	2.2	2.0	2.3	2.8	2.9	3.0	3.5	4.3	5.1	5.6	5.5	4.9	3.3	4	H
7								3.3	0.56	0.71	0.96	1.1	1.4	1.7	2.0	1.1	1.4	1.5	1.9	1.7	2.0	2.5	2.6	2.7	3.2	4.0	4.8	5.3	5.2	4.6	3.0	1	V
8									0.30	0.38	0.62	0.87	1.3	1.6	1.9	0.81	1.0	1.2	1.7	1.5	1.7	2.1	2.2	2.3	2.9	3.7	4.5	5.0	4.8	4.2	2.7	2	H
9										0.33	0.85	1.0	1.5	1.9	2.2	0.56	0.88	1.2	1.7	1.2	1.5	2.0	2.1	2.3	2.7	3.5	4.3	4.8	4.6	4.1	2.6	3	V
10											0.33	0.75	1.3	1.6	1.9	0.48	0.67	0.84	1.4	1.2	1.3	1.8	1.8	2.0	2.5	3.3	4.1	4.6	4.4	3.8	2.3	5	H
11												0.54	1.1	1.4	1.8	0.64	0.82	0.57	1.1	1.3	1.2	1.6	1.6	1.7	2.4	3.2	4.1	4.5	4.3	3.7	2.1	4	V
12													0.56	0.88	1.2	1.2	1.1	0.84	0.93	1.8	1.7	1.8	1.8	1.8	2.8	3.6	4.5	4.8	4.5	3.9	2.1	1	H
13														0.33	0.86	1.7	1.6	1.3	1.1	2.4	2.2	2.2	2.1	2.8	3.2	4.0	4.9	5.1	4.8	2.7	2.4	2	V
14															0.33	2.1	2.0	1.6	1.3	2.7	2.4	2.5	2.3	2.2	3.5	4.2	5.2	5.3	5.0	4.4	2.5	3	H
15																2.4	2.3	1.9	1.5	3.0	2.8	2.7	2.5	2.4	3.8	4.5	5.4	5.5	5.2	4.6	2.7	5	V
16																	0.38	0.85	1.5	0.61	0.91	1.5	1.7	1.9	2.2	2.9	3.7	4.2	4.1	3.5	2.2	1	V
17																		0.54	1.2	0.76	0.82	1.1	1.3	1.5	1.9	2.7	3.5	3.9	3.8	3.2	1.8	2	H
18																			0.85	1.3	0.91	1.1	1.1	1.2	2.0	2.8	3.6	4.0	3.7	3.1	1.5	3	V
19																				1.9	1.4	1.2	1.0	0.91	2.2	3.0	3.9	4.0	3.7	3.1	1.2	4	H
20																					0.88	1.4	1.7	2.0	1.7	2.4	3.1	3.8	3.7	3.2	2.2	5	H
21																						0.75	1.0	1.2	1.3	2.1	2.8	3.3	3.2	2.6	1.5	4	V
22																							0.33	0.88	1.0	1.8	2.7	2.9	2.7	2.1	0.77	5	H
23																								0.33	1.3	2.0	2.9	3.8	2.7	2.1	0.48	2	V
24																									1.6	2.2	3.1	3.1	2.8	2.2	0.33	1	H
25																										0.81	1.7	2.1	2.0	1.5	1.5	1	V
26																											0.92	1.4	1.4	1.1	2.0	2	H
27																												1.2	1.5	1.6	2.0	3	V
28																													0.46	0.88	2.8	4	H
29																														0.83	2.5	1	V
30																															1.9	5	H
31																																3	V

ORIGINAL PAGE IS
OF POOR QUALITY

Figure C-2. Interbeam Separation Matrix

Next, the frequencies and polarizations have to be assigned with the aid of figure C-1. Since they are close together, the cities numbered 1 to 5 are assigned band numbers 1 to 5 in order, with alternating polarizations except for city 5 which is a member of a triangle of circles 3, 4, and 5, which touch. Two of these must have the same polarization and two will have to use smaller horns (see discussion on horn size, page 126). This effect will be taken into account. All other cities are assigned bands and polarizations after assignments to cities in their immediate vicinity, i.e., within 2° have been considered. One reasonable assignment of bands and polarizations is shown at the right of the beam separation matrix. Another triangle of circles occurred for beams 8, 9, and 10 where 8 and 10 were assigned the same polarization.

Isolation Results

The isolation performance of the assignment scheme must next be analyzed. Probably no two beams are more closely surrounded by other beams than numbers 3 and 8. The calculation made uses figure C-1, which shows the beams; figure C-2, which gives the separations and band assignments; and figures C-3 and C-4, which give the patterns and sidelobe levels of the beams.

Consider beam 3: all the beams having band 3, are listed in table C-1. The first column shows the other beams in the band. Beam 3 is protected from other bands by filtering.

Column two lists the angular separations from beam 3 of the other beams which reuse band 3. The separations are employed to find the highest sidelobe level from these beams within beam 3 by using the patterns of figure C-3 or C-4 as appropriate. To be conservative, the peak of the sidelobe level is taken, rather than the exact value at the angle of separation. For angular separations greater than the range in figures C-3 and C-4, the observed rate of fall off with angle of the sidelobe peaks is used up to -70 dB. The level assigned is entered in the third column. The fourth column lists the polarization of the interfering beam. If it is cross-polarized, a conservative -20 dB is added to the interference level. The final interference levels are added in power to determine the resultant level, which is expressed in decibels. As can be seen, the interference level at beam 3 was found to be -45.6 dB.

Another beam surrounded by many beams is beam number 8. Table C-2 is constructed for beam 8 in the manner described.

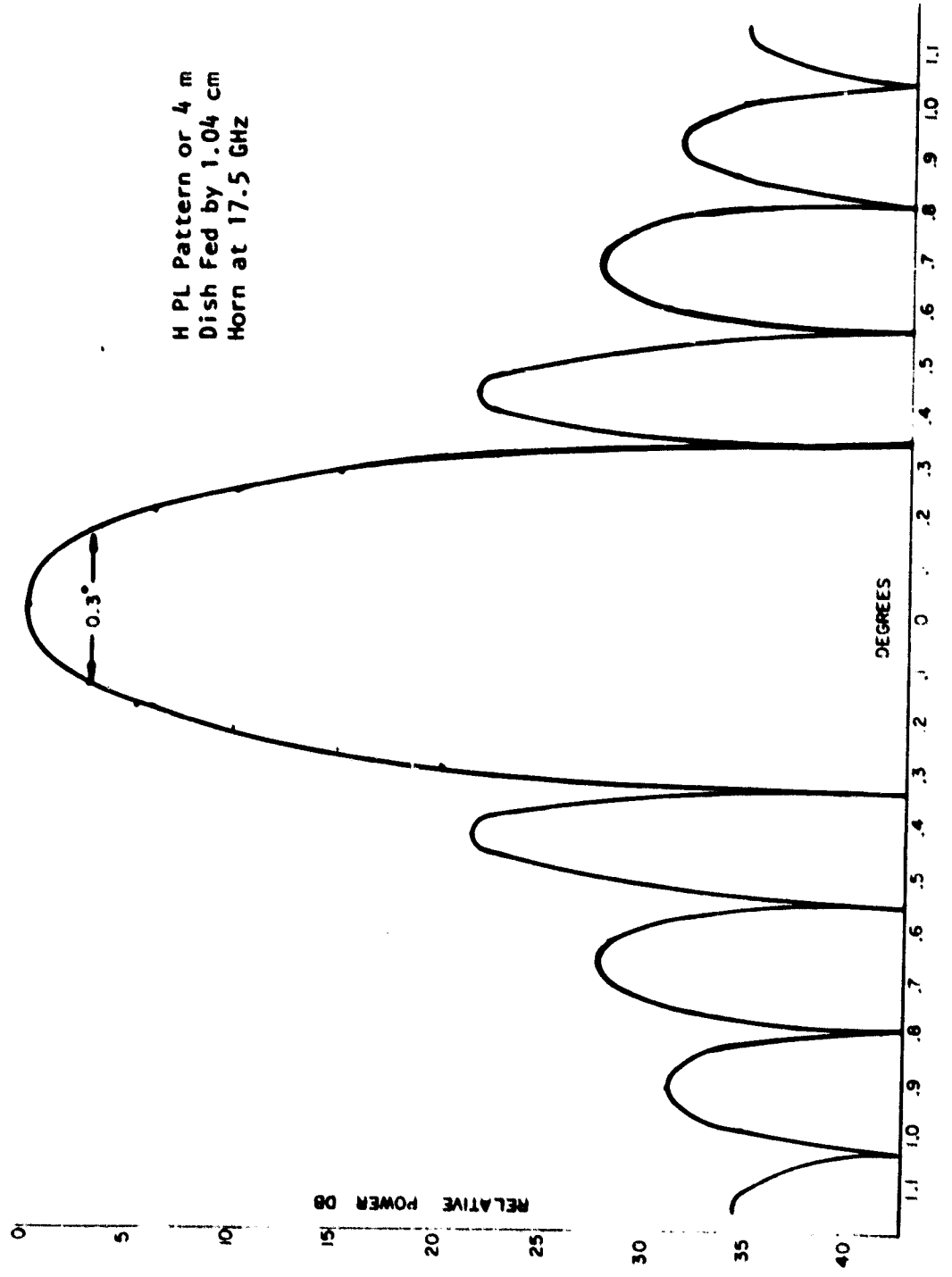

Figure C-3. H Plane Pattern for Aperture Illumination of Table 9-1

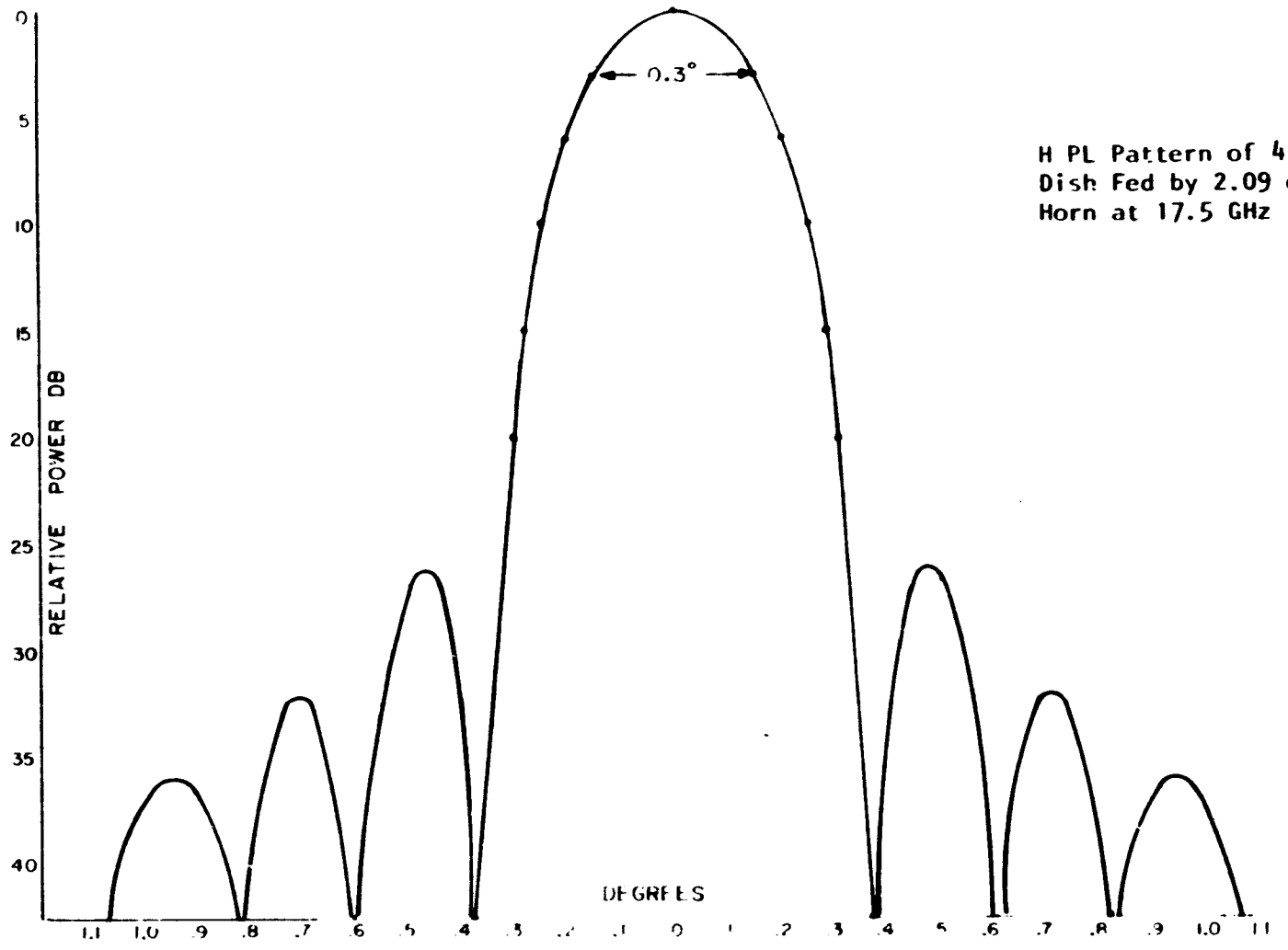

Figure C-4. H Plane Pattern for Aperture Illumination of Table 9-2

Table C-1

Interferences in Beam 3 by Other Band 3 Antenna Beams
Horizontal Polarization of Beam 3

Contributing Beam #	Angular Separation (degrees)	Interference Level (dB)	Polarization	Interference Level (dB)
9	1.0	-36	V	-56
14	1.5	-46	H	-46
18	1.8	-52	V	-72
27	5.2	70	V	-90
31	3.2	70	V	-90

Sum of powers (resultant level: -45.6 dB)

Table C-2

Interference in Beam 8 by other Band 2 Beams
Horizontal Polarization of Beam 8

Contributing Beam #	Angular Separation (degrees)	Interference Level (dB)	Polarization	Interference Level (dB)
2	0.92	-36	V	-56
13	1.30	-42	V	-56
17	1.00	-36	H	-36
23	2.20	-60	V	-80
26	3.70	-70	H	-70

Resultant Level at Beam 8: -35.94 dB

Beam 8 is a member of one of the triangles of touching beams. As such it has the same polarization as beam 10 and both beams use the small horn. This results in the secondary pattern of figure C-3 for beam 8 which has sidelobes about 4.5 dB higher than those of figure C-4. A centrally located beam such as 17, having the same polarization as 8, might have a higher beam interference. Table C-3 confirms this; the calculation yields an interference level of 31.5 dB.

Table C-3

Interferences in Beam 17 by other Band 2 Beams
Horizontal Polarization of Beam 17

Contributing Beam #	Angular Separation (degrees)	Interference Level (dB)	Polarization	Interference Level (dB)
2	2.0	-56.0	V	-76.0
8	1.0	-31.5	H	-31.5
13	1.6	-48.0	V	-68.0
23	1.3	-42.0	V	-62.0
26	2.7	-70.0	H	-70.0

Resultant Level at Beam 17: -31.5 dB

The results displayed in tables C-1, C-2, and C-3 are for beams in the most densely surrounded situations of figure C-1. These are considered the worst cases in the entire beam set. The analysis leads to the following conclusions:

1. An antenna beam design for first sidelobe levels of -26 dB appears feasible. All but a few beams can have horn apertures which permit this if a polarization screen is used to create two focal surfaces.

2. The summed interference level at any beam can be kept at -31 dB or lower due to polarization protection and beam separations. A major contribution is made by utilizing five separate 500 MHz bandwidths so that only five or six beams contribute sidelobe interference to any one main beam. The object is to provide the largest supportable bandwidth in each beam. This includes the traffic handling capability and earning power of the satellite.

3. This analysis demonstrates calculated cases. Careful construction is necessary to achieve the performance indicated.

4. This method avoids the complexity of using multiple horns for each beam plus horn sharing between beams. The isolation achievable in the worst case for the single horn per beam technique is about -30 dB for the beam plan of figure C-1.

Design Concept

The previous subsection described a "color" method of assigning frequency bands and polarizations to the 31 uplink and downlink beams which were deployed to satisfy Traffic Model A, shown in figure C-1. The conclusions of the color study were that the method of frequency band assignment could limit crosstalk in the worst case to a minimum of -31 dB. The antenna design is suitable for supporting an FDM processor which uses the beam isolations made available.

This subsection covers a system design in which the color assignments described are fully utilized. There are 31 beams, each supporting a bandwidth of 500 MHz, so that the total bandwidth throughput for 31 beams is 15.5 GHz. The frequency band of each beam is reused six times in this case. However, the frequency reuse factor should be used very carefully in calculating throughput since it can give misleading results. Counting the beam bands as above is more reliable.

The objective of this subsection is to determine the benefits and costs making maximum use of the potential 15.5 GHz throughput.

Link Calculation

A beam should be able to support a 500 MHz bandwidth. Manufacturers of millimeter wave TWTs are offering to develop tubes whose amplitude and phase response are equalized over this and even

larger bandwidths.(Hughes, 1980) Communication to the satellite is power limited on the downlink. However, for the parameters given in table C-4, the link is shown to be supportable.

It is further assumed that the 10 W power emanates from the satellite antenna, and that the preamplifier is located at the feed in the earth terminal antenna. The downlink budget which results is given in table C-5.

Table C-5 indicates that the factors increasing the link sensitivity exceed those opposing it by 3 dB. The ground station antenna does not have to be 4 m (13.12 ft) in diameter if the station accepts a concomitant reduction in bandwidth. Since 500 MHz is used for routing, that reduction is highly unlikely. A large aperture is also necessary to prevent ground beams from different satellite systems from interfering.

Traffic Capability of Maximum Throughput System

With an instantaneous bandwidth of 15.5 GHz, most of the traffic in Model A could be serviced. This subsection examines the subject to see how much can be accomplished within the 500 MHz per beam limitation. The traffic specification is in terms of data rate, R (in b/s). The required bandwidth for MSK modulation, for example, is approximately 1.2R. To accomodate rain, rate 1/2 coding is used by those users that experience rain attenuation in excess of the rain margin. Assuming that 20% of the users in a beam need coding results in an additional bandwidth expansion factor of 1.2. It is further assumed that the ratio of guard bands to channel bands obtained in current commercial satellites (which have 12 channels 38 MHz wide in a 500 MHz transponder bandwidth) applies. This factor is 1.09. A factor of 1.57 represents the ratio of hertz to b/s, and a 500 MHz channel can support about 319 Mb/s.

Next, the CPS traffic of Model A must be examined. The definition of CPS traffic in this model includes all links in which at least one CPS terminal is involved. The CPS traffic is listed in table C-6, which also shows the trunking only (TR) traffic and the grand total (GT) of the traffic as well. The traffic of Model A is distributed among the 31 beams serving CONUS and this distribution is given in table C-6.

Table C-4

Downlink Parameters

Frequency	17.5 GHz
Range	22,400 miles
Satellite Downlink Power	10 W
Satellite Antenna Diameter	4 m
Ground Antenna Diameter	4 m
Ground System Noise Figure	7 dB
Bandwidth	600 MHz
Antenna Efficiency	75%

Table C-5

Downlink Budget

Factors Increasing Link Sensitivity	Factors Opposing Link Closure
-10 dBW power	-208 dB space loss
-112 dB gain 2 antennas	-10 dB C/N required
-197 dBW system sensitivity	-1 dB attitude control
-319 dBW/Hz	-3 dB edge of coverage
	-1 dB atmospheric loss
	-6 dB rain margin
	-87 dB Hz 500 MHz bandwidth units
	-316 dBW

Table C-6

Distribution of Model A Traffic Among the 31 Beams of Figure C-1
(Mb/s)

Beam		CPS	TR	GT
1.	Boston/Hartford	90	497	587
2.	New York/Philadelphia	381	994	1375
3.	Washington/Harrisburg	193	656	849
4.	Norfolk	33	0	33
5.	Greensboro	126	0	126
6.	Rochester/Syracuse	111	0	111
7.	Pittsburg/Buffalo	141	154	295
8.	Cleveland/Colombus	123	248	371
9.	Detroit/Lansing	182	248	430
10.	Cincinnati/Indianapolis	201	164	365
11.	Nashville/Louisville	58	0	58
12.	Atlanta	59	158	217
13.	Jacksonville	25	0	25
14.	Tampa	121	0	121
15.	Miami	65	163	228
16.	Chicago/Milwaukee	347	575	922
17.	St. Louis	60	158	218
18.	Memphis	25	0	25
19.	New Orleans	68	0	68
20.	Minneapolis/St Paul	70	158	228
21.	Kansas City/Omaha	67	103	170
22.	Oak City	33	0	33
23.	Dallas	99	248	347
24.	Houston	117	248	365
25.	Denver	52	103	155
26.	Salt Lake City	116	0	116
27.	Seattle/Portland	158	103	261
28.	San Francisco/Sacramento	199	497	696
29.	Los Angeles/San Diego	317	575	892
30.	Phoenix	121	0	121
31.	San Antonio	25	0	25
TOTALS:		3783	6050	9833

An examination of the traffic table shows that the 500 MHz beams will support:

1. 100% of the CPS traffic except for

   a. Chicago/Milwaukee (92% only), and

   b. New York/Philadelphia (84% only)

2. 100% of the CPS and trunking traffic for eight beams which have both services

   The cities so covered and their beam numbers are:

   Pittsburg/Buffalo (7)

   Atlanta (12)

   Miami (15)

   St. Louis (17)

   Minneapolis/St. Paul (20)

   Kansas City/Omaha (21)

   Denver (25)

   Seattle/Portland (27)

The 12 cities which have CPS traffic only, along with the eight in group 2, comprise a total of 20 whose requirements completely satisfied under Model A. Of the 11 beams (cities) whose requirements are not completely satisfied, five are served to a level of 74% or more. These regions are:

Cleveland/Columbus (8)	85.9%
Detroit/Lansing (9)	74.1%
Cincinnati/Indianapolis (10)	87.4%
Dallas (23)	91.9%
Houston (24)	87.4%

The percentages for these cities are so high that no further assignment of resources should be made to accommodate their traffic needs.

The six regions whose total needs are not substantially met by the color scheme are:

Boston/Hartford (1)	54.3%
New York/Philadelphia (2)	23.4%
Washington/Harrisburgh (3)	37.5%
Chicago/Milwaukee (16)	34.6%
San Francisco/Sacramento (28)	45.8%
Los Angeles/San Diego (29)	35.8%

These six mega-regions are not fully satisfied because of their trunking requirements. Except for cities 1 and 2, their CPS traffic is satisfied. The city 1 and city 2 CPS traffic (as noted above) is satisfied 92 and 84% respectively.

The communcations shortfall requires that more resources be applied. This cannot be done by furnishing another FDM transponder on the satellite. The beam interferences for the six new additional links in the band would drive the crosstalk above the -31 dB level. Servicing the remaining traffic can only be accomplished by an additional satellite transponder located at another orbital station. In that case, the beam interferences can be held to -31 dB even though system operation is in the same band. These remarks apply to all FDM systems using the 31 beam grouping.

The second transponder must to be crosslinked via space to the first to provide the necessary trunking connectivity. This link must support 3407 Mb/s in a bandwidth of 4.46 GHz. The expansion ratio for this link contains only factors for guardbands and modulation as there is no rain. The band can be divided approximately into two 2.23 GHz bands, one transmitted with vertical polarization and the other with horizontal. Earth/space beam isolation would be well served if the second transponder were 5° from the first. This would place them only 2000 miles apart in space, an easy link to close. Lower transmitted power and smaller antennas could be used because the crosslink path loss will decrease by 21 dB and rain loss by 6 dB while the bandwidth increases only by 6.5 dB

compared to that for the earth/space link of table C-6. The extra 21.0 dB can be apportioned as desired.

Since two satellites are used, it would be possible to reapportion all the traffic between them so that the load is shared more equally. This subject will not be developed here. Renting space for the auxiliary transponder on another stationary satellite orbited for a different purpose is also possible. There is no need to increase the capacity of the other channels in the main satellite to handle the special trunking links. This loading is already included in the Model A traffic allocations. A crosslink transponder with proper frequency multiplexing/demultiplexing is required in the original satellite. The channels it contributes to/or absorbs from the FDM processor would be treated like any other channels. To the main satellite, the crosslink is like any link to the ground. If multiple TWTs are needed for each 2.23 GHz channel, the TWT outputs are multiplexed into the two polarizations in the way usually employed for current commercial communications satellites.

Beam Considerations for the Second Transponder

An additional satellite transponder at an orbital position 5 removed from the main transponder offers the opportunity to service the outsized trunking requirements of cities 1, 2, 3, 16, 28, and 29. The same principles used for the main transponder to minimize beam interferences must again be used in the auxiliary transponder. If this is done, a notable improvement in total traffic handling for these six cities becomes possible. For convenience the total traffic loads of these cities are extracted from table 9-8 and repeated in table C-7 along with supporting data.

Table C-7 shows how it is possible to serve the traffic of these six megacities almost completely. For example, the sum of the CPS and TR traffic of Boston requires a bandwidth of 922 MHz. This can be served via beam number 1 of the main satellite and via one new beam from the auxiliary satellite package, provided that some of the TR traffic is carried by the under-utilized CPS beam of Boston. In other words flexibility of assignment between CPS and trunking beams will go far to satisfy all the traffic. Chicago, Washington/Harrisburg, and San Francisco/Sacramento can be helped in this manner. The final score in servicing the megacities is given in table C-8.

Table C-7

High Capacity Cities of Model A

City and #	CPS Mb/s	TR Mb/s	TOT Mb/s	TOT MHz	Assigned 500 MHz Beams CPS	TR
Boston/Hartford (1)	90	497	587	922	1	1
New York/Philadelphia (2)	381	944	1325	2080	1	3
Washington/Harrisburg (3)	193	656	849	1333	1	2
Chicago/Milwaukee (16)	347	575	922	1448	1	2
San Francisco/Sacramento (28)	199	497	696	1093	1	1
Los Angeles/San Diego (29)	317	575	892	1400	1	2
TOTALS	1527	3744	5271	8275	6	11
Equiv MHz	2397	5878	8275	8275	3000	5500

Table C-8

Percentage of Megacity Traffic Served by Equalizing Loading Density on CPS + TR Beams

City and #	CPS	TR
Boston/Hartford (1)	100	100
New York/Philadelphia (2)	87	100
Washington/Harrisburg (3)	100	97
Chicago/Milwaukee (16)	100	100
San Francisco/Sacramento (28)	100	88
Los Angeles/San Diego (29)	100	100

As can be seen from table C-7, 11 earth/space beams are to be provided by the auxiliary transponder. Their assignments are based on principles developed earlier. There are additional constraints because these beams must be multiplexed onto the crosslink between the auxiliary and the main satellite. Band interferences in the crosslink must be considered as well as beam interferences in the earth/space link. A possible solution is given in table C-9.

The two groups of frequencies add to approximately equal bandwidths for transmission on the crosslinks. Earth/space beam isolations are also maintained using different bands and polarizations. The number 1 band for Boston/Hartford must be translated to another band for transmission on the crosslink to avoid interference with the second band from Washington/Harrisburg (3).

With the auxiliary satellite transponder it is possible to service the CPS and trunking traffic of all cities in Model A at 100% except for the following cities which are serviced at the lesser percentages shown in table C-10.

Table C-9

Earth/Space Band Assignments for Auxiliary Beams
(Principally Trunking)

City and #	Beam Band	Beam Band	Beam Band	Cross TOT BW	Beam
Boston/Hartford (1)	1H			461	1
Washington/Harrisburg (3)	5H	1V		888	1
San Francisco/Sacramento (28)	4V			500	1
Los Angeles/San Diego (29)	2V	3H		934	1
New York/Philadelphia (2)	2V	3H	4V	1500	1
Chicago/Milwaukee (16)	1V	5V		966	2

BW. Sum 1, 2, 28, 29; 2783 MHz
BW. Sum 2,16; 2466 MHz

Table C-10

Cities Not Serviced at 100% in Either CPS or TR Traffic

City and #	CPS	TR
New York/Philadelphia (2)	87	100
Washington/Harrisburg (3)	100	97
San Francisco/Sacramento (28)	100	88
Cleveland/Columbus (8)	86	86
Detroit/Lansing (9)	74	74
Cincinnati/Indianapolis (10)	87	87
Dallas (23)	92	92
Houston (24)	87	87

Of eight cities whose needs are not completely served, seven are served at 86% or better, and only one is served at 74%. To sum up, the potential of the color scheme system with auxiliary transponder for total CPS and trunking service is:

23 cities served 100%

7 cities served 86% to 97%

1 city (Detroit) served 74%

Frequency Assignment Plans

To minimize the number of components in the satellite, a plan for frequency assignment within the uplink beams is used. The master control station will assign frequencies in each beam based on destination in accordance with this plan. A number of message channels will come up to the transponder in each beam on different frequencies. The transponder will route each message to its destination by filtering processes. First, it disassembles a beam into sub-bands, then routes the sub-bands to the destination beam, and finally adds the sub-bands in the beam so they can be sent back to earth. For bandwidth conservation, the sub-bands to be added must be contiguous in frequency. This is the guiding principle for the entire process.

Sub bands can always be made contiguous by a sufficient number of translation processes. Translation consists of amplification, mixing with an LO, and post mix filtering. One process uses four components. A plan is needed to minimize the number of translations necessary for the traffic within the transponder. However, this plan must maintain the independence of the beams so that the throughput described above can section 9.2.3 is achieved.

The number of different subbandwidths expected among the 42 beams must be determined first from the bandwidth distributions derived by apportioning the traffic in Model A among the 42 beams shown in tables C-6 and C-7. The sum of the grand total column in these tables is 9,833 Mb/s which corresponds to a total system throughput bandwidth of 15,438 MHz. If the total CPS and trunking traffic for each city is divided by 9,833 for normalization, the percentage of the average beam bandwidth destined for each city could be found. When these percentages are multiplied by the bandwidth of the average beam, the distribution of subband sizes is found. The average beam bandwidth is determined to be 370 MHz on dividing the system throughput among 42 beams. When the process was carried out, a beam was found to be composed of 5, 10, and 15 MHz sub-bands with populations as given in table C-11.

Table C-11

Channel Size Distribution Based on Traffic Model A and Tables C-6 and C-7 for the Average Beam

Sub Bandwidth (MHz)	Number of Sub Bands
5	12
10	9
15	21

The beams will be distributed among five bands, each 500 MHz wide. Three bands will have eight beams, and two bands will have nine beams. In most cases, the number of sub-bands of a given size does not equal the number of beams in a 500 MHz band. A scheme for obtaining channel contiguity for this situation is illustrated in figure C-5. Here one of the channel sub bandwidth groups has been filtered from each of the beams in a certain band. For example, the 60 MHz bands containing the twelve 5 MHz sub-bands are filtered from the nine beams in band 1. The 60 MHz bands are displaced in frequency from each other in echelon by 5 MHz steps. Then the 5 MHz sub-bands are assigned beam destinations in order as shown in the figure. When the sub-bands are filtered out of the 60 MHz band, they can be added directly and will form 12 contiguous 45 MHz bands suitable for further adding and transmission to their destination cities. The mixers performing the echelon process will also move the 60 MHz bands to frequencies suitable for addition to the 5 MHz frequencies of the other 500 MHz bands in the system.

The echelon process thus determines the frequency plan for the entire FDM system. Each of 42 beams is first translated to IF, then sliced into three bands: containing the 5 MHz, one the 10 MHz, and one the 15 MHz channels. These bands are echeloned for filtering and addition with similar sub-bands from the other beams in the 500 MHz band. The echelon mixers displace all the frequencies so that the sub-bands will also add contiguously system wide. For example, the 45 MHz bandwidths containing the 5 MHz sub-bands/derived from band 1 and destined for city number 4 would be 500 MHz away from the 45 MHz band summed from the beams of band 2. Therefore, the band two contribution must be displaced by 500 - 45 = 455 MHz, so that the two 45 MHz bands will be contiguous. A similar process is followed for the 90 MHz band sums containing the 10 MHz channels and the 135 MHz band sums containing the 15 MHz channels.

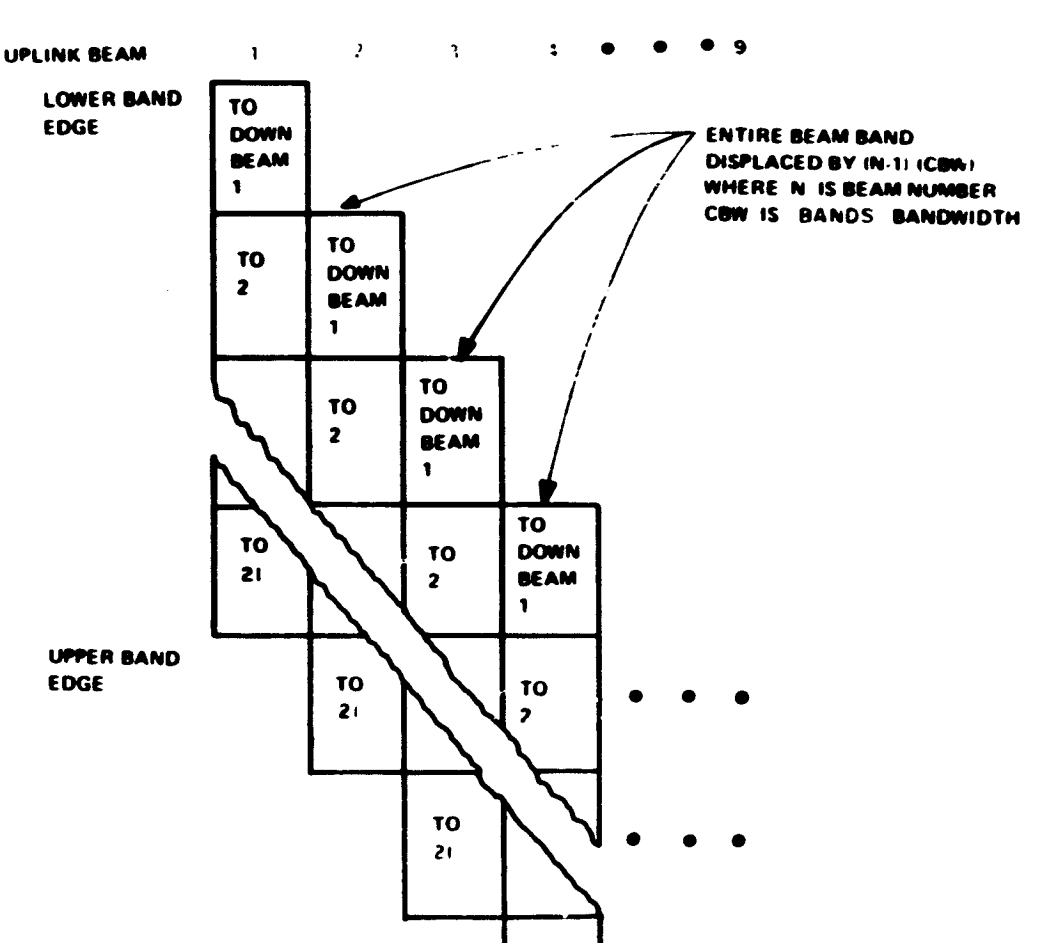

Figure C-5. Echelon Displacement of Entire Beam Band and Band Assignments to Make Assembled Downlink Beam Bands Contiguous

An illustration of the system in the main transponder is given in figures C-6 and C-7. The 15 MHz sub-bands will be followed through the system. The beam signal enters the transponder from the antenna where it is preselection filtered and amplified. Next, it is translated to IF where it is more easily filtered into the three bands required by table C-11 i.e., the 60 MHz containing the 5 MHz sub-bands, the 90 MHz containing the 10 MHz sub-bands, and the 315 MHz containing the 15 MHz sub-bands. Hereafter only the 15 MHz bands are followed. The other bands are treated similarly.

The next step translates the 315 MHz band containing the 15 MHz sub-bands to a band which is echeloned among eight beams and translated among five, 500 MHz bands so that the sub-bands in any 15 MHz slot, when channel filtered and combined in two successive combiners, will fit into a contiguous frequency band ready to be radiated down to the ground or to the auxiliary satellite. The 315 MHz band is channel filtered into twenty-one 15 MHz sub-bands after being echeloned and translated. Next, all the same numbered channels in the eight beams in a 500 MHz band are combined in a sub-band combiner. There are twenty-one 15 MHz combiners, each with eight or nine inputs for the eight beams of one band. The output of any one sub-band combiner is added in a band combiner with the four other sub-band combiner outputs from the remaining 500 MHz bands. A band combiner output contains the traffic for one downlink beam. The same process is performed with different channel counts for the 5 MHz and 10 MHz sub-bands.

Figure C-7 continues the FDM process through the satellite. Blocks representing the 12, 9, and 21 band combiners for the 5, 10, and 15 MHz channel downlink beams are shown. Their individual output lines, which now contain the traffic for one downlink beam, are routed to a 42-input 42-output 126-cross point switch which is usually quiescent. It is exercised only to exchange bandwidths between links when the traffic statistics of the model changes so that traffic to one city grows while that of another city diminishes.

The signals are next upconverted from IF to the downlink frequency bands. A total of 31 beams goes down to earth from the main satellite, and eleven beams are multiplexed onto two orthogonal polarizations for radiating on the crosslink to the auxiliary satellite. This is done in the fashion usual for current communications satellites.

An FDM system has been outlined which handles substantially all the traffic in Model A, both CPS and trunking. Figures C-6 and C-7 suggest the numbers of components required. These numbers are given explicitly in table C-12.

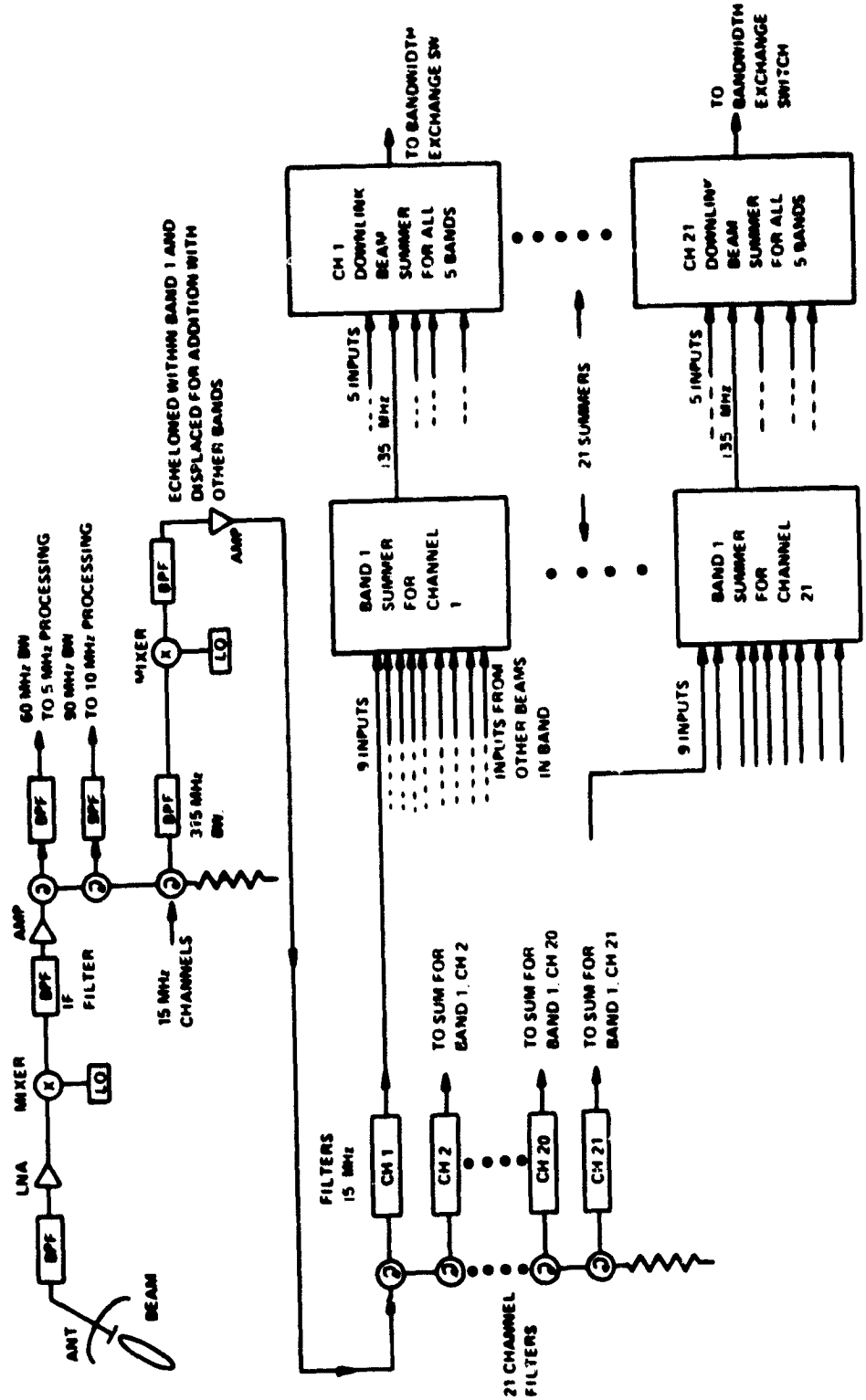

Figure C-6. Band Separation, Echeloning, and Summing Illustrated for the 15 MHz Bands

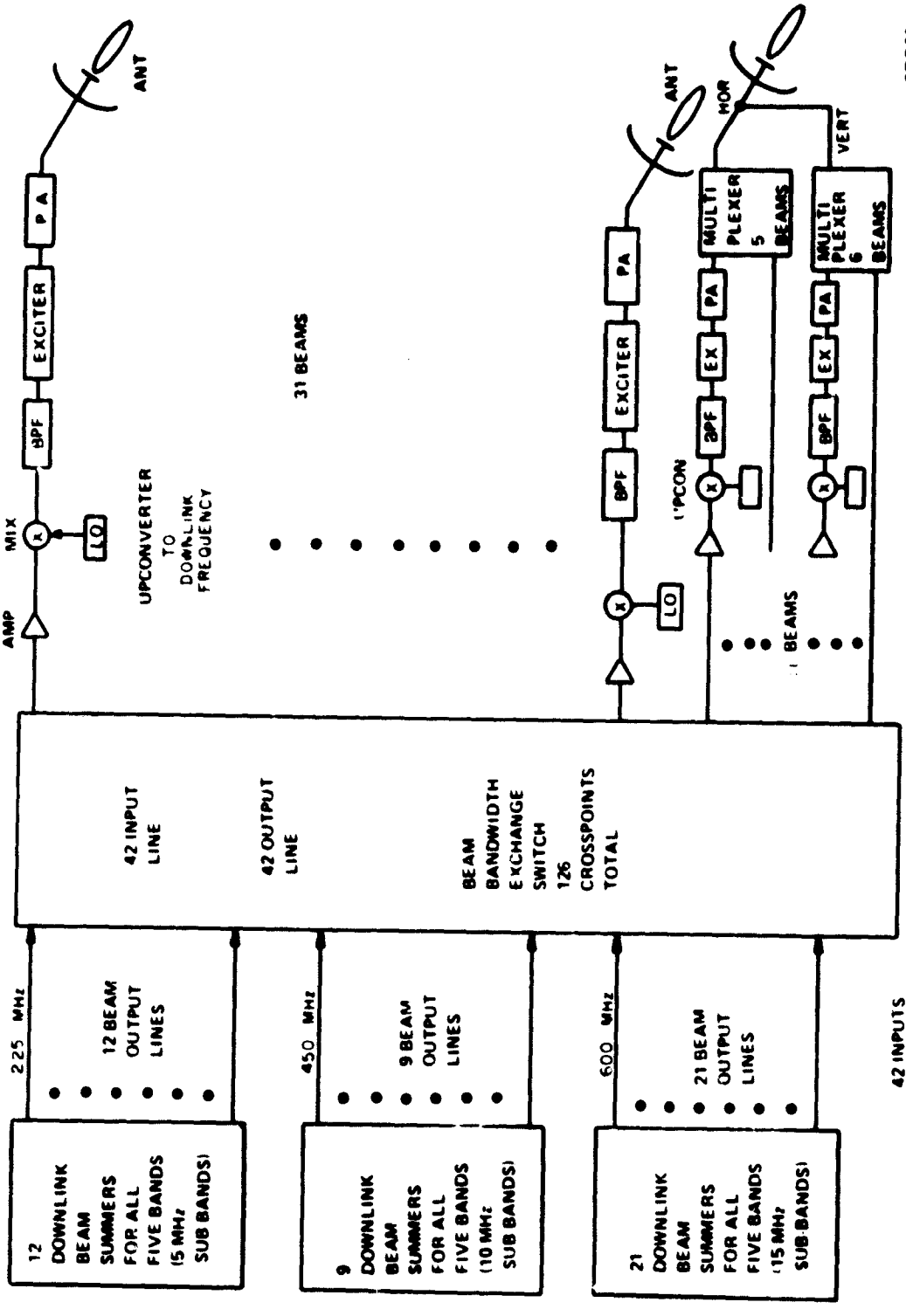

Figure C-7. Summing, Bandwidth Exchange, Upconversion and Transmitting for Downlink Beams

Table C-12

Color Beam FDM Transponder Component Count
Total CPS and Trunking
Main Satellite Plus Auxiliary Including Crosslink

Item	Number
Antennas	12
Low Noise Amplifiers	66
Preselector Filters	66
IF Translators	42
IF Amplifiers	42
Band Separation Filters	126
Echelon Translators	126
Channel Separation Filters	1764
Channel Summers	210
Beam Summers	42
Band Exchange Switch (BES)	1
Cross Points for BES	126
UP Converters	66
Bandpass Filters	66
Exciters	66
Power Amplifiers	66
Antenna Feeds	66

All the numbers except for channel filters are reasonable in size. The channel filters operate at IF, perhaps 3 GHz, and can take the extremely compact and lightweight form of the stripline interdigital filter with built in circulator. The adoption of the echelon process has thus reduced the parts count of the color FDM system to an economical level.

The (color) scheme completely satisfies the CPS and trunking requirements of 23 cities. Seven cities are satisfied to better than 86%, and one to better than 74%. Six regions need additional resources for trunking. In addition, there is unused capacity for expansion in 20 regions. CPS and trunking traffic are interlinked in a single system. The color beam system is worthy of serious consideration.

APPENDIX D

SAW DEVICE FILTERS

Filtering of beam traffic down to the 10 to 30 MHz band has been considered for SSFDMA satellites. This directs attention to the characteristics of SAW filters which were studied. Some of the state-of-the-art results may not be commercially available as most of the research and development work has been sponsored by large companies that have produced SAW devices for their own internal uses and have been reluctant to give away secrets. This doesn't persist indefinitely, however -- e.g., Sawtek, Inc. was recently founded by a group of SAW-device design experts who left Texas Instruments.

Some of the generalities and specifics on SAW bandpass filters garnered from the study are:

- Center frequencies from 20-500 MHz are routinely achievable with 3-4 μm design rules; and center frequencies from 0.6-1.0 GHz are realizable with 1 μm design rules, but not in volume production as yet.

- Fractional bandwidths range from less than 0.1% to around 50%.

- Ultimate stop-band rejections of 100 dB have been reported, and with proper care, 60 dB is routine.

- Insertion loss, depending on the substrate material used, the matching networks employed, the center frequency, and the fractional bandwidth, is often on the order of 15-20 dB.

- Pass-band ripple of 0.1 dB is readily achievable.

- 3 dB - 40/50 dB transition or skirt region shape factors of 1.1 to 1.2 are quite common.

- Being non-minimum-phase devices, SAW-device bandpass filter phase response can be specified independently of the magnitude; ±3° phase linearity over the pass-band is not uncommon.

- The temperature coefficient of a SAW-device bandpass filter depends upon the substrate used:

- Lithium Niobate -- mostly used for filters with 3-50% fractional bandwidth and (due to its very high coupling coefficient) low insertion loss; has a temperature coefficient of 94 ppm/°C.

- ST-Quartz -- used for filters with less than 3% fractional bandwidth; has negligible temperature coefficient.

- Lithium Tantalate -- the temperature coefficient of 69 ppm/°C is only slightly better than that of lithium niobate, but its coupling coefficient is much better than that of quartz.

- Prototyping SAW components -- as with any IC -- is fairly expensive. The nonrecurring engineering charges required to design a high-resolution photomask can easily run as high as $20,000. Using CAD techniques, design turnaround times range from a few weeks to a month or so. Actual passband responses typically match theoretical designs to within 0.1 dB.

Some of the areas for further research include:

- Use of GaAs as a SAW-device filter substrate. Under Army and Air Force contracts, United Technologies Research Center is building SAW filters, delay lines and resonators on GaAs substrates for operation in the 100-to-200 MHz range, with hopes of eventually pushing the operational frequency to 1 GHz. On the same GaAs substrate it may also be possible to form MOSFET amplifiers which could offset the SAW-device insertion losses.

- Reduction of insertion loss. The bidirectional nature of the filter's interdigital transducer leads to a minimum device loss of 6 dB (3 dB at generation, and 3 dB at detection) and concomitant triple transit signals only 12 dB below the principal output. For adequate suppression of multi-transit signals, losses of 15-20 dB have had to be accepted. Development of three- and four-phase unidirectional transducers has shown losses as low as 1.5 dB with triple transit suppression of about 40 dB.

Some of the key specifications of several SAW-device bandpass filters encountered in the literature are given below.

- Hughes program for Ft. Monmouth:
  - Quartz Bandpass Filter: f_o = 100 MHz; 3-dB ΔF = 2 MHz; IL = 20 dB; sidelobe suppression = 40 dB
  - Lithium Niobate Bandpass Filter: f_o = 150 MHz; 3-dB ΔF = 30 MHz; IL = 20 dB; sidelobe suppression = 20 dB
- Anderson Labs: f_o = 70 MHz; 3-dB ΔF = 280 kHz; sidelobe suppression = 30 dB; 3-30 dB shape factor = 1.7; phase linearity = [illegible]
- IF filter used in ECM D/F telemetry and radar receivers: f_o = 160 MHz; 3-dB Δf = 650 kHz; sidelobe suppression = 35 dB; IL = 20 dB; phase linearity = ±3°
- JTID/TIES modular SAW filters

f_o (MHz)	70	70	70	70
1-dB Δf (kHz)	40	-	-	7 MHz
3-dB Δf (kHz)	52	70	350	9 MHz
40-dB Δf (kHz)	130	140	1050	17.5 MHz
Shape factor	(3-40)		(3-50)	
	2.5	2.0	3.0	2.5
IL (dB)	15	15	12	12
Ripple (dB)	±0.5	±1.0	±0.4	±0.4
Rejection (dBO	40	40	50	40
Phase Linearity	-	-	±3°	±3°

- GE NASA Report: GE has developed some SAW filters required for a sidelobe canceler receiver in a radar system with the following parameters: f_o = 300 MHz; BW (3-dB Δf) = 5 MHz; 35-dB Δf = 13.5 MHz; sidelobe attenuation $\gtrsim$ 37 dB; insertion loss = 22 dB; pass-band ripple = $\pm$0.25 dB; phase linearity = $\pm$1.25°; and the 3-35 MHz shape factor = 2.7.

A list of vendors from whom more current and detailed information on SAW-device bandpass filters may be obtained follows:

SAW Device Vendors

Andersen Labs, Inc.
Advance Systems Div.
1280 Blue Hills Ave.
Bloomfield, Conn. 06002
(203) 242-0761

Anders, Inc.
77 Wolcott Rd
Simsbury, Conn. 06070
(203) 658-7666

Crystal Technology
1035 Meadow Circle
Palo Alto, CA 94303
(415) 856-7911

Hughes Aircraft Co.
Box 3310
Fullerton, CA 92634
(714) 871-3232

Kyocera International, Inc.
8600 Balboa Ave.
San Diego, CA 92123
(714) 279-8310

Marconi Electronics, Inc.
Marconi Instrument Div.
100 Stonehurst Ct.
Northvale, N.J. 07647
(201) 767-7250

Damon Corporation
Electronics Div.
80 Wilson Way
Westwood, MA 02090
(617) 449-0800

Fujitsu America, Inc.
910 Sherwood Dr-23
Lake Bluff, Ill. 60044
(312) 295-2610

Hughes Aircraft Co.
Aerospace Groups
Centinela Ave. & Teale St.
Culver City, CA 90230
(213) 391-0711

Rockwell International
Collins Radio
Electronic Devices
(Filter Products)
4311 Jamboree Rd
Newport Beach, CA 92660
(714) 833-4632

Rockwell International
Microelectronic Devices
Box 3669
Anaheim, CA 92803
(714) 632-3729

Sawtek, Inc.
P.O. Box 7756
Orlando, FL 32854
(305) 299-4441

Microsonics Div.,
Sangamo-Weston Inc.
60 Winter St.
Weymouth, MA 02188
(617) 337-4200

Plainview Electronics Corp
28 Cain Drive
Plainview, N.Y. 11803
(516) 822-5357

Plessey Semiconductors
1641 Kaiser Ave.
Irvine, CA 92714
(714) 540-9979

Tauber-Dreyer Corp.
17074 Dearborn St.
Northridge, CA 91325
(213) 993-0048

Teledyne MEC
3165 Porter Drive
Palo Alto, CA 94304
(415) 493-1770

Valpey-Fisher Corp.
75 South St.
Hopkinton, MA 01748
(617) 435-6831

APPENDIX E

LARGE SCALE INTEGRATION SWITCHING 10-30 MHz

Initial thinking for SSFDMA satellite system design considered filtering channels down to the 10 to 30 MHz band. This led to consideration of RF cross bar switches with as many as 1000 input and 1000 output ports. The straightforward or standard approach would then require one million switching elements. In last year's Project 8680 Final Report (MTR-3787), it was pointed out that substantial reduction in the number of the cross points of an N x N cross-bar switch could be realized by the special partitioning and interconnection techniques of C. Clos of Bell Labs. For instance, his partitioning of an entire switching array into certain three-stage submatrices, while retaining the non-blocking character of the standard approach, reduces the total number of cross points, N_{cp}, to

$$N_{cp} = 6 (N_L)^{3/2} - 3 N_L$$

where N_L is the number of lines (ports) in and out of the switch. The fractional reduction (relative to the standard approach) in the total number of cross points due to this three-stage version of the Clos approach is given by

$$\frac{N_{cp}}{N_L^2} = \sqrt{\frac{6}{N_L}} - \frac{3}{N_L}$$

Also, the (average?) number of input lines crossing over an output line is N_L for the standard approach and

$$\frac{N_{cp}}{N_L} = 6\sqrt{N_L} - 3$$

for the Clos approach. The table below gives some idea of the reductions possible:

N_L (Lines)	Total No. Cross Points		Cross Points/Line		Fract'l Red'n
	Std Meth	Clos Meth	Std Meth	Clos Meth	
30	9×10^2	8.96×10^2	30	30	0.995
100	10^4	5.70×10^3	100	57	0.57
300	9×10^4	3.03×10^4	300	101	0.34
1000	10^6	1.87×10^5	1000	187	0.19

CONSEQUENCES OF LARGE NUMBERS OF CROSS POINTS

The number of cross points per output line is particularly significant in that the open-switch capacitive feed-through of each cross-point switching element contributes to the noise on a given output line, in addition to the cross-talk induced by the (primarily) immediately adjacent output lines. If a fraction, f_{xc}, of the standard signal carrier power, P_c, on an input line is cross-coupled onto an output line by one open switching element, then the carrier-to-interference power ratio of an output line is given by:

$$\frac{P_c}{P_I} = \frac{P_c}{N_{cp} \times (f_{xc} \times P_c)} = \frac{1}{N_{cp}\, f_{xc}}$$

so that

$$10 \log f_{xc} = -\left[10 \log \frac{P_c}{P_I} + 10 \log N_{cp}\right]$$

For a 1000 x 1000 cross-bar switch, the standard approach requires

$$10 \log f_{xc} = -10 \log \frac{P_c}{P_I} - 30 \text{ dB}$$

and for the Clos approach

$$10 \log f_{xc} = -10 \log \frac{P_c}{P_I} - 22.7 \text{ dB}$$

If $10 \log (P_c/P_I)$ is to be 30 dB, then $10 \log f_{xc}$ should be less than -60 dB for the standard and -52.7 dB for the Clos approach.

Also, the number of closed switches (in series) between an input and output port is important due to insertion losses at each switch. (Treating the (most likely printed-circuit strip-line) cross-bar over a ground plane as a transmission line of characteristic impedance, Z_o, then joining it to another line with a series resistance, R_{sw}, introduces a two-fold insertion loss. One is due to termination mismatch of the source line by the sum of the switch resistance and the parallel (due to center-point contact) driven bar impedance:

$$T_1 = \frac{2 Z_L}{Z_o + Z_L}, \text{ where } Z_L = \frac{Z_o(R_{sw} + \frac{1}{2} Z_o)}{(R_{sw} + \frac{3}{2} Z_o)}$$

The other element of loss is due to the voltage division across the series switch resistance:

$$T_2 = \frac{\frac{1}{2} Z_o}{R_{sw} + \frac{1}{2} Z_o}$$

The total insertion loss then becomes

$$T = T_1 T_2 = \frac{\frac{1}{2} Z_o}{(Z_o + R_{sw})}$$

$$= \frac{\frac{1}{2}}{1 + \frac{R_{sw}}{Z_o}}$$

So that the $Z_o = 50\Omega$ and $R_{sw} = 50\Omega$

$T = 0.25$

or

20 log T ≃ -12 dB/series closed-switch.

Thus the presence of four or five switches in series between input and output ports could result in substantial losses.

PROBLEMS WITH CROSS-BAR SWITCH AND ITS FET IMPLEMENTATION

Since the total number of cross-point switches is quite large, the only apparently feasible approach would be to employ a substantial degree of medium- to large-scale integration in the implementation of the design. Thus, the switching elements would be semiconductor switches, and most likely fabricated with FETs.

Most analog FET switches consist of a switching transistor connecting input and output terminals, and several switch-driven transistors; e.g.:

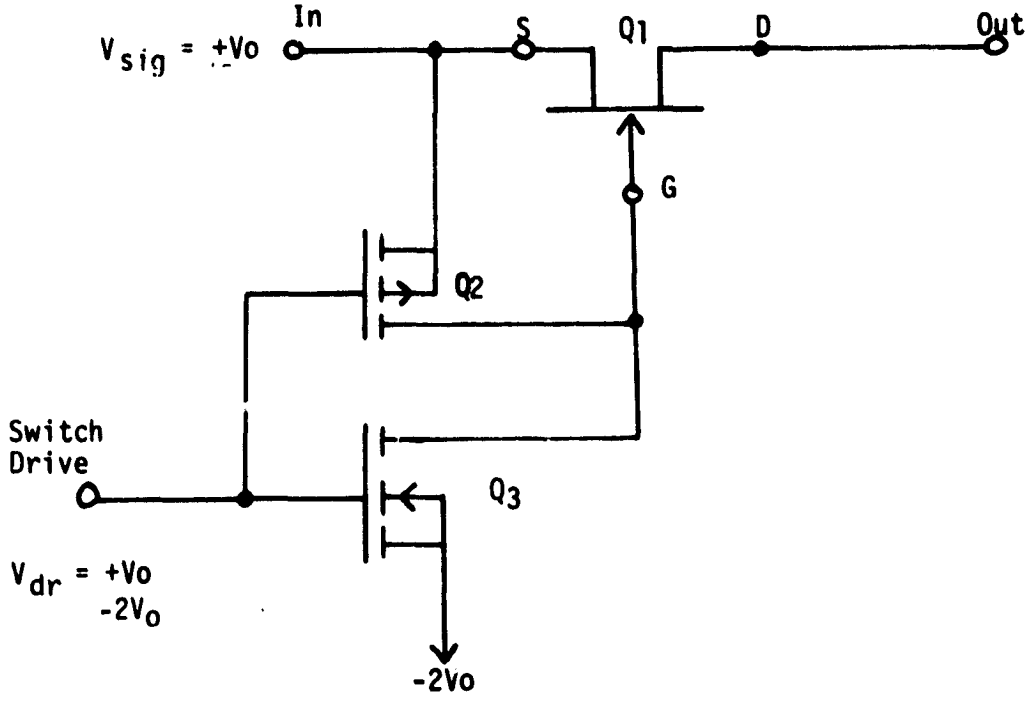

When the switching transistor, Q_1, is to be ON (i.e., switch closed), the switch-drive signal turns drive transistors Q_2 ON and Q_3 OFF; when Q_1 is to be OFF (i.e., switch open), the drive signal turns transistors Q_2 OFF and Q_3 ON.

As a result, a rough model of the closed switch is given by

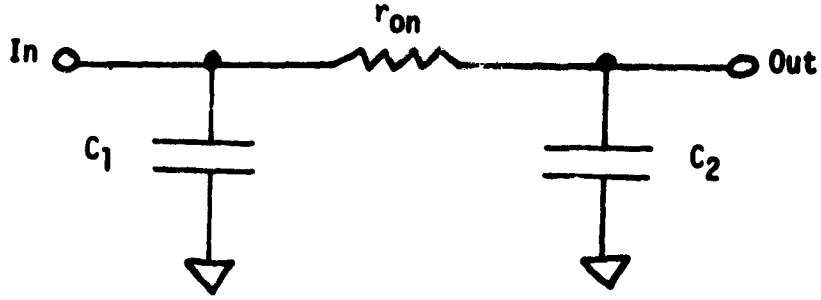

where $C_1 \approx C_2$ are on the order of 5-30 pf and r_{on} can be 20-200Ω, depending upon the particular FET considered. Likewise, a rough model of the open switch is given by

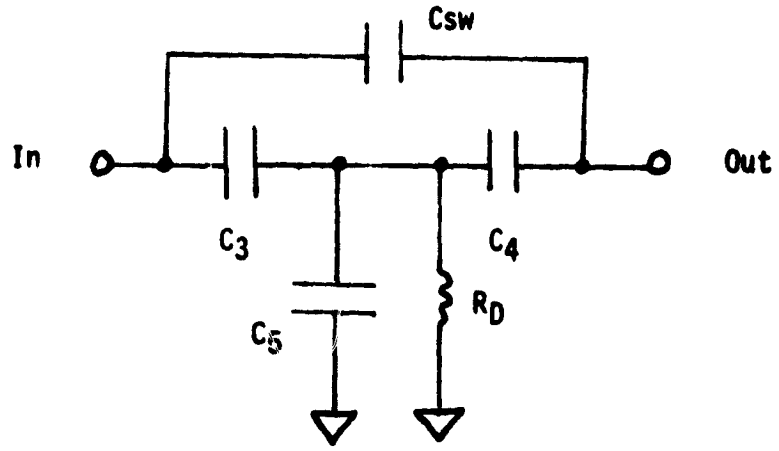

where $C_3 \approx C_4 \sim$ 2-4 pf; $C_5 \sim$ 7-15, $R_D \sim$ 200 - 2000Ω; and the switch capacitance, C_{sw}, is on the order of 0.1 pf.

Calculation with these and other more detailed models agree well with measurements on several types of FET switches. A measurement of the OFF isolation of a typical FET switch (Siliconix DG181) vs. frequency is shown below for a 75Ω - load:

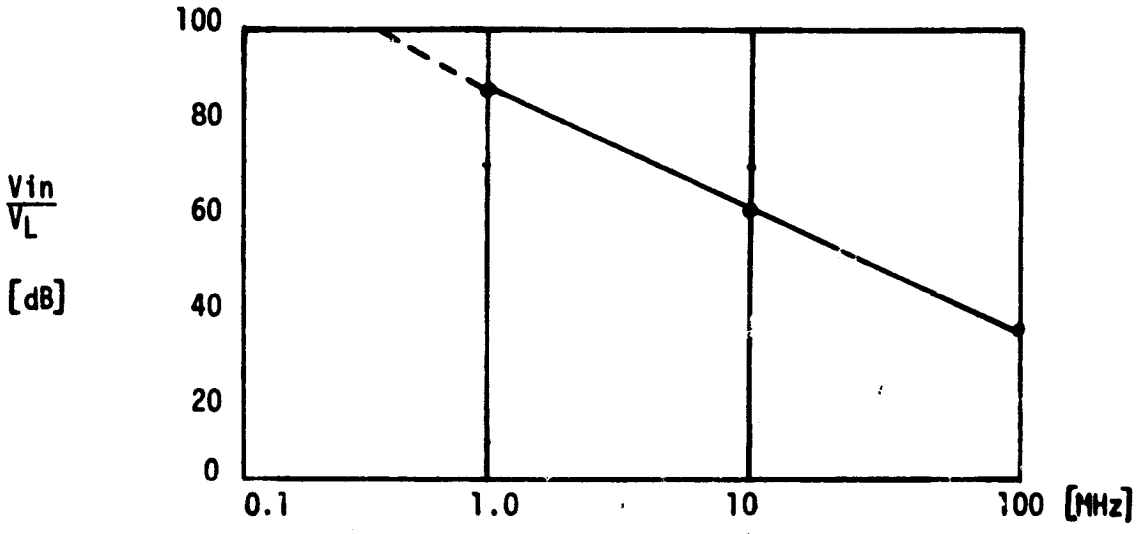

A table is given below summarizing the relative switch performance of three types of FET switches (all Siliconix):

- DG172 -- PMOS
- DG181 -- JFET
- DG200 -- CMOS

Switch	r_{on} (Ω)	C_{on} (pf)	R_L (Ω)	OFF Isol. @10MHz (dB)	ON/OFF (dB)	Insert'n Loss (dB)
DG172	100-150	25-35	100 75 50	51 54 57	43 44.5 45	8.0 9.5 12
DG181	15-25	10-14	100 75 50	55.9 58.4 61.9	53.9 55.9 58.3	2.0 2.5 3.6
DG200	45-60	18-24	100 75 50	43.8 46.3 49.8	39.7 41.2 43.0	4.1 5.1 6.8

Accordingly, some of the non-ideal aspects of the FET switch, arising from stray and residual parameters, are:

- Switch-feed through (noise) -- due to switch-shunting capacitance
- decreased channel bandwidth -- due to line-shunting capacitance
- insertion loss -- due to series switch ON-resistance

The output line noise pickup is further increased by capacitively coupled cross-talk from the switch matrix itself:

- from adjacent parallel lines
- from passing over crossing lines

SOME IMPLICATIONS OF A STRAIGHTFORWARD APPROACH

If the output line has some 187 open switches capacitively coupled to it, then, according to the OFF isolation curve given above, the isolation at 30 MHz is about -43 dB, so that the carrier-to-interference introduced would be around:

$$\left(\frac{P_c}{P_I}\right)_{dB} \simeq -\left(-43\ dB\right) - 22.7\ dB$$

$$\simeq 20.3\ dB$$

The total shunting capacitance of all the open switches would be about 187 x 15 pf ≈ 2.8 nf, which presents a reactance of -1.9jΩ in parallel with the assumed load impedance of 75Ω. In passing through 3-4(?) submatrices, some 40 dB of insertion losses could arise.

Since each switch has two signal terminals and one switch-control terminal, then (excluding power supply terminals) an IC package with multiple FET switches must have three pins for each switch. The 64-pin IC package is about the largest currently available, which would put a pin-out restricted limit of about 20 switches per IC package. If such an IC package (currently about 1.7 in. x 0.9 in.) was allowed 1/4 in. spacing on a printed circuit board, then the 187,000/20 = 9350 IC switch packages would occupy a total area of about 146 square feet i.e., about a 12 ft x 12 ft

square. This might be accommodated by stacking 16 3 ft x 3 ft or 36 2 ft x 2 ft printed circuit boards.

POSSIBLE ALTERNATIVES

With only some 20 simple FET switches on an IC chip, the chip's LSI potential has scarcely been tapped. With such a large number of chips being required, custom design of an "improved" switch chip is economically quite feasible. Accordingly, by on-chip buffering the input and output of the FET switch (e.g., with source-followers -- or even op-amps) the insertion loss and line shunt-loading could be greatly reduced.

Since switch setting (i.e., opening or closing) is done relatively infrequently in this NASA system design, a high degree of large scale integration might be achieved by incorporating an entire M x N switching submatrix on one chip using TDM switch control. For example, a 30 x 30 submatrix, with 30 input and 30 output lines, and several power and TDM switch control lines, can be accomodated in one 64-pin IC package. The resulting 900 cross-point switches would each have a control latch which is set (or reset) one at a time. A 10-time-slot TDM digital pulse train (furnishing 1024 possible binary state combinations) could be serial-to-parallel converted (also on-chip) into a 10-bit address which could then be decoded and routed to the control latch on any of the 900 switches (much as is done in a 1k x 1 ROM).

If the OFF isolation of a single FET switch is not adequate, a (triple-switch) T-configuration switch could be employed: two FET switches in series with their junction point shunted to ground by a third FET switch. When the T-switch is to be open, the two series switches are also open with the third (shunting) switch loading down the junction point, which leads to a very much smaller feed through. When the T-switch is closed, the series ON-resistance is, of course, doubled but if the T-switch is also input- and output-buffered as suggested before, this should make little difference.

Even if each of the 900 cross-points had: (3 switches) x (5 transistors/switch) + 5 transistors/buffer (input + output) + 5 transistors/switch-control latch, the required 22,500 transistors make a relatively modest demand on present LSI technology (e.g., 64K RAMS have at least 64K transistors on a chip). A little over 200 such chips would provide the 187K cross points of the Clos method; 1100 such chips would provide the million cross points of the standard approach -- and occupy only about five 2 ft x 2 ft printed circuit boards.

For the very large number of chips required -- whether using the standard or Clos approach -- CMOS is probably the best technology, not only for the primary consideration of power consumption, but for noise immunity and temperature stability as well.

GLOSSARY

AGC	automatic gain control
AWGN	additive white Gaussian noise
BCH	Bose-Chaudhuri-Hocquenghem
BER	bit error rate
BO	backoff
BOL	beginning of life
BPF	bandpass filter
BPSK	binary phase shift kaying
CC	convolutional code
CCIR	International Radio Consultative Committee
C/IM	carrier-to-intermodulation
CONUS	continental United States
CNR	carrier-tc-noise ratio
CPS	Customer Premises Service
CSC	common signaling channel
DAMA	demand assignment multiple access
DC	direct current
EIRP	effective isotropic radiated power
FET	field effect transistor
FDM	frequency division multiplexed
FDMA	frequency division multiple access
FOV	field of view

GLOSSARY (Continued)

FSP	full scale production
G&A	general and administration
G/T	gain-to-noise temperature ratio
GT	grand total
HDW	hardware
HPA	high power amplifier
HPBW	half power beamwidth
IF	intermediate frequency
IM	intermodulation
IUS	interim upper stage
LeRC	Lewis Research Center
LO	local oscillator
LRP	low rate production
LSI	large scale integration
MBA	multibeam antenna
MSK	minimum shift keying
NASA	National Aeronautics and Space Administration
NCC	network control center
QPSK	quadriphase shift keying
RAM	random access memory
RF	radio frequency
R&D	research and development

GLOSSARY (Concluded)

SAMSO	Space and Missile Systems Organization (now SD)
SAW	surface acoustic wave
SD	Space Division
SFSK	sinusoidal frequency shift keying
SMSA	Standard Metropolitan Statistical Area
SNR	signal-to-noise ratio
SQPSK	staggered quadriphase shift keying
SR	satellite routed
SS	satellite switched
T	trunking
TDM	time division multiplexed
TDMA	time division multiple access
TR	trunking only
TWT	traveling wave tube
VBFN	variable beam forming network
VPD	variable power divider